UNSW SYDNEY | Australia's Global University

Australian Centre for Advanced Photovoltaics
Australia-US Institute for Advanced Photovoltaics

Annual Report 2017

Table of Contents

Director's Report

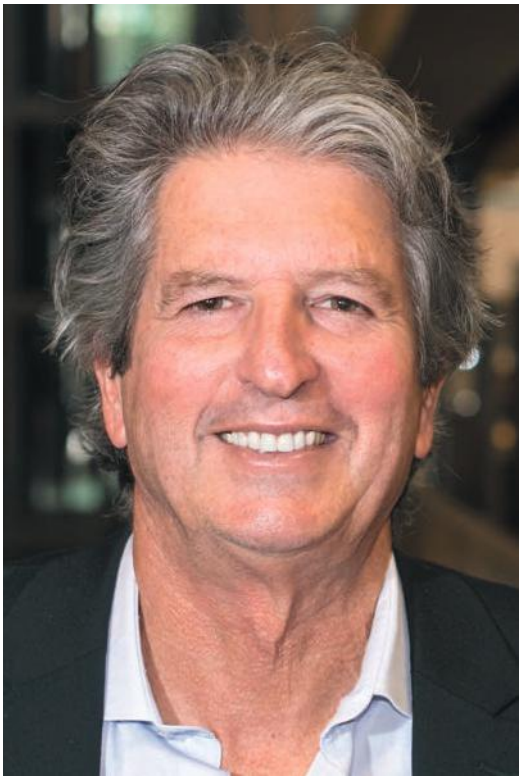

Solar photovoltaics involves the direct generation of electricity from sunlight, when it shines upon devices known as solar cells. Silicon is the most common material used to make these photovoltaic cells, similarly to its key role in microelectronics, although several other photovoltaic materials are being actively investigated.

During 2017, photovoltaics reinforced its position as the lowest cost option for electricity production yet developed. In August 2016, bids were submitted for the long-term supply of electricity in Chile using solar photovoltaics at US$29.10/MWh, appreciably lower than from any other bidding technology including coal, where the corresponding bid was nearly twice as high at US$57/MWh (itself quite low by international standards, with Bloomberg estimating the cost of electricity from a new black coal plant in Australia in 2016 at an appreciably higher AU$120/MWh). In 2017, appreciably lower bids were received in multiple power auctions. In September, a consortium led by Abu Dhabi's renewable energy company Masdar submitted the lowest bid to date for a project in Saudi Arabia, as OPEC's top crude producer diversifies its economy away from hydrocarbons. Masdar and its French partner EDF submitted an offer of US$17.86/MWh, lower than even the short-run marginal cost of generation from most existing Australian black coal plants.

Australia has played a major role in achieving these past cost reductions and is expected to play a key role in future cost reductions through the activities of the Australian Centre for Advanced Photovoltaics (ACAP), documented in this 2017 Annual Report. According to EnergyTrend, the global manufacturing capacity for the Australian-invented and -developed PERC (Passivated Emitter and Rear Cell) technology grew by a massive 160.5% in 2017, reaching 42.38GW by the end of the year, about one-third of all capacity. With such high growth rates, PERC should account for the majority of photovoltaic manufacturing before 2020.

ACAP researchers are working closely with a consortium of manufacturers and equipment suppliers to further increase PERC performance while reducing costs through patented hydrogenation technology. The buoyant mood created by the accelerating uptake of photovoltaics and of Australian technology was dampened by the sudden passing in December of close colleague and solar pioneer, Professor Stuart Wenham. Stuart has been involved with the UNSW group for over 34 years, playing a major role in most of the group's major achievements over this period, including the development of the first 20% and 25% efficient silicon cells, the latter using PERC technology, the invention and commercialisation of the "buried contact", "semiconductor finger" and "Pluto" solar cells, as well as the hydrogenation approaches mentioned above (see obituary at end of Report).

This is the fifth annual ACAP report also incorporating that of the Australia–US Institute for Advanced Photovoltaics (AUSIAPV), supported by the Australian Government through the Australian Renewable Energy Agency (ARENA). ACAP encompasses the activities of Australian-based researchers while, through synergistic research activities with US partners, AUSIAPV aims to significantly accelerate photovoltaic development beyond that achievable by Australia or the US individually. This objective is to be reached by leveraging development

of “over the horizon” photovoltaic technology, providing a pipeline of improved technology for increased performance and ongoing cost reduction.

A second aim is to provide high quality training opportunities for the next generation of photovoltaic researchers, particularly through enhanced collaborations between Australian and US researchers, with one targeted outcome being to consolidate Australia’s position as the photovoltaic research and educational hub of the Asia-Pacific manufacturing region.

ACAP/AUSIAPV came into being on 1 February 2013 after the signing of a Head Agreement between the University of New South Wales (UNSW) and ARENA. During 2013, related Collaboration Agreements were signed between UNSW and the other ACAP nodes, Australian National University (ANU), University of Melbourne (UoM), Monash University, University of Queensland (UQ) and CSIRO (Materials Science and Engineering, Melbourne) and, additionally, with the ACAP industrial partners, Suntech Research and Development, Australia (SRDA) (partnership now transferred to Wuxi Suntech Power Co., Ltd), Trina Solar Ltd, BlueScope Steel, BT Imaging, PV Lighthouse, Greatcell Pty Ltd and RayGen Resources. Our major international partners include the NSF-DOE Engineering Research Center for Quantum Energy and Sustainable Solar Technologies (QESST) and the US National Renewable Energy Laboratory (NREL), as well as the Molecular Foundry (Berkeley), Stanford University, Georgia Institute of Technology and the University of California, Santa Barbara.

This report covers the period from 1 January to 31 December 2017. Over the past five years, both ACAP and AUSIAPV have moved quickly to establish a high profile within the international research community. Following on from the world record 24.4% energy conversion efficiency rear junction cell developed at ANU during 2013, a system based on splitting focused sunlight into different colour bands, designed and fabricated at UNSW with performance then certified by US partner NREL, became, in late 2014, the first in history to convert sunlight to electricity with over 40% energy conversion efficiency. In 2015, a similar approach was extended to a one-sun minimodule with performance subsequently confirmed at 34.5%, the highest ever for non-concentrated sunlight. In 2016, additional world-record results were confirmed for “thin-film” cells made from the compound CZTS (Cu_2ZnSnS_4), based on “Earth abundant”, relatively benign materials, and also for perovskite solar cells. An efficiency record of 9.5% was confirmed for a small area CZTS cell, with an efficiency of 18.0% independently confirmed for a 1.2 cm^2 perovskite cell, the highest ever for a cell of this size.

The tradition of world records was continued in 2017 with the CZTS record improved to a new value of 11.0% and that for a perovskite cell increased to 19.6%, the highest confirmed efficiency reported for a perovskite cell larger than 1 cm^2 in area at that time. These and several other key achievements during 2017 are summarised in the highlight pages immediately following my report. More detailed results described in the body of this 2017 Annual Report contributed to making 2017, once again, an extremely successful year for both ACAP and AUSIAPV.

I would like to thank ARENA for its ongoing financial support and also for the very effective involvement of ARENA personnel in supporting the ACAP/AUSIAPV program, both informally and via the ACAP National Steering Committee and the AUSIAPV International Advisory Committee. I would additionally like to thank, in particular, all researchers affiliated with the Institute for their contributions to the broad range of progress reported in the following pages.

Finally, I am pleased to be able to report that ACAP/AUSIAPV has taken another major step towards attaining its significant long-term objectives by achieving its key fifth-year milestones, on time and within budget. We look forward to similar progress in 2018 and in subsequent years.

Martin Green
Director

Highlights

Record Cu_2ZnSnS_4 (CZTS) solar cells

CZTS solar cells are of international interest since, like silicon, they use only abundant, non-toxic elements. They can be fabricated in the form of thin films deposited onto a supporting substrate or on top of silicon to form a tandem cell stack. In 2017, two new world records were independently confirmed for CZTS cells fabricated at UNSW Sydney in work supported by ACAP. The first of these was 10.0% efficiency for a 1-cm^2 CZTS device (certified by NREL), substantially improving upon the previously best result of 7.6%, also established by UNSW. The second was 11.0% efficiency (certified by NREL) for a smaller area, sub-1 cm^2 device, also improving on the previous record of 9.5%, again established by UNSW.

Figure 2.1: Dr Xiaojing (Jeana) Hao, leader of the UNSW CZTS team, holding a batch of CZTS cells similar to those setting the recent world records.

High-efficiency four-terminal CZTS/Si and CIGS/Si tandem cells by spectrum splitting

Chalcogenide semiconductors, including copper zinc tin sulphide (CZTS) and copper indium tin sulphide (CIGS), are promising as absorber materials for solar cells due to their direct bandgaps, high absorption coefficient, high energy conversion efficiency, low-cost potentiality and high stability. The baseline efficiency of high bandgap pure-sulphide CZTS solar cells has been improved, such that the highest certified performance by NREL is 11% (see above item). Great progress has been made in improving the efficiency of CZTS/Si tandem cells by increasing the CZTS solar cell efficiency and designing tandem cells combining CZTS family cells and Si cells. UNSW has demonstrated 22.7% efficiency CZTS/PERL tandem solar cells and 19% CZTS/PERC-Si tandem solar cells by a spectrum splitting method (in-house measurements), which are comparable to the performance of corresponding high bandgap CIGS (by Solar Frontier)/Si tandem cells, fabricated using a similar spectrum splitting method.

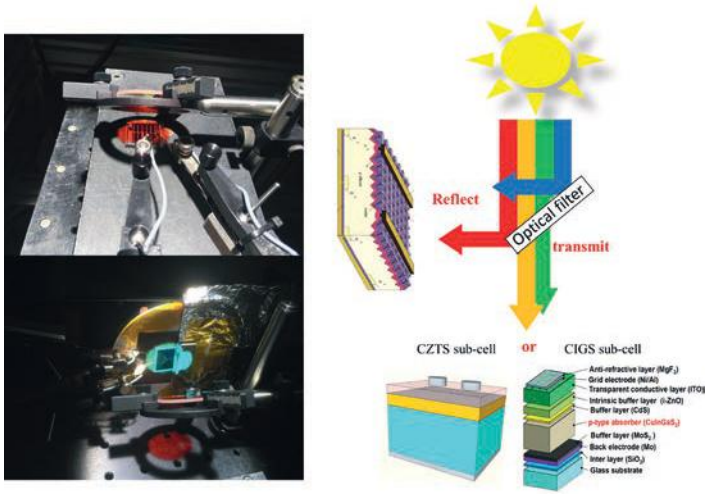

Figure 2.2: Chacogenide/Si four terminal tandem by spectrum splitting

High performance perovskite – silicon tandem cells

Tandem cells consist of a stack of cells made of materials which absorb different parts of the solar spectrum. Such tandem devices can dramatically lift the conversion efficiency of sunlight to electricity compared to conventional solar cells. Tandem cells consisting of a combination of perovskite and silicon are particularly interesting since they combine two low-cost, highly efficient materials with the right absorption properties. As a result, perovskite – silicon tandems are a hot topic in research.

In work led by PhD student The Duong, ANU's perovskite and silicon cell teams combined forces to push the boundaries of the respective technologies, and demonstrated a record 26.4% efficiency perovskite – silicon tandem cell (in-house measurement). In this tandem, the two sub-cells are independently wired. The result, reported in *Advanced Energy Materials*, was achieved through a careful analysis of loss mechanisms and the optimisation of each of the sub-cells. Importantly, the work also identified a clear path to 30% efficiency tandem cells, which is the longer term goal in order to ensure the cells offer a clear efficiency benefit even over the very best conventional silicon cells.

In a separate project led by PhD student Yiliang Wu, the ANU team fabricated monolithic perovskite – silicon tandem cells, where the two sub-cells are fully integrated, resulting in a less complex process sequence. Here, they were able to demonstrate an efficiency of 22.5% (in-house measurement) using a silicon sub-cell fabricated with conventional, diffused junction technology, a record for this type of cell. The result is of commercial significance since diffused junction technology is the dominant technology in solar cell production and because such cells are more temperature tolerant than many alternatives, thus allowing substantially greater process flexibility for the fabrication of the subsequent perovskite cell on top of the silicon cell. This work was published in *Energy and Environmental Science.*

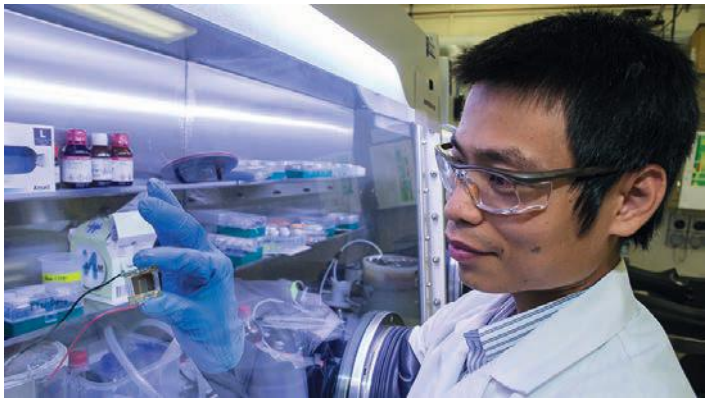

Figure 2.3: The Duong with a high efficiency perovskite cell.

Complementing this work at ANU, at the end of 2017, UNSW Sydney and the Institute Materials for Electronics and Energy Technology (i-MEET), Friedrich-Alexander University, Erlangen-Nuremberg, Germany reported a 26.7% efficient (measured externally to ACAP) mechanical stack (four-terminal) that uses a PERL (Passivated Emitter rRear Localised) Si cell as the bottom cell and an ITO-fused silica/CuSCN/$MAPbI_3$/PC60BM/ZnO:Al nps/AgNW perovskite cell as the top cell. After the application of MgF_2 anti-reflection coating, the efficiency improves to 26.9%. These are the highest efficiencies reported to date for a four-terminal perovskite–Si tandem and have surpassed the record for a single-junction silicon cell at 26.7%. The results were published in *Journal of Materials Chemistry A*.

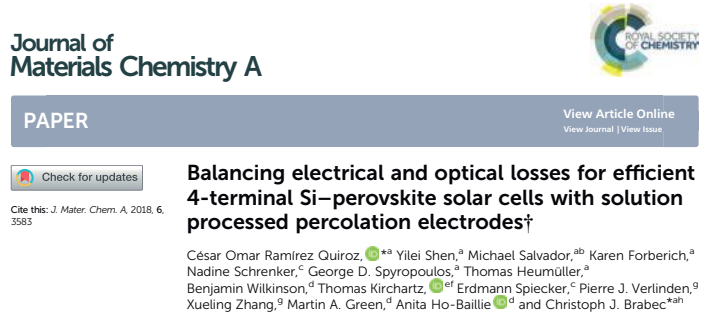

Journal of Materials Chemistry A

PAPER

View Article Online
View Journal | View Issue

Check for updates

Cite this: *J. Mater. Chem. A*, 2018, 6, 3583

Balancing electrical and optical losses for efficient 4-terminal Si–perovskite solar cells with solution processed percolation electrodes†

César Omar Ramírez Quiroz,*[a] Yilei Shen,[a] Michael Salvador,[ab] Karen Forberich,[a] Nadine Schrenker,[c] George D. Spyropoulos,[a] Thomas Heumüller,[a] Benjamin Wilkinson,[d] Thomas Kirchartz,[ef] Erdmann Spiecker,[c] Pierre J. Verlinden,[g] Xueling Zhang,[g] Martin A. Green,[d] Anita Ho-Baillie[d] and Christoph J. Brabec*[ah]

Figure 2.4: Broad collaboration achieved outstanding silicon-perovskite efficiency.

Record perovskite cell efficiency

Along with stability, achieving large-area perovskite devices has been a global challenge. Great progress has been made in ACAP in the demonstration of >1 cm^2 devices. In particular, certified efficiency at 19.6% has been achieved on a 1.02 cm^2 cell at UNSW in 2017.

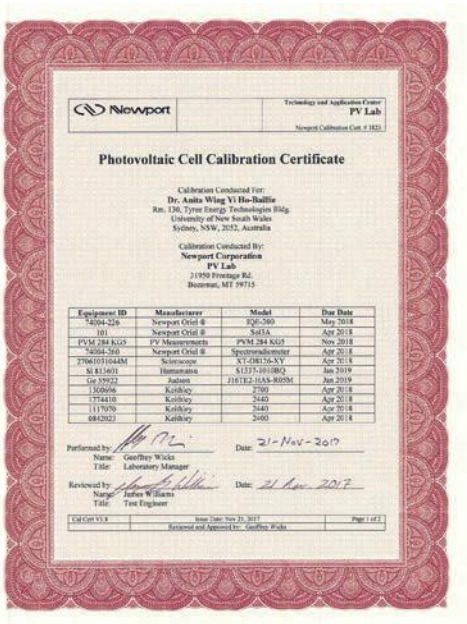

Newport

Technology and Application Center
PV Lab

Photovoltaic Cell Calibration Certificate

Calibration Conducted For:
Dr. Anita Wing Yi Ho-Baillie
Rm. 130, Tyree Energy Technologies Bldg.
University of New South Wales
Sydney, NSW, 2052, Australia

Calibration Conducted By:
Newport Corporation
PV Lab
19550 Frontage Rd.
Bozeman, MT 59715

Equipment ID	Manufacturer	Model	Due Date
54304-326	Newport Oriel #	IQE-200	May 2018
101	Newport Oriel #	Sol3A	Apr 2018
PVM 284 KG5	PV Measurements	PVM 284 KG5	Nov 2018
54304-260	Newport Oriel #	Spectroradiometer	Apr 2018
270610T1044M	Scienscope	XT-DB126-XY	Apr 2018
SI 813601	Humanatus	S1337-1010BQ	Jan 2019
Ge 35922	Judson	J16TE2-16A8-R05M	Jun 2019
1320696	Keithley	2700	Apr 2018
1774418	Keithley	2440	Apr 2018
1117970	Keithley	2440	Apr 2018
0842921	Keithley	2400	Apr 2018

Performed by: Geoffrey Wicks, Laboratory Manager — Date: 21-Nov-2017
Reviewed by: Jarhen Williams, Test Engineer — Date: 21 Nov. 2017

Cal Cert V3.8 | Issue Date: Nov 21, 2017 | Page 1 of 2
Reviewed and Approved by: Geoffrey Wicks

Figure 2.5: Certificate for 19.6% perovskite cell with area exceeding 1 cm^2.

Polysilicon passivated contacts with 735 mV implied-V_{OC} and low contact resistance

As silicon photovoltaic technology advances, charge carrier losses at the contacted interfaces of the silicon absorber are coming to dominate power conversion efficiency. Development of passivated contacts, which provides selective charge-carrier extraction while simultaneously reducing interface recombination, is thus of significant interest for next generation silicon solar cells. However, achieving both low recombination and low resistance to charge carrier extraction has proven challenging.

In research activities led by Dr Kean Chern Fong at ANU, a novel method of n^+ polysilicon-oxide stack deposition was developed which achieves simultaneously very low reverse saturation current density below below 1 $fAcm^{-2}$, low specific contact resistivity below 1 $m\Omega cm^2$, while retaining very high bulk lifetimes exceeding 140 ms, indicating an implied-V_{OC} above 735 mV in test wafers. The key to this technology is the fine control over the in-situ oxidation conditions performed within the low pressure chemical vapour deposition (LPCVD) furnace under low pressure conditions, and at high temperatures. The passivated contact structure maintains its electronic properties at temperatures up to 950˚C, and can withstand subsequent deposition of optically optimised films or masking and patterning films for device fabrication.

The developed technology is compatible with both high efficiency laboratory device fabrication and industrial fabrication processes, utilising an industrially applicable high throughput process. This work therefore represents a significant advancement in industrially applicable passivated contact technology.

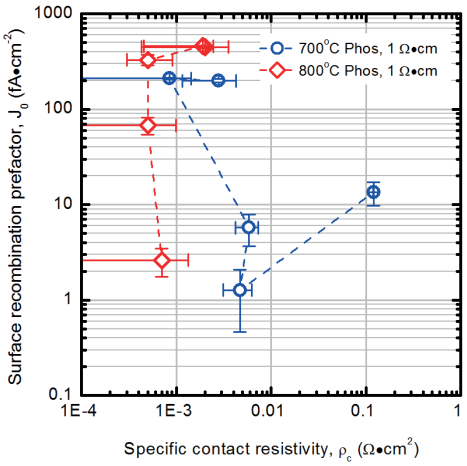

Figure 2.6: Summary of J_0 and ρ_c for the range of phosphorus diffusion between 700 and 850˚C, and oxidation temperature between 650 and 800˚C.

Record open circuit voltage for Cz silicon solar cell

High open circuit voltage (V_{OC}) is a necessary (but not sufficient, since high short circuit current is needed too) condition for high efficiency. This 703 mV record V_{OC} for p-type Cz silicon, achieved in collaboration between UNSW Sydney and Arizona State University (ASU), brings together high efficiency n-type heterojunction solar cell technology with conventional solar cell processing that naturally improves the quality of silicon throughout the fabrication of industrial p-type solar cells. It uses a novel prefabrication gettering (concentration of undesirable impurities in regions where they have less impact on performance) and a multi-stage hydrogenation process to overcome the usual limitations of conventional heterojunction solar cells that have previously restricted the fabrication of such solar cells to expensive, high-lifetime n-type silicon wafers. This result represents almost a 20 mV improvement in V_{OC} over the current state-of-the-art industrial PERC solar cells and could lead to a new generation of industrial high efficiency p-type solar cells featuring a heterojunction with amorphous silicon.

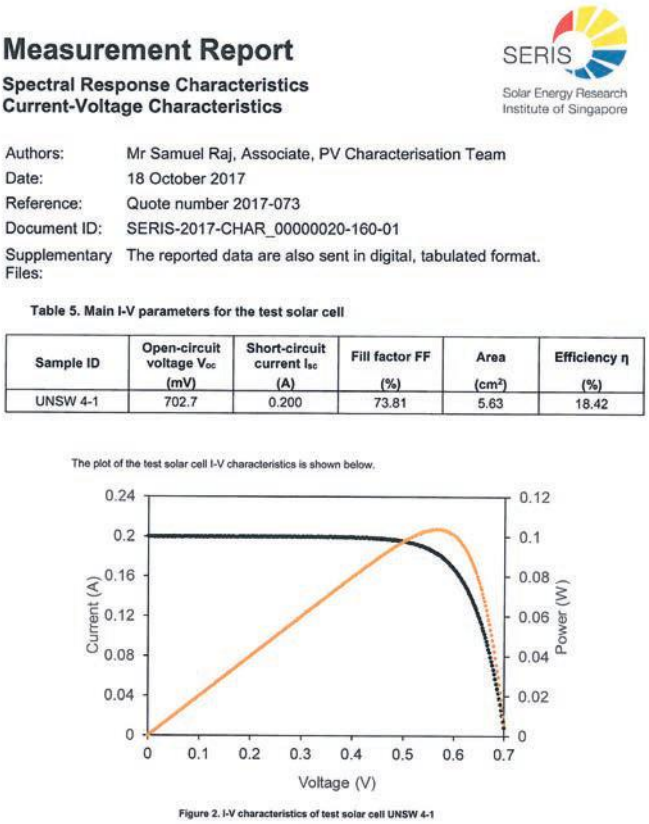

Measurement Report

Spectral Response Characteristics
Current-Voltage Characteristics

SERIS
Solar Energy Research Institute of Singapore

Authors:	Mr Samuel Raj, Associate, PV Characterisation Team
Date:	18 October 2017
Reference:	Quote number 2017-073
Document ID:	SERIS-2017-CHAR_00000020-160-01
Supplementary Files:	The reported data are also sent in digital, tabulated format.

Table 5. Main I-V parameters for the test solar cell

Sample ID	Open-circuit voltage V_{oc} (mV)	Short-circuit current I_{sc} (A)	Fill factor FF (%)	Area (cm^2)	Efficiency η (%)
UNSW 4-1	702.7	0.200	73.81	5.63	18.42

The plot of the test solar cell I-V characteristics is shown below.

Figure 2. I-V characteristics of test solar cell UNSW 4-1

Figure 2.7: Certification of 703 mV open circuit voltage.

High Impact Papers

An additional ten papers published under the ACAP program in 2017 have already been identified as making a large impact at the international level. These have been classified as “Highly Cited Papers”, earning a ranking within the top 1% in their field. Three of these have earned the additional distinction of being identified as “Hot Papers”, within the top 0.1% in their field. This is a disproportionately high number relative to the ACAP total and brings the total to 42 papers earning the “Highly Cited” distinction over the first five years of ACAP operation.

Five of the 2016 “Highly Cited Papers” were based on results generated in ACAP program strand PP2: “Thin-Film, Third Generation and Hybrid Devices”. The first of these, with lead author Jianfeng Yang affiliated with the UNSW Sydney node, discusses up-conversion and a hot-phonon bottleneck in lead-halide perovskites. The second, with lead author Daniel Jacobs affiliated with the ANU node, addresses the issue of hysteresis in perovskite solar cells. The third, with lead author Meng Zhang, with UNSW Sydney node affiliation, describes high efficiency rubidium-incorporated perovskite cells. The fourth, with lead author Jun Peng affiliated with ANU, describes improved electron transport layers for perovskite solar cells. The final highly cited paper in the PP2 strand, with lead author Mathias Rothmann affiliated with the Monash node, describes the direct observations of twin domains in these perovskite materials.

Outside the PP2 strand, a paper by Martin Green and Stephen Bremner, both with the UNSW Sydney node, assesses a range of approaches for improving solar cell efficiency beyond that possible with standard devices. A somewhat related paper, with lead author James Banal affiliated with the University of Melbourne node, describes emissive molecular aggregates and energy migration in luminescent solar concentrators. A third paper, spanning PP1 and PP2 strands, with lead author The Duong of the ANU node, describes high efficiency perovskite-silicon tandem solar cells.This paper has the additional distinction of being identified as a “Hot Paper” (within the top 0.1% in its field).

The final two “Highly Cited Papers” arose from collaboration between AUSIAPV partners, UNSW and Colorado-based NREL, documenting recent efficiency improvements in photovoltaics across a range of technologies, including the recent UNSW record 10% and 11% CZTS cell results and the record 19.9% result for a multicrystalline silicon module obtained by ACAP industrial partner, Trina Solar, using UNSW-invented and -developed PERC (Passivated Emitter and Rear Cell) technology. Both papers also received the additional “Hot Paper” distinction, being within the top 0.1% in their field.

From a slightly different perspective, Australia published 3.7% of all papers between 2013 and 2016 with “Perovskite Solar Cell” included in the title, but 9.5% in the highest impact category of “Hot Papers”, according to the Web of Science. Similarly, Australia published 7.4% of all papers with “Silicon Solar Cell” in the title over the same period, but a massive 13.3% in the top category of “Highly Cited Papers”, if perovskite and graphene papers are excluded. All the papers in the most highly cited category had ACAP authorship in both cases.

Figure 2.8: Professor Henry Snaith workshop at Monash University, January 2017, lecturing on "Stability studies of perovskite solar cells".

Distinguished scholar Professor Henry Snaith visits Monash University and UNSW Sydney

Henry Snaith is a professor at the University of Oxford, one of the co-inventors of the perovskite solar cell, and a co-founder of the company Oxford PV. He has co-authored 16 papers in Nature and Science journals in the area of perovskite solar cells. In January 2016 Professor Snaith was named as "the world's second most influential scientific mind" by Thomson Reuters. He spent two weeks at Monash University in 2017, giving lectures, public talks, and having detailed conversations with individual academics and researchers from the Renewable Energy Group, laying down the foundations for future collaborations, research exchanges and joint grants applications. Professor Snaith also visited other ACAP nodes, giving a public lecture at UNSW on 23 January 2017.

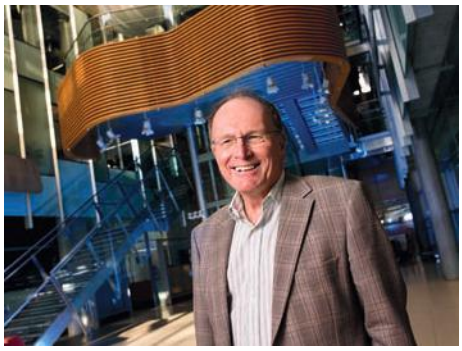

Figure 2.9: Professor Andrew Holmes. Photo courtesy of Bio21. Photographer: Peter Casamento.

Andrew Holmes AC

Andrew Holmes, an ACAP Chief Investigator at the University of Melbourne, was recognised in the 2017 Australia Day Honours list with Australia's highest honour, Companion in the General Division of the Order of Australia. This recognition was received for his lifetime of service to science including his research at the interface of chemistry, biology and materials science (including contributions to the development of LEDs and solar cells), as an academic leader and mentor, and through leadership of scientific organisations. In 2017 Professor Holmes was also named a Fellow of the American Association for the Advancement of Science (AAAS). Election as an AAAS Fellow is an honour bestowed upon AAAS members by their peers because of their scientifically or socially distinguished efforts to advance science or its applications. During July Professor Holmes presented a Plenary Lecture on the opening day of the Royal Australian Chemical Institute's Centenary Congress held in Melbourne highlighting the contributions of chemistry to materials development for light emitting diodes and solar cells. Professor Holmes is the current President of the Australian Academy of Science.

Figure 2.10: Dr Brett Hallam received his award in Government House from the NSW Premier, Gladys Berejiklian.

Dr Brett Hallam, NSW Premier's Award for Energy Innovation

Dr Brett Hallam, from the UNSW node, won the Premier's Award for Energy Innovation in New South Wales.

His research has resulted in a significant increase in electrical output of solar panels which will lead to cheaper photovoltaic-generated electricity. His focus is on developing techniques for manipulating the charge state of atomic hydrogen in silicon to neutralise performance-limiting defects in solar cells (see Section PP1.1). He has managed multiple international collaborations with industrial solar cell manufacturers and research institutes, achieving world record silicon solar cell efficiencies.

A/Prof Renate Egan lauded as one of Eight Great Women in the Business and Science of Solar

Chief Investigator for the UNSW node, A/Prof Renate Egan was honoured by Renewable Energy World in its 15 December 2017 issue as one of Eight Great Women in the Business and Science of Solar, models for young women of what is possible.

The citation by Paula Mints, a leading photovoltaics market research analyst states, "Dr Egan's commitment to the science, engineering and to the analytics required to keep the global PV industry on its trajectory to becoming a mainstream electricity source serves as an example to young women considering a career in the solar industry."

Figure 2.11: A/Prof Renate Egan, one of Eight Great Women in the Business and Science of Solar

EU PVSEC Student Award for UNSW's Appu Rshikesan Paduthol

Appu Rshikesan Paduthol, from the UNSW ACAP node, received an EU PVSEC Student Award for his paper, "Efficient carrier injection from amorphous silicon into crystalline silicon determined from photoluminescence" at the 33rd European Photovoltaic Solar Energy Conference (EU PVSEC) in Amsterdam on 29 September 2017. These awards are delivered in recognition of the most remarkable and outstanding research work in the field of PV.

Figure 2.12: Appu Rshikesan Paduthol, from the UNSW ACAP node, receives the EU PVSEC Student Award in Amsterdam (Image credit: Eu PVSEC).

Awards and front covers for Monash PhD student Wenxin Mao

Wenxin Mao won best poster award at the recent 2017 International Symposium on Energy Conversion and Storage Materials in Brisbane in July–August 2017. Wenxin's recent paper "Controlled Growth of Monocrystalline Organo-Lead Halide Perovskite and Its Application in Photonic Devices" appeared on the front cover of Angewandte Chemie (see Figure 2.13).

Wenxin Mao also won the People's Choice award for a poster presentation at the Chemical Engineering Postgraduate Association (CEPA) conference at Monash University (see Figure 2.14).

Congratulations to Mathias Rothmann

Congratulations to Mathias Rothmann who won the best poster presentation award at the Asia-Pacific International Conference on Hybrid and Organic Photovoltaics (AP-HOPV17) in Yokohama, as well as another award in Wuhan.

Figure 2.13: Cover of issue 2017–56/41 of Angewandte Chemie International Edition.

Figure 2.14: Wenxin Mao at the Chemical Engineering Postgraduate Association (CEPA) conference at Monash University.

Organisational Structure and Research Overview

The Australian Centre for Advanced Photovoltaics (ACAP) coordinates the activities of the Australian partners in the Australia–US Institute for Advanced Photovoltaics (AUSIAPV), established to develop the next generations of photovoltaic technology and to provide a pipeline of opportunities for performance increase and cost reduction. The Australian partners in ACAP are UNSW, ANU, University of Melbourne, Monash University, University of Queensland and CSIRO, plus our industrial partners Suntech Power, Trina Solar, BlueScope Steel, BT Imaging, PV Lighthouse, Greatcell Solar and RayGen Resources. AUSIAPV links ACAP with international partners, specifically the National Science Foundation and Department of Energy–supported Engineering Research Center for Quantum Energy and Sustainable Solar Technologies (QESST), based at Arizona State University, the National Renewable Energy Laboratory (NREL), Sandia National Laboratories, Lawrence Berkeley National Laboratory, Stanford University, Georgia Institute of Technology and University of California, Santa Barbara. These national and international research collaborations provide a pathway for highly visible, structured photovoltaic research collaboration between Australian and American researchers, research institutes and agencies, with significant joint programs based on the clear synergies between the participating bodies.

AUSIAPV/ACAP is driving significant acceleration of photovoltaic development beyond that achievable by institutes acting individually, with significant leveraging of past and current funding. This program is supported by the Australian Government through the Australian Renewable Energy Agency (ARENA). The Australian Government, through ARENA, is supporting Australian research and development in solar photovoltaic and solar thermal technologies to help solar power become cost competitive with other energy sources. (The views expressed herein are not necessarily the views of the Australian Government, and the Australian Government does not accept responsibility for any information or advice contained within this report.)

The AUSIAPV/ACAP organisational chart is shown in Figure 3.1. The international activities of AUSIAPV are coordinated by an International Steering Committee with membership drawn from ARENA, the US Department of Energy (DOE), ACAP and the ACAP National Steering Committee, QESST and NREL. The International Steering Committee is also charged with identifying opportunities for synergistic photovoltaic research initiatives between Australia and international partners and for facilitating staff and student exchanges. Some examples of current international activities, many arising from competitive ACAP Collaboration Grants, are reported in Section 6 of this report.

As well as these collaborative activities, the major partners in AUSIAPV, specifically ACAP, QESST and NREL, conduct their own largely independent research programs meeting the specific research and training objectives of their major supporters and sponsors. In the case of ACAP, research is milestone driven with annual milestone targets established under the Funding Agreement with ARENA. ACAP is managed by a Management Committee, which consists of the node directors or delegates from each of the nodes. The Management Committee takes advice from the National Steering Committee, with an independent Charter, but with membership including a representative of ARENA and NREL, the ACAP and QESST directors, and other members drawn from industrial partners.

As indicated in Figure 3.1, the ACAP program is organised under five Program Packages (PP1–PP5), each supported by multiple nodes. PP1 deals with silicon wafer–based cells, by far the dominant photovoltaic technology commercially, and likely to remain so for at least the next 10 years. Here the challenge is to continue to reduce manufacturing costs, while maintaining or preferably, improving, energy conversion efficiency. PP1 focuses on three main areas: cells made from solar-grade silicon, rear contact cells and silicon-based tandem cells, both monolithic and mechanically stacked.

PP2 involves collaborative research into a range of organic, organic-inorganic hybrid cells and "earth abundant" thin-film materials, including Si and Cu_2ZnSnS_4 (CZTS), as well as more futuristic "third-generation" approaches. Recently, the relatively new photovoltaic material, the organic-inorganic perovskites, has been included within the scope and additional funding provided from 2016 to expand and intensify the research on these materials and devices. The program now has the overall goal of demonstrating high efficiencies for these new thin-film cells of above 1 cm^2 area and of demonstrating the feasibility of costs below the US Department of Energy SunShot targets for cost reductions.

PP3, optics and characterisation, targets experimental demonstration that theoretical conversion limits can be increased by the use of structures that have a high local density of optical states, with particular emphasis on thin-film organic and inorganic solar cells.

PP4, manufacturing issues, aims at delivery of a substantiated methodology for assessing manufacturing costs of the different technologies under investigation by ACAP. The overall cost target is to undercut the US Government's SunShot targets, for one or more of the technologies, in at least one major SunShot targeted application, as deduced by a substantiated costing methodology. Environmental costs are also considered by ACAP, through application of the rigorous life cycle assessment regime.

Additional targets for PP1–PP4 relate to the established academic measures assessing research performance, specifically the number and quality of publications, with strong collaboration being encouraged by placing emphasis on publications involving authors from multiple nodes within the Australian-based Centre or the Australia–US Institute, on invited keynote and plenary presentations, on patent applications and on indicators of commercial interest, such as the number of projects jointly supported by industry, with active commercialisation of key developments for at least one technology by Year Eight.

PP5 involves education, training and outreach. ACAP has specific targets for the number of researchers in different categories benefiting from the infrastructural support it provides and for the quality and number of researcher exchanges. Additionally, a significant number of major outreach events are targeted for each year. As well as major events such as those reported in the PP5 section of this annual report, other outreach activities include public lectures on material relevant to ACAP activities, newspaper and magazine articles, responses to governmental calls for submissions, visits by policy developers and their advisors, information papers prepared and presentations to both policy developers and their advisors.

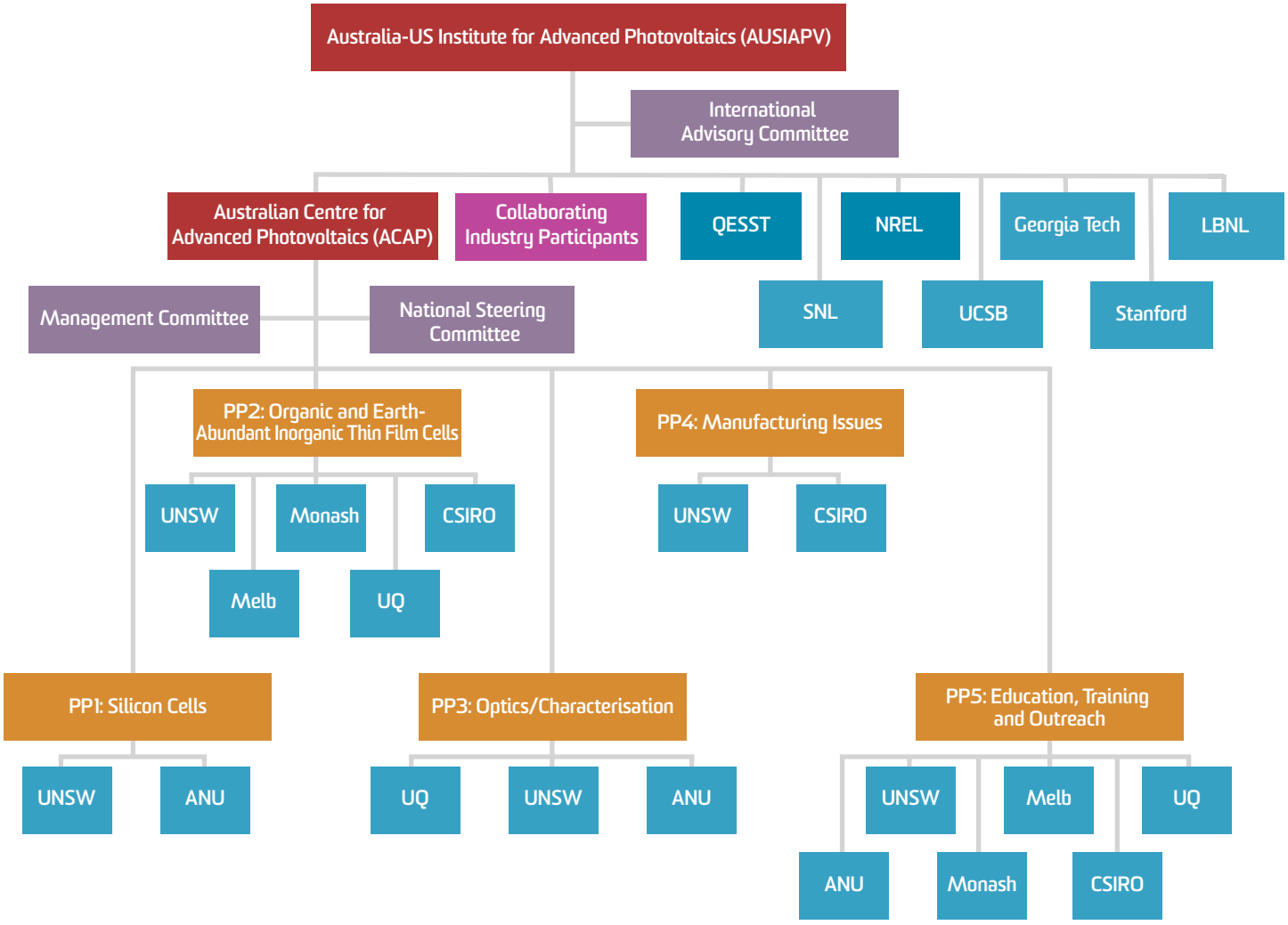

Figure 3.1: Organisational chart.
Collaborating industry participants are involved in collaborative research as well as in the Advisory and Steering Committees.

Affiliated Staff and Students

University of New South Wales

Green, Martin (Centre Director)
Corkish, Richard (Centre Chief Operating Officer)

Academic Staff and Senior Researchers

Egan, Renate (Node Leader)
Abbott, Malcolm
Bagnall, Darren (until Jun 2017)
Bremner, Stephen
Chong, Chee Mun
Conibeer, Gavin
Edwards, Matthew
Ekins-Daukes, Nicholas (from Aug 2017)
Hao, Xiaojing
Hameiri, Ziv
Ho-Baillie, Anita
Hoex, Bram
Huang, Shujuan
Keevers, Mark
Lennon, Alison
Mehrvarz, Hamid
Perez-Wurfl, Ivan
Shrestha, Santosh
Trupke, Thorsten
Uddin, Ashraf
Wen, Xiaoming
Wenham, Stuart
Young, Trevor

ECR and Postdoctoral Fellows

Chan, Catherine
Cui, Hongtao
Edwards, Matthew
Evans, Rhett
Feng, Yu
Hameiri, Ziv
Hallam, Brett
Hsiao, Pei-Chieh
Huang, Jialiang
Ishwara, Thilini
Jiang, Yajie
Juhl, Matthias
Kampwerth, Henner
Li, Zhongtian
Liu, Fangyang
Liu, Ziheng
Ma, Fajun
Mahboubi Soufiani, Arman
Mai, Ly
Mehrvarz, Hamid
Patterson, Robert
Payne, David
Pillai, Supriya
Pollard, Michael
Römer, Udo
Song, Ning
Sugianto, Adeline
Telford, Andrew (from Nov 2017)
Wen, Xiaoming
Western, Ned
Wright, Matthew
Yan, Chang
Zhang Tian
Zhang, Meng

PhD Students

Abdullah, Taufiq Mohammad
Allen, Vincent (until Jun 2017)
Amin, Samiul
Bhoopathy, Raghavi
Bing, Jueming
Chan, Kah Howe
Chan, Kai-Yuen Kevin (from Jul 2017)
Chan, Yuan-Chih
Chang, Nathan
Chen, Daniel
Chen, Ran
Chen, Sheng (until Aug 2017)
Chen, Weijian
Chen, Zihan
Chung, Daniel
Colwell, Jack Killian
Concha Ramon, Bruno Gustavo
Cui, Xin
Dai, Xi
Deng, Xiaofan
Disney, Claire (until Aug 2017)
Duan, Leiping (from Jul 2017)
Dumbrell, Robert
Evans, Rhett (until Aug 2017)
Fung, Tsun Hang
Gao, Yijun

Hall, Charles Aram Mandela
Haque, Faiazul
He, Mingrui (from Jul 2017)
Hu, Yicong
Jiang, Yu
Kim, Jincheol
Kim, Kyung Hun (until Aug 2017)
Kim, Moonyong
Kim, Taehyun
Lambert, Daniel
Lau, Cho Fai Jonathan
Lau, Derwin
Lee, Chang-Yeh
Liao, Anqi
Limpert, Steven
Lin, Simao
Liu, Shaoyang
Liu, Xu (until Aug 2017)
Lunardi, Marina Monteiro
Ma, Qingshan (until Aug 2017)
Mahmud, Md Arafat
Noh, Shinyoung
Nomoto, Keita
Park, Jongsung (until Aug 2017)
Phua, Benjamin
Pu, Aobo
Samadi, Aref
Sen, Chandany
Shen, Xiaowei
Shi, Lei
Soeriyadi, Anastasia
Song, Ning
Sun, Heng (from Jul 2017)
Sun, Kaiwen
Tabari-Saadi, Yasaman
Teymouri, Arastoo
Thapa, Bharat
To, Alexander (until Aug 2017)
Upama, Mushfika Baishakhi
Vargas Castrillon,Carlos Andre
Varshney, Utkarshaa
Wang, Bo
Wang, Dian
Wang, Hongfeng
Wang, Pei (until Aug 2017)
Wang, Sisi
Wang, Xi
Xu, Cheng
Xu, Xiaoqi
Yang, Jianfeng (until Aug 2017)
Ye, Qilin
Yi, Chuqi
Yi, Haimang
Yuan, Lin (until Aug 2017)
Yu, Jae Sung
Zafirovska, Iskra
Zeng, Yiyu (until Aug 2017)
Zhang, Qiuyang (until Aug 2017)
Zhang, Yian
Zhang, Yuanfang
Zhang, Zewen (until Aug 2017)
Zhang, Zhilong, (until Aug 2017)
Zhao, Jing
Zhao, Xin
Zhou, Fangzhou
Zhou, Zibo
Zhu, Yan

Masters Students

Chen, Longran
Ding, Lei (until Jun 2017)
Feng, Qingge (from Jun 2017)
Haydous, Zeinab (until Jun 2017)
Ibrahim, Ahmad (until Jun 2017)
Li, Mengchen (until Jun 2017)
Li, Yin (from Jul 2017)
Lu, Xiaosheng (until Jun 2017)
Myint, Ye Win (until Jun 2017)
Sang, Borong (until Jun 2017)
Tan, Xinyan (from Jul 2017)
Uzer, Ugur Can (until Jun 2017)
Wang, Anbang (from Jul 2017)
Wilkinson, Benjamin (until Jun 2017)
Zhang, Chen (from Jul 2017)
Zhang, Chuanjing (until Jun 2017)
Zhang, Xinyi (from Jul 2017)

Honours Students

Hull, Clifford
Neoh, Jia
Tan, Xingru
Tang, Peter
Wang, Anbang
Wang, Kun
Wang, Shaozhou
Zhang, Chen

Australian National University

Academic Staff and Senior Researchers

Blakers, Andrew (Node Leader)
Bi, Qunyu (until 10 Aug1207)
Catchpole, Kylie
Chern Fong, Kean
Cuevas, Andres
Franklin, Evan (until 28 Jul 2017 - Adjunct status)
Macdonald, Daniel
Rougieux, Fiacre

Stocks, Matthew
Thomson, Andrew
Wan, Yimao
Weber, Klaus
White, Tom

ECR and Postdoctoral Fellows
Baerhujin, Qiaoke (aka Barugkin, Chog)
Booker, Katherine
Duong, The
Ernst, Marco
Liu, Anyao
Mulmudi , Hemant Kumar
Nguyen, Hieu
Osorio Mayon, Yahuitl (Azul)
Shen, Heping
Sieu Phang, Pheng
Sio, Hang Cheong
Sun, Chang
Walter, Daniel
Yan, Di

PhD Students
Basnet, Robin
Dolati Ilkhechi, Noushin
Fu, Xiao
Goodarzi, Mohsen
Lu, Bin
Peng, Jun
Wu, Huiting
Wu, Nandi
Wu, Yiliang

CSIRO Manufacturing

Academic Staff and Senior Researchers
Scholes, Fiona (Node Leader)
Wilson, Gerry (Node Leader)
Chantler, Regine
Faulks, Andrew
Gao, Mei
Ramamurthy, Jyothi
Vak, Doojin

ECR and Postdoctoral Fellows
Sears, Kallista (until June 2017)
Weerasinghe, Hasitha

PhD Students
Kim, Juengeun (visiting)
Peng, Xiaojin (visiting, from Sep 2017)
Song, Seyeong (until March 2017)
Tan, Boer (co-supervised with Monash)
Zuo, Chuantian (visiting)

University of Melbourne

Academic Staff and Senior Researchers
Ghiggino, Ken (Node Leader)
Goerigk, Lars
Holmes, Andrew
Jones, David
Smith, Trevor
Wong, Wallace

ECR and Postdoctoral Fellows
Kumar, John
Lai, Yuying
Lu, Shirong
Mitchell, Valerie (from October 2017)
Subbiah, Jegadesian

PhD Students
Banal, James
Belic, Ognjnen
Dkhissi, Yasmina
Farooq, Umer
Gao, Can
Geraghty, Paul
Hong, Quentin
Lee, Calvin
Lovel, Mathew
Masoomi, Saghar
Mitchell, Valerie (until October 2017)
Novakovic, Sacha
Saker-Neto, Nicolau
Saxena, Sonam
Schwarz, Kyra (until October 2017)
Song, Aaron
Zhang, Bolong

Masters Students
Duan, Ruoyu
Fabig, Thomas
Gallant, Ben (visiting, Cambridge University)
Jameel, Mohammed A.
Kartika, Monica
Kroh, Daniel (visiting Bayreuth)
Seow, Jia Yi
Vu, Khuyen
Wang, Hao-Tian
Zhang, Bolong

Monash University

Academic Staff and Senior Researchers
Cheng, Yi-Bing (Node Leader until Sep 2017))
Bach, Udo (Node Leader from Sep 2017)
Simonov, Alexandr

ECR and Postdoctoral Fellows
Fürer, Sebastian
Kashif, Kalim
Li, Feng
Li, Wei
Liu, Chang
Lu, JianFeng
Ruiz Raga, Sonia
Zhang, Jinbao

PhD Students
Bacal, Dorota
Benesperi, Iacopo
DeLuca, Giovanni (exchange from Georgia Tech)
Jiang, Liangcong
Lin, Xiongfeng
Mao, Wenxin
Milhuisen, Rebecca
Pai, Narendra
Rothmann, Mathias
Sepalage, Anuradha
Surmiak, Adam
Tan, Boer (co-supervised with CSIRO)
Xiao, Manda

Honours Students
Paz, Simon
Wang, Yuhe
Zhang, Shuoxuan
Zhang, YuchungGu, Qinying

University of Queensland

Academic Staff and Senior Researchers
Burn, Paul (Node Leader)
Meredith, Paul (Node Leader, until 14 Apr 2017)

ECR and Postdoctoral Fellows
Armin, Ardalan
Donaghey, Jenny (until February 2016)
Fang, Yuan (until April 2016)
Jin, Hui
Raynor, Aaron (from 11 Apr 2017)
Shaw, Paul
Stephen, Meera (from 31 Oct 2017)
Stoltzfus, Dani (until 31 Jan 2017)

PhD Students
Kim, Il Ku (Benjamin) (until January 2016)
Kitchens, Luke (started 9/10/17)
Li, Xin (until October 2016)
Lin, Qianqian (until September 2016)
McGregor, Sarah
Stolterfoht, Martin (until April 2016)
Wang, Xiao (UQ/UESTC)
Yazmaciyan, Aren (until 27 January 2017)
Zhang, Shanshan

QESST
Honsberg, Christiana
Augusto, Andre
Bertoni, Mariana
Bowden, Stuart
Buonassisi, Tonio
Burrell, Anthony
Goodnick, Stephen
Jensen, Mallory
Mitchell, John
Peters, Ian Marius
Fraser, Matthew

National Renewable Energy Laboratory
Friedman, Dan
Geisz, John
Johnston, Steve
Levi, Dean
Osterwald, Carl
Page, Mathew
Reid, Obadiah
Rumbles, Garry
Schnabel, Manuel
Stradins, Paul
Teeter, Glenn
Wilson, Gregory
Woodhouse, Michael
Young, Mathew

Molecular Foundry, Lawrence Berkeley National Laboratories
Chen, Teresa
Javey, Ali
Knapstein, Jessie
Neaton, Jeffrey
Yang, Yang

Stanford University
Dauskardt, Reinhold
McGehee, Mike
Rolston, Nick

Georgia Technology Institute
Kippelen, Bernard
Jradi, Fadi
Marder, Seth
Reichmanis, Elsa
Rohatgi, Ajeet
Samuel, Graham
Upadhyaya, Ajay

Wuxi Suntech Power Co. Ltd.

Chen, Rulong
Zhou, Min

Trina Solar

Verlinden, Pierre

BT Imaging

Bardos, Robert
Trupke, Thorsten

BlueScope Steel

Nolan, David
Zappacosta, Dion

PV Lighthouse

Abbott, Malcolm
McIntosh, Keith

Dyesol/Greatcell

Milliken, Damion
Thompson, Gordon

Raygen

Lasich, John
Mosley, Will

Research Reports

PP1 Silicon Solar Cells

Overview

Silicon solar cells continue to dominate the global solar photovoltaic (PV) market, making up more than 90% of commercially available products. This share is unlikely to change significantly over the next few years. Silicon's dominance in the global PV market can be attributed to its abundance, moderate cost, low toxicity, high and stable cell efficiency, robustness, bankability, highly advanced and widespread knowledge of silicon and extensive and sophisticated supply chains.

The ongoing challenge for the industry is to continue to reduce the cost per watt of power produced from silicon solar cells, through lowering the cost of silicon solar cells, improving the power conversion efficiency of the cells or both. Program Package 1 (PP1) supports the fundamental investigation and demonstration of novel technology leading towards improved cost-effectiveness of silicon-based solar cells. Specifically, research activities are carried out in the areas of low-cost solar- grade silicon, rear contact high efficiency solar cells, and silicon-tandem structures.

PP1.1 Solar-grade silicon

Solar-grade silicon feedstocks offer a low-cost alternative to the standard electronic-grade silicon feedstocks used in the PV industry today. Research into fabricating high efficiency solar cells on low-cost upgraded metallurgical-grade (UMG) silicon wafers is being carried out through a collaboration between ANU (cell fabrication), UNSW (defect hydrogenation) and Apollon Solar (solar-grade silicon supplier). The aim is to demonstrate that the use of less pure solar-grade silicon does not reduce cell efficiency. A key outcome to date has been the world-first demonstration of solar cell efficiencies above 21% for devices made with UMG wafers. A modified fabrication sequence to maintain wafer quality during thermal processing has been developed that is capable of efficiencies above 24% on electronic-grade wafers. Using this process, combined with UNSW's expertise on defect hydrogenation, we aim to demonstrate efficiencies above 23% on UMG wafers in the near term.

PP1.2a Rear contact silicon cells

Rear contact solar cells are the epitome of single junction silicon solar cell design. Formation of metal contacts of both polarities on the rear eliminates the trade-off between front optics to electrical requirements, and allows maximum photon collection from the absence of front optical obstructions. The highest efficiency measured on a rear contact cell fabricated at ANU to date is 24.7%. Since then, significant progress has been made in surface passivation and LPCVD polysilicon passivated contacts, which is expected to demonstrate significantly higher device efficiencies upon implementation to laboratory cells in 2018.

PP1.2b Passivated contacts

The ongoing improvements in both the silicon material and surface passivation quality of silicon solar cells has meant that one of the dominant loss mechanisms in silicon solar cells is now the recombination occurring at the metal/silicon contact interface. To reduce this loss, "passivated contacts" which suppress interface recombination while selectively transporting electrons and holes towards the cell's terminals are being developed. We are developing several types of such contacts, from the synthesis and characterisation of the component layers to the fabrication of proof-of-concept devices. In the high temperature approach, we have further optimised the polysilicon/tunnelling oxide contacts and, in collaboration with PP1.1, achieved a 24.7% solar cell efficiency, which indicates that efficiencies above 25% are within reach. In the low temperature approach, we have achieved a 21.8% n-type cell with partial rear passivating contacts based on TiO_x, Ca and Al. We aim to demonstrate efficiencies in the range of 23% with alternative passivating contact materials and a re-designed device structure.

PP 1.3a Silicon tandem cells (monolithic)

One approach to convert more of the sun's spectrum into electricity is to use multiple solar cells which absorb different wavelengths of light. Work continued in 2017 to develop monolithic silicon tandem cells, tandem cells where a wide bandgap top cell (or cells) is grown onto a silicon cell with the two (or more) cells operating in series. Several different approaches to forming these structures are being explored and are explained in section PP1.3a. Highlights in 2017 included improved understanding of forming abrupt Si/Ge layers, an efficiency of 23.2% for a triple-junction cell consisting of InGaP/GaAs and silicon sub-cells attached via bonding, an efficiency of 22.67% for a CZTS/Si (PERL) tandem solar cell by the spectrum splitting method, and 22% for a two-terminal perovskite/Si solar monolithic tandem device (26.9% when using the same materials in a mechanically stacked four-terminal configuration).

PP1.3b Silicon tandem cells (mechanically stacked)

In a mechanically stacked tandem system, a high bandgap top cell is independently operated in conjunction with a standard silicon bottom cell. Two approaches, involving series or parallel connection of top and bottom cells, enable high annual energy yields under simulation of real weather conditions. Each approach involves scaling the area of the top cell relative to the bottom cell to enable voltage or current matching. This area scaling enables the use of a much wider range of top cell bandgaps with ideal four-terminal efficiencies approached for a broad range of bandgaps. GaAs cells developed in a related ACAP collaboration project are being paired with silicon to demonstrate the potential for efficiencies well above 30%.

PP1.1 Solar Silicon

ANU Team
Prof Daniel Macdonald, Dr Fiacre Rougieux

Partner
Apollon Solar (France)

ANU Students
Peiting Zheng, Chang Sun, Rabin Basnet

Funding Support
ACAP, ARENA, ARC, ANU

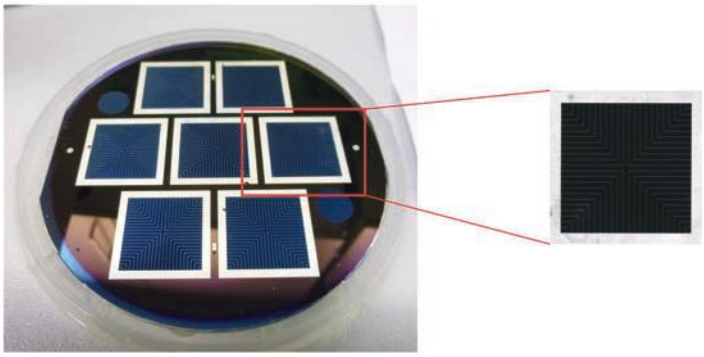

Figure PP1.1.1: 2cm x 2 cm high efficiency PERL cells fabricated at ANU.

Aims

The use of low-cost solar-grade silicon materials is likely to play an important role in achieving further cost reductions for photovoltaic modules. However, to create a compelling case for the industrial application of such solar-grade materials, it is necessary to demonstrate that the resulting cell efficiencies are indistinguishable from those obtained when using standard silicon wafers. In support of this broader objective, the aims for the previous period were: to further develop methods for improving the electronic quality and high temperature tolerance of solar-grade wafers; to develop a new cell process with a selectively doped front surface to allow higher efficiency potential; and to further optimise the deactivation of the boron-oxygen defect in these devices through collaboration with colleagues at UNSW.

Progress

Good progress has been achieved during the reporting period, with the key achievement being a new cell efficiency record of 21.2% (in-house measurement) using n-type Czochralski-grown (Cz) wafers grown from 100% solar-grade silicon, also known as upgraded metallurgical-grade (UMG) silicon, supplied by our industry partner Apollon Solar. This record device was a heterojunction solar cell fabricated at Arizona State University (ASU) on UMG wafers pre-processed at ANU, and supported by a related small ACAP collaboration grant.

The progress across various topics of investigations are as follows:

1. Optimisation of a new selective emitter PERL cell process at ANU for UMG wafers, especially in relation to potential thermal degradation during high temperature oxidation steps required for masking layers. We have made excellent progress in this area. An optimised Passivated Emitter and Rear Locally-diffused (PERL) cell process has been developed which can achieve efficiencies of up to 24.3% (in-house measurement) on electronic-grade wafers. We have also demonstrated that the use of a pre-anneal step, known as a Tabula Rasa, combined with phosphorus gettering, results in carrier lifetimes of up to 5 ms on UMG wafers, and that these lifetimes are stable during subsequent boron diffusion and oxidation steps. This stability arises from the fact that the Tabula Rasa step dissolves in-grown precursor particles that otherwise form recombination-active oxygen precipitates during subsequent processing. Combining these advances, we expect efficiencies on UMG wafers of well above 22% to be achieved during 2018.
2. Incorporation of a SiN firing step in the cell fabrication process and the demonstration of almost complete deactivation of the boron-oxygen defect during subsequent illuminated annealing. This task is on track to be completed in early 2018. Pre-fired UMG wafers were fabricated into heterojunction cells at ASU in late 2017. In collaboration with colleagues at UNSW, these devices are currently being subjected to defect deactivation and degradation tests to demonstrate the ability of charge-state-controlled hydrogenation to completely passivate the boron-oxygen defect in a stable way.
3. Fabrication of solar-grade silicon cells using the above techniques with efficiencies above 21.5%. As described above, we expect to achieve efficiencies above 22% when we apply our new PERL process at ANU to UMG wafers which have been pre-processed with Tabula Rasa and gettering steps. However, this has been delayed somewhat due to unavailability of our thin-film deposition tools at ANU (primarily PECVD SiN) since September 2017. These tools will be available again in March/April 2018.

Highlights

- Fabrication of a 21.2% efficient (in-house measurement) n-type solar-grade silicon heterojunction solar cell at Arizona State University (ASU) on n-type Cz UMG wafers pre-processed at ANU.
- Development of pre-processing steps including a Tabula Rasa anneal and phosphorus gettering, that allow stable lifetimes above 5 ms to be achieved in UMG wafers.
- Development of a high efficiency PERL process at ANU capable of solar cell efficiencies above 24% on electronic-grade wafers.

Future Work

Future work will aim to achieve confirmed solar-grade cell efficiencies of over 22% by March 2019, by applying our new PERL cell process to UMG wafers which have been pre-treated with Tabula Rasa and phosphorus gettering steps. In collaboration with UNSW, ANU aims to demonstrate the ability of charge-state-controlled hydrogenation to eliminate the degradation associated with the boron-oxygen defect in compensated UMG n-type silicon wafers.

References

Zheng, P., Rougieux, F.E., Zhang, X., Degoulange, J., Einhaus, R., Rivat P. and Macdonald, D., 2017, “21.1% UMG silicon solar cells”, IEEE Journal of Photovoltaics 7(1), 58–61.

Sun, C., Nguyen, H.Y., Rougieux F.E. and Macdonald, D., 2017, "Activation kinetics of the boron-oxygen defect in compensated n- and p-type silicon studied by high-injection micro-photoluminescence", IEEE Journal of Photovoltaics 7(4), 988–995.

Shen, D., Sun, C., Zheng, P., Macdonald, D. and Rougieux, F., 2017, "Carrier induced degradation in compensated n-type solar cells: Impact of temperature, light-intensity and forward bias voltage on the reaction kinetics", Japanese Journal of Applied Physics, 56 (8), 08MB23.

Basnet, R., Rougieux, F.E., Nguyen, H.T. and Macdonald, D., 2017, "Investigating relationship between local oxygen precipitates and their recombination activities in n-type Cz silicon", 27th International Photovoltaic Science and Engineering Conference, Kyoto, Japan, 12–17 November 2017.

Basnet, R., Rougieux, F.E., Nguyen, H.T. and Macdonald, D., "Investigating relationship between local oxygen precipitates and their recombination activities in n-type Cz silicon", 4th Asia-Pacific Solar Research Conference, Melbourne, 5–7 December 2017.

PP1.2a Rear Contact Silicon Cells

ANU Team
Prof Andrew Blakers, Dr Evan Franklin, Dr Matthew Stocks, Dr Kean Chern Fong, Dr WenSheng Liang, Dr Marco Ernst, Dr Daniel Walter, Dr Teck Kong Chong

Industry Partner
PV Lighthouse: Dr Keith McIntosh

ANU Students
Teng Choon Kho

Funding Support
ACAP, ARENA, ANU

Aims

The objectives of this project are twofold: to develop very high efficiency laboratory-based silicon solar cells; and, in parallel, to develop cell fabrication techniques and processes compatible with industrially feasible low-cost implementation of interdigitated back contact (IBC) solar cells. IBC cells, by their very nature, are both inherently capable of very high efficiencies owing to superior optics compared to conventional cell architectures and owing to an improved ability to tailor fabrication processes to meet specific goals of cell features. However, such cells are also characterised by more complex and expensive fabrication processes. The target for the end of the program is to fabricate cells using any techniques with efficiencies of 26% or above, and in parallel to produce cells using industrially applicable techniques, and by doing so meeting an informal or internal efficiency target of 24% or above.

Progress

The highest efficiency ANU IBC solar cell to date is measured to be 24.7%. Significant progress in the crucial areas of surface passivation and passivated contacts for rear contact solar cells have been achieved since then, and is expected to provide further efficiency improvements once incorporated into device fabrication.

Polysilicon passivated contact rear contact cells were planned for 2017, but progress was halted due to unavailability of silane in the laboratory. The laboratory has undergone an independent audit and is performing the necessary safety upgrades in order to have silane reconnected. This is expected to be completed by early Q2 2018.

ONO Passivation

Further optimisation to the front Oxide-Nitride-Oxide (ONO) surface passivation currently yields measured lifetimes exceeding established Auger limits for a large range of wafer resistivities, and achieves a record 170 ms on 100 Ωcm n-type wafers. Figure PP1.2a.1 presents the measured maximum effective lifetimes as compared to other results in literature, as well as the measured effective lifetime as compared to the Auger lifetime mode of Richter et al. Excellent surface passivation is also achieved on boron and phosphorus diffused surfaces, where J_0 of 1 fAcm^{-2} is achieved on a lightly diffused 520 Ω/sq phosphorus surface, and J_0 of approximately 20 fAcm^{-2} is achieved on a light boron diffused surface.

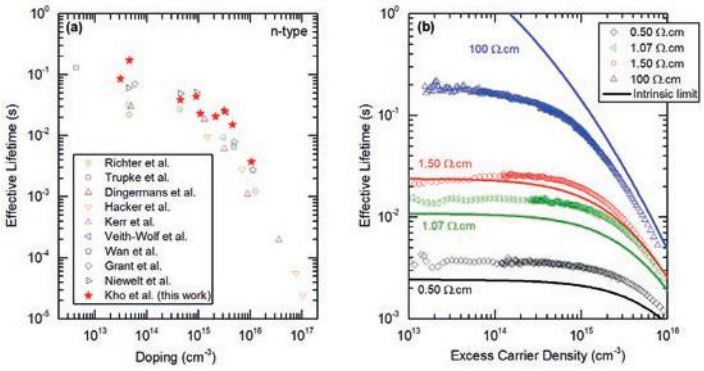

Figure PP1.2a.1: (a) Maximum lifetime as a function of dopant concentration measured at 300 K on n-type silicon together with literature data; and (b) ONO passivation with a range of n-type silicon resistivity in comparison to parameterised Richter Auger including radiative recombination (lines).

LPCVD Passivated Contacts

ANU has achieved significant advancement in this area, attaining very low surface recombination and low contact resistivity, enabling its application to IBC solar cells without the need for carefully tuned trade-off in the electrical characteristics. The novelty of this work lies in the use of low-pressure thermal oxidation to provide precise control of the growth conditions for the interfacial oxide. Furthermore, the oxidation is performed in situ to the polysilicon deposition, where the oxide is not exposed to the atmosphere prior to being capped with polysilicon, allowing fine control of ultra-thin (<1 nm) oxide layers with high repeatability.

A summary of data of measured ρ_c and J_0 is presented in Figure PP1.2.a.2, with the dotted line indicating samples where the oxidation temperature is varied. Excellent surface passivation with J_0 below 3 fAcm^{-2} and low ρ_c below 1 mΩcm^2 is achieved simultaneously, representing among the lowest values measured in combination.

Highlights

- Improved ONO passivation exceeds Auger lifetimes, achieving 170 ms on 100 Ω-cm n-type wafers.
- n^+ LPCVD polysilicon passivated contacts achieves J_0 < 3 fAcm^{-2} and contact resistivities ρ_c < 1 mΩcm^2.

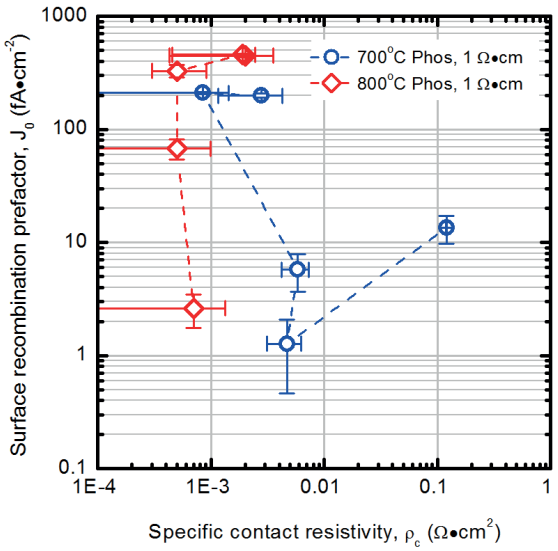

Figure PP1.2a.2: Summary of measured J_0 and ρ_c for n^+ LPCVD polysilicon of various phosphorus diffusion and oxidation temperature.

Future Work

Continual optimisation using small local contact openings is demonstrating diminishing returns due to high sensitivity to bulk lifetimes and current crowding effects, which are exacerbated by the complex fabrication procedures. Over the next 12 months, we envisage a significant shift in device design to incorporate LPCVD polysilicon passivated contacts in the device fabrication. This is expected to take place starting the second quarter of 2018.

Further development of p^+ LPCVD polysilicon is planned, along with development of compatible masking dielectrics to enable n^+ and p^+ doping on the same side as is necessary for rear contact cells.

PP1.2b Passivated Contacts

ANU Team
Prof Andres Cuevas, Dr Di Yan, Dr Yimao Wan, Dr Thomas Allen, Mr Christian Samundsett

Academic Partners
University of California Berkeley: Dr James Bullock
EPFL

Funding Support
ACAP, ARENA, ARC, ANU

Aims

Crystalline silicon (c-Si) solar cells keep getting cheaper and better. Today's record solar cells use "passivated contacts" to selectively transport electrons and holes towards the cells' terminals. There is a strong motivation for bringing such passivated contacts to the broader PV industry, and this small project, with synergistic support from other sources of funding, aims to do that. ANU, together with collaborators at University of California at Berkeley and EPFL in Switzerland, is following a two-pronged approach at developing novel silicon solar cells that incorporate passivated contacts. Part of our work is on the well-proven high temperature approach of depositing a silicon film onto an ultrathin dielectric layer (or layers), so that quantum-mechanical tunnelling can take place. We also pursue a low temperature approach, based on depositing materials that have either a very high or a very low work function, which makes them selective to the transport of holes or electrons, respectively.

Progress

Progress in the low temperature approach during 2017 has lifted the conversion efficiency of n-type cells with localised rear passivated contacts from 20.3% to 21.8%. Progress in the high temperature approach has surpassed our own expectations, from 21.1% last year to 24.7%. This represents the highest independently confirmed silicon solar cell result achieved at ANU laboratories.

Collaboration with University of California at Berkeley and EPFL in Neuchatel has continued, and significant progress has been made by improving the stability of some dopant-less passivated contacts. A separate report (see Section 6.9 of this report) describes additional achievements of that collaborative work. Additional collaboration with UNSW (Drs Allen and Hameiri) focused on the early stages of development of novel characterisation techniques for passivating contacts.

n-type silicon solar cells with partial rear contacts based on calcium and titanium oxide

Building on the work reported last year, we have improved electron-selective contacts based on calcium. Low resistivity passivated contacts have been developed that combine reduced titania (TiO_x) for interface passivation and the low work function metal calcium (Ca) for electron selection. By using Ca as the overlying metal in the contact structure we are able to achieve a reduction in the contact resistivity of TiO_x passivated contacts of up to two orders of magnitude compared to previously reported data on Al/ TiO_x contacts, allowing for the application of the Ca/ TiO_x contact to n-type c-Si solar cells with partial rear contacts. Implementing this contact structure on the cell level results in a power conversion efficiency of 21.8% where the Ca/ TiO_x contact comprises only ≈6% of the rear surface of the solar cell, an increase of 1.5% absolute compared to a similar device fabricated without the TiO_x interlayer.

24.7% efficient silicon solar cells incorporating an industrially compatible n^+ polySi/SiO_x electron-selective passivated rear contact

An overlap of equipment and techniques facilitates the adoption of new technologies by the industry. Passivating contacts based on silicon films deposited onto a thin SiO_x layer combine high performance with a degree of compatibility with industrial metallisation steps. We have developed an approach to form n^+ polySi/SiO_x electron-selective contacts that maximises the overlap with common industrial equipment. It is based on depositing an intrinsic amorphous silicon layer by PECVD and then doping and recrystallising it by means of thermal phosphorus diffusion from $POCl_3$. By optimising the a-Si thickness and the phosphorus diffusion temperature very low recombination current densities $J_{0c} \approx 3$ fAcm^{-2} and contact resistivities $\rho_c \approx 3$ mΩcm^2 have been achieved. The application of these optimised electron-selective contacts to n-type silicon solar cells has permitted Dr Di Yan in collaboration with Dr Pheng Phang (see Section 1.1 of this report) to achieve a conversion efficiency of 24.7%. This result, independently confirmed, is among the highest reported worldwide for solar cells with a polysilicon passivating contact.

Highlights

- 24.7% efficient silicon solar cell with a rear full-area SiO_x/polysilicon passivated contact.
- 21.8% efficient n-type silicon solar cells with partial-area rear contacts based on TiO_x and Ca.

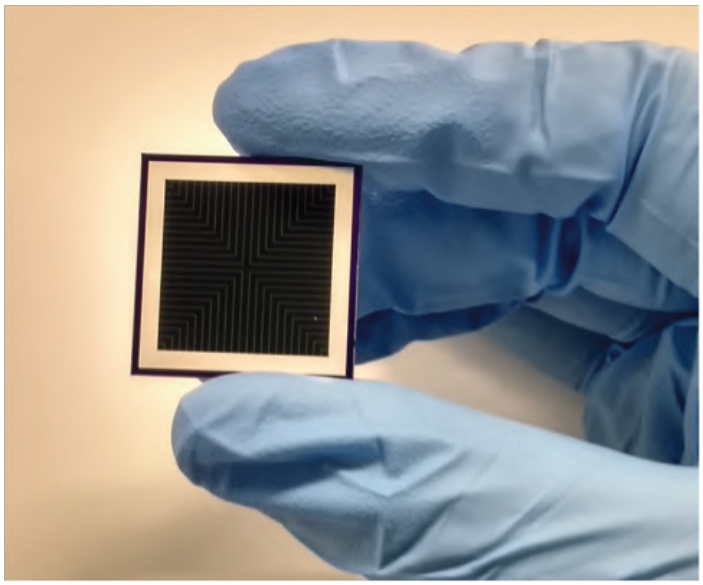

Figure PP1.2b.1. Photograph of a 4cm^2 n-type silicon solar cell fabricated at ANU with a double boron diffusion at the front and a phosphorus diffused polySi/SiO_x full-area rear passivated contact.

Future Work

Five years after the beginning of this project, the development of passivated contact technologies has become one of the most active areas of research in silicon PV. This is exemplified by the fact that it is the largest area (27% of accepted papers) at the 2018 SiliconPV conference. Our five-year-old vision for advancing silicon solar cell technology is now widely supported by the international research community. We will continue working on both the low and high temperature approaches, supported by strong collaboration links with University of California Berkeley, EPFL, KAUST and UNSW. During 2018 we will aim to increase further the conversion efficiency of solar cells based on low temperature passivating contacts, as well as to improve their thermal stability. Instead of Ca, which is difficult to work with, we will focus on other low work function materials, such as LiF_x, to implement the contacts. We will fabricate solar cells with passivating contacts based on LiF_x, combined with TiO_x or a-Si:H, either in a partial or full area configuration. On the high temperature front, a priority will be to newly optimise boron-doped polysilicon contacts and develop proof-of-concept devices on p-type silicon wafers.

References

Allen, T.G., Bullock, J., Jeangros, Q., Samundsett, C., Wan, Y., Cui, J., Hessler-Wyser, A., De Wolf, S., Javey, A. and Cuevas, A., 2017, “A Low Resistance Calcium/Reduced Titania Passivated Contact for High Efficiency Crystalline Silicon Solar Cells”, Adv. Energy Mater., 7.

Yan, D., Phang, S.P., Cuevas, A., Wan, Y., Liu, A., Macdonald, D. and Bullock, J., 2017, accepted for oral presentation at SiliconPV 2018.

Yan, D. and Cuevas, A., 2017, “Solar cell fabrication”, Australian provisional patent application No:2016905022, priority date 6 December 2016.

PP1.3a Silicon Tandem Cells (Monolithic)

III-V Cells on Silicon Using Atomically Abrupt Si/Ge Transition

Program Package 1.3a aims, for the first time, to successfully mate the commercially dominant PV technology based on silicon solar cells with other promising PV materials, including the III-V semiconductors, the chalcogenides and perovskite technologies.

A major challenge for monolithic silicon tandem cells is addressing the crystal lattice mismatch between the top cell and the silicon bottom cell. Of the Group III-V materials of interest, only GaP offers a good lattice match to silicon, with the other III-V semiconductors as used in high performance III-V cells having about 4% mismatch, being better matched to Ge. We previously reported on the progress of a project that used the approach of growing a series of SiGe buffer layers in order to change the lattice constant from that of Si to Ge after the growth of a micron or more of buffer material. This project ceased in early 2017 with the departure of key personnel.

Work continued on several other approaches to building high quality tandem cells using III-V materials on silicon wafers. An atomically abrupt Si/Ge transition is being investigated, where the lattice mismatch is taken up in a single atomic layer, which is thermodynamically feasible since it is a low energy configuration. UNSW has filed patent applications on approaches that have given promising results of this type. This would allow the Ge layer to be very thin, creating negligible absorption loss or, alternatively, thick enough to be used as an active cell in a novel “out-of-sequence tandem”. Another method under investigation for creating III-V/Si tandem cells takes the approach of using Pd nanoparticles for bonding a triple-junction InGaP/GaAs cell to a crystalline Si cell. The aim is to demonstrate multi-junction III-V/Si tandem without epitaxial growth on a crystalline Si template while achieving high performance. The use of bonding allows two-terminal configuration to still be achieved without the additional wiring that would otherwise be required to interconnect a mechanically stacked four-terminal tandem.

Chalcogenides are also being investigated as an alternative to III-V materials for the upper cells in the tandem stack. Although the established chalcogenide cell materials (copper indium gallium selenide (CIGS) and CdTe) have shown high efficiency potential, they are not lattice-matched to silicon and have problems for long-term use arising from the use of toxic and/or scarce materials. More promising for the long term are devices made from materials based on the CZTS (CuZnSnS) system. Despite the relatively small effort so far devoted to the development of this material, solar cells using it have already demonstrated energy conversion efficiency above 12%. Moreover, the lattice constant of CZTS and that of related alloys is a close match to silicon and the CZTS bandgap, at circa 1.5 eV, and is almost ideal for the lower cell in a two-cell stack on silicon. Moreover, alloying with related compounds to replace, for example, Zn or Sn with lighter elements, such as Fe(ii) or Si, will increase the bandgap making values such as the 1.7 eV required for a one-cell stack or the circa 2 eV required for the top cell in a two-cell stack on silicon also accessible in a highly compatible materials system.

Lastly, metal halide perovskite materials that do not require lattice matching to silicon for good cell performance are being investigated for top cells. The details for all of these monolithic silicon tandem projects are given below.

UNSW Team

Dr Anita Ho-Baillie, Dr Ziheng Liu, Dr Xiaojing Hao, Prof Martin Green, Prof Gavin Conibeer, Dr Stephen Bremner, Dr Hamid Mehrvarz

Partners

Korea Advanced Nano Fab Center (KANFC)
Institute of Nuclear Energy Research (INER), Taiwan
Tianjin Institute of Power Sources (TIPS), China
Applied Physics Division, National Institute of Standards and Technology (NIST), USA
Helmholtz-Zentrum Berlin (HZB), Germany
Shinshin
Epistar

UNSW Students

Shinyoung Noh, Chuqi Yi

Funding Support

ACAP, ARENA, ARC

Aims

This project aims to build low-cost high efficiency Si/III-V tandem cells by using the sputtered heteroepitaxial Ge/Si. The high quality sputtered heteroepitaxial Ge/Si will be used as a virtual Ge substrate or interconnecting layer for integrating Si wafers with overlying III-V solar cells. For the latter, an atomically abrupt Si/Ge transition is used, where the lattice mismatch is taken up in a single atomic layer, which is thermodynamically feasible since it is a low energy configuration.

Progress

Good progress has been made on the novel methods developed in this project for reducing defects in the Virtual Ge. The methods are (i) laser annealing and (ii) aluminium-assisted crystallisation of Ge on Si.

It has been previously demonstrated that threading discolouration density (TDD) in magnetron-sputter-deposited Ge on Si can be effectively reduced by laser annealing to a range of 106 to 107 cm^2 in a large area. By laser scanning the sample, the Ge layer is melted and recrystallised laterally following the laser beam at a high speed. Due to the lateral regrowth, Ge acts as the crystallisation seed instead of Si. This changes the mechanism from Ge/Si heteroepitaxy to Ge/Ge homo-epitaxy. In addition, the high recrystallisation speed might result in the vacancies' super-saturation which could induce the dislocations climbing and moving to the lateral surface. As a result, Ge films with low TDD are obtained after diode laser annealing. However, the melting and regrowth process is also accompanied by the overheating issue which can induce the line pattern on Ge surfaces and the diffusion of Si into Ge which pose challenges to the subsequent growth of group III-V materials and their quality.

The surface pattern observed could be due to the Si and Ge inter-diffusion induced by local overheating during laser annealing. To demonstrate this, an Si on Insulator (SOI) substrate with limited supply of Si is used for an experiment which involves the laser annealing of a 100 nm Ge grown on an SOI (4 nm of SOI) substrate resulting in a structure: Ge/Si/Insulator/Si substrate). Raman spectra were taken on Ge on an SOI annealed by laser at different energy intensities. Results are shown in Figure PP1.3a.1. As the laser dose increases, the Si content in the top layer increases and then saturates indicating complete melting of the Ge and thin Si layers.

Transmission electronic microscopy (TEM) and energy-dispersive X-ray spectroscopy (EDS) were performed on the same sample before and after laser annealing at 130 J/cm^{-2}. Results are shown in Figure PP1.3a.2. It can be seen that defects in the now SiGe layer are greatly reduced after laser annealing without any change in surface roughness after laser annealing. Only a very small amount of Si is present in the SiGe layer and is distributed uniformly due to the limited amount of Si available from SOI.

To investigate whether inserting an SiO_2 layer between the grown Ge and the Si substrate is effective in minimising Si-Ge inter-diffusion thereby minimising the surface roughening that causes the surface pattern, test structures consisting of Ge/SiO_2/Si substrates were fabricated. SiO_2 layers with different thicknesses from 0.5 to 3 nm were trialled. Unfortunately, the Ge layer on the SiO_2 fails to remain intact.

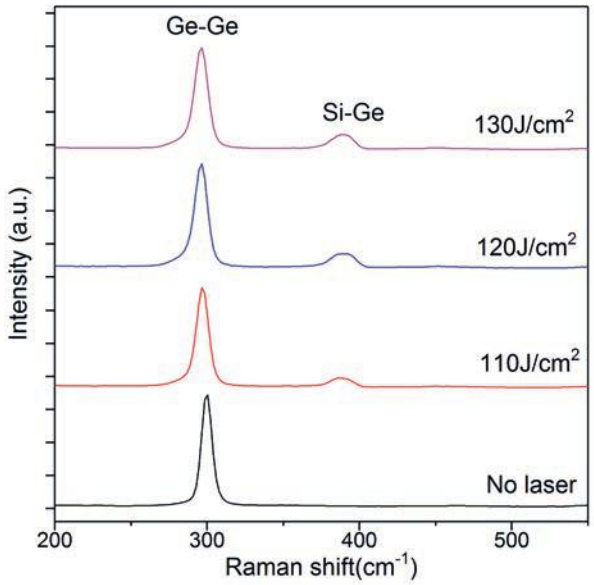

Figure PP1.3a.1: Raman spectra of 100 nm Ge on 4 nm SOI sample before and after laser treatments at 110 J cm^{-2}, 120 J cm^{-2}, and 130 J cm^{-2}.

Therefore Al_2O_3 is considered instead, which has an advantage of maintaining the epitaxy growth of Ge. Test structures using sapphire (Al_2O_3) substrates were first used to study the property of the Ge epitaxy and the effect of laser annealing. Figure PP1.3a.3 shows the XRD patterns for as-deposited Ge on sapphire at different temperatures. Regardless of substrate temperature, the Ge as-deposited film is largely single crystalline but has some parts that are polycrystalline. Laser annealing was employed to improve the crystalline quality of the Ge films. The XRD patterns in Figure PP1.3a.4 show that the polycrystalline portion is completely removed, and the Ge peak becomes much stronger as the twin defect density is significantly reduced after laser annealing. Future work that flows on from this will be the development of Ge/Al_2O_3/Si structure.

Another approach to minimise the surface pattern is capping layer engineering (SiO_2/Ge/Si structure) which has been reported previously. It has been found that when the thickness of the SiO_2 capping layer increases from 150 nm to 450 nm, the height of the surface line pattern is significantly reduced from 50 nm to 10 nm. In 2017, the effect of doping of the capping layer on the surface roughness was investigated. Ge doping of the SiO_2 layer is achieved by co-sputtering alternating SiO_2 with an ultrathin Ge layer (1 nm). This has been shown (see Figure PP1.3a.5) to be very effective in suppressing surface roughening and hence the formation of surface pattern when compared to the use of an undoped SiO_2 capping layer alone.

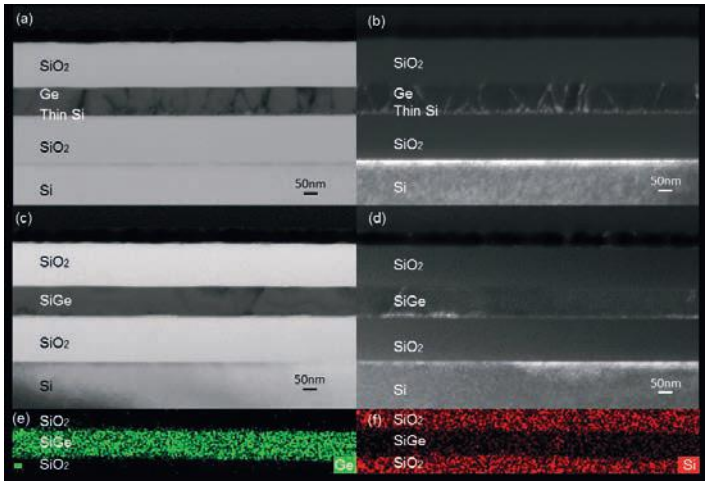

Figure PP1.3a.2: TEM and EDS of the cross-sectional structures of the 100 nm Ge on 4 nm SOI sample before and after laser treatment at 130 Jcm^{-2}: (a) bright-field and (b) dark-field TEM images of the sample before laser treatment; (c) bright-field and (d) dark-field TEM images of the sample after laser treatment; EDS mapping of (e) Ge and (f) Si of the sample after laser treatment.

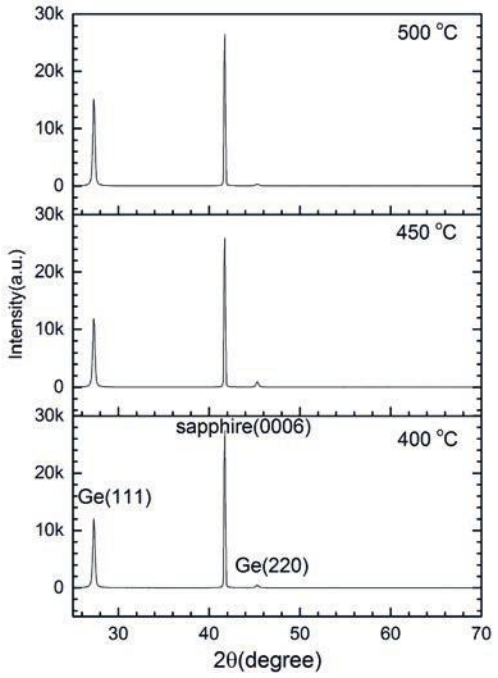

Figure PP1.3a.3: XRD 2θ-Ω profiles of the Ge on sapphire samples deposited at 400˚C, 450˚C and 500˚C.

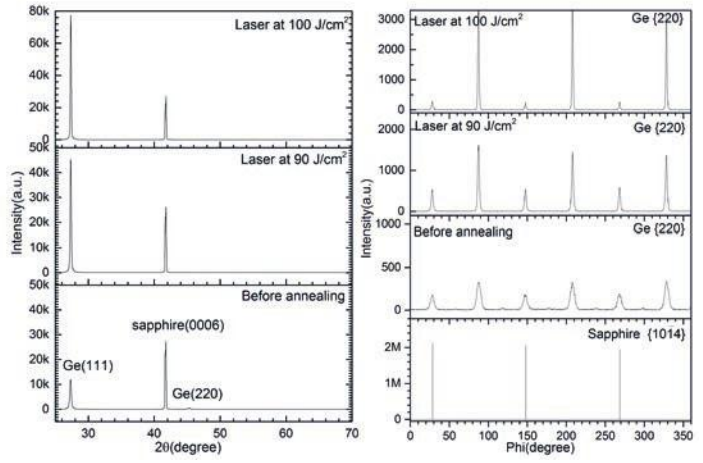

Figure PP1.3a.4: XRD results of (a) 2θ-Ω profiles of the 400˚C deposited Ge samples before annealing, after laser annealing at 90 J cm^{-2} and 100 J cm^{-2}; and (b) Φ scan patterns of sapphire {104} and Ge {220} before and after laser annealing.

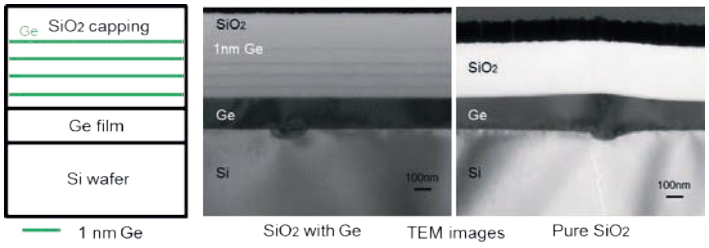

Figure PP1.3a.5: (a) Schematic diagram of the SiO_2 capping layer with Ge doping. Cross-sectional TEM images of the (b) Ge samples with the Ge-doped SiO_2 capping layer; and (c) pure SiO_2 capping layer after laser annealing.

Previously, aluminium-assisted crystallisation has also been investigated for Ge epitaxial growth on Si because the temperature required for Ge crystallisation is reduced with the presence of aluminium (Al). This is because the covalent bonds of the Ge and Si are weakened when in contact with Al. As a result of the bond weakening, these Si and Ge atoms have relatively high mobility and tend to lower the Gibbs energy of the system by crystallising at sites of low energy. The higher mobility of the Ge atoms may help to eliminate the growth of dislocations and improve the Ge film quality.

In 2017, the effects of Al layer thickness on one-step aluminium-assisted crystallisation of Ge on Si were investigated to better understand the Ge growth mechanism. With increasing Al thickness, sharper Ge peaks are observed in both the XRD and Raman measurements (see Figure PP1.3a.6) revealing improved Ge quality. The cross-sectional TEM images in Figure PP1.3a.7 show that the Ge layer is more continuous when the Al to Ge thickness ratio is lower. This is different from that reported in the conventional two-step aluminium-induced crystallisation (AIC) process which could be attributed to the different crystallisation mechanisms. The different stages of the Ge growth are investigated by TEM measurements shown in Figure PP1.3a.8. The results suggest that the Ge growth in one-step aluminium-assisted crystallisation can be divided into two stages: (i) a predominantly vertical growth until the Ge reaches the Al surface followed by (ii) a predominantly lateral growth with a slow vertical growth rate in order to form a continuous film. The results suggest that surplus Ge is required to obtain continuous Ge layers in one-step aluminium-assisted crystallisation.

The combined process of aluminium-assisted crystallisation and laser annealing was also investigated to capitalise on the advantages from both processes. Our previous in situ XRD study on the effect of annealing time in aluminium-assisted crystallisation revealed that the Si content of the epitaxial film keeps increasing with time throughout the process. This increase is rapid during the initial layer exchange but is gradual during the diffusion into Si substrate. These results suggest that the Si content can be minimised by reducing the annealing time through the employment of laser annealing. The exposure time for our laser process is only milliseconds which is much shorter than the minutes of annealing in the furnace annealing. As shown in Figure PP1.3a.9, pure Ge peak is achieved by using laser annealing in the aluminium-assisted crystallisation. Further optimisation of the laser conditions and Ge/Al layer thicknesses will be conducted.

Highlights

- Developed understanding of the laser-induced recrystallisation.
- Developed understanding of the surface roughening caused by the laser annealing process.

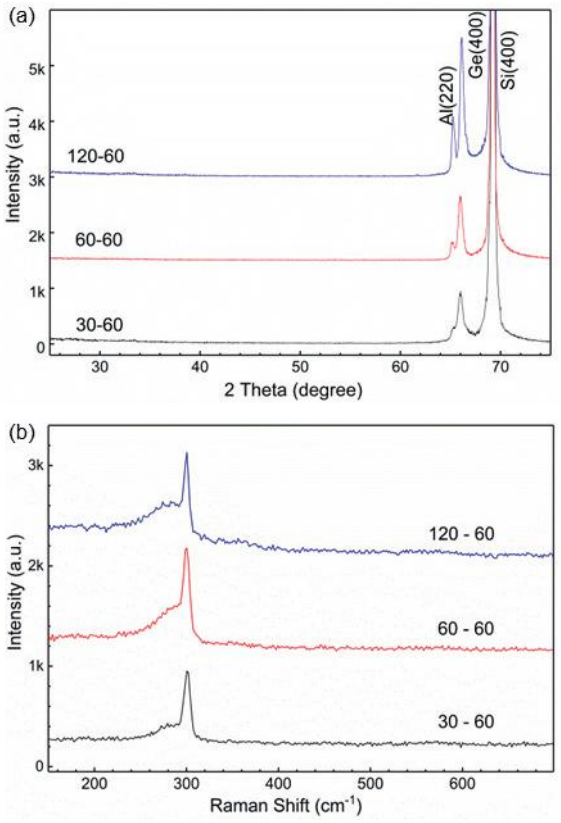

Figure PP1.3a.6: (a) XRD 2theta diffraction patterns; and (b) Raman spectra of samples 30-60; 60-60 and 120-60 (Al thickness-Ge thickness, nm).

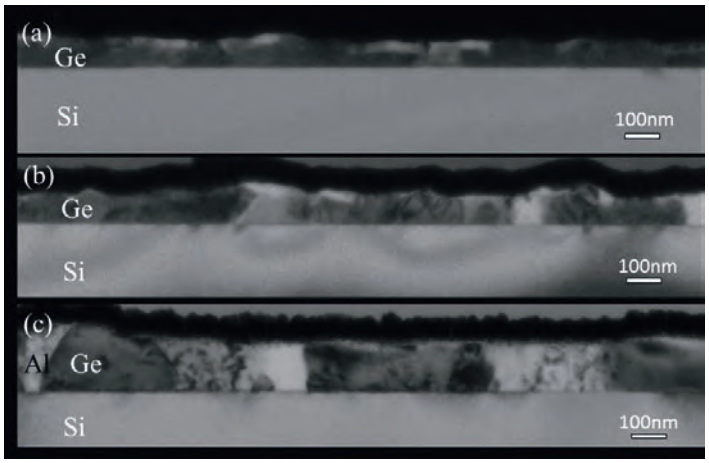

Figure PP1.3a.7: Cross-sectional TEM images of samples (a) 30-60; (b) 60-60; and (c) 120-60.

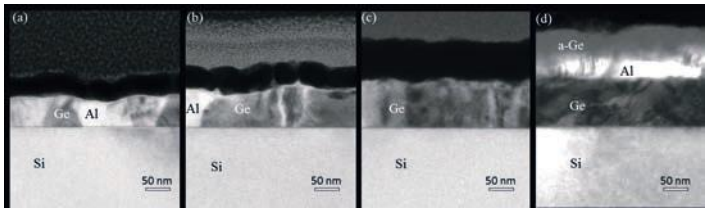

Figure PP1.3a.8: Cross-sectional TEM images of samples (a) 60-5; (b) 60-15; (c) 60-60; and (d) 60-150.

- Devised strategies for reducing surface roughening and Si diffusion into the Ge layer caused by the laser annealing process.
- Developed Ge-doped capping layer to reduce surface roughening during laser annealing process.
- Developed understanding of the mechanism of Ge epitaxial growth on Si by one-step aluminium-assisted crystallisation.

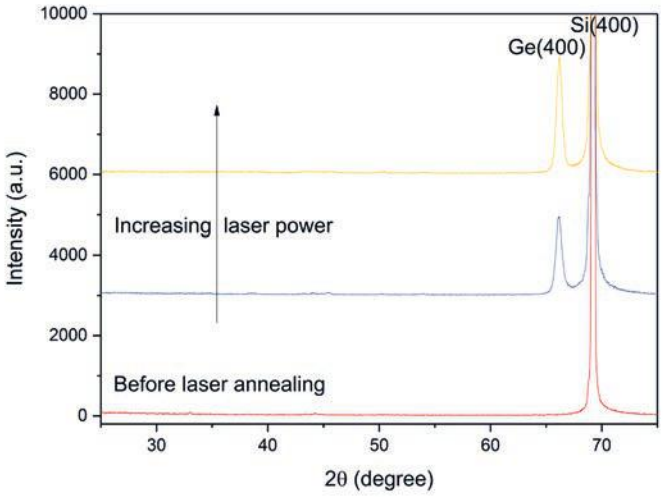

Figure PP1.3a.9: XRD 2theta diffraction patterns of the Ge/Al/Si sample before and after laser annealing with different doses.

Future Work

The aim of future work is to improve the laser annealing process and the structure of capping layer to reduce surface roughening and Si diffusion into the Ge layer caused by the laser annealing process. The optimisation of capping layer dopant amount, position and ratio will be investigated.

Other future work may include the further optimisation of the laser conditions and Ge/Al layer thicknesses of the aluminium-assisted crystallisation by laser annealing

References

Liu, Z., Hao, X., Ho-Baillie, A. and Green, M.A., 2017, "Effects of Al thickness in one-step aluminium-assisted crystallization of Ge epitaxy on Si by magnetron sputtering", Materials Letters, 209, 32–35.

Liu, Z., Hao, X., Ho-Baillie, A., Varlamov, S. and Green, M.A., 2017, "Diode laser annealing of epitaxy Ge on sapphire (0001) grown by magnetron sputtering", Materials Letters, 208, 35–38.

Liu, Z., Hao, X., Ho-Baillie, A. and Green, M.A., 2017, "Epitaxial growth of Ge on Si at low temperatures for III-V tandem solar cells", Asia-Pacific Solar Research Conference, December 2017, Melbourne, Australia (Oral).

Liu, Z., Hao, X., Ho-Baillie, A., Huang, J., Noh, S., Varlamov, S. and Green, M.A., 2017, "Defect density reduction in Ge hetero-epitaxy by diode laser treatment, towards a cost-effective substrate for high efficiency III-V solar cells", China Photovoltaic Technology International Conference (CPTIC) 2017, March 2017, Xi'an, China (Oral).

Non-Epitaxial Tandem Cells on Si – Two Terminal III-V/Silicon Tandem via Bonding

Team

UNSW: A/Prof Anita Ho-Baillie, Mr Chuqi Yi, A/Prof Stephen Bremner, Dr Hamid Mehrvarz, Prof Martin Green

Partner

National Institute of Advanced Industrial Science and Technology (AIST), Japan: Dr Hidenori Mizuno, Dr Toshimitsu Mochizuki, Dr Hidetaka Takato, Dr Kikuo Makita, Dr Takeshi Tayagaki, Dr Takeyoshi Sugaya

Funding Support

ARENA, New Energy and Industrial Technology Development Organization (NEDO) under Ministry of Economy, Trade and Industry (METI), Japan

Aim

The aim is to demonstrate multi-junction III-V/Si tandem without epitaxial growth on a crystalline Si template while achieving high performance. The use of bonding allows two-terminal configuration to still be achieved avoiding the additional interconnection required in a mechanically stacked tandem that requires a four-terminal configuration.

Last year, we demonstrated a 23.2% triple-junction tandem consisting of InGaP/GaAs cells by AIST on UNSW's crystalline Si sub-cell using the "Smart Stack" approach developed by AIST. The advantages of the choice of a Si sub-cell include abundance, low cost, non-toxicity, proven technology and ideal bandgap as a bottom cell in a multi-junction tandem. This year, we aim to boost the conversion efficiency by improving the current matching between the multi-junctions. This is achieved by reducing front surface reflection and light trapping in Si cells through the application of a front surface textured cover on the planar multi-junction cells.

Details for the fabrication of UNSW's PERL Si cell, AIST's InGaP/GaAs cell via epitaxial lift-off (ELO) and the Pd nanoparticle (NP) bonding can be found in last year's report and in the references. Figure PP1.3a.10(a) shows a typical scanning electron microscopy (SEM) image of such a Pd NP array on the Si bottom cell. The InGaP/GaAs/Si stacked cell structure (cross-section) and photo of the smart stack cell are shown in Figure PP1.3a.10(b) and (c) respectively.

The energy conversion efficiency of the device under AM1.5G solar spectrum illumination was 23.2% with a short-circuit current density (J_{SC}) of 10.46 mAcm^{-2}, open-circuit voltage (V_{OC}) of 2.81 V and a fill factor of 0.79.

J_{SC} calculated from the EQE spectra (see Figure PP1.3a.11) of the smart stack cell were 11.1, 10.5 and 9.2 mAcm^{-2}, respectively for the InGaP, GaAs and Si sub-cells, suggesting that the overall performance of the smart stack cell is mainly limited by the Si bottom cell due to optical loss from high reflection from a planar device and lack of light trapping in the bottom cell.

This year, we fabricated polydimethylsiloxane (PDMS) layers with different textured features (Figure PP1.3a.12) using Si wafers as moulds. The Si wafers used have random upright pyramids that range from 2 to 4 μm in size, slightly larger upright pyramids (8-10 μm) and regular inverted pyramids (10 um), for surface texturing.

These PDMS layers are then applied onto a test cell which has a slightly higher series resistance. Figure PP1.3a.13 shows the reflectance (R%) measure for this cell before and after applying PDMS layers with geometries replicated from silicon wafers

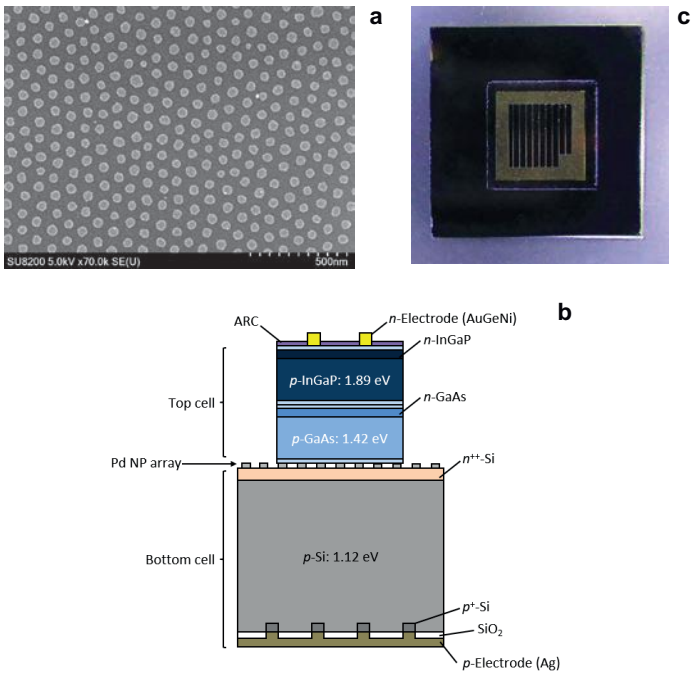

Figure PP1.3a.10 (a) SEM image of the Pd NP array formed on the front side of the Si bottom cell; (b) schematic cross-section of the InGaP/GaAs/Si smart stack cell; and (c) photo of InGaP/GaAs/Si smart stack cell.

textured with random small pyramids (2 to 4 μm), larger random pyramids (8 to 10 μm) and regular inverted pyramids (8 to 10 μm). It can be seen that the humps observed in the R% of the planar cells have been reduced. This is because the surface texturing has altered the optical path length inside the cell thus alleviating the interference caused by the presence of an air-gap that is not avoided between the nanoparticle bonding. In addition, it is found that the PDMS with random large pyramids (8 to 10um) is most effective in reducing surface reflectance followed by PDMS with regular pyramids (10 um) and lastly the small regular pyramids (2 to 4 um). This is because as the texture size of the mould gets small, the limitation of the PDMS fabrication process results in artefacts in the surface texture (see Figure PP1.3a.12(a)) making it less effective. When the pyramid sizes are comparable (~10 um), random textures perform better than regular textures and hence the results observed. For all samples, we can see that light trapping of light at long wavelength in the Si cell has been highly effective due to the reduction of R% for all cells after the application of PDMS at wavelength > 1150 nm.

Figure PP1.3a.14 and Table 1 show the light IV data for a test before and after applying PDMS with random small pyramids (2 to 4 μm); with larger random pyramids (8 to 10 μm); and with regular pyramids (8 to 10 μm). We can see that the application of the PDMS is highly effective in boosting J_{SC} by 3% to 10% which results in a boost in V_{OC} by 1%. The efficiency boosts are 5%, 8% and 11% respectively when textured PDMS with random small pyramids (2 to 4 μm); larger random pyramids (8 to 10 μm); and large regular pyramids (8 to 10 μm) are applied. It is anticipated that when a better test cell is used without the high series resistance, the cell efficiency can be boosted from 23.2% to 25.8%

Highlights

- A triple-junction cell consisting of InGaP/GaAs and crystalline Si sub-cells based on AIST's smart stack approach is demonstrated achieving an energy conversion efficiency of 23.2%.

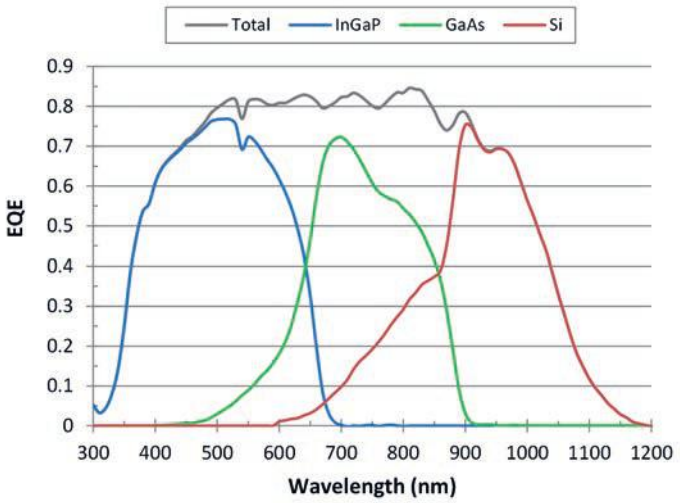

Figure PP1.3a.11 EQE spectra of the InGaP/GaAs/Si smart stack cell and sub-cells.

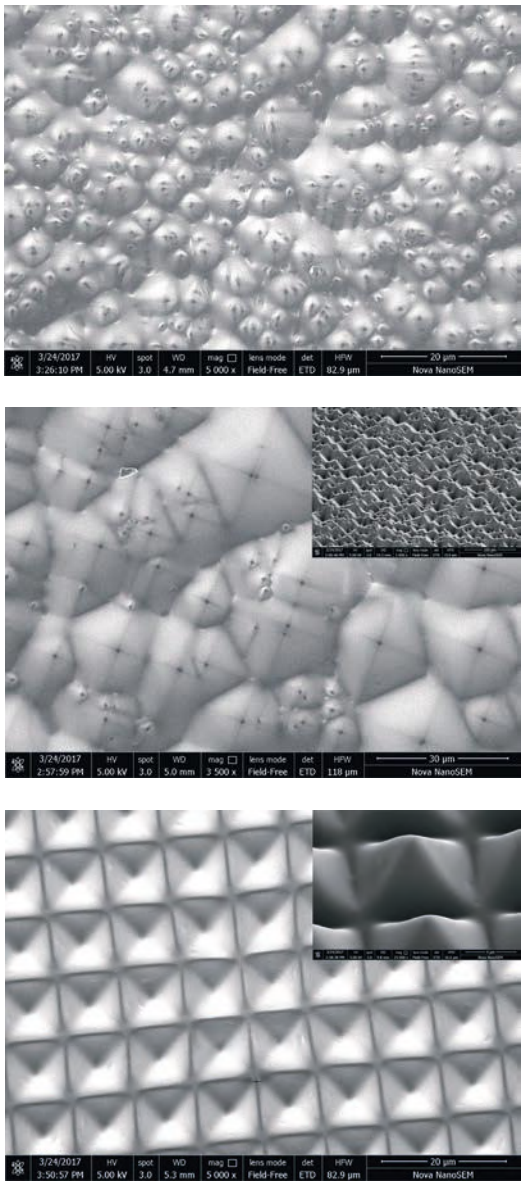

Figure PP1.3a.12: Scanning electron microscope (SEM) images of replicated PDMS layers with (a) random small pyramids; (b) larger random pyramids (inset is tilted view; scale bar = 500 um); and (c) regular (10 um) pyramids (inset is tilted view; scale bar = 1 µm);.

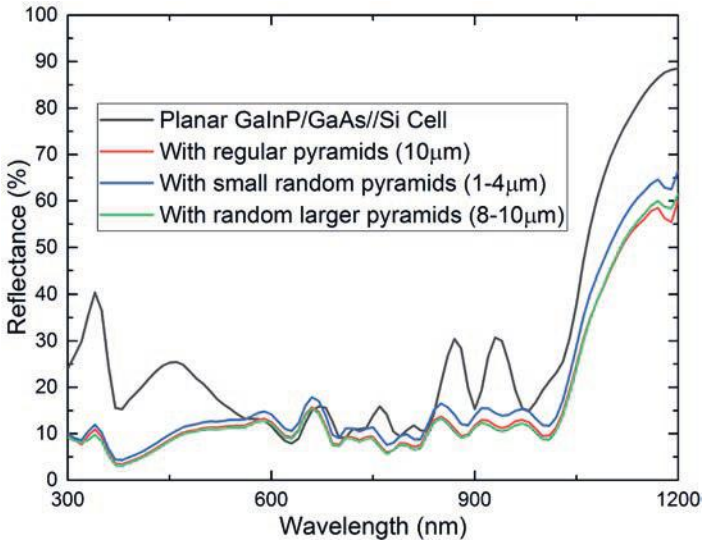

Figure PP1.3a.13 Measured reflectance of a InGaP/GaAs/Si cell before and after the application of textured PDMS layers with small random pyramids (1–4 µm) (blue); regular pyramids (10 µm) (red); and random larger pyramids (8–10 µm) (green).

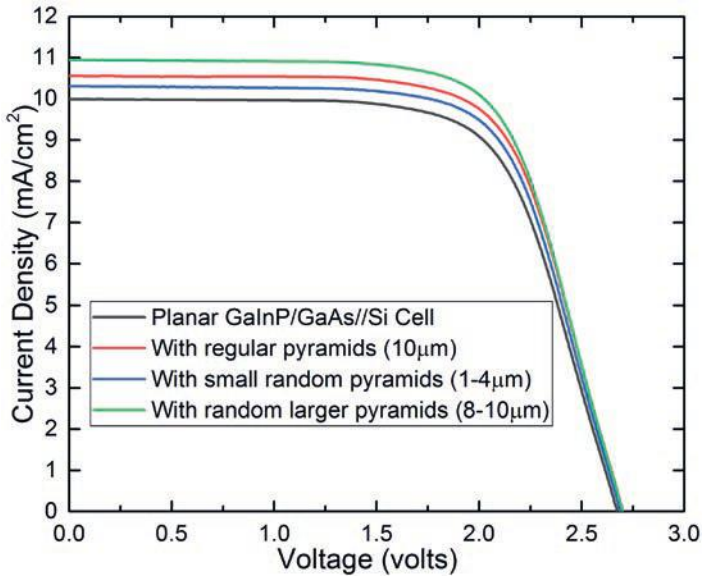

Figure PP1.3a.14 Measured light IV curves of an InGaP/GaAs/Si test cell before and after applying textured PDMS layers with random small pyramids (1–4 µm) (blue); regular pyramids (10 µm) (red); and random larger pyramids (8–10 µm) (green).

- External surface texturing using PDMS layers with replicated surface geometries are applied onto the fabricated InGaP/GaAs//Si wafer bonded solar cell. The short circuit current density was increased by 0.95 mAcm2, while the overall cell efficiency is boosted by more than 2% absolute.

Future Work

The light IV measurement shows the light-trapping ability of PDMS layers. To further optimise this external surface texturing layer, optical simulations are required to gain insight into the mechanism of this layer.

Table I Summary of light IV data

	J_{SC} (mAcm^2)	V_{OC} (V)	Efficiency (%)
Planar INGaP/GaAs/Si Cell	9.99	2.67	18.19
Plus small random pyramids (1–4 µm)	10.31	2.69	19.01
Plus regular pyramids (10 µm)	10.56	2.70	19.58
Plus random larger pyramids (8–10 µm)	10.94	2.70	20.25

References

Mizuno, H., Makita, K., Tayagaki, T., Mochizuki, T., Takato, H., Sugaya, T., Mehrvarz, H., Green, M. and Ho-Baillie, A., 2016, "A 'Smart Stack' Triple-Junction Cell Consisting of InGaP/GaAs and Crystalline Si", Proceedings of 43rd IEEE Photovoltaic Specialists Conference, 5–10 June 2016, Portland, Oregon, USA., 1923–1925.

Tayagaki, T., Makita, K., Mizuno, H. and Sugaya, T., 2017, "Investigation of the properties of semiconductor wafer bonding in multijunction solar cells via metal-nanoparticle arrays", Journal of Applied Physics, 122(2), 023101.

Chalcogenide on Silicon Tandem Cells

Team

UNSW: Dr Xiaojing Hao, Prof Martin Green, Dr Jialiang Huang, Dr Ouyang Zi, Dr Fajun Ma, Chang Yan

Partners

NREL: Dr Glenn Teeter, Dr Mathew Young, Dr Steve Johnston

Colorado School of Mines: A/Prof Brian Gorman

Students

UNSW: Aobo Pu, Jongsung Park, Xu Liu, Kaiwen Sun, Yuanfang Zhang, Yiyu Zeng, Yasaman Tabari-Saadi

Funding Support

ACAP, ARENA

Aims

As an alternative to III-V materials described in the previous projects, chalcogenide semiconductors are promising as absorber materials for solar cells due to their direct bandgaps, high absorption coefficient (>10^4 cm^{-1}), high energy conversion efficiency and low-cost potential and high stability. As an ideal candidate to substitute for toxic and rare elements in CIGS ($Cu(In,Ga)Se_2$), CZTS (Cu_2ZnSnS_4), a quaternary absorber material with a bandgap of 1.5 eV has been identified. This bandgap energy is close to the optimal bandgap for a single-junction solar cell of 1.35 eV, and is also optimal for a middle cell in a three-cell tandem with an Si bottom cell. Bandgap tuning of CZTS, by substituting a lower atomic number group IV element for some of the Sn, Ag for Cu, allows exploration of CZTS-based cells for the top cell in a CZTS/Si stack for a two- or three-cell tandem. The combination of optimal bandgap as a middle cell, and tunable bandgap as a top cell for a three-cell stack and low lattice mismatch shows that this material system is well suited for the top cell on Si cells. The aim of the present project is to work with NREL and Colorado School of Mines, which has world-leading expertise on I-II-VI chalcogenide solar cells and characterisation, to exploit the complementary synergies to develop a new generation of Si wafer cell technology by using chalcogenide materials, with performance of the Si cell substantially improved by deposition of thin layers of high performance chalcogenide cells on its surface to produce tandem devices.

Progress

Great progress has been made in improving the efficiency of CZTS/Si tandem cells by increasing the CZTS solar cells' efficiency and designing tandem cells with CZTS (family) cells and Si cells. Highlighted research progress is mainly in the following aspects.

The baseline efficiency of high bandgap pure sulphide CZTS solar cells has been improved. The highest in-house measured CZTS cell efficiency is 11.5% and certified performance by NREL is 11% (see Table PP1.3a.1). This certified 11% efficiency is the highest reported so far and listed in the Solar Cell Efficiency Tables (Version 50 and Version 51). A paper that resulted from this record cell has been submitted to *Nature Energy* and is currently under review.

Further progress has been made on transparent conductive electrodes (Ag NW) (see Figure PP1.3a.15) to replace the traditional transparent conductive oxide (TCO) (i.e. indium tin oxide (ITO) and aluminium-doped zinc oxide (AZO)). Ag NW, compared with ITO and AZO, can boost the photo-generated carrier density not only in the long wavelength region by the reduced free carrier absorption but also in the UV region (see Figure PP1.3a.17). However, most reported Ag NW networks required post-annealing in order to minimise junction resistance between Ag NWs. It is desirable to minimise the impact of the Ag NW' process on the underlying heterojunction so that the application of Ag NWs will not be limited by the buffer options and their associated post-annealing treatment and the cell performance can be more robust and reproducible. Room-temperature processed highly transparent and conductive Ag NW is developed as the front electrode. A comparable conductivity but more transparent Ag NW is achieved by using the hybrid structure of low density Ag NW on an ultrathin ITO. By adding the antireflection coating layer, a novel highly transparent and conductive hybrid Ag NW structure composed of thin ITO/Ag NW/thin ZnO is developed, enabling improved lateral conductivity and mechanical adhesion, reduced reflection and Ag oxidisation (see Figure PP1.3a.17). This room-temperature synthesised hybrid network of ultrathin ITO/Ag NW/ZnO, when integrated in the CZTS solar cells, greatly improved current density and efficiency while maintaining comparable fill factor (FF) and V_{OC} (see Figure PP1.3a.16). CZTS solar cells with this Ag NW show increased J_{SC}, with about 2% increase in the efficiency compared with the reference cells with ITO electrodes. This process is ready to be applied to other thin-film solar cells.

With the developed novel diode laser post-treatment on the CZTS absorber (see Figure PP1.3a.18), the crystallinity of the CZTS absorber is improved and the Cu/Zn disordering is reduced (see Figure PP1.3a.19). As a result of this, the power conversion efficiency of the laser annealed device is boosted by 9%, with a major increase in the short circuit current (see Table PP1.3a.2). The effectiveness and reproducibility of the diode laser post-treatment is currently under test.

With the characterisations by NREL, and our established TCAD simulation analysis of our champion CZTS solar cells, the key factors responsible for the voltage loss are identified and prioritised (see Figure PP1.3a.20). The cell performance loss is still likely dominated by the heterojunction interface recombination. More work on the buffer layer and heterojunction engineering is planned.

Classification	Efficiency (%)	Area (cm^2)	V_{oc} (V)	J_{sc} (mA/cm^2)	Fill Factor (%)	Test Centre (date)	Description
Cells (silicon)							
Si (crystalline)	25.0 ± 0.5	4.00 (da)	0.706	42.7[a]	82.8	Sandia (3/99)[b]	UNSW p-type PERC top/rear contacts[40]
Si (crystalline)	**25.7 ± 0.5**[c]	**4.017 (da)**	**0.7249**	**42.54**[d]	**83.3**	**FhG-ISE (3/17)**	**FhG-ISE, n-type top/rear contacts**[41]
Si (large)	**26.6 ± 0.5**	**179.74 (da)**	**0.7403**	**42.5**[d]	**84.7**	**FhG-ISE (11/16)**	**Kaneka, n-type rear IBC**[5]
Si (multicrystalline)	21.3 ± 0.4	242.74 (t)	0.6678	39.80[e]	80.0	FhG-ISE (11/15)	Trina Solar, large p-type[42]
Cells (III-V)							
GaInP	21.4 ± 0.3	0.2504 (ap)	1.4932	16.31[f]	87.7	NREL (9/16)	LG Electronics, high bandgap[43]
Cells (chalcogenide)							
CIGS (thin-film)	22.6 ± 0.5	0.4092 (da)	0.7411	37.76[f]	80.6	FhG-ISE (2/16)	ZSW on glass[44]
CIGSS (Cd free)	**22.0 ± 0.5**	**0.512 (da)**	**0.7170**	**39.45**[f]	**77.9**	**FhG-ISE (2/16)**	**Solar Frontier on glass**[12]
CdTe (thin-film)	22.1 ± 0.5	0.4798 (da)	0.8872	31.69[g]	78.5	Newport (11/15)	First Solar on glass[45]
CZTSS (thin-film)	12.6 ± 0.3	0.4209 (ap)	0.5134	35.21[h]	69.8	Newport (7/13)	IBM solution grown[46]
CZTS (thin-film)	**11.0 ± 0.2**	**0.2339(da)**	**0.7306**	**21.74**[d]	**69.3**	**NREL (3/17)**	**UNSW on glass**[14]
Cells (other)							
Perovskite (thin-film)	22.1 ± 0.7[i]	**0.0946 (ap)**	1.105	24.97[j]	80.3	Newport (3/16)	KRICT/UNIST[17]
Organic (thin-film)	**12.1 ± 0.3**[k]	**0.0407 (ap)**	**0.8150**	**20.27**[d]	**73.5**	**Newport (2/17)**	**Phillips 66**

Table PP1.3a.1: "Top 10" confirmed cell and modules results not class records under the global AM1.5 spectrum (1000 Wm^{-2}) at 25°C (IEC 60904-3: 2008, ASTM G-173-03 global) (reused Table from Solar Cell Efficiency Tables (version 51) [M.A. Green et al., Prog. Photovolt. Res Appl., 2018; 26:3-12].

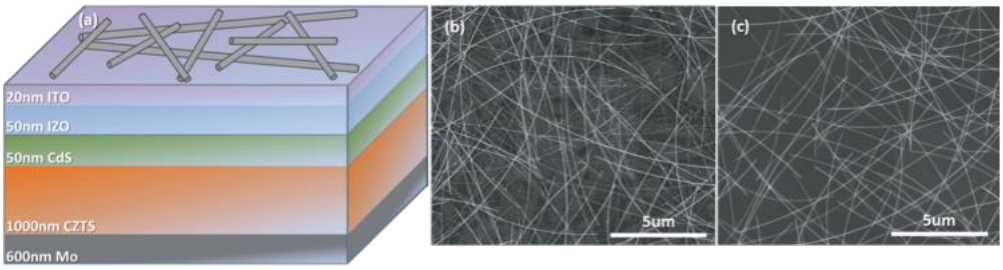

Figure PP1.3a.15: (a) Schematic structure of CZTS device with the hybrid electrode and morphology of Ag NW networks; (b) high density (20 Ω/□) Ag NW network / 20 nm ITO; and (c) low density (36 Ω/□) Ag NW network / 20 nm ITO.

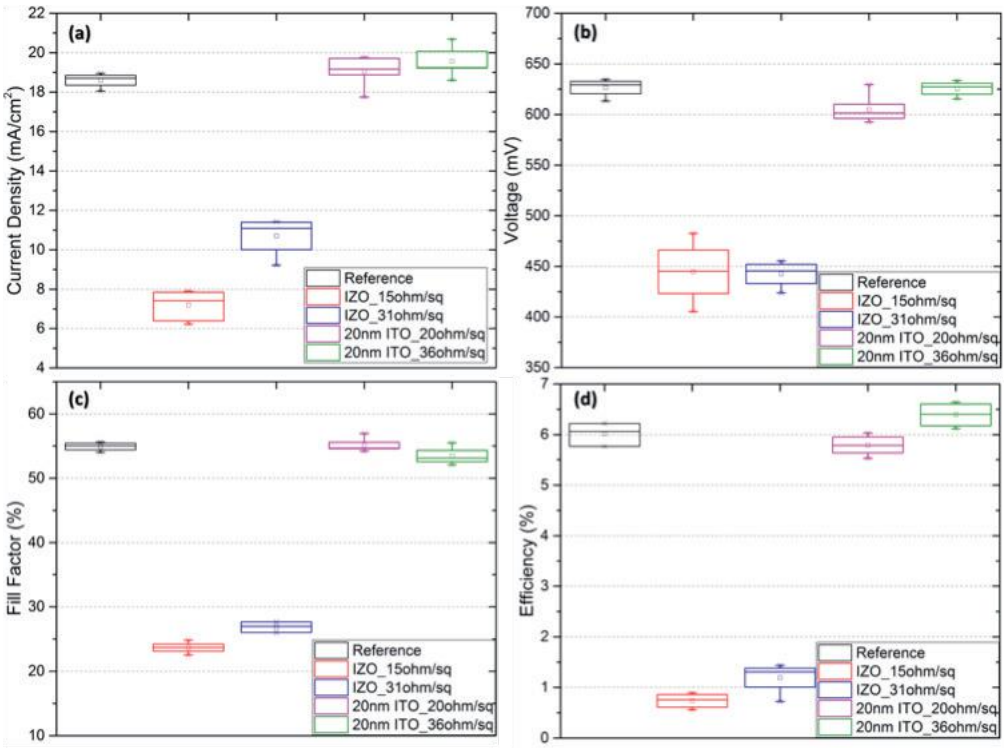

Figure PP1.3a.16: J-V characteristics of CZTS devices with different types of electrodes. (The numbers of samples measured were between 10 and 15 for each device, sample labelling with IZO and 20 nm ITO is the type of substrates, and numbered ohm/sq is R_{sheet} of the hybrid electrodes.)

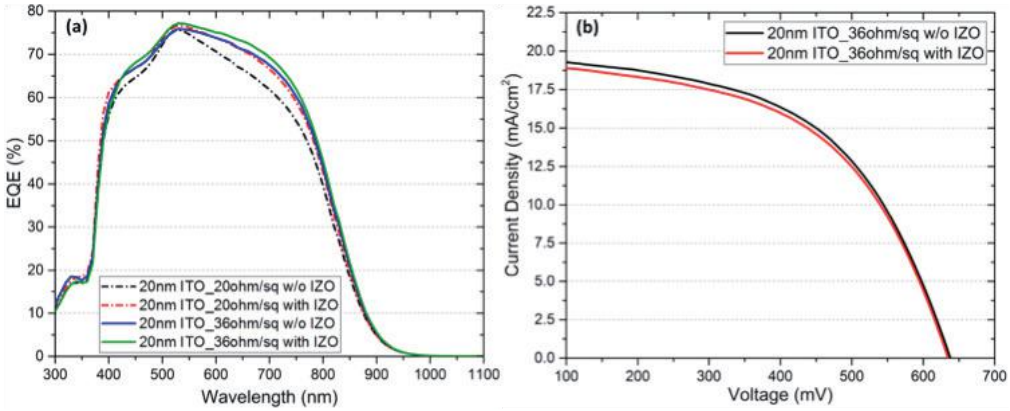

Figure PP1.3a.17: (a) EQEs of the CZTS devices with hybrid electrodes before and after IZO deposition; and (b) J-V curves of the CZTS device which shows the highest efficiency before and after IZO deposition.

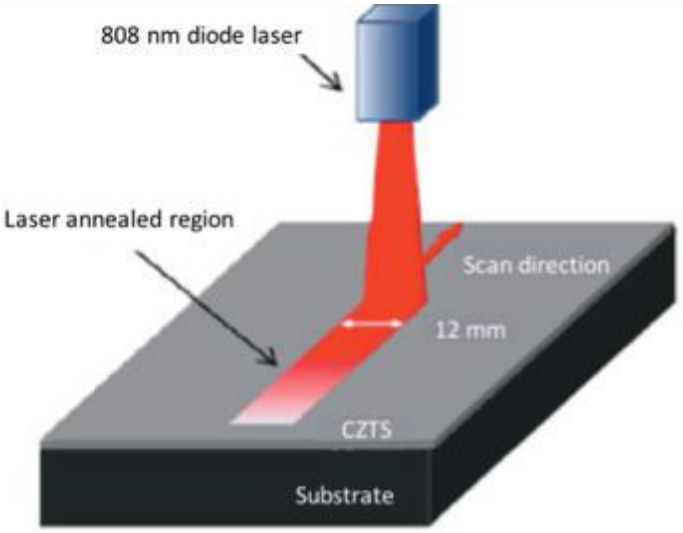

Figure PP1.3a.18: Schematic of laser annealing treatment.

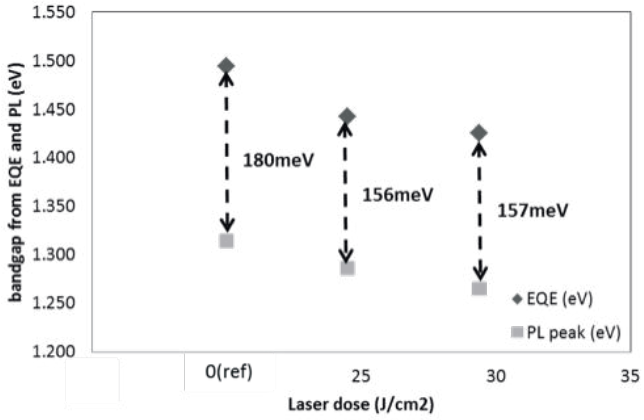

Figure PP1.3a.19: The difference of optical bandgap and electrical bandgap of laser annealed CZTS with different laser dose and reference sample showing the reduced disordering.

With the new champion CZTS solar cell, four-terminal CZTS family /Si tandem cells with efficiency exceeding 20% were demonstrated by a spectrum splitting method (Table PP1.3a.3, Figure PP1.3a.21). The tandem cells with high bandgap CZTS are comparable with the cells with the high bandgap CIGS provided by Solar Frontier, i.e. 22.67% CZTS/PERL vs. 23.35% CIGS/PERL (+4.7 diff%), 19.04% CZTS/PERC vs. 19.72% CIGS/PERC (+3.79 diff%). It is notable that the champion CZTS solar cell uses ITO as the front electrode, which will be replaced by the hybrid Ag NW network/ultrathin ITO in our future work to reduce its parasitic absorption and improve the optical gain in both CZTS and underneath Si cells. In addition, the 11% efficient champion CZTS solar cell uses the CdS buffer. With our previously developed $Zn_xCd_{1-x}S$ buffer, offering the more favorable conduction band alignment, the open circuit voltage of CZTS solar cells is expected to be further increased by about 100 mV (according to our previous work comparing the CZTS devices with these two different buffer options).

Two new chalcogenide PV materials have been explored for the high bandgap cell for tandem stacks, including Sb_2S_3, $CuSbS_3$. Our synthesised Sb_2S_3 has a bandgap of 1.7 eV, direct bandgap, high absorption coefficient of over 105 cm^{-1}, made of earth-abundant and non-toxic materials. With the device configuration of $TiO_2/Sb_2S_3/Au$, we obtained a 3.36%

Sample No. C#	V_{oc} [mV]	FF [%]	J_{SC} (With ARC) [mA cm-2]	PCE (With ARC) [%]	Laser Dose [J cm^{-2}]
C1	680.31	46.21	19.97	6.28	24.50
C2	682.92	54.13	19.31	7.14	24.50
C3	667.96	52.64	18.76	6.60	24.50
C4	664.36	56.32	19.60	7.33	34.30
C5	664.10	55.99	19.72	7.33	34.30
C6	486.56	44.37	17.50	3.78	44.10
C7(reference)	674.24	55.51	18.00	6.74	0.00

Table PP1.3a.2: Device parameters of laser annealed CZTS and reference.

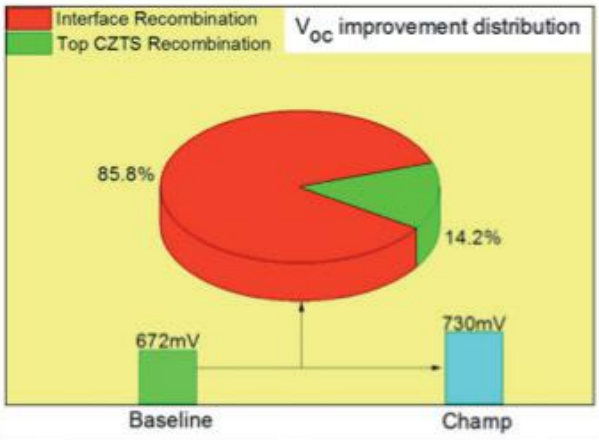

Figure PP1.3a.20: Simulations to reveal the recombination contributions to the V_{OC} deficit of our champion CZTS device.

efficient Sb_2S_3 solar device (see Figure PP1.3a.22). Similarly, our synthesised $CuSbS_2$ PV materials are made of earth-abundant and environmentally friendly constituents. As one of the most promising candidates for emerging thin-film solar cells, $CuSbS_2$ also possesses great potentials such as optimal direct bandgap of 1.5 eV, high optical absorption coefficient of over 105 cm^{-1} and low melting point of 551°C. Through the heterojunction engineering, we demonstrated a record V_{OC} of 622 mV for $CuSbS_2$ based thin-film solar cells (see Figure PP1.3a.23).

Highlights

- Base-line efficiency of CZTS solar cells has been significantly improved with the in-house highest efficiency of 11.5% and NREL-certified highest efficiency of 11%.
- Demonstrated beyond 22.67% efficiency CZTS/PERL tandem solar cells and 19.04% CZTS/PERC-Si tandem solar cells by spectrum splitting method, which are comparable to the performance of corresponding high bandgap CIGS/Si tandem cells by a similar spectrum splitting method.
- Developed room-temperature processed transparent and conductive hybrid Ag NW/ultrathin ITO front electrode and demonstrated about 2% J_{SC} improvement in CZTS solar cells with hybrid Ag NW electrode.
- Identified the key factors limiting the present champion CZTS device performance.
- Developed new abundant and non-toxic materials for top cell of the tandem stacks, and demonstrated working devices, i.e. 3.5% efficient Sb_2S_3 solar cell, and 2% efficient $CuSbS_2$ solar cell with a record V_{OC} of 622 mV.

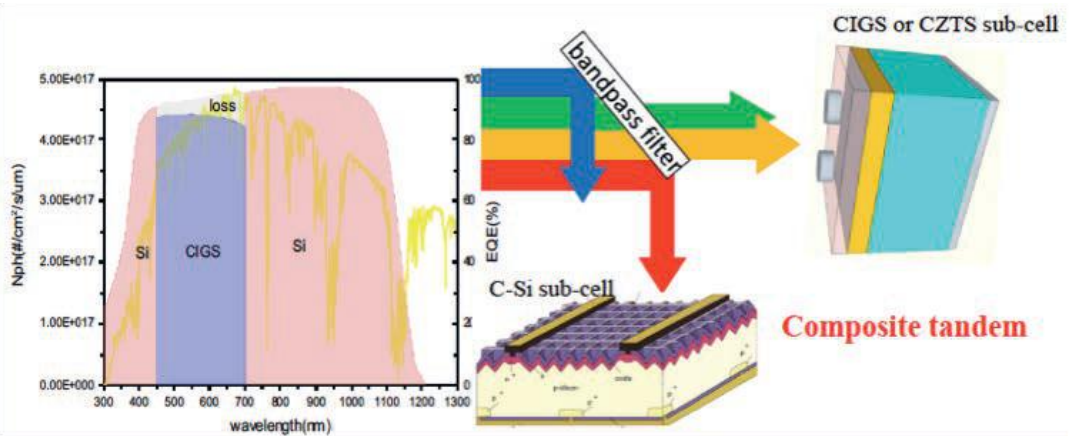

Figure PP1.3a.21: Schematic of four-terminal CZTS/Si and CIGS/Si tandem cells by spectrum splitting

	Previous record 9.5% CZTS	New Record 11% CZTS	High bandgap CIGS
PERL Si	21.44	*22.67*	23.35
PERC Si	17.81	*19.04*	19.72
SP Si	15.58	*16.81*	17.49

Table PP1.3a.3:. Four-terminal CZTS/Si and CIGS/Si tandem cells by spectrum splitting.

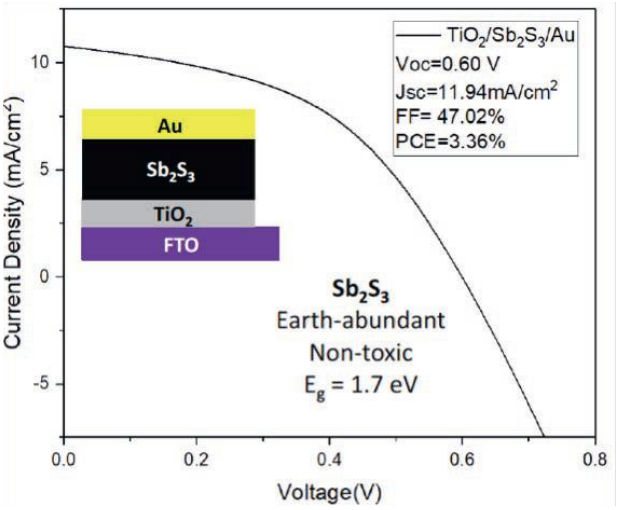

Figure PP1.3a.22: Earth-abundant and non-toxic Sb_2S_3 solar cells.

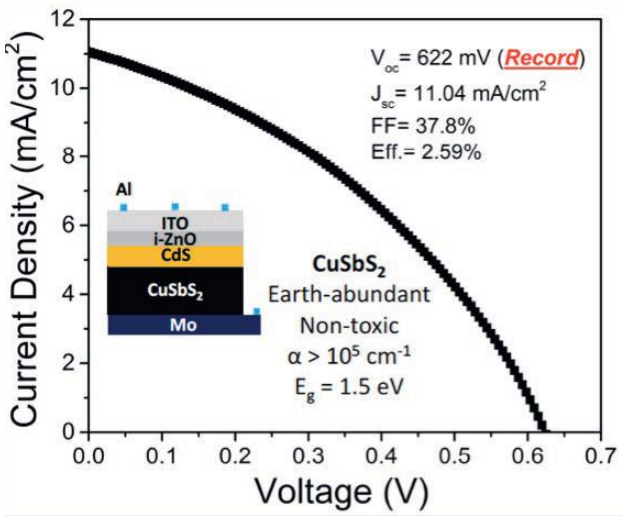

Figure PP1.3a.23: Earth-abundant and non-toxic $CuSbS_2$ solar cells.

Future Work

Future work in 2018 will be focused on (1) further improving the efficiency of high bandgap CZTS solar cells, in particular reducing the open circuit voltage deficit; (2) integrating the room-temperature processed highly transparent and conductive hybrid Ag NW network in chalcogenide/Si tandem cells; (3) integrating and developing strategies for beyond 25% chalcogenide/Si tandem cells; (4) further understanding the properties of new chalcogenide PV materials and performance loss.

References

Yan, C., Huang, J., Sun, K., Pu, A., Johnston, S., Zhang, Y., Liu, F., Eder, K., Yang, L., Cairney, J.M., Ekins-Daukes, N.J., Sun, H., Hameiri, Z., Stride, J.A., Chen, S., Green, M. A. and Hao, X.J., [year?] "Heat treated heterojunction Cu2ZnSnS4 solar cell breaks 10% power conversion efficiency barrier", Nature Energy (under review).

Huang, J., Yan, C., Sun, K., Liu, F., Sun, H., Pu, A., Green, M. A. and Hao, X.J., 2018, "Boosting the kesterite Cu2ZnSnS4 solar cells performance by diode laser annealing", Solar Energy Materials and Solar Cells, 175, 71–76.

Lunardi, M.M., Moore, S., Alvarez-Gaitan, J.P., Yan, C., Hao, X.J. and Corkish, R., 2018, "A comparative life cycle assessment of chalcogenide/Si tandem solar modules", Energy, 145, 700–709.

Cui, H., Liu, X., Sun, L., Liu, F., Yan, C. and Hao, X.J., 2017, "Fabrication of efficient Cu2ZnSnS4 solar cells by sputtering single stoichiometric target", Coatings, 7(2), 19; doi: 10.3390/coatings7020019.

Teymouri, A., Pillai, S., Ouyang, Z., Hao, X.J., Liu, F., Yan, C. and Green M. A., 2017, "Low temperature solution processed random silver nanowire as promising replacement for indium tin oxide", ACS Applied Materials & Interfaces, DOI: 10.1021/acsami.7b13085.

Park, J., Ouyang, Z., Yan, C., Sun, K., Sun, H., Liu, F., Green, M. and Hao X.J., 2017, "Hybrid Ag nanowire-ITO as transparent conductive electrode for pure sulphide kesterite Cu2ZnSnS4 solar cells", Journal of Physical Chemistry C, DOI: 10.1021/acs.jpcc.7b05776.

Liu, F., Huang, J., Sun, K., Yan, C., Shen, Y., Park, J., Pu, A., Zhou, F., Liu, X., Stride, J.A., Green, M.A. and Hao, X.J. , 2017, "Beyond 8% ultrathin kesterite Cu2ZnSnS4 solar cells by interface reaction route controlling and self-organised nano-pattern at the back contact", NPG Asian Materials, 9, e401, doi:10.1038/am.2017.103.

Song, N., Huang, J., Green, M.A. and Hao, X.J., "Diode laser annealing on sputtered epitaxial Cu2ZnnS4 thin films", 2017, Physica Status Solidi RRL, 1700033, DOI: 10.1002/pssr.201700033.

Cazzaniga, A.C., Crovetto, A., Yan, C., Sun, K., Hao, X.J., Estelrich, R., Canulescu, S., Stamate, E., Pryds, N., Hansen, O. and Schou J., 2017, "Ultra-thin Cu2ZnSnS4 solar cell by pulsed laser deposition", Solar Energy Materials and Solar Cells, DOI: 10.1016/j.solmat.2017.03.002.

Liu, X., Huang, J., Zhou, F., Liu, F., Stride, J.A. and Hao, X.J., 2017, "Spatial grain growth and composition evolution during sulfurizing meta-stable wurtzite Cu2ZnSnS4 nanocrystal-based coating", Chemistry of Materials, 29(5), 2110-2121. DOI: 10.1021/acs.chemmater.6b04603.

Yan, C., Sun, K., Liu, F., Huang, J., Zhou, F. and Hao X.J., 2017, "Boost Voc of pure sulphide kesterite solar cells via a double CZTS layer stacks", Solar Energy Materials and Solar Cells, 160, 7–11.

Non-Epitaxial Tandem Cells on Silicon

Team

UNSW: Dr Anita Ho-Baillie, Dr Shujuan Huang, Dr Xiaojing Hao, Dr Jae S. Yun, Dr Meng Zhang, Dr Trevor Young, Prof Martin Green

Partners

Monash: Prof Udo Bach, Prof Yi-Bing Cheng, Prof Leone Spiccia, Dr Wei Li, Dr Yasmina Dkhissi, Dr Tian Zhang

ANU: Dr Mulmudi Hemant Kumar, Dr Heping Shen, Dr Tom White, Prof Klaus Weber, Prof Kylie Catchpole

Korea Research Institute of Chemical Technology (KRICT)

Ulsan National Institute of Science and Technology (UNIST)

School of Materials Science and Engineering, UNSW

School of Physics, UNSW

Institute Materials for Electronics and Energy Technology (i-MEET) at Department of Materials Science and Engineering, Friedrich-Alexander University Erlangen-Nuremberg, Germany

Some of these tasks are conducted under the ARENA RND075 program in collaboration with Monash University, Australian National University, Arizona State University, Suntech Power Co. Ltd and Trina Solar Energy Co. Ltd.

Students

UNSW: Qingshan Ma, Sheng Chen, Adrian Shi, Arman M. Soufiani, Jincheol Kim, Cho Fai Jonathan Lau, Xiaofan Deng, Benjamin Wilkinson, Nathan Chang, Jianghui Zheng, Daseul Lee, Yongyoon Cho, Jueming Bing, Nathan Chang

Monash: Liangcong Jiang, Qicheng Hou

ANU: The Duong, Jun Peng, Daniel Jacobs, Yiliang Wu

Funding Support

ACAP, ARENA

Aim

The aim of this project is to investigate material systems where epitaxial growth on a crystalline template is not required for good cell performance. One such material system is organic metal halide perovskite.

Progress

In 2017, significant progress was made towards high efficiency tandem cells. Since the demonstrations of split spectrum tandems at 23% (Sheng, et al., 2015; Duong, et al., 2016), the team improved on the four-terminal perovskite/Si solar tandem device produced by stacking with 24.5% efficiency measured in-house in 2016 (Peng, et al., 2017). In 2017, ANU reported a 26.4% efficient mechanical stack that uses an interdigitated back contact (IBC) Si cell as the bottom cell and a textured cover/ITO quartz/c-TiO_2/mp-TiO_2/Rb0.05$(FA_{0.75}MA_{0.15}Cs_{0.1})_{0.95}$ PbI_2Br/PTAA/MoO_x/ITO/Au grid perovskite cell as the top cell (Duong, et al., 2017). At the end of 2017, UNSW and Institute of Materials for Electronics and Energy Technology (i-MEET) at the Department of Materials Science and Engineering, Friedrich-Alexander University, Erlangen-Nuremberg, Germany reported a 26.7% efficient mechanical stack that uses a passivated emitter rear localised (PERL) Si cell as the bottom cell and an ITO fused silica/CuSCN/$MAPbI_3$/$PC_{60}BM$/ZnO:Al nps/AgNW perovskite cell as the top cell. After the application of MgF_2 anti-reflection coating, the efficiency improves to 26.9% (Quiroz, et al., 2018). These are the highest efficiencies reported to date for a four-terminal perovskite-Si tandem and have surpassed the record for a single-junction silicon cell at 26.7%.

In terms of monolithic integration for a two-terminal tandem, ANU has reported a 22% efficient tandem on 1 cm^2 using a mesoscopic perovskite top sub-cell and a high temperature tolerant homo-junction c-Si bottom sub-cell with a p emitter on an n-substrate.

Most commercial cells have an n-emitter on p-substrate requiring an "inverted" perovskite cell for monolithic integration for a two-terminal perovskite/Si tandem. NiO_x has been investigated by UNSW (Zheng, et al., 2018) as a hole transport layer for such an "inverted" perovskite cell structure. Additional criteria including ease of fabrication (e.g., solution-process) and low processing temperature (e.g., 300°C) need to be considered for compatibility with Si cells. It was found that Ag doping is effective in improving conductivity, improving carrier extraction and enhancing the p-type property of the NiO_x film confirmed by electrical characterisation, photoluminescence measurements and ultraviolet photoelectron spectroscopy. In addition, Ag doping has no negative effect on the optical transmittance, morphology and stability of the NiO_x film, the overlying perovskite film and the complete perovskite solar cells respectively. The demonstrated ITO/Ag:NiOx/CH3NH3PbI3/PCBM/BCP/Ag devices have improved the average FF (from 69% to 75%), enhanced the average J_{SC} (by 1.2 mA cm^{-2} absolute) and enhanced the average V_{OC} (by 29 mV absolute). The average efficiency of these devices is 16.3% while the best device achieves a power conversion efficiency (PCE) of 17.3% with negligible hysteresis and a stabilised efficiency of 17.1%. In comparison, devices that use undoped NiO_x have an average efficiency of 13.5%. This work demonstrates the use of a low temperature simple solution processed NiO_x for high-performance inverted perovskite solar cells (PSCs) and for future monolithic perovskite-Si tandems.

First a 10 x 10 cm^2 operated cell has been demonstrated using low temperature processes comprising a combination of SnO_2 with C60 for electron transport material. Further development on large area deposition for various layers and new cell patterning methods will be performed in 2018 to improve device performance to be comparable with that on a small area device.

It has been demonstrated that a full area encapsulation scheme is most effective in limiting the moisture and heat exposure to perovskite solar devices. A low-cost encapsulation method using this scheme has been developed for encapsulated cells passing the International Electrotechnical Commission (IEC) thermal cycling test 200 cycles between –40˚C and 85˚C with less than 5% efficiency loss (Shi, et al., 2017).

Highlights

- Demonstrated small area 26.9% four-terminal perovskite/Si solar tandem device produced by stacking.
- Demonstrated 1 cm^2 26.9% two-terminal perovskite/Si solar monolithic tandem device.
- Developed low-cost encapsulation method for perovskite solar cells that pass IEC thermal cycling test 200 cycles between –40 °C and 85°C with less than 5% efficiency loss.

Future Work

- Exploration of alternative perovskite materials including fabrication of solar devices, modelling of material properties and characterisations for better understanding of the materials and device operation including loss mechanisms and factors affecting stability.
- Demonstrate perovskite/Si monolithic tandem with various cell designs and extending to large areas.
- Stability study and encapsulation strategies for perovskite/Si tandem technology, extending to large areas.

References

Sheng, R., Ho-Baillie, A.W.Y., Huang, S.J., Keevers, M., Hao, X.J., Jiang, L.C., Cheng, Y.B. and Green, M.A., 2015, "Four-Terminal Tandem Solar Cells Using CH3NH3PbBr3 by Spectrum Splitting", Journal of Physical Chemistry Letters, 6(19), 3931–3934.

Duong, T., Grant, D., Rahman, S., Blakers, A., Weber, K.J., Catchpole, K.R. and White, T.P., 2016, "Filterless Spectral Splitting Perovskite-Silicon Tandem System With >23% Calculated Efficiency ", IEEE Journal of Photovoltaics, 6(6), 1432–1439.

Peng, J., Duong, T., Zhou, X.Z., Shen, H.P., Wu, Y.L., Mulmudi, H.K., Wan, Y.M., Zhong, D.Y., Li, J.T., Tsuzuki, T., Weber, K.J., Catchpole, K.R. and White, T.P., 2017, "Efficient Indium-Doped TiOx Electron Transport Layers for High-Performance Perovskite Solar Cells and Perovskite-Silicon Tandems ", Advanced Energy Materials, 7(4) DOI:10.1002/aenm.201601768.

Duong, T., Wu, Y.L., Shen, H.P., Peng, J., Fu, X., Jacobs, D., Wang, E.C., Kho, T.C., Fong, K.C., Stocks, M., Franklin, E., Blakers, A., Zin, N., McIntosh, K., Li, W., Cheng, Y.B., White, T.P., Weber, K. and Catchpole, K., 2017, "Rubidium Multication Perovskite with Optimized Bandgap for Perovskite-Silicon Tandem with over 26% Efficiency ", Advanced Energy Materials, 7(14) DOI: 10.1002/aenm.201700228.

Quiroz, C.O.R., Shen, Y., Salvador, M., Forberich, K., Schrenker, N., Spyropoulos, G.D., Heumüller, T., Wilkinson, B., Kirchartz, T., Spiecker, E., Verlinden, P.J., Zhang, X., Green, M.A., Ho-Baillie, A. and Brabec, C.J., 2018, "Balancing electrical and optical losses for efficient 4-terminal Si–perovskite solar cells with solution processed percolation electrodes", J. Mater. Chem. A, DOI:10.1039/C7TA10945H.

Zheng, J., Hu, L., Yun, J.S, Zhang, M., Lau, C.F.J., Bing, J., Deng, X., Ma, Q., Cho, Y., Fu, W., Chen, C., Green, M.A., Huang, S. and Ho-Baillie, A.W.Y., 2018, "Solution-Processed, Silver-Doped NiOx as Hole Transporting Layer for High-Efficiency Inverted Perovskite Solar Cells", ACS Appl. Energy Mater., DOI: 10.1021/acsaem.7b00129.

Shi, L., Young, T.L., Kim, J., Sheng, Y., Wang, L., Chen, Y.F., Feng, Z.Q., Keevers, M.J., Hao, X.J., Verlinden, P.J., Green, M.A. and Ho-Baillie, A.W.Y., 2017, "Accelerated Lifetime Testing of Organic-Inorganic Perovskite Solar Cells Encapsulated by Polyisobutylene ", ACS Applied Materials & Interfaces, 9(30), 25073-25081.

PP1.3b Silicon Tandem Cells (Mechanically Stacked)

An alternative approach to implementing silicon tandem cells is mechanical stacking with independent connection to each cell in the stack. This removes constraints upon the matching of current, lattice constant and thermal expansion coefficients, albeit at the cost of additional mounting and interconnection costs. The best available silicon and wide bandgap cells can be separately optimised and mounted together.

Current proof-of-concept work is focused on reflector-based architectures to direct long wavelength light to the silicon cell. This enables the use of commercially available conventional GaAs cells as the top cell in the stack. Design of the mounting, optics and interconnection is critical to maximising performance. Longer term design preferences are for transparent top cells which offer more flexibility in the application of the tandem structure.

Team
ANU: Dr Matthew Stocks, Prof Andrew Blakers, A/Prof Klaus Weber, Dr Thomas White

Partner
Monash: Prof Udo Bach, Prof YiBing Cheng

Funding Support
ARENA, ANU

Aims

Demonstrate potential of mechanically stacked tandems to increase silicon module efficiency.

Progress

The primary activity has been preparing for integrating the GaAs top cells with ANU's high efficiency IBC silicon bottom cell. Unfortunately, progression to testing GaAs-Si tandem devices has not been made as originally planned this year.

GaAs cell development has been undertaken in collaboration with NREL. Information on the cell processing activities are described in Section 6.8.

Contacting problems that were previously mentioned have been resolved. A jig has been developed that enables voltage and current measurement of all ten contacts of the cells while

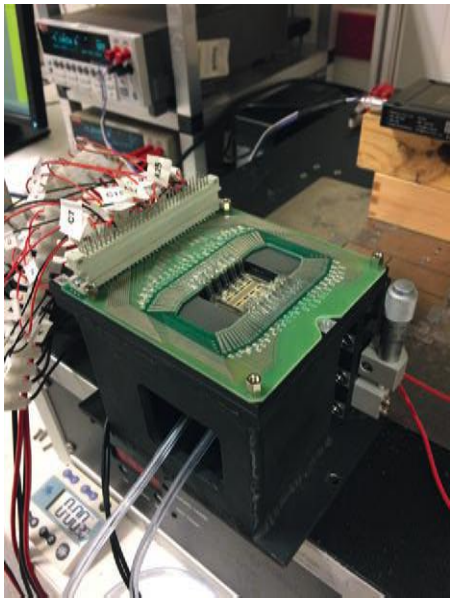

Figure PP1.3b 1. Jig for measuring open rear GaAs tandem

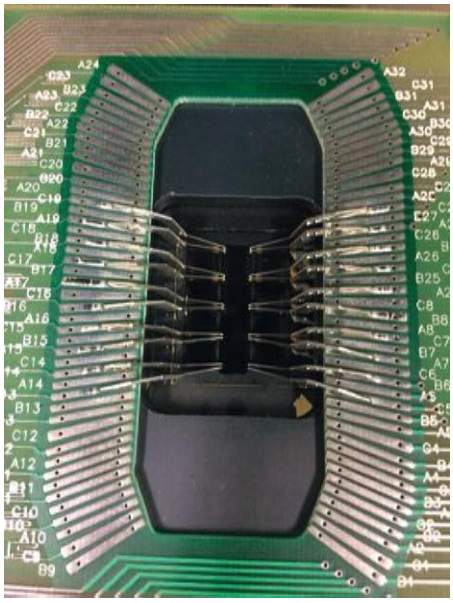

Figure PP1.3b 2. GaAs cell measurement showing the jig contact arrangement

retaining an open rear. A full image and close-up of the jig can be seen in Figures PP1.3b.1 and PP1.3b.2. This will enable characterisation of the GaAs cells under high concentration.

The addition of the gold pads on the rear contacts has enabled the connection of wires to the cells for on lens testing. The previous chromium surface was not able to be reliably contacted with soldering or conductive adhesives. The addition of the gold contacts have been added, as can be seen at the top and bottom contacts in Figure PP1.3b.3.

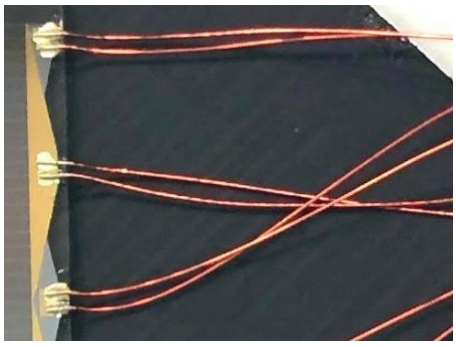

Figure PP1.3b 3. Close-up of successful GaAs cell wiring

The addition of the anti-reflection coatings has been the barrier to demonstration of high performance. Previously, ZnS had been used but has been restricted in the sputter chamber in the Australian Nanofabrication Facility (ANFF). Sputtered TiO_2 and SiO_2 was deposited on test samples and demonstrated good optical properties. Optimisation of the film thickness using the optical tools at PV Lighthouse indicated that a boost in short circuit current of 25% was expected. This was then demonstrated on earlier processed cells with the old contacting arrangements.

Results on cells were not as expected. The process delivered only a 5% increase in current as can be seen comparing the black and red curves in Figure PP1.3b.4. This was not due to the optical properties of the films but due to damage to the GaAs cells during the TiO_2 sputtering, as indicated by the decrease in open circuit voltage for the cells. This is supported by the reduction in IQE in the cells. It is currently hypothesised that this was due to heating during the relatively slow TiO_2 deposition. The good current achieved in earlier ZnS processes can be seen in the blue curve in Figure PP1.3b.4. ANU is exploring options for ZnS deposition elsewhere in the ANFF.

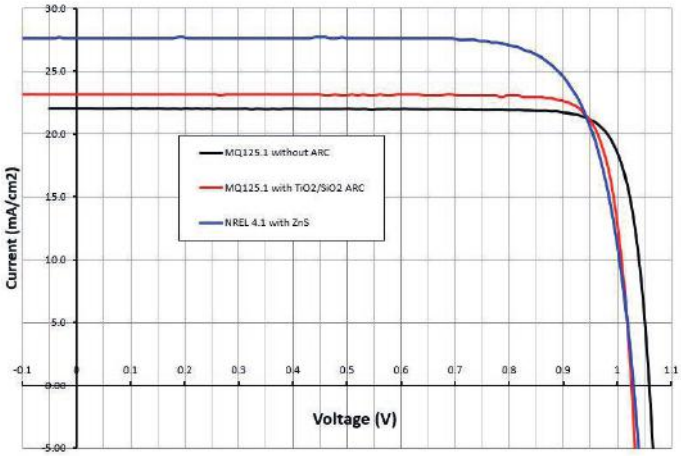

Figure PP1.3b 4. IV curves for GaAs cells with and without AR coatings

Highlights

- Resolution of contact problems for GaAs stacked tandems.

Future Work

- Resolution of anti-reflection coating integration.
- Integration of GaAs in stacked tandem.
- Characterisation of GaAs top cells under concentration.

PP2 Thin-Film, Third Generation and Hybrid Devices

Overview

Program Package 2 (PP2) encompasses research into a range of next generation cell technologies with the overall goals of demonstrating efficiency above 16% for cells of greater than 1 cm² area and of demonstrating the feasibility of significantly reduced costs. The program is divided into tasks to address the key materials groups: organic solar cells (OPV), organic-inorganic hybrid cells, "Earth-abundant" inorganic thin-film materials, "third generation" approaches and the hot topic of organic-inorganic perovskites.

Great progress has been made in 2017 in a number of target areas including that UNSW broke its own international records for large-area cell efficiency in CZTS and perovskite technologies.

The thin-film organic photovoltaics task (PP2.1) aims to identify and address roadblocks in organic photovoltaics to enable cost-effective, mass manufacture of modules using this technology. The research targets lower cost materials and/or processes compared to those of conventional cells or, alternatively, applications such as flexible or partly transparent cells for which conventional cells are not well suited. In 2017, in the materials area, the team demonstrated the ability to scale the synthesis of the high performance molecular donor benzodithiophene-quaterthiophene-rhodanine (BQR), allowing for extensive collaborative research, device optimisation, and large-scale roll-to-roll (R2R) printed OPV to be initiated. Two new series of molecular donors have been synthesised and understanding the impact of side-chain engineering has led to the synthesis of a series of oligothiophenes with improved OPV performance, compared to similar materials reported in the literature. Key structural aspects for the isolation of chromophores in luminescent solar concentrator materials have led to increased hopes for viability of such concentrators.

The characterisation work has led to the ability to improve device performance through application of vapour and thermal annealing and to improved understanding of the mechanism of initial photo-degradation of OPV devices. Indium-tin-oxide (ITO)-free flexible organic solar cells have been developed with efficiencies approaching those of ITO on glass.

Printing and scale-up developments in 2017 include achievement of 3.6% efficiency for 100 cm^2 modules via R2R printing process, successful translation of the reported high efficiency material of PPDT2FBT to R2R slot-die coating process, and excellent result of non-fullerene-based polymer solar cell with 10% PCE via batch processed slot-die coating on glass.

Thin films of the compound semiconductor Cu_2ZnSnS_4 (CZTS) are the focus of PP2.2. In 2017, the team beat its own record with 10.0% efficiency for a 1-cm^2 CZTS device (certified by NREL), substantially improving upon the previously best result of 7.6%, also established by UNSW and established a second world record efficiency for small area CZTS solar cells of 11%, breaking the previous 9.5% record, again established by UNSW.

Work on advanced third generation devices forms the focus of PP2.4. Hot carrier cells are a topic of particular interest given their long-term potential with efforts directed to understanding fundamentals as well as to implementing the different elements required for their successful implementation. Advances in work on both absorbers and contacts are reported in this section.

A new work program was started in 2016, to advance the organohalide perovskite technologies, addressing scale and durability. The work program was established as an internal project within ACAP and outcomes are reported under PP2.5.

Advances in 2017 include:

- Achievement of certified efficiency of 19.63% for a 1.02 cm^2 cell;
- Improved methods for measuring perovskite solar cells, involving inter-comparison amongst the accredited PV measurement and PV research laboratories;
- Progress on inorganic higher bandgap perovskite cells suitable for multi-junction tandems reporting some of the highest efficiencies for $CsPbI_2Br$ and $CsPbI_3$ cells;
- Development of a low-cost glass–glass encapsulation technique for perovskite solar cells and encapsulated $FAPbI_3$ planar cells have been demonstrated to pass the IEC61215:2016 thermal cycling test; and
- The successful translation of batch-printing-on-glass to roll-to-roll-printing-on-flexible-substrate.

PP2.1 Organic Photovoltaic Devices

PP2.1 Overview

Organic photovoltaic (OPV) devices have continued to make steady progress towards their theoretical photoconversion efficiency (PCE) of >20%, with single-junction cells now reported with claimed PCEs of over 13%. One of the advantages of organic semiconductor materials is the ability to molecular engineer materials, and there is still considerable parameter space that is yet to be explored. For example, up to a few years ago fullerenes were considered the acceptor of choice for bulk heterojunction devices, with donors designed to complement their properties. However, more recently, non-fullerene acceptors, an area in which ACAP members undertook pioneering work, have now surpassed fullerenes. Questions are now being raised as to whether the bulk heterojunction is necessary if the dielectric constant of the materials can be increased. While significant progress is being made on the photoactive materials there is still room for improvement in areas such as device architecture, including choice of interlayers, transparent conducting electrodes, and inverted and standard device architectures. Underpinning these activities are key structure-property relationship measurements that can guide the development of the next generation materials. Finally, while the team has made significant strides in these fundamental areas it has also had an important focus of up-scaling of materials and printing large-area solar cells. Thus, the team provides cohesive activities from basic to application at scale.

For ease of reading, the program has been divided into three sections: Materials, Characterisation and Device Architectures, and Printing and Scale-up.

Team

University of Melbourne: Dr David Jones, Dr Jegadesan Subbiah, Dr Wallace Wong, Prof Kenneth Ghiggino

CSIRO: Dr Fiona Scholes, Dr Gerry Wilson, Dr Doojin Vak, Dr Hasitha Weerasinghe, Dr Mei Gao, Dr Andrew Scully, Mr Andrew Faulks, Ms Jyothi Ramamurthy, Dr Kallista Sears, Mrs Régine Chantler

UNSW: A/Prof Ashraf Uddin, Prof Gavin Conibeer, Dr Naveen Kumar Elumalai, Dr Matthew Wright, Dr Supriya Pillai, Dr Binesh Puthen-Veettil, Dr Arman Mahboubi Soufiani, Dr Vinicius R. Goncales

University of Queensland: Prof Paul Burn, Dr Hui Jin, Dr Aaron Raynor

Students

University of Melbourne: Valerie Mitchell, Nicolau Saker Neto, Paul Geraghty, Calvin Lee, Sonam Saxena, Bolong Zhang, Saghar Massomi, Sacha Novakovic, Can Gao, Jia Yi Seow, Ruoyu Duan, Ms Kyra Schwarz, Paul Hibbert

CSIRO: Xiaojin Peng, Chuantian Zuo, Juengeun Kim

UNSW: Mushfika Baishakhi Upama, Cheng Xu, Arafat Mahmud, Dian Wang, Kah Chan, Faiazul Haque, Haimang Yi, Leiping Duan

University of Queensland: Sarah McGregor, Xiao Wang

Foreign University Team

Georgia Tech: Prof Samuel Graham, Prof Seth Marder;

Stanford: Prof Reinhold H. Dauskardt

NIST: Dr Lee Richter, Dr Sebastian Engmann

University of Bayreuth: Prof Anna Koehler, Prof Mukundan Thelakkat, Dr Sven Huettner, Daniel Kroh (student)

Imperial College London: Prof Jenny Nelson

University of St Andrews: Prof Ifor Samuel

Karlsruhe Institute of Technology: Dr Alexander Colsmann

KAUST: Prof Pierre Beaujuge

Institute of Metal Research, Chinese Academy of Sciences: Prof Jinhong Du

Academic Partners

Georgia Tech, USA; Stanford, USA; Imperial College, UK; St Andrews, UK; KAUST, Saudi Arabia; Chimie Paris Tech, France; UIsan National Institute of Science and Technology, South Korea; Dongguk University, South Korea; Wuhan University of Technology, China; University of Bayreuth, Germany; NIST; Kunsan National University, South Korea; Chinese Academy of Science, China; Gwangju Institute of Science and Technology (GIST), South Korea; Chonbuk National University, South Korea; Institute of Metal Research, Chinese Academy of Sciences, China

Funding Support

ACAP, ARENA, CSIRO, UoM, UNSW, UQ, DAAD, Chinese Science Council, NIST, Lord Mayor's Charitable Foundation

Materials

Aims

Commercialisation of emerging technologies requires performance profiles sufficiently high to allow confidence that translation to large-scale modules will give commercial performance. For organic solar cells being developed within ACAP, key materials properties are: (1) high power conversion efficiency (PCE) (>10%); (2) material stability during processing; (3) processability in industrial relevant solvent systems; and (4) long-term stability under operational conditions. For organic solar cells, it is expected that efficiencies for printed modules of between 8% and 10% PCE could provide commercial opportunities. Therefore, lab-based devices with a >10% PCE are required.

To this end the materials development program has had the following aims.

- Development of amphiphilic block copolymers for compatibility with industrially relevant solvents.
- Development of high performance p-type organic semiconductor materials.
- Improving polymer poly(dispersity).
- Development of materials for luminescent solar concentrators.
- Creation of organic semiconductor materials with a high dielectric constant.

Progress

Amphiphilic block-copolymers: The team had a major achievement in synthesising the first pure amphiphilic block-copolymers, where side-chain engineering has replaced the alkyl side-chains on the acceptor block with tetraethylene glycol (TEG) side-chains to promote the use of an extended range of solvents (see Figure PP2.1.1). The new materials show excellent solubility in non-chlorinated solvents and have been processed from industrially relevant and acceptable solvent systems. The block copolymers show excellent morphology control in thin films.

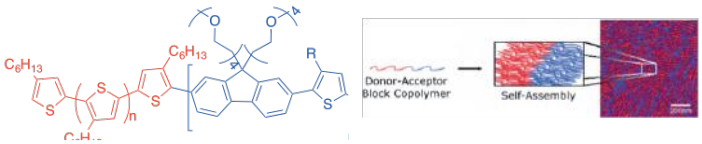

Figure PP2.1.1: We have demonstrated the development of amphiphilic block copolymers for morphology control and solubility in industrially relevant solvents. P3HT-b-PF_{TEG}T(R)BT, where P3HT (red) Donor and PF_{TEG}T(R)BT (blue) Acceptor, self-assemble in thin films.

High performance p-type organic semiconductors: As part of an extensive range of collaborations, 20 g of the high performance molecular donor benzodithiophene-quaterthiophene-rhodanine (BQR) (see Figure PP2.1.2) has been prepared. BQR has been extensively examined by team members within the ACAP network, NIST (on the development of OPV devices with non-fullerene acceptors), Imperial College London and the University of St Andrews (elucidation of the fundamental materials properties of BQR), and researchers at KAUST, Northwestern University and Karlsruhe Institute of Technology (devices). A detailed in situ X-ray analysis of BQR containing active layers has been completed and the results will be reported shortly.

The importance of BXR (benzodithiophene-X-rhodanine, where X may be monothiophene, bithiophene, terthiophene, quaterthiophene or quinquethiophene) molecular materials as donors in OPV devices, and the demonstrated ability to improve device performance through material modification, suggested that we could expand this key group of materials through molecular engineering of the energy levels by the incorporation of a higher electron affinity group in place of the rhodanine. We have now extended the series of molecular materials to generate the benzo[d][1,2,3]triazole (BTA) series of molecular donors (see Figure PP2.1.3). By modifying the electron density of the acceptor group, we have been able to tune the key energy levels (see Figure PP2.1.3), significantly reducing the ionisation energy

(HOMO energy levels) and decreasing the optical gap. Initial device testing suggests that these new materials may be poorly matched with fullerenes as the acceptor in OPV devices, but further work is ongoing.

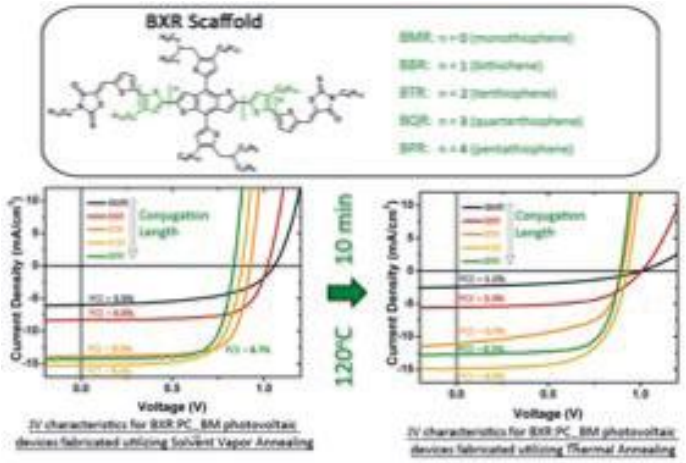

Figure PP2.1.2: The synthesis of BQR, the best material from the BXR series, has been scaled to 20 g to allow printing trials to commence.

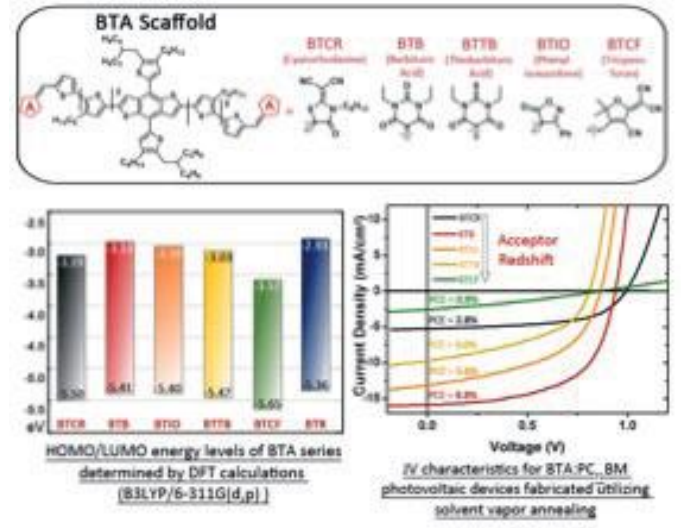

Figure PP2.1.3: Development of the BTA series of molecular donors for OPV by varying the electron density of the acceptor unit.

In developing the BXR series of molecular donors we have investigated the role of alkyl side-chain placement on device performance, with the idea that well-engineered placement of alkyl side-chains would allow the chromophore to be more planar, giving better performance. This key concept of side-chain engineering has been translated, in conjunction with Prof Seth Marder at Georgia Tech, to a series of oligothiophenes where we see a significant improvement in OPV device performance, compared to published efficiencies of the same chromophore, when the alkyl side-chains are arranged in a regioregular manner (see Figure PP2.1.4). Final X-ray characterisation of these materials is underway in preparation for publication.

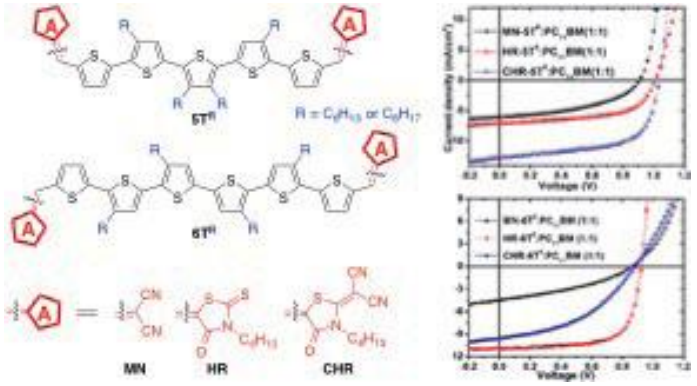

Figure PP2.1.4: Side-chain engineered oligothiophenes for OPV.

Improving polymer poly(dispersity): In addition, to developing non-polymeric donors the team has also been exploring strategies to control the poly(dispersity) of polymeric donor materials. Synthesis of polymers with a single molecular weight are of great interest for analytical standards, understanding the fundamental materials properties, as well as a route to controlled polymer architectures, which could lead to more reliable device fabrication and performance. We have developed a concept of exponential iterative coupling (see Figure PP2.1.5) as a technique for the completely deterministic synthesis of oligomeric and polymeric conjugated materials. The basic mathematical theory behind the process and methods for achieving high molecular weight materials has been developed and progressed towards a practical implementation based on the widely applicable Suzuki-Miyaura cross-coupling, using recently developed boron protecting group chemistry. Applications for these monodisperse and low-dispersity conjugated polymers and the synthetic methods developed are being investigated.

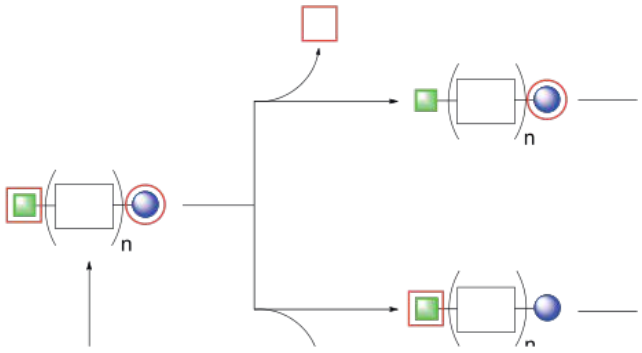

Figure PP2.1.5: Simplified scheme for exponential iterative coupling.

Luminescent solar concentrators (LSCs): LSCs may provide the advantage of improving light collection in the urban environment where direct sunlight is often not available. The LSC research has focused on new fluorophore designs to achieve greater light harvesting efficiency. By extending our concepts of emissive aggregates and energy migration systems, we have demonstrated state-of-the-art performance in LSC devices with a thin light-harvesting layer. Two key results published this year include a full study on molecularly insulated perylene diimide dyes (see Figure PP2.1.6) that have very high solid-state photoluminescence quantum yields, and the development of a new class of fluorescent betaine dyes which have been applied in transparent LSC devices.

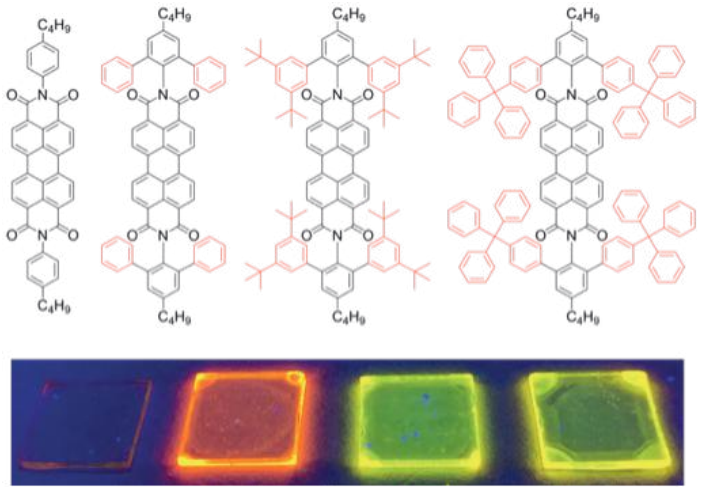

Figure PP2.1.6: Design of molecularly insulated perylene diimide fluorophores for use in LSCs. As the chromophore is isolated in the solid state with larger groups the fluorescent quantum yield increases and the emission approaches that of the isolated perylene in solution.

High dielectric materials: Recent work has shown that the inclusion of glycol ether chains can dramatically increase the dielectric constant at low frequency, while maintaining both the optical and electronic properties of their alkylated derivatives. Additionally, it has been shown that the inclusion of these glycolated units has the ability to increase the molecular packing density of the film, enhancing the optical frequency dielectric constant, and thus, homojunction device performance. As a result, we have synthesised a series of glycolated materials incorporating different functional end groups (see Figure PP2.1.7) to further investigate the structure-dielectric constant relationship.

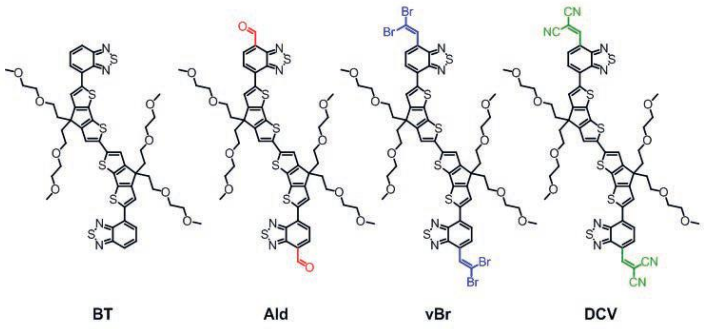

Figure PP2.1.7: Glycolated material series with varying end group functionality.

The materials with an enhanced optical frequency dielectric constant (ε_{opt} 4.0 or above), had improved homojunction device performance. Most significantly, **DCV** and **Ald** (ε_{opt} 4.0 and 4.6, respectively) show significant charge generation at energies near their optical gap (see Figure PP2.1.8). **BT** and **vBr**, with an optical frequency dielectric constant less than 4.0 (ε_{opt} 3.3 and 3.2, respectively) only show an external quantum efficiency (EQE) response contribution at energies well above their optical gap, suggesting excess thermal energy is required for exciton separation.

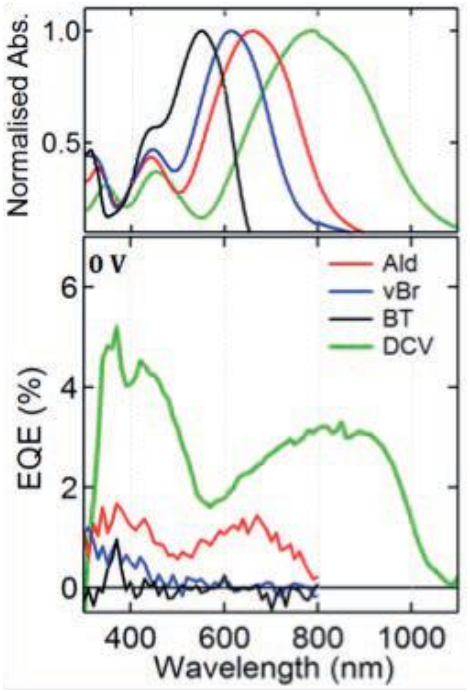

Figure PP2.1.8: Normalised absorption spectrum (top), and EQE (bottom).

Highlights

- Demonstrated the ability to scale the synthesis of BQR to >20 g, allowing for extensive collaborative research, device optimisation, and large-scale roll-to-roll (R2R) printed OPV to be initiated.
- Based on the ability to scale BTR and BQR intermediates, two new series of molecular donors have been synthesised where the energy levels have been modified by replacing the high electron affinity rhodanine moiety with alternatives leading to the BTA and BQA series of molecular donors.
- Understanding the impact of side-chain engineering has led to the synthesis of a series of oligothiophenes with improved OPV performance, compared to similar materials reported in the literature.
- Amphiphilic block copolymers have been synthesised, leading to new materials that can be deposited from industrially relevant solvent systems.
- Development of asymmetric monomers has commenced for the development of monodispersed advanced polymers via an exponential iterative coupling method.
- Key structural aspects for the isolation of chromophores in luminescent solar concentrator materials have been developed.
- Examples of homojunction devices have been produced with EQE responses near the optical gap energy showing that the optical frequency dielectric constant is important for charge generation.

Future Work

- New high performance amphiphilic conjugated block copolymers to be examined for device performance.
- The relationship between a high temperature nematic liquid crystalline phase in p-type organic semiconductors and improved organic solar cell performance will be probed.
- Complete characterisation and device optimisation of a series of BTA/BQA analogues. Investigate structure-property relationships and the energy landscape of high performance p-type organic solar cells.

- Complete scale-up for printing trials using the BQR material and to enable deeper collaboration with ACAP and AUSIAPV partners.
- The synthesis of a series of n-type organic semiconductors will be completed and materials characterised.
- New singlet fission will be fully characterised and incorporated into OPV devices.
- New up-conversion materials will be developed and characterized.
- Further development of synthetic methodologies to desymmetrised building blocks to enable controlled assembly of polymers or molecular materials.
- Application of LSC devices in light-harvesting windows.
- Manipulation of the dielectric constant for homojunction devices will be studied.

References

Armin, A., Stoltzfus, D.M., Donaghey, J.E. et al., 2017, "Engineering dielectric constants in organic semiconductors", Journal of Materials Chemistry C 5, 3736–3747.

Banal, J.L., Zhang, B., Jones, D.J., Ghiggino, K.P., Wong, W.W., 2017, "Emissive Molecular Aggregates and Energy Migration in Luminescent Solar Concentrators", Acc. Chem. Res. 50 (1), 49–57. DOI: 10.1021/acs.accounts.6b00432.

Chandrasekharan, A., Hambsch, M., Jin, H. et al., 2017, "Effect of capping group on the properties of non-polymeric diketopyrrolopyrroles for solution-processed bulk heterojunction solar cells", Organic Electronics 50, 339–346.

Gendron, D., Maasoumi, F., Armin, A. et al., 2017, "A thiocarbonyl-containing small molecule for optoelectronics", RSC Advances 7, 10316–10322.

Liang, R.-Z., Babics, M., Seitkhan, A., Wang, K., Geraghty, P.B., Lopatin, S., Cruciani, F., Firdaus, Y., Caporuscio, M., Jones, D.J., Beaujuge P.M., 2017, "Additive-Morphology Interplay & Loss Channels in 'All-Small-Molecule' BHJ Solar Cells with the Nonfullerene Acceptor IDTTBM", accepted Adv. Funct. Mater. DOI: 10.1002/adfm.201705464.

Mitchell, V.D., Gann, E., Huettner, S., Singh, C.R., Subbiah, J., Thomsen, L., McNeill, C.R., Thelakkat, M., Jones, D.J., 2017, "Morphological and Device Evaluation of an Amphiphilic Block Copolymer for Organic Photovoltaic Applications", Macromolecules 50 (13), 4942–4951. DOI: 10.1021/acs.macromol.7b00377.

Mitchell, V.D., Wong, W.W.H., Thelakkat, M., Jones, D.J., 2016, ""The synthesis and purification of amphiphilic conjugated donor–acceptor block copolymers", Polym. J. 49 (1), 155–161.

Xu, J., Zhang, B., Jansen, M., Goerigk, L., Wong, W.W.H., Ritchie, C., 2017, "Highly Fluorescent Pyridinium Betaines for Light Harvesting", Angew. Chem. Int. Ed. Engl. 56 (44), 13882–13886. DOI: 10.1002/anie.201704832.

Zarrabi, N., Stoltzfus, D.M., Burn, P.L. et al., 2017, "Charge Generation in Non-Fullerene Donor-Acceptor Blends for Organic Solar Cells", Journal of Physical Chemistry C 121, 18412–18422.

Zhang, B., Soleimaninejad, H., Jones, D.J., White, J.M., Ghiggino, K.P., Smith, T.A., Wong, W.W.H., 2017, "Highly Fluorescent Molecularly Insulated Perylene Diimides: Effect of Concentration on Photophysical Properties". Chem. Mater. 29 (19), 8395–8403. DOI: 10.1021/acs.chemmater.7b02968.

Characterisation and device architectures

Aims

For organic solar cells being developed within ACAP it is important to understand the device architectural factors that lead to high PCE (>10%); long- term stability under operational conditions; and features that enable their unique deployment.

To this end the characterisation and device architecture program has had the following aims.

- Examine the fundamental processes involved in exciton formation and charge separation when BQR was incorporated into the active layer in comparison to BTR.
- Understand morphology control of donor and acceptor systems and light trapping in organic solar cells.
- Engineer interfaces of buffer layers in organic solar cells.
- Investigate the photo-degradation of organic solar cells.
- Create efficient semi-transparent organic solar cells.
- Fabricate ITO-free solar cells.

Progress

Comparison of BQR and BTR devices: OPV devices containing BQR show increased resistance to thermal stress once formed compared to previously reported BTR containing devices. Increasing the chromophore length to generate BQR is thought to slow down the diffusion of BQR in comparison to BTR leading to improved thermal stability. We have used transient absorption (TA) spectroscopy to examine the changes in exciton formation and charge separation for BQR containing thin films, so that we can then compare these processes before and after solvent vapour or thermal annealing. The TA studies on BQR have now been completed and will be published in the near future. Rapid exciton formation and charge separation is seen in solvent vapour annealed devices without the generation of triplet species in the un-annealed BTR films (see Figure PP2.1.9). The BTR and BQR materials are of great interest to the broader community and both BTR and BQR have been shared with a number of research groups so that fundamental physical properties, e.g., diffusion length, CT state energy levels and electro absorption coefficients, can be measured.

Morphology: Work completed in collaboration with NIST has mapped the in situ structural changes for BQR/$PC_{71}BM$ films during annealing to map impact of crystallisation on device performance. Using in situ wide and small angle X-ray techniques the crystal growth parameters were followed indicating an Ostwald-type ripening process with overgrowth of crystallites during thermal annealing. Differences between BTR and BQR were noted for the optimal solvent vapour annealing. With tetrahydrofuran (THF) a domain size of around 30 nm was measured, while for BQR after thermal annealing an overgrowth of the domains was not seen (see Figure PP2.1.10).

Inverted solar cells: We have designed and developed a new inverted OPV device to address the challenge of improving the device stability and efficiency by interface engineering buffer layers. In line with this approach, we achieved non-fullerene PBDB-T:ITIC-based OPV devices with high PCE of ~12.3% complemented with good device lifetime of ~7–8 months without any encapsulation under ambient conditions. Compared to traditional/conventional device structures, which only last for a few days, our devices with inverted architecture possess extended lifetimes lasting for about a year. The device structure and current-voltage characteristics are shown in Figure PP2.1.11.

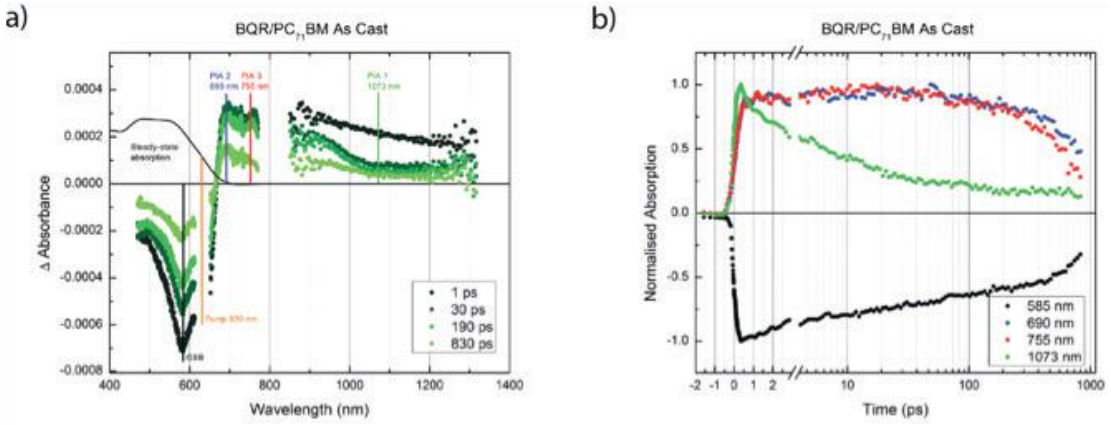

Figure PP2.1.9: Transient absorption spectra on BQR:$PC_{71}BM$ as cast thin films (a) after 1, 30, 190 and 830 ps; and (b) kinetic traces at 585 nm (ground state bleach), 690 and 755 nm (radical cation), and 1073 nm (exciton). No indication of triplet is observed as was seen for BTR:$PC_{71}BM$ as cast films.

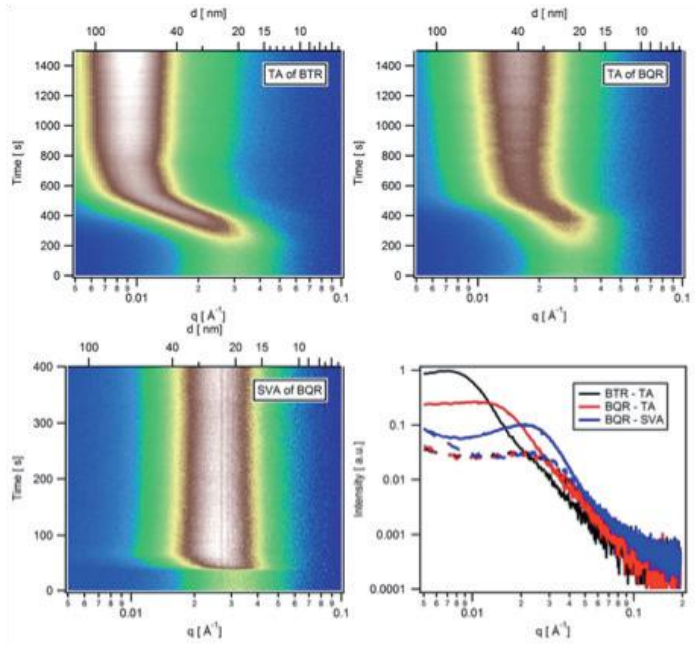

Figure PP2.1.10: Initial in situ GiSAX measurements comparing BTR:$PC_{71}BM$ and BQR:$PC_{71}BM$ thin films after thermal annealing (TA) (top) and solvent vapour annealing of BQR:$PC_{71}BM$ (bottom left). Thermal annealing of BTR:$PC_{71}BM$ leads to average domain sizes of 77 nm, while for thermally annealed BQR:$PC_{71}BM$ thin films domain sizes remain around 40 nm.

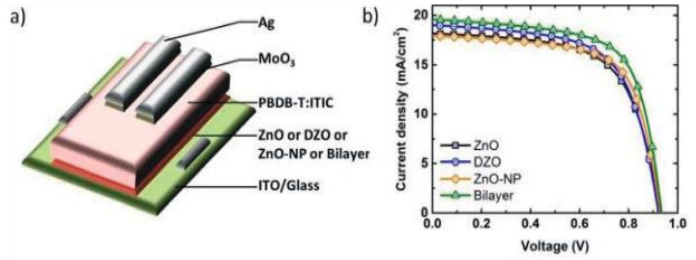

Figure PP2.1.11: (a) Schematic diagram of device structure of the fabricated inverted non-fullerene PBDB-T:ITIC based organic solar cells with different ETLs (ZnO, DZO, ZnO-NP and bilayer); (b) I-V characteristics of the solar cells at room temperature under AM1.5G illumination at 100 mWcm^{-2}.

ETL description	J_{sc} (mAcm^{-2})	V_{oc} (V)	FF (%)	Avg. PCE (%)	Max. PCE (%)	R_s (Ω.cm^2)	R_{sh} (Ω.cm^2)
ZnO	18.64±0.34	0.924±0.00	61.1±1.6	10.5±0.14	10.69	7.5±0.63	748.4±71.9
DZO	18.87±0.11	0.925±0.00	63.3±0.1	11.1±0.04	11.11	7.0±0.48	762.4±9.67
ZnO-NP	17.97±0.04	0.932±0.00	66.2±1.1	11.1±0.12	11.21	5.9±0.26	750.0±88.8
Bilayer	19.42±0.17	0.936±0.00	65.3±2.0	11.9±0.35	12.24	6.0±0.78	681.6±49.2

Table PP2.1.1 Photovoltaic performance parameters of non-fullerene PBDB-T:ITIC-based organic solar cells with different ETLs (ZnO, DZO, ZnO-NP and bilayer) under AM1.5G 100 mWcm^{-2} illumination.

Investigation of photo-degradation: The burn-in or photo-degradation in non-fullerene PBDB-T:ITIC-based organic solar cells has been investigated using photothermal deflection spectroscopy (PDS). This method enables the in-depth evaluation of short-term degradation of organic devices under continuous illumination. The PDS technique facilitates: (i) measurement of absorption features in the sub-optical gap region in polymer–polymer and polymer–acceptor blend films; and (ii) measurement of weak absorption near the optical gap, which is normally difficult with traditional methods. The schematic diagram of the device structure and the current-voltage characteristics of fresh and aged devices are shown in Figure PP2.1.12. The sub-band absorption in PDS signals are observed in aged samples as shown in figure PP2.1.13. We believe that the formation of these trap states is the mechanism underpinning the initial degradation in PBDB-T:ITIC-based devices.

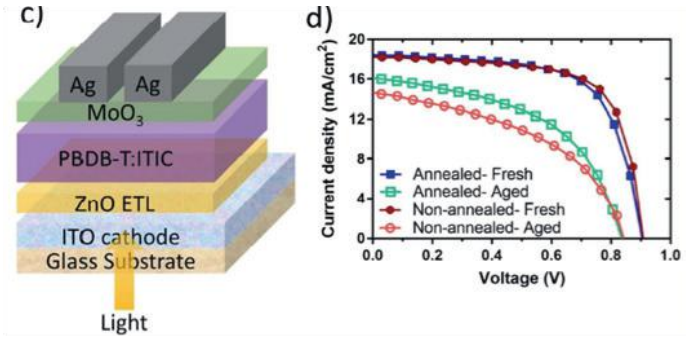

Figure PP2.1.12: (a) Schematic diagram of the device structure of the fabricated inverted non-fullerene PBDB-T:ITIC-based OPV devices; and (b) current-voltage characteristics under AM1.5G 100 mWcm^{-2} illumination of the fabricated non-annealed and annealed solar cells.

Device description	J_{sc} ($mAcm^2$)	V_{oc} (V)	FF (%)	PCE (%)	R_s ($\Omega.cm^2$)	R_{sh} ($\Omega.cm^2$)
Non-annealed (Fresh)	18.3 ± 0.12	0.912 ± 0.00	68.8 ± 0.11	11.5 ± 0.06	4.7 ± 0.07	939 ± 104
Non-annealed (Aged)	14.5 ± 0.22	0.836 ± 0.01	45.4 ± 1.41	5.5 ± 0.29	10 ± 0.47	209 ± 8.5
Annealed (Fresh)	18.3 ± 0.16	0.911 ± 0.00	66.8 ± 0.75	11.1 ± 0.10	5.8 ± 0.25	789 ± 24.6
Annealed (Aged)	16.0 ± 0.51	0.826 ± 0.02	50.4 ± 2.21	6.7 ± 0.20	13.3 ± 0.53	315 ± 28.3

Table 2: Photovoltaic performance parameters of non-fullerene PBDB-T:ITIC-based organic solar cells of fresh and aged devices after five hours burn-in under AM1.5G 100 $mWcm^{-2}$ illumination.

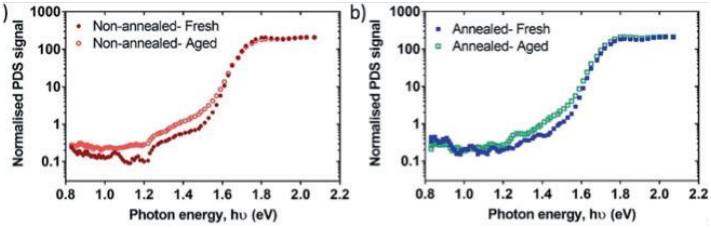

Figure PP2.1.13: Photothermal deflection spectroscopy (PDS) absorption spectra of (a) non-annealed and (b) annealed PBDB-T:ITIC-based BHJ blend films under both fresh and aged conditions. Absorption below 1.7 eV increased after photo-aging in both non-annealed and annealed films.

Semitransparent organic solar cells: A highly efficient bulk heterojunction semitransparent inverted organic solar cell has been developed that incorporates D/M/D electrode (MoO_3/Ag/MoO_3) and non-fullerene PBDB-T:ITIC-based photo-absorbing layer. The change in device transparency was studied by varying the active layer thickness and outer MoO_3 layer thickness. Changing these parameters also affects the number of absorbed photons and, hence, the photocurrent density. By tuning the active layer thickness, the average device efficiency increased from 5.8% to 7.3%. An impressive PCE of 7.3% was achieved for the best device at an average visible transmittance (AVT) of 25% as shown in figure PP2.1.14. A semitransparent OPV device with an AVT of 25% is required for window applications.

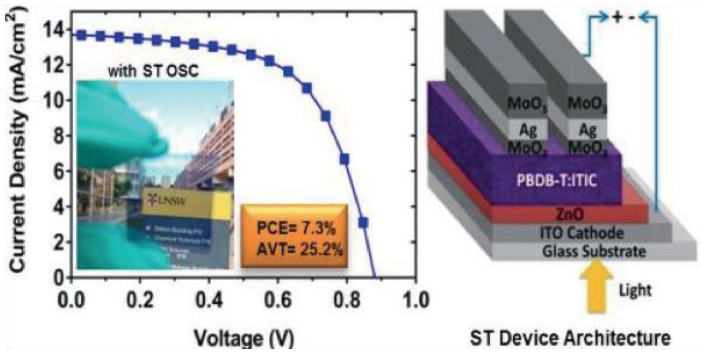

Figure PP2.1.14: J-V curve of non-fullerene PBDB-T:ITIC-based high performance semitransparent organic solar cell and device structure. Efficiency was 7.3% with 25.2% AVT.

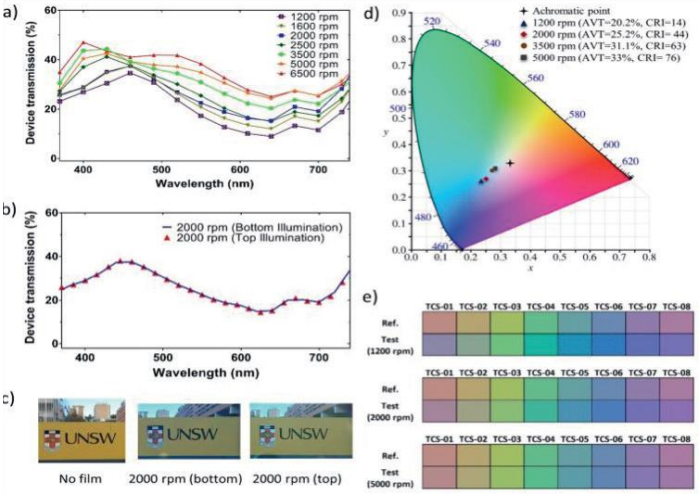

Figure PP2.1.15: (a) Total transmittance spectra of the semitransparent organic solar cells under bottom illumination for different active layer thicknesses; (b) device transmittance spectra (active layer spin rate = 2000 rpm, (93 nm thick)) under both top and bottom illumination; (c) comparison of images through ST device from both top and bottom side; photographs of the devices with 93 nm active layer thickness (2000 rpm); (d) The colour coordinates (x, y) of the semitransparent solar cells with different active layer thicknesses under standard illumination; and (e) simulated colour appearance of eight CRI reflective samples for different semitransparent solar cells (test – 1200, 2000 and 5000 rpm) and when illuminated by CIE Standard Illuminant D65.

ITO-free organic solar cells: We have used a multilayer poly(3,4-ethylenedioxythiophene):poly(styrenesulfonate) (PEDOT:PSS) transparent electrode for ITO-free organic solar cells (OSCs). Two-layer PEDOT:PSS films treated with methanol or formic acid were found to exhibit high transmittances in the visible wavelength range and have low sheet resistances: 66% with 34.9 Ω/square, and 63% with 30.9 Ω/square, respectively. The sheet resistance reduction by methanol/formic acid treatment has been reported to remove PSS leading to a film thickness reduction, and better connected PEDOT chains within PEDOT:PSS. In addition, instead of using common plastic substrates, we fabricated the devices on a 100 mm thick Corning® Willow® Glass substrate to yield high efficiency ITO-free bulk heterojunction OSCs. The ITO-free devices with standalone PEDOT:PSS anodes treated with methanol using BQR:$PC_{71}BM$ as the active layer showed a high PCE of up to 8.1%, which was comparable to the corresponding devices based on the traditional ITO anode. We have also used graphene prepared by chemical vapour deposition (CVD) as an alternative to ITO as the transparent conducting electrodes. By oxidising the top layer of three-layer graphene films with an ozone treatment, a graphene oxide/graphene (GO/G) vertical heterostructure can be formed. The heterostructure had greatly improved optical transmittance, a deeper work function and higher stability. Importantly, the introduction of an MoOx interfacial layer not only reduced the energy barrier between the graphene anode and the active layer, but also decreased the resistance of the GO/G film by nearly eight times. The OSCs with the structure of polyethylene terephthalate/G/GO/MoOx/BQR:$PC_{70}BM$/Ca/Al were flexible and ITO-free, and had a PCE of up to 5.8%, compared to 9.2% of the devices with an equivalent structure prepared on commercial ITO on glass. The open-circuit voltages were quite similar for both electrodes, with the lower performance for the graphene-based device arising from a lower short-circuit current and fill factor, which is related to the relatively high sheet resistance of the graphene-based transparent electrode.

Highlights

- TA spectroscopy on films containing BQR has identified significant differences from the previously reported BTR containing films with no involvement of triplet states in as-cast films for BQR. Upon solvent vapour annealing and thermal annealing the device performance improves.
- In situ X-ray characterisation of printed films (doctor bladed) continues to highlight changes induced through molecular or side-chain engineering.
- Morphology control of donor and acceptor systems for different donor/acceptor-based OPV devices.
- Understanding of the mechanism of initial photo-degradation of OPV devices.
- Improved the OPV device efficiency and stability by interface engineering of buffer layers.
- Developed highly efficient semitransparent OPV devices with good colour rendering index and transparency.
- Developed ITO-free flexible organic solar cells with efficiencies approaching those of ITO on glass.

Future Work

- Continue investigation into morphology control of donor/acceptor materials in bulk heterojunction solar cells.
- Extend lifetimes study and degradation mechanism in OPV devices.
- Exploit light-trapping prospects in OSCs by plasmonic nanoparticles.
- Develop highly efficient semitransparent OPV devices with high AVT for window application.
- Scale ITO-free organic solar cells.

References

Chan, K.H., Elumalai, N.K., Tayebjee, M.J.Y. et al., 2017, "Dark carrier dynamics and electrical characteristics of organic solar cells integrated with Ag-SiO_2 core-shell nanoparticles", Synthetic Metals 223, 34–42.

Upama, M.B., Elumalai, N.K., Mahmud, M.A. et al., 2017, "Interfacial engineering of electron transport layer using Caesium Iodide for efficient and stable organic solar cells", Applied Surface Science, 416, 834-844.

Upama, M.B., Elumalai, N.K., Mahmud, M.A. et al., 2017, "Organic solar cells with near 100% efficiency retention after initial burn-in loss and photo-degradation", Thin Solid Films, 636, 127–136.

Upama, M.B., Elumalai, N.K., Mahmud, M.A. et al., 2017, "Role of fullerene electron transport layer on the morphology and optoelectronic properties of perovskite solar cells", Organic Electronics, 50, 279–289.

Upama, M.B., Wright, M., Elumalai N.K. et al., 2017, 2017b, "Optical modelling of P3HT:PC71BM semi-transparent organic solar cell", Optical and Quantum Electronics, 49, 28.

Upama, M.B., Wright, M., Elumalai, N.K. et al., 2017a, "High performance semitransparent organic solar cells with 5% PCE using non-patterned MoO_3/Ag/MoO_3 anode", Current Applied Physics, 17, 298–305.

Upama, M.B., Wright, M., Elumalai, N.K. et al., 2017, "High-Efficiency Semitransparent Organic Solar Cells with Non-Fullerene Acceptor for Window Application", ACS Photonics 4, 2327–2334.

Upama, M.B., Wright, M., Mahmud, M.A. et al., 2017, "Photo-degradation of high efficiency fullerene-free polymer solar cells", Nanoscale 9, 18788–18797.

Upama, M.B., Wright, M., Puthen-Veettil, B. et al., 2016, "Analysis of burn-in photo degradation in low bandgap polymer PTB7 using photothermal deflection spectroscopy", RSC Advances, 6, 103899–103904.

Printing and Scale-Up

Aims

The overall aim of this sub-package is to address challenges associated with scale-up of printed solar films. The activities are articulated around the key research area of organic photovoltaics (OPV) with the aim of "lab-to-fab" translation, i.e. accelerating the translation of laboratory-based small-scale results to larger-scale devices using industry-relevant manufacturing methods.

These activities include:

- Expansion of CSIRO's lab-to-fab translation tools.
- Exploration of different materials (ACAP and commercial) for enhanced performance.
- Exploration of a more robust printing process to accelerate progress towards roll-to-roll printed organic solar cells.

Progress

CSIRO's custom-developed mini slot-die coating capabilities were significantly expanded in 2016 with the commissioning of four new mini slot-die coaters. The design of these units was refined from previous versions, with additional functionality incorporated in selected units (e.g. thermal control) and improved ease of operation, making them more amenable to utilisation by collaborators. These lab-to-fab translation tools have been utilised this year by ACAP partners from the University of Melbourne (UoM) for their high performing OPV donor material, BQR. Demonstrated high performance on the laboratory scale by spin-coating (glass, 0.1 cm^2) has been translated to mini slot-die coater processing, resulting in devices with a PCE of 6% (glass, 0.1 cm^2) representing 60% of the performance achieved by spin-coating. The BQR material has now been scaled to allow a significantly expanded printing program and has encompassed new work with NIST looking at in situ X-ray analysis of printed (doctor blade) films, as well as preliminary work to date (ongoing in 2018) with Prof Anna Koehler from the University of Bayreuth looking at spectroscopic changes on adding a third component to the printed films to improve performance, stability and durability. Masters student Daniel Kroh from Prof Koehler's group is currently in Melbourne at CSIRO completing a five-month research project printing BQR containing OPV devices (see Figure PP2.1.16).

Investigations on understanding film morphology during the printing process are being conducted in collaboration with Dr Lee Richter at NIST (USA). Dr Richter is an expert in the development of in situ and static X-Ray techniques and we have recently completed a series of preliminary synchrotron-based GiWAX and RSoXs experiments on BQR containing thin films in preparation for a more detailed series of in situ R2R experiments on BQR containing blends.

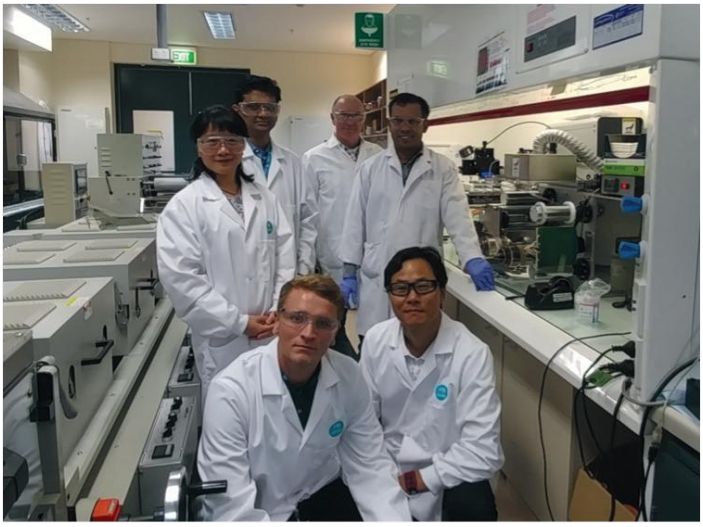

Figure PP2.1.16: Daniel Kroh (Bayreuth, bottom left) in the printing laboratories at CSIRO with Doojin Vac (CSIRO, bottom right) and Mei Gao (CSIRO), Jegadesan Subbiah (UoM), David Jones (UoM) and Hasitha Weerisinghe (CSIRO) back row from left to right.

Figure PP2.1.17: Dr David Jones (left) and Dr Lee Richter (right) during a recent collaborative visit to NIST during the IEEE PVSC-44 in Washington DC.

We have also used CSIRO's printers to investigate PI-4, a commercially available formulation that has been designed and optimised for large-scale roll-to-roll (R2R) fabrication of organic solar cells. In comparison with the previously used P3HT/PCBM blend, this solar ink yields a much better performance and is superior in its processing properties. The initial trial of R2R printed small-scale cells (0.1 cm^2 device area) resulted in a PCE of 4.5%. After further optimisation, this material was successfully translated to the larger-scale R2R printer, leading to a PCE of 3.6% for 100 cm^2 modules, a 38% improvement compared with a P3HT/PCBM blend (2.2%) for devices of the same size. These fully printed 10 cm wide modules were also encapsulated and their stability has been studied under different exposure conditions.

One of the challenges in lab-to-fab translation for organic solar cells is the need for a thicker active film (>150 nm) to compensate for the roughness of the substrate, especially for ITO/PET, in order to avoid shorting. To address this, we have investigated a PPDT2FBT:PC_{70}BM blend which has been reported to give devices with PCEs of 9% at a film thickness over 300 nm. This work, in collaboration with Chonbuk National University of South Korea, resulted in a PCE of 7.1% obtained by continuous R2R hot slot-die coating on flexible substrate. Moreover, unlike the original PCE of 9.3% which was achieved by spin-coating on glass, this outstanding R2R result was achieved in air and without additives. These findings indicate that PPDT2FBT:PC_{70}BM blend has great potential for further scale-up investigations.

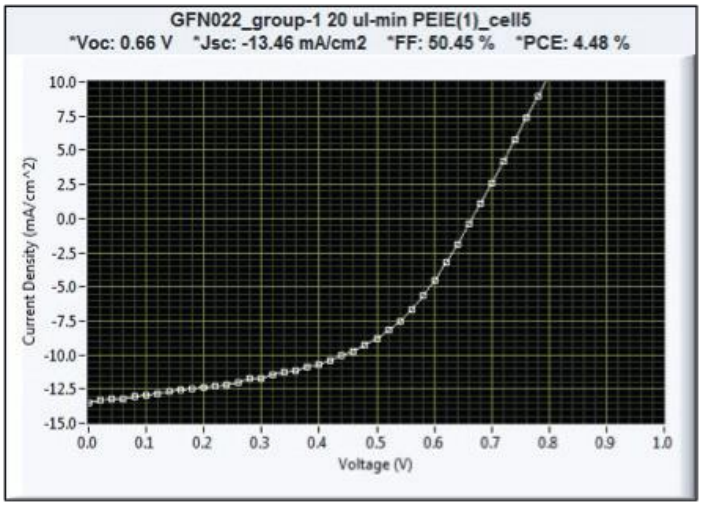

Figure PP2.1.18: Current density-voltage characteristic of the PI-4 polymer solar cell prepared by roll-to-roll printing in air. Device structure: ITO/PET/PEIE/PI-4 solar ink/PEDOT:PSS/Ag (size = 0.1 cm^2).

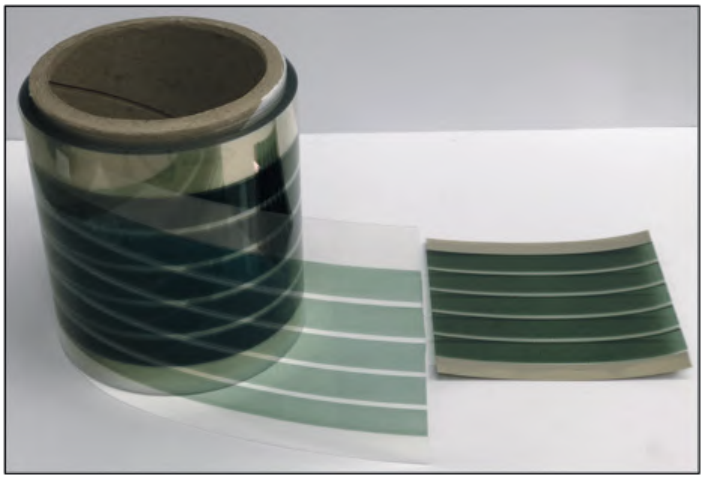

Figure PP2.1.19: Large-scale (10 cm wide) roll-to-roll printed PI-4 film (left) and 10 cm × 10 cm encapsulated working module (right) with PCE of 3.6%.

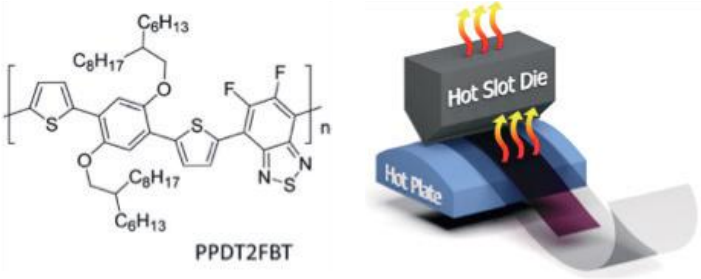

Figure PP2.1.20: Chemical structure of PPDT2FBT donor (left); and schematic drawing of roll-to-roll hot slot-die coating on ITO/PET substrate (right) with which lab-to-fab translation from 9.3% PCE (lab) to a very encouraging 7.1% PCE via roll-to-roll coating was achieved.

PBDB-T:ITIC is a non-fullerene-based polymer solar cell blend, with the PCBM being replaced by ITIC. It is currently the most efficient non-fullerene acceptor used in organic solar cells. Laboratory results of PCE >11% and excellent demonstrated thermal stability motivated CSIRO to explore its feasibility for printing. A bespoke bench-top slot-die coater was used with a well-controlled coating speed, gas blowing rate and coating environment. A PCE of 10% on ITO/glass substrate was achieved, a very promising result and one of the highest reported so far by slot-die coating without the use of additives. The printed active layer was found to be extremely stable after annealing at 160°C in air. This work was also done in collaboration with Chonbuk National University as well as Kunsan National University in South Korea. The small difference in cell efficiencies fabricated by slot-die (10%) and spin coating (11.3%) suggests that non-fullerene-based polymer solar cells have high lab-to-fab translation potential. Further optimisation and R2R trials will be conducted in the next 12 months.

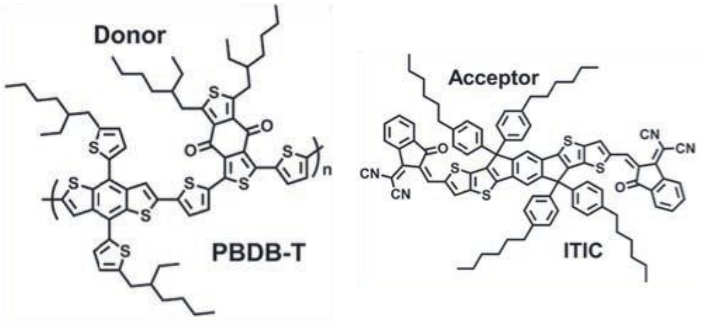

Figure PP2.1.21: Chemical structures of PBDB-T as donor and non-fullerene ITIC as an acceptor which showed excellent lab-to-fab translation with achieved PCE of 10%.

Highlights

- Superior performance using PI-4 solar ink with 3.6% of PCE at 100 cm^2 modules via R2R printing process (compared with previously used standard blend for large-scale OPV printing, i.e. P3HT/PCBM for 2.2% @ 100 cm^2).
- Successful translation of the reported high efficiency material of PPDT2FBT to R2R slot-die coating process with PCE of 7.1% achieved on PET film (compared with 9.3% PCE by spin-coating).
- Excellent result of non-fullerene-based polymer solar cell with 10% PCE via batch processed slot-die coating on glass (compared with 11.3% PCE by spin-coating).
- All printing executed under ambient conditions, thereby satisfying requirements for lower cost, industry-scale production.

Future Work

- Continue optimisation of the PI-4 blend and other commercially available materials (e.g. PI-5 blend) using R2R printing processes.
- R2R coating of PBDB-T:ITIC non-fullerene-based polymer solar cell.
- Further optimise slot-die coating of BQR containing OPV cells to achieve PCE >8%.
- Stability monitoring on fully encapsulated modules.

References

Mitchell, V.D., Wong, W.W.H., Thelakkat, M. and Jones, D.J., 2016, "The synthesis and purification of amphiphilic conjugated donor–acceptor block copolymers", Polym. J., 49(1), 155–161.

https://infinitypv.com/

Nguyen, T.L., Choi, H., Ko, S.J., Uddin, M.A., Walker, B., Yum, S., Jeong, J.E., Yun, M.H., Shin, T.J., Hwang, S., Kim, J.Y. and Woo, H.Y., 2014, "Semi-crystalline photovoltaic polymers with efficiency exceeding 9% in a ~300 nm thick conventional single-cell device", Energy & Environmental Science, 7, 3040–3051.

Zhao, W., Qian, D., Zhang, S., Li, S., Inganäs, O., Gao, F. and Hou, J., 2016, "Fullerene-free polymer solar cells with over 11% efficiency and excellent thermal stability", Advanced Materials, 28, 4734–4739.

Geraghty, P.B., Lee, C., Subbiah, J., Wong, W.W.H., Banal, J.L., Jameel, M.A., Smith, T. and Jones, D.J., 2016, "High Performance p-type Molecular Electron Donors for OPV Applications via alkylthiophene catenation chromophore extension", *Beilstein J. Org. Chem., 12*, 2298–2314.

PP2.1b Organic Tandem Solar Cells

UNSW Team

A/Prof Ashraf Uddin, Prof Gavin Conibeer, Dr Naveen Kumar Elumalai, Dr Matthew Wright, Dr Supriya Pillai, Dr Arman Mahboubi Soufiani, Dr Vinicius R. Goncales

UNSW PhD Students

Arafat Mahmud, Dian Wang, Kah Chan, Faiazul Haque, Haimang Yi, Mushfika Baishakhi Upama, Cheng Xu, Leiping Duan

Funding Support

ACAP, ARENA, ARC, UNSW

Motivation

The advantage of organic-perovskite and organic-organic tandem solar cells is process and material compatibility. The highest improvements in efficiency and durability of a device can be achieved through the proposed tandem device structure by selection of suitable materials and optimisation of device performance. Australia has a number of companies, such as Future Solar Technologies Pty Ltd, with an interest in establishing a manufacturing position in the organic and tandem cells area, with initial applications of organic and tandem cells likely to be in consumer products. The project involves two parallel device fabrication and optimisation streams: (i) perovskite solar cells; and (ii) organic solar cells. The optimised functional units (i) and (ii) are then concatenated via an interconnection layer (ICL) to make a fully functional tandem solar cell. As an example, the design of a perovskite solar cell (stream 1), organic solar cell (stream 2) and tandem solar cell structure are shown in figure PP2.1.22.

Figure PP2.1.22: Schematic device structure of perovskite solar cell (stream 1), organic solar cell (stream 2) and their tandem structure are shown.

The fabrication of a tandem solar cell with the abovementioned configuration necessitates the deposition of a perovskite cell via low temperature processing – in order to maintain the structural integrity of the bottom layer. We are also working on other possible device structures to build the tandem solar cell without using the thermal evaporator, which is quite a challenge. We are currently evaluating all possible options and working on solution processable material systems to fabricate the tandem solar cells.

Aims

(i) Develop a low temperature solution processed technology for perovskite device fabrication – compatible with tandem structures, which has an added advantage for flexible substrates and roll-to-roll (R2R) manufacturing.

(ii) Test novel perovskite materials, along with numerous charge transfer buffer layers including metal oxide nanostructures and polymers for improved photon harvesting and stability.

(iii) Interface engineering of electron transport layer (ETL) to improve the device efficiency and stability.

(iv) Interface engineering of hole transport layer (HTL) to improve the device efficiency and stability.

(v) Develop a process technology for the fabrication of tandem solar cells with perovskite and organic solar cells concatenated together.

Progress

(i) Low temperature solution processed perovskite solar cells

We have developed low temperature processed (<150 °C), highly reproducible perovskite solar cells with sol-gel processed ZnO thin film as the ETL. The optimised ZnO film also provides coherent surface morphology for the proper crystalline growth of the overlying perovskite layer and suppresses the deep trap states existing at the ZnO/perovskite interface. The electronic properties such as contact resistance, recombination resistance, flat-band potential and depletion width of the best performing device have been investigated. The interfacial charge transfer characteristics between methyl ammonium lead triiodide perovskite and low temperature sol-gel ZnO have also been elaborated based on the interface electronic properties.

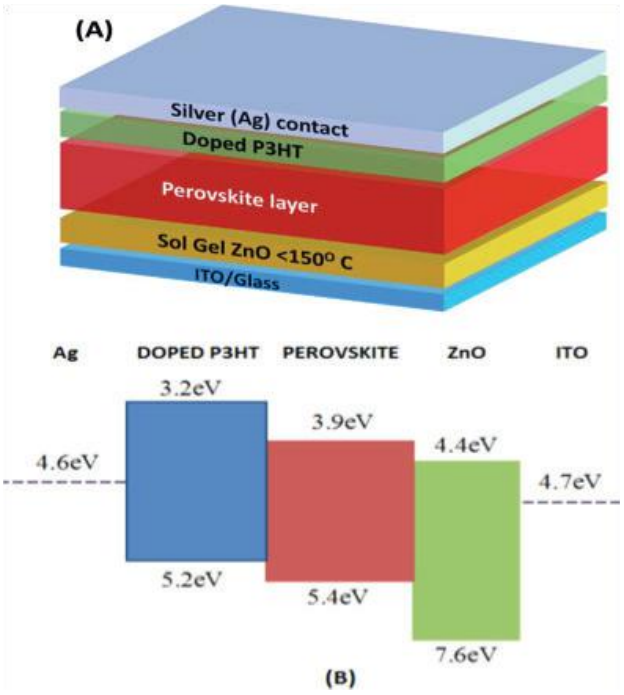

Figure PP2.1.23: (A) Schematic representation of the fabricated device structure at low temperature process; and (B) energy band diagram of the device showing the individual HOMO and LUMO levels with work function of the electrodes.

(ii) Low temperature processed single vs mixed organic cation-based perovskite solar cells

We performed a comparative study between single and mixed organic cation-based $MAPbI_3$ and $MA_{0.6}FA_{0.4}PbI_3$ perovskite devices fabricated in conjunction with low temperature processed (<150 °C) ZnO electron transport layers. A controlled primary nucleation aided restricted volume solvent annealing (RVSA) method was used for the mixed organic cation-based perovskite film for highly efficient (highest PCE: 16.78%) and thermally stable perovskite solar cells (PSCs). To the best of our knowledge, this is the highest efficiency ever reported with PSCs incorporating low temperature processed ZnO as the electron transport layer (ETL). The reported RVSA method raises the degree of supersaturation of the precursor solution due to the high solvent evaporation rate during the crucial primary nucleation phase that ensures smooth and uniform perovskite grain distribution during the rapid crystal growth phase. The enhanced power conversion efficiency (PCE) attained with the RVSA method has been explained with elaborate surface morphology and topography study, along with charge transport analysis with electrochemical impedance spectroscopy and Mott–Schottky analysis.

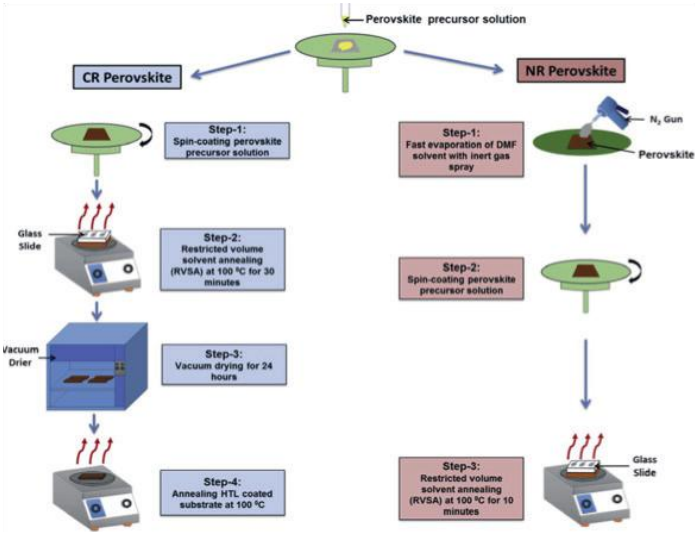

Figure PP2.1.24: The process of fabricating single and mixed organic cation-based $MAPbI_3$ and $MA_{0.6}FA_{0.4}PbI_3$ perovskite films with conventional restricted (CR) volume solvent annealing method (on right) compared to the reported controlled nucleation assisted restricted volume solvent annealing (NR or RVSA) method (on left) on top of identically fabricated sol-gel ZnO film. The NR process includes an inert gas spray step that facilitates fast evaporation of DMF solvent for a high degree of supersaturation at primary perovskite nucleation. CR necessitates an additional vacuum drying step at the post-RVSA phase and an additional annealing session at the post-HTL deposition stage.

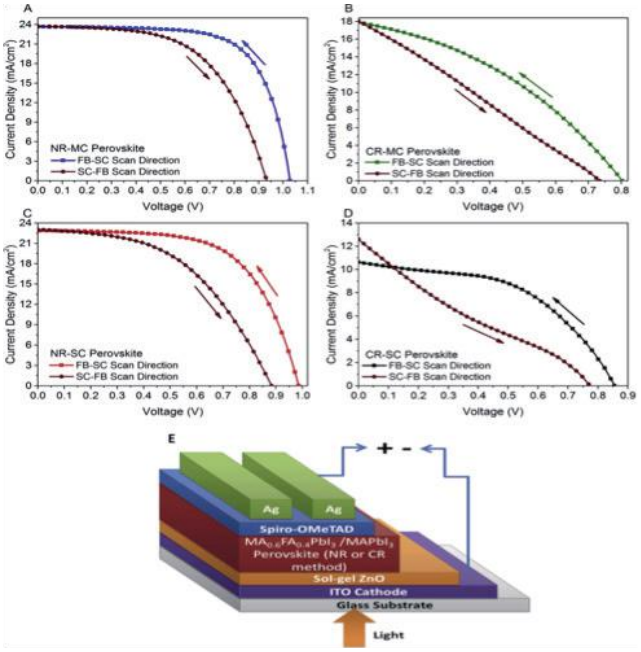

Figure PP2.1.25: Current voltage (J-V) characteristics (both FB-SC and SC-FB direction at 0.2 V/s) of the best performing (A) RSVP process, (B) CR-process, (C) RSVP process and (D) CR process PSCs; and (E) schematic diagram of fabricated PSCs device structure.

(iii) Interface engineering of ETL

We have fabricated the low temperature, solution-processed triple cation-based $MA_{0.57}FA_{0.38}Rb_{0.05}PbI_3$ (MA: methyl ammonium, FA: formamidinium, Rb: rubidium) PSCs by adsorbed carbon nanomaterials at the perovskite/electron transporting layer interface. Carbon derivatives namely fullerene (C_{60}) and $PC_{71}BM$ ([6,6]-phenyl C_{71} butyric acid methyl ester) are employed as adsorbents in conjunction with ZnO and together serve as a bilayer electron transporting layer (ETL). The adsorbed fullerene passivates the interstitial trap-sites of C-ZnO with interstitial intercalation of oxygen atoms in the ZnO lattice structure. C-ZnO ETL-based PSCs demonstrate about a 19% higher average PCE compared to conventional ZnO ETL-based devices. C-ZnO ETL-based PSCs demonstrate a superior device stability retaining about 94% of its initial PCE in the course of a month-long, systematic degradation study conducted. The enhanced device stability with C-ZnO PSCs is attributed to their high resistance to aging-induced recombination phenomena and a water-induced perovskite degradation process, due to a lower content of oxygen related chemisorbed species on the C-ZnO ETL.

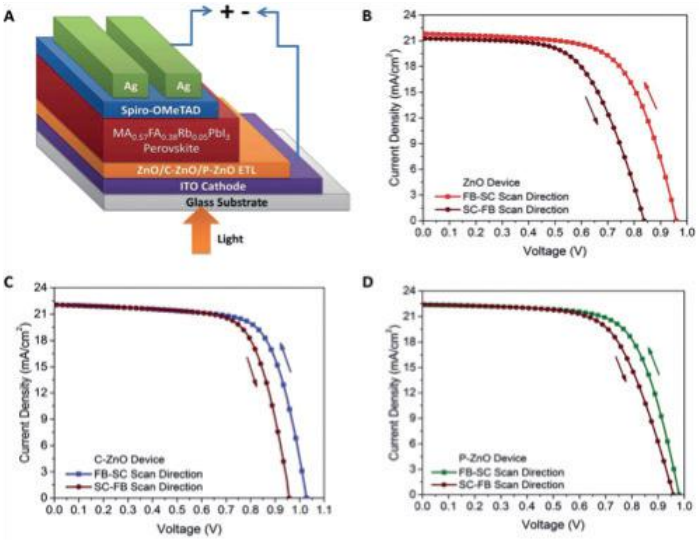

Figure PP2.1.26: (A) Schematic diagram of the fabricated PSCs device structure with ETL ZnO, C-ZnO and (PCBM-based) p-ZnO. Current voltage (J-V) characteristics of (both FB-SC and SC-FB directions at 0.05 V s^{-1}) the best performing of (B) ZnO, (C) C-ZnO and (D) P-ZnO ETL-based PSC devices.

(iv) Interface engineering of HTL

We have fabricated the PSCs with pristine and F4TCNQ doped P3HT as an HTL at low temperature process. All the devices under study were fabricated in ambient conditions. The

F4TCNQ doped P3HT (HTL)-based devices exhibit 14 times higher device stability compared to the conventional Li-TFSI/TBP doped P3HT devices. The underlying mechanism behind the enhanced device lifetime in F4TCNQ doped P3HT (HTL)-based devices was investigated via in-depth electronic, ionic and polaronic characterisation.

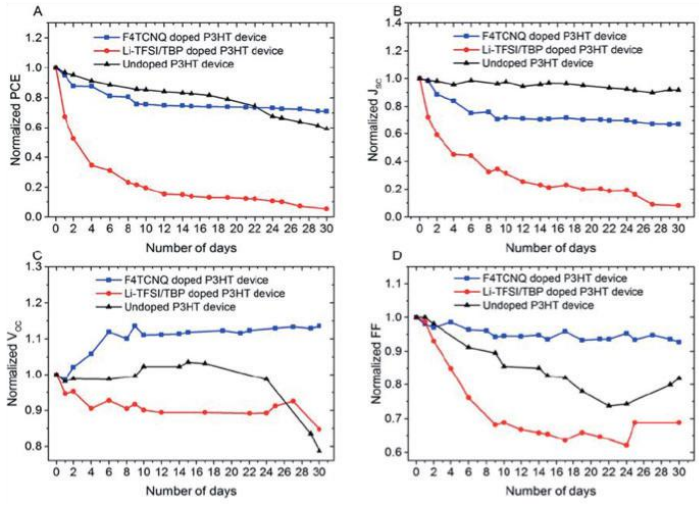

Figure PP2.1.27: Normalised device performances of Li-TFSI/TBP doped P3HT and F4TCNQ doped P3HT HTL devices as a function of sample storage time in an N2 filled glove box. (A) Normalised PCE, (B) normalised J_{SC}, (C) normalised V_{OC} and (D) normalised FF. Overall, F4TCNQ doped P3HT HTL devices show higher device stability compared to Li-TFSI doped P3HT HTL device.

We have investigated the PSCs with vanadium pentoxide (V_2O_5) and Poly(3,4-ethylenedioxythiophene)-poly(styrenesulfonate) (PEDOT: PSS) bilayer (PVO) as a hole transport layer (HTL). The device with PVO bilayer HTL exhibits 20% higher PCE than conventional PEDOT-only devices. The PSCs with PVO bilayer HTL demonstrated superior electronic properties as evaluated using impedance spectroscopy measurements. The recombination resistance of the bilayer-based devices are 57% higher than the reference cells. In addition to high charge selectivity, the bilayer PSCs exhibit low interfacial capacitance originating from electrode polarisation and almost zero hysteresis.

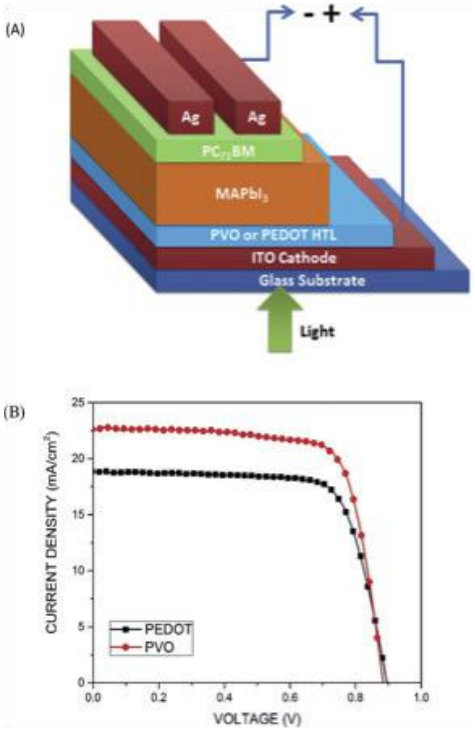

Figure PP2.1.28: (A) Schematic diagram of PSC with PVO or PEDOT:PSS HTL; and (B) current-voltage (I–V) characteristics of PVO and PEDOT-based PSC devices. The PCE of PVO and PEDOT-based devices are 15% and 12.5%, respectively.

Highlights

- Investigation of novel perovskite materials, electron and hole interfacial materials in the device structure.
- Use of advanced characterisation techniques to evaluate the charge transport properties in the bulk and interfaces.
- Development of highly efficient and robust interconnection layers for developing the organic-perovskite and organic-organic tandem solar cells.

Future Work

- Establish reproducible benchmark devices for future improvements.
- Test novel perovskite materials to improve thermal and moisture stability of the devices.
- Evaluate novel interfacial layers including polymers for improved charge selectivity and collection across the electrodes.
- Investigate interfacial compatibility with inorganic and organic materials, develop highly functional metal oxide nanostructures, self-assembling materials for surface modification, quantum dots etc. to improve the PCE and stability.
- Develop state-of-the-art interconnection layers for fabricating organic-perovskite and organic-organic tandem solar cells.

References

Mahmud, M.A., Elumalai, N.K., Upama, M.B., Wang, D.A., Chan, K.H., Wright, M., Xu, C., Hague, F. and Uddin, A., 2017, "Low temperature processed ZnO thin film as electron transport layer for efficient perovskite solar cells", Solar Energy Materials and Solar Cells, 159, 251–264.

Mahmud, M.A., Elumalai, N.K., Upama, M.B., Wang, D.A., Goncales, V.R., Wright, M., Gooding, J.J., Haque, F., Xu, C. and Uddin, A., 2018, "Cesium compounds as interface modifiers for stable and efficient perovskite solar cells", Solar Energy Materials and Solar Cells, 174, 172–186.

Mahmud, M.A., Elumalai, N.K., Upama, M.B., Wang, D.A., Goncales, V.R., Wright, M., Xu, C., Haque, F. and Uddin, A., 2017, "A high performance and low-cost hole transporting layer for efficient and stable perovskite solar cells", Physical Chemistry Chemical Physics, 19(31), 21033–21045.

Mahmud, M.A., Elumalai, N.K., Upama, M.B., Wang, D., Haque, F., Wright, M., Xu, C. and Uddin, A., 2017, "Controlled nucleation assisted restricted volume solvent annealing for stable perovskite solar cells" Solar Energy Materials and Solar Cells, 167, 70–86.

Mahmud, M.A., Elumalai, N.K., Upama, M.B., Wang, D., Haque, F., Wright, M., Chan, K.H., Xu, C. and Uddin, A., 2016, "Enhanced stability of low temperature processed perovskite solar cells via augmented polaronic intensity of hole transporting layer" Physica Status Solidi-Rapid Research Letters, 10(12), 882–889.

Mahmud, M.A., Elumalai, N.K., Upama, M.B., Wang, D., Puthen-Veettil, B., Haque, F., Wright, M., Xu, C., Pivrikas, A. and Uddin, A., 2017, ""Controlled Ostwald ripening mediated grain growth for smooth perovskite morphology and enhanced device performance" Solar Energy Materials and Solar Cells, 167, 87–101.

Mahmud, M.A., Elumalai, N.K., Upama, M.B., Wang, D., Soufiani, A.M., Wright, M., Xu, C., Haque, F. and Uddin, A., 2017, "Solution-Processed Lithium-Doped ZnO Electron Transport Layer for Efficient Triple Cation (Rb, MA, FA) Perovskite Solar Cells" ACS Applied Materials & Interfaces, 9(39), 33841–33854.

Mahmud, M.A., Elumalai, N.K., Upama, M.B., Wang, D., Wright, M., Chan, K.H., Xu, C., Haque, F. and Uddin, A., 2016, ""Single Vs Mixed Organic Cation for Low Temperature Processed Perovskite Solar Cells" Electrochimica Acta, 222, 1510–1521.

Mahmud, M.A., Elumalai, N.K., Upama, M.B., Wang, D., Wright, M., Sun, T., Xu, C., Haque, F. and Uddin, A., 2016, "Simultaneous enhancement in stability and efficiency of low-temperature processed perovskite solar cells" RSC Advances, 6(89), 86108–86125.

Mahmud, M.A., Elumalai, N.K., Upama, M.B., Wang, D., Zarei, L., Goncales, V.R., Wright, M., Xu, C., Haque, F. and Uddin, A., 2018, "Adsorbed carbon nanomaterials for surface and interface-engineered stable rubidium multi-cation perovskite solar cells" Nanoscale, 10(2), 773–790.

Upama, M.B., Elumalai, N.K., Mahmud, M.A., Wang, D., Haque, F., Goncales, V.R., Gooding, J.J., Wright, M., Xu, C. and Uddin, A., 2017, "Role of fullerene electron transport layer on the morphology and optoelectronic properties of perovskite solar cells" Organic Electronics, 50, 279–289.

Wang, D., Chan, K.H., Elumalai, N.K., Mahmud, M.A., Upama, M.B., Uddin, A. and Pillai, S., 2017, ""Interfacial engineering of hole transport layers with metal and dielectric nanoparticles for efficient perovskite solar cells" Physical Chemistry Chemical Physics, 19(36), 25016-25024.

Wang, D., Chan, K. H., Elumalai, N. K., Mahmud, M. A., Upama, M. B., Uddin, A., and Pillai, S., 2017, "Interfacial engineering of hole transport layers with metal and dielectric nanoparticles for efficient perovskite solar cells." Physical Chemistry Chemical Physics, 19(36), 25016–25024.

Wang, D., Elumalai, N.K., Mahmud, M.A., Wright, M., Upama, M.B., Chan, K.H., Xu, C., Haque, F., Conibeer, G. and Uddin, A., 2018, "V2O5-PEDOT: PSS bilayer as hole transport layer for highly efficient and stable perovskite solar cells" Organic Electronics, 53, 66–73.

PP2.2 CZTS solar cells

Lead Partner
UNSW

UNSW Team
Dr Xiaojing Hao, Prof Martin Green, A/Prof Nicholas (Ned) Ekins-Daukes, Dr Fangyang Liu, Dr Yansong Shen, Dr Hongtao Cui, Dr Jialiang Huang, Dr Chang Yan, Dr Fajun Ma, Caiwei Xue

UNSW Students
Kaiwen Sun, Xu Liu, Jongsung Park, Aobo Pu, Yuanfang Zhang, Heng Sun, Xin Cui, Mingrui He

Industry Partner
Baosteel

Other Partners
IREC, IBM, NTU, Corning Research & Development Corp.

Funding Support
ACAP, ARC, Baosteel

Visitors
A/Prof Zhao Fang (Xi'An University of Architecture and Technology, China)

Aim

All successfully commercialised non-concentrating photovoltaic technologies to date are based on silicon or chalcogenides (semiconductors containing Group VI elements, specifically Te, Se and S). The successful chalcogenide materials, CdTe and $Cu(In,Ga)Se_2$ (CIGS), can be regarded as "synthetic silicon" where the balance between atoms in these materials provides the same average number of valence band electrons as in silicon, resulting in the same tetrahedral coordination (see Figure PP2.2.1). Cd and Se are toxic while Te and In are among the 12 most scarce elements in Earth's crust. These factors would seem to clearly limit the long-term potential of the established chalcogenide technologies. By delving more deeply into the Periodic Table, an alternative option can be uncovered with the same number of valence band electrons on average but involving only Earth-abundant, non-toxic elements.

Kesterite Cu_2ZnSnS_4 (CZTS) compound semiconductor has emerged, based on such reasoning, as a promising candidate for thin-film solar cells. Analogous to the chalcopyrite structure of CIGS, CZTS shares similar optical and electrical properties. CZTS has a bandgap of around 1.5 eV, a large absorption coefficient of over $10^4\,cm^{-1}$. Notable is that the bandgap of the CZTS family can be tuned to span a wide range beyond 2.25 eV, even above the accessible range of the highest efficiency III-V cells. This makes the material suitable for tandem cells. For thin-film solar cells, energy conversion efficiency up to 12.6% and 11% have been achieved so far for CZTSSe and CZTS solar cells by IBM and UNSW, respectively.

Classification	Efficiency (%)	Area (cm^2)	V_{oc} (V)	J_{sc} (mA/cm^2)	Fill Factor (%)	Test Centre (date)	Description
Cells (silicon)							
Si (crystalline)	25.0 ± 0.5	4.00 (da)	0.706	42.7[a]	82.8	Sandia (3/99)[b]	UNSW p-type PERC top/rear contacts[40]
Si (crystalline)	**25.7 ± 0.5[c]**	**4.017 (da)**	**0.7249**	**42.54[d]**	**83.3**	**FhG-ISE (3/17)**	**FhG-ISE, n-type top/rear contacts[41]**
Si (large)	**26.6 ± 0.5**	**179.74 (da)**	**0.7403**	**42.5[d]**	**84.7**	**FhG-ISE (11/16)**	**Kaneka, n-type rear IBC[5]**
Si (multicrystalline)	21.3 ± 0.4	242.74 (t)	0.6678	39.80[e]	80.0	FhG-ISE (11/15)	Trina Solar, large p-type[42]
Cells (III-V)							
GaInP	21.4 ± 0.3	0.2504 (ap)	1.4932	16.31[f]	87.7	NREL (9/16)	LG Electronics, high bandgap[43]
Cells (chalcogenide)							
CIGS (thin-film)	22.6 ± 0.5	0.4092 (da)	0.7411	37.76[f]	80.6	FhG-ISE (2/16)	ZSW on glass[44]
CIGSS (Cd free)	**22.0 ± 0.5**	**0.512 (da)**	**0.7170**	**39.45[f]**	**77.9**	**FhG-ISE (2/16)**	**Solar Frontier on glass[12]**
CdTe (thin-film)	22.1 ± 0.5	0.4798 (da)	0.8872	31.69[g]	78.5	Newport (11/15)	First Solar on glass[45]
CZTSS (thin-film)	12.6 ± 0.3	0.4209 (ap)	0.5134	35.21[h]	69.8	Newport (7/13)	IBM solution grown[46]
CZTS (thin-film)	**11.0 ± 0.2**	**0.2339(da)**	**0.7306**	**21.74[d]**	**69.3**	**NREL (3/17)**	**UNSW on glass[14]**
Cells (other)							
Perovskite (thin-film)	22.1 ± 0.7[i]	**0.0946 (ap)**	1.105	24.97[i]	80.3	Newport (3/16)	KRICT/UNIST[17]
Organic (thin-film)	**12.1 ± 0.3[k]**	**0.0407 (ap)**	**0.8150**	**20.27[d]**	**73.5**	**Newport (2/17)**	**Phillips 66**

Table PP2.2.1: "Top 10" confirmed cell and modules results not class records under the global AM1.5 spectrum (1000 Wm-2) at 25 oC (IEC 60904-3: 2008, ASTM G-173-03 global) (Table from Solar Cell Efficiency Tables (version 51) (M.A. Green and et al., Prog. Photovolt. Res Appl., 2018, 26:3-12).

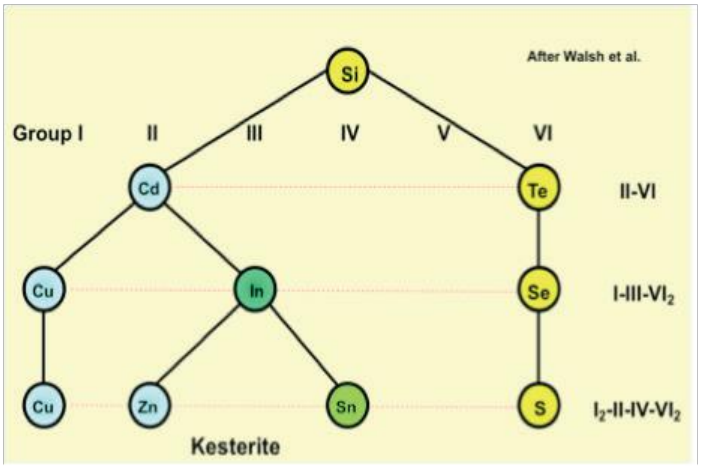

Figure PP2.2.1: The schematic of "Synthetic Si" showing how the CZTS is derived.

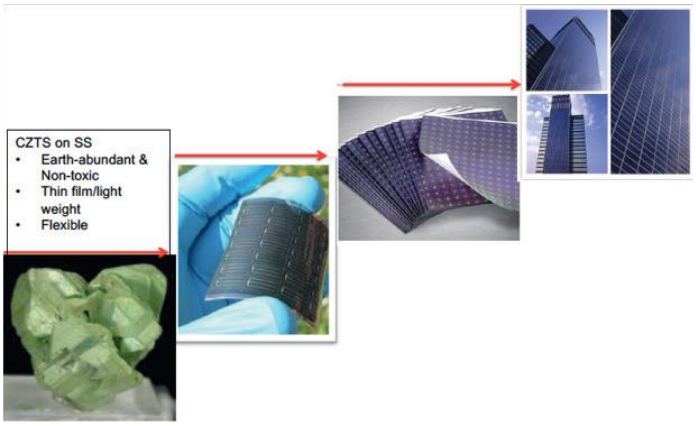

Figure PP2.2.2: Flexible CZTS solar cells on stainless steel.

ACAP's work in the CZTS area takes the sputtering fabrication direction, a low-cost, high-throughput and upscalable manufacturing process which has been used in the commercialised high performance CIGS solar cells. In this regard, CZTS offers a realistic potential to achieve the efficiency levels required for transferring lab-scale processes to commercialisation in the short term, since it is fully compatible with current CIGS production lines. Using kesterite materials less than two micron-thick, cells can be flexible and integrated into buildings (BIPV) (see Figure PP2.2.2), harvesting light and reducing greenhouse emissions.

Work in this strand includes the development of high efficiency CZTS solar cells on soda lime glass and flexible stainless steel.

Progress

Based on the absorber and interface engineering strategies developed in 2015 and 2016, we demonstrated certified beyond 10% efficiency CZTS solar cells by heterojunction engineering in 2017. This breaks our previous world record efficiency of 9.5%, marking a milestone for high bandgap CZTS solar cells as the record power conversion efficiency of CZTS devices has been stagnant at around 9% for several years. The highest in-house measured CZTS cell efficiency is 11.5% and certified performance by NREL is 11% (see Table PP2.2.1). This certified 11% efficiency is included in the Solar Cell Efficiency Tables (version 50 and version 51, Green et al., Prog. Photovolt. Res Appl., 2018, 26:3–12). Our analysis shows that the efficiency improvement mainly results from the reduced non-radiative recombination. A paper resulted from this record cell and understandings of underlying mechanism is under review by Nature Energy. With the same approach, we also demonstrate a certified centimetre-scale (1.11 cm^2) 10% efficiency CZTS solar cell, which is the first kesterite cell (including selenium-containing) of standard centimetre size breaking the 10% efficiency barrier (see Table PP2.2.2). This 10% efficiency standard-sized CZTS cell is also included in the Solar Cell Efficiency Tables (version 50 and version 51).

Based on the electrical properties of CZTS characterised by NREL and UNSW, the performance loss mechanisms of current champion CZTS solar cells is analysed by the established Sentaurus TCAD device simulation based on the combination of experimental characterisation results and empirical data from literature. The heterojunction recombination is likely to still dominate the V_{OC} deficit. More detailed performance loss analysis is currently under investigation by more detailed electrical properties measurement.

Classification	Efficiency (%)	Area (cm^2)	V_{oc} (V)	J_{sc} (mA/cm^2)	Fill Factor (%)	Test Centre (date)	Description
Silicon							
Si (crystalline cell)	**26.7 ± 0.5**	**79.0 (da)**	**0.738**	**42.65[a]**	**84.9**	**AIST (3/17)**	**Kaneka, n-type rear IBC[5]**
Si (multicrystalline cell)	**21.9 ± 0.4[b]**	**4.0003 (t)**	**0.6726**	**40.76[a]**	**79.7**	**FhG-ISE (2/17)**	**FhG-ISE, n-type[6]**
Si (thin transfer submodule)	21.2 ± 0.4	239.7 (ap)	0.687[c]	38.50[c,d]	80.3	NREL (4/14)	Solexel (35 μm thick)[7]
Si (thin film minimodule)	10.5 ± 0.3	94.0 (ap)	0.492[c]	29.7[c]	72.1	FhG-ISE (8/07)[e]	CSG Solar (<2 μm on glass)[8]
III-V cells							
GaAs (thin film cell)	28.8 ± 0.9	0.9927 (ap)	1.122	29.68[f]	86.5	NREL (5/12)	Alta Devices[9]
GaAs (multicrystalline)	18.4 ± 0.5	4.011 (t)	0.994	23.2	79.7	NREL (11/95)	RTI, Ge substrate[10]
InP (crystalline cell)	**24.2 ± 0.5[b]**	**1.008 (ap)**	**0.939**	**31.15[a]**	**82.6**	**NREL (9/12)**	**NREL[11]**
Thin film chalcogenide							
CIGS (cell)	**21.7 ± 0.5**	**1.044 (da)**	**0.718**	**40.70[a]**	**74.3**	**AIST (1/17)**	**Solar Frontier[12]**
CdTe (cell)	21.0 ± 0.4	1.0623 (ap)	0.8759	30.25[d]	79.4	Newport (8/14)	First Solar, on glass[13]
CZTS (cell)	**10.0 ± 0.2**	**1.113 (da)**	**0.7083**	**21.77[a]**	**65.1**	**NREL (3/17)**	**UNSW[14]**
Amorphous/microcrystalline							
Si (amorphous cell)	10.2 ± 0.3[g,b]	1.001 (da)	0.896	16.36[d]	69.8	AIST (7/14)	AIST[15]
Si (microcrystalline cell)	**11.9 ± 0.3[b]**	**1.044 (da)**	**0.550**	**28.72[a]**	**75.0**	**AIST (2/17)**	**AIST[16]**
Perovskite							
Perovskite (cell)	19.7 ± 0.6[g,h]	0.9917 (da)	1.104	24.67[i]	72.3	Newport (3/16)	KRICT/UNIST[17]
Perovskite (minimodule)	**16.0 ± 0.4[g,h]**	**16.29 (ap)**	**1.029[c]**	**19.51[c,a]**	**76.1**	**Newport (4/17)**	**Microquanta, 6 serial cells[18]**
Dye sensitised							
Dye (cell)	11.9 ± 0.4[j]	1.005 (da)	0.744	22.47[k]	71.2	AIST (9/12)	Sharp[19]
Dye (minimodule)	10.7 ± 0.4[j]	26.55 (da)	0.754[c]	20.19[c,j]	69.9	AIST (2/15)	Sharp, 7 serial cells[19]
Dye (submodule)	8.8 ± 0.3[j]	398.8 (da)	0.697[c]	18.42[c,m]	68.7	AIST (9/12)	Sharp, 26 serial cells[20]
Organic							
Organic (cell)	11.2 ± 0.3[n]	0.992 (da)	0.780	19.30[d]	74.2	AIST (10/15)	Toshiba[21]
Organic (minimodule)	9.7 ± 0.3[n]	26.14 (da)	0.806	16.47[c,j]	73.2	AIST (2/15)	Toshiba (8 series cells)[22]

Table PP2.2.2. Confirmed single-junction terrestrial cell and submodule efficiencies measured under the global AM1.5 spectrum (1000 Wm-2) at 25 oC (IEC 60904-3: 2008, ASTM G-173-03 global). (Table from Solar Cell Efficiency Tables (version 51) [M.A. Green and et al., Prog. Photovolt. Res Appl., 2018; 26:3-12].

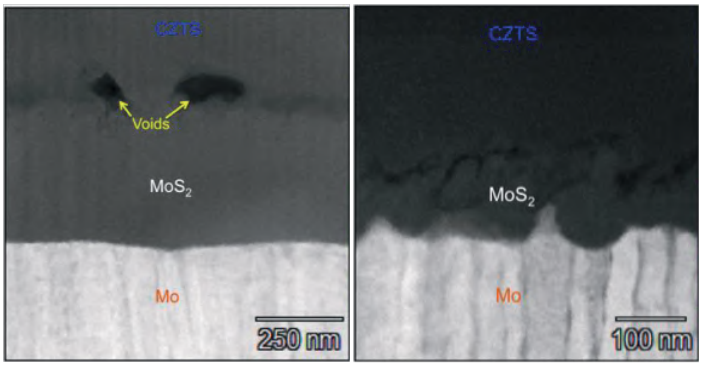

Figure PP2.2.3: Cross-sectional TEM images for back contact regions of CZTS devices without (left) and with (right) Al_2O_3 intermediate layer.

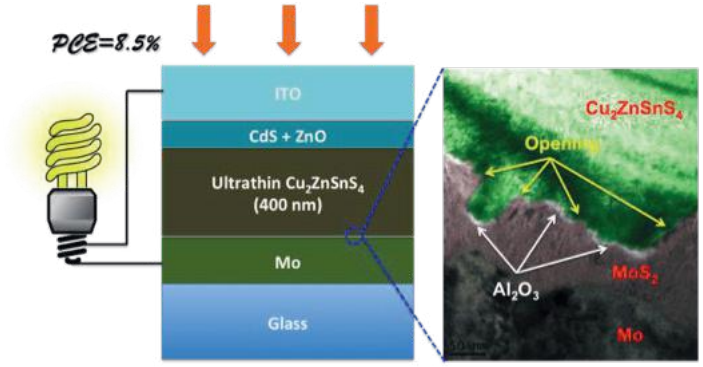

Figure PP2.2.4: Schematic of ultrathin CZTS solar cells.

Two key interface engineering strategies developed in 2016 were the use of Al_2O_3 at the interface of back contact and CZTS absorber, and the development of $Zn_xCd_{1-x}S$ buffer materials replacing CdS buffer. The former intermediate Al_2O_3 layer at the back contact results in a significant improvement in the film quality of CZTS absorber, solving the traditional problems of voids, secondary phases and highly resistive thick MoS_x resulting from the reaction between CZTS absorber and Mo back contact (see Figure PP2.2.3). This enables 8.4% efficiency ultrathin CZTS solar cells with the absorber thickness of 400 nm (see Figure PP2.2.4) and our first world record 7.6% efficiency standard-sized CZTS solar cells. The latter $Zn_xCd_{1-x}S$ buffer enables a more favourable conduction bad alignment (see Figure PP2.2.5), resulting in significant V_{oc} improvement (see Figure PP2.2.6) and our previous world record 9.5% efficiency CZTS solar cells (listed in the Solar Cell Efficiency Tables (version 49) (see Figure PP2.2.7)). In 2017, the interface engineering strategy has been further advanced.

Following the collaboration with Nanyang Technological University on the Cd-free buffer, we set up the atomic layer deposited-$Zn_{1-x}Sn_xO$ (ALD-ZTO) baseline at UNSW to address the V_{OC} deficit issue in CZTS solar cells. Compared with CBD-CdS buffer, a more favourable band alignment of CZTS/ZTO is formed resulting in increased V_{OC} by up to 10% through optimising the composition of ZTO (see Figure PP2.2.8). Further optimisation on the ZTO thickness, we demonstrated 9.3% efficiency CZTS solar cells, which is the highest reported for Cd-free pure sulphide CZTS solar cells to the best of our knowledge (see Figure PP2.2.9).

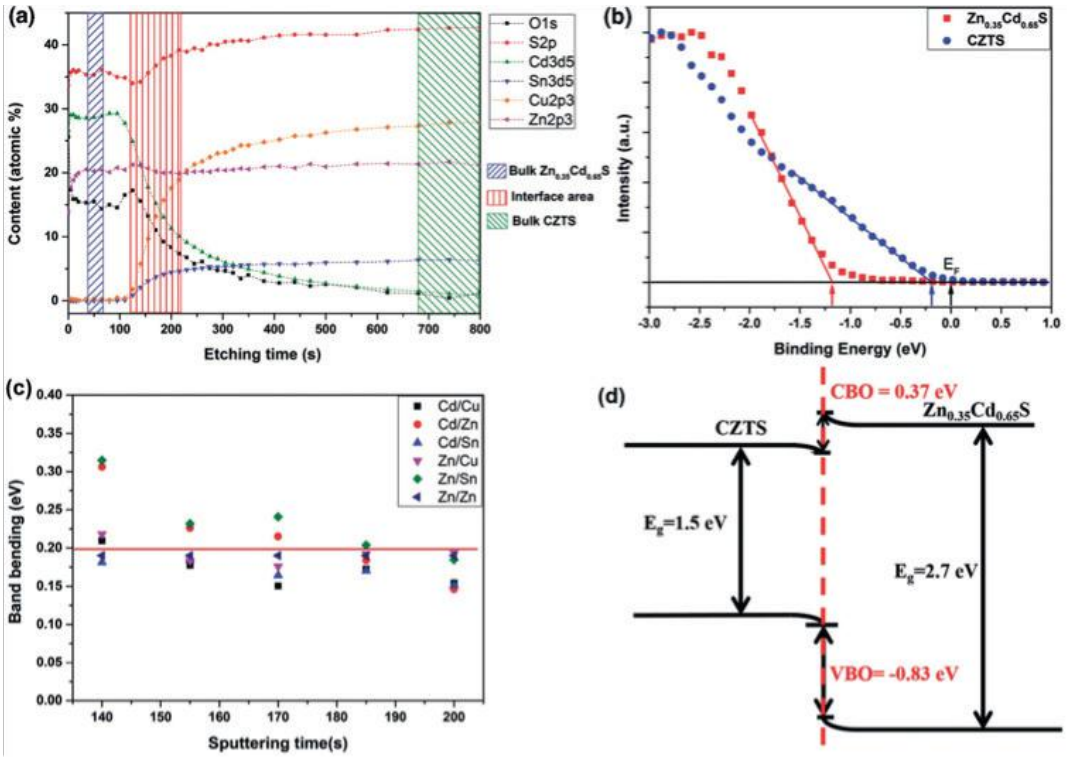

Figure PP2.2.5: a) The XPS composition profile from $Zn_{0.35}Cd_{0.65}S$ to CZTS as a function of sputtering time. According to composition profile, the blue, red, and green area can be regarded as bulk $Zn_{0.35}Cd_{0.65}S$, interface, and bulk CZTS area, respectively. b) Normalized VB data of CZTS/$Zn_{0.35}Cd_{0.65}S$ heterojunctions measured by XPS. Binding energies are measured with respect to the Fermi energy (EF). c) Band bending as a function of sputtering time shown for six data sets. d) Schema of the band alignment at CZTS/$Zn^{0.35}Cd_{0.65}S$ interface. Values of the VBO, CBO, and E_g are indicated.

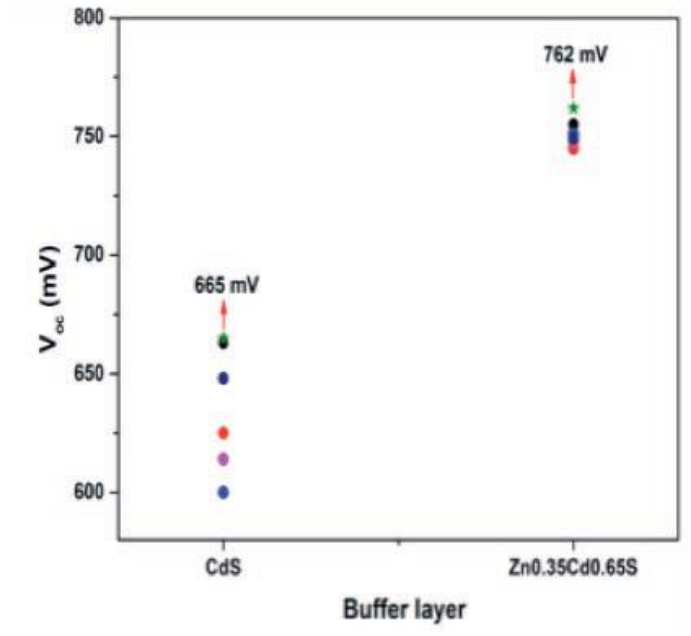

Figure PP2.2.6: The Voc of CZTS solar cells as a function of Zn content of $Zn_xCd_{1-x}S$ buffer.

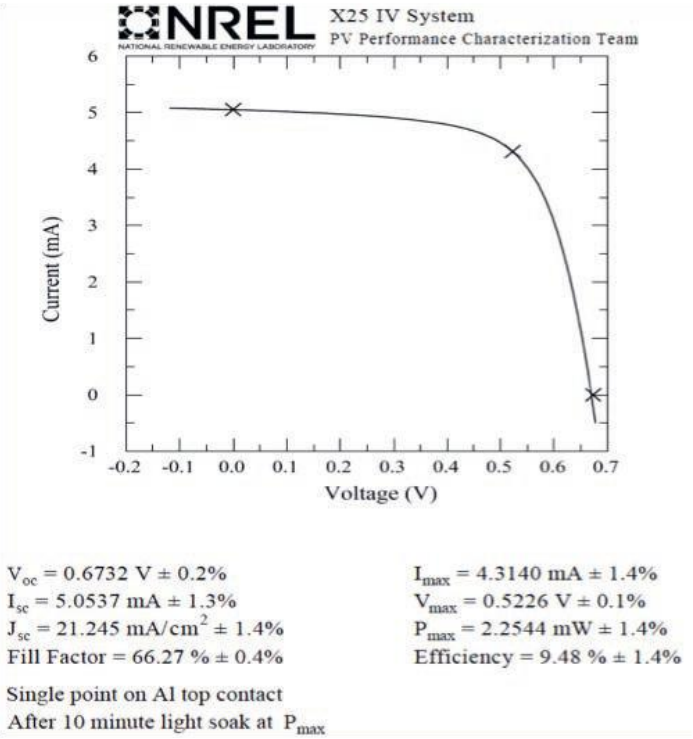

Figure PP2.2.7: Certified J-V characteristic of 9.5% efficiency CZTS solar cells.

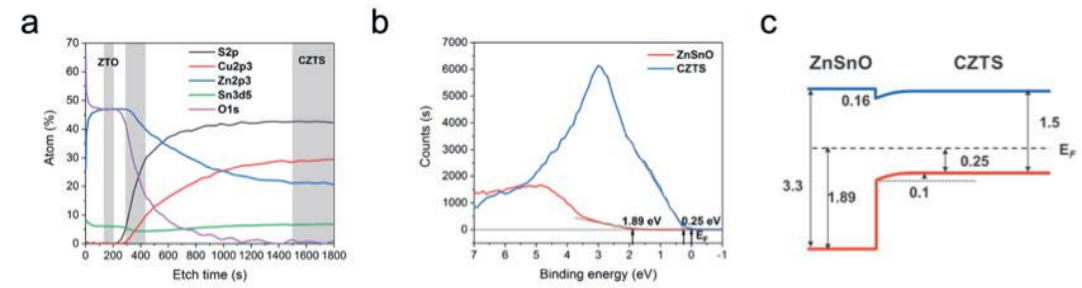

Figure PP2.2.8: (a) The XPS composition profile for CZTS cells with ZnSnO emitter. (b) Normalized VB data of CZTS/$Zn_{0.77}Sn_{0.23}O$ heterojunction measured by XPS. Binding energies are measured with respect to the Fermi energy (EF). (c) Schematic of the band alignment at CZTS/$Zn_{0.77}Sn_{0.23}O$ interface.

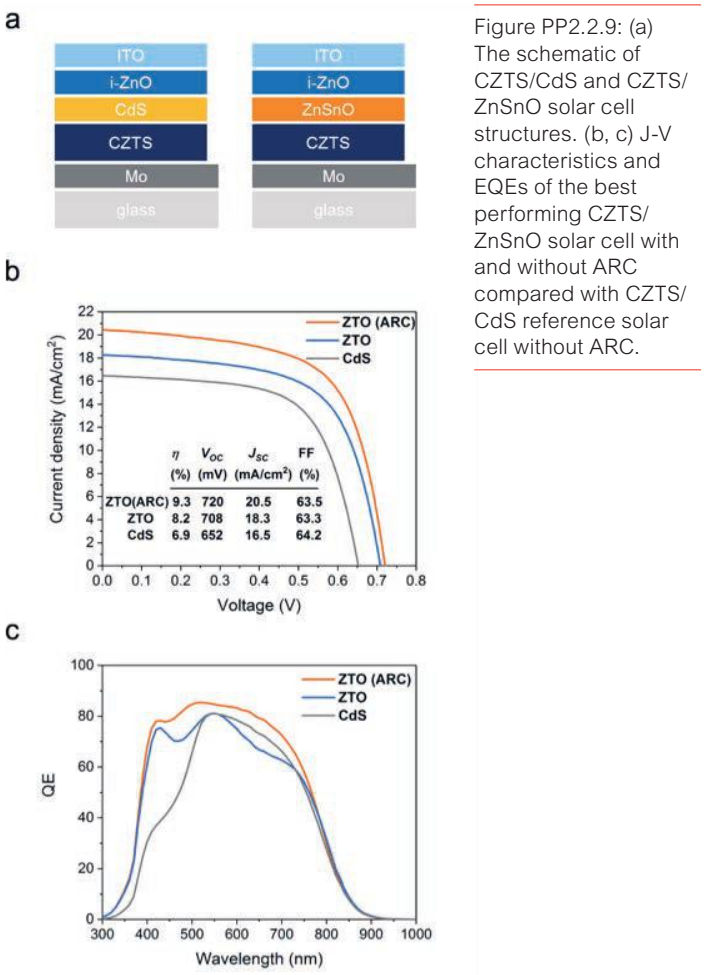

Figure PP2.2.9: (a) The schematic of CZTS/CdS and CZTS/ZnSnO solar cell structures. (b, c) J-V characteristics and EQEs of the best performing CZTS/ZnSnO solar cell with and without ARC compared with CZTS/CdS reference solar cell without ARC.

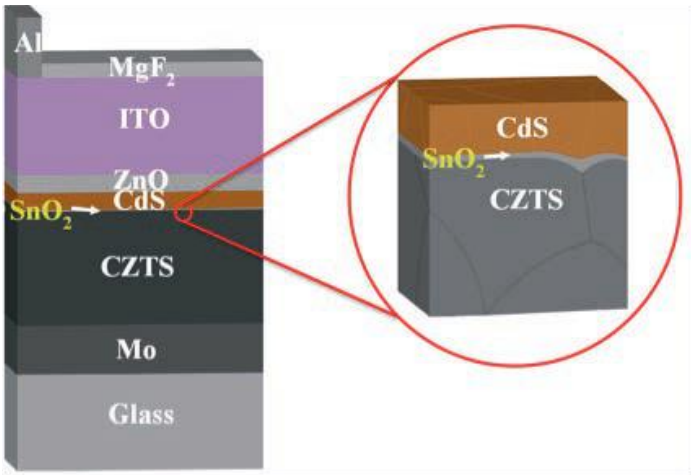

Figure PP2.2.10: Schematic of device structures with details of CdS/SnO_2/CZTS heterojunctions (not to scale).

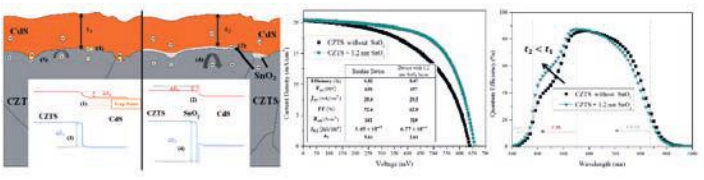

Figure PP2.2.11: Schematic of band alignment (left), J-V curve (middle) and EQE spectra (right) of CZTS devices with and without SnO_2 passivation layer at CZTS/CdS heterojunction interface.

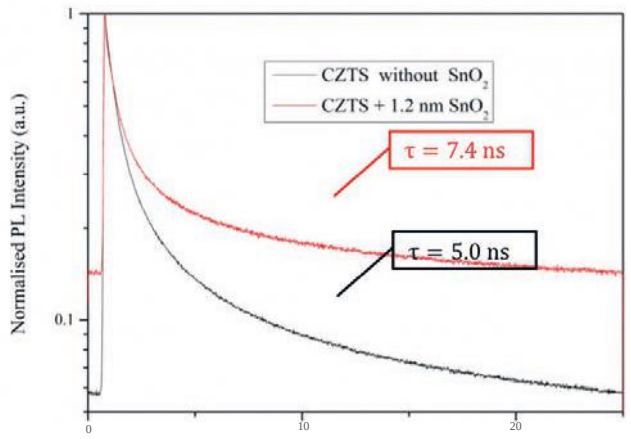

Figure PP2.2.12: (a) TRPL transient of reference CZTS device and the device with a 1.2 nm SnO_2 at the CZTS/CdS heterointerface, with 470 nm excitation wavelength.

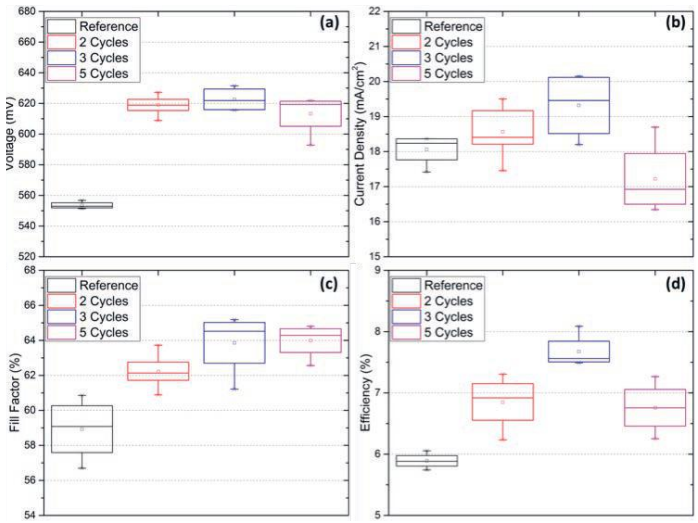

Figure PP2.2.13: J-V characteristics of the CZTS devices with different cycles ALD-Al_2O_3 on absorber layer.

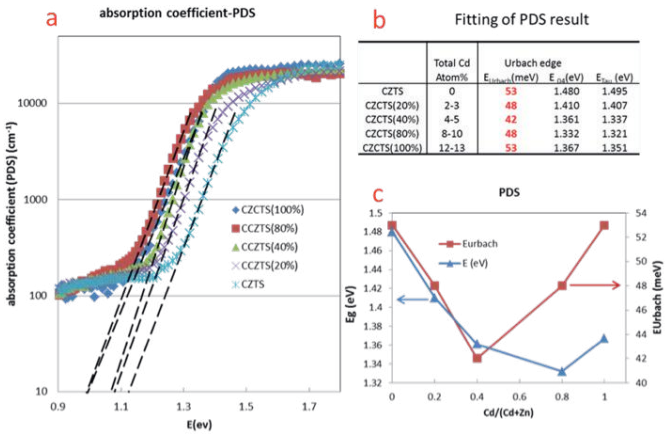

Figure PP2.2.14: (a) Absorption coefficient vs. photo energy of different Cd alloy concentration determined by PDS measurement, (b) table of the fitting result of the Urbach energy and band-gaps and (c) plot of the dependence of bandgap and Urbach energy on Cd ratio.

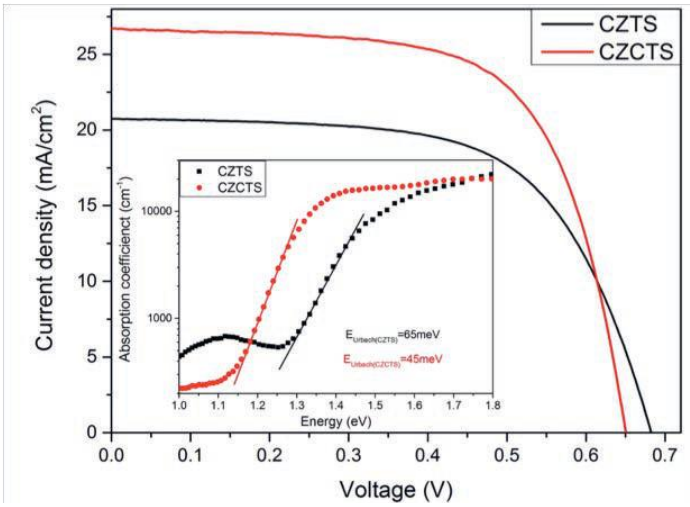

Figure PP2.2.15: J-V characteristic of CZTS and CZCTS (with Cd alloying) with inset showing estimated Urbach energy from PDS measurement.

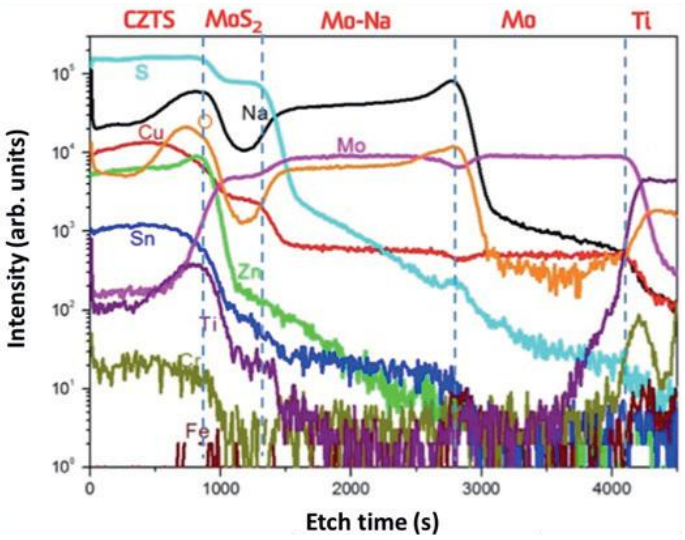

Figure PP2.2.16: TOF-SIMS depth compositional profiles of relevant elements for CZTS absorbers on optimised back contact configurations. (showing Ti barrier is effective in blocking Fe diffusion from stainless steel; Moderate diffusion of Ti accumulates at the bottom of the CZTS absorber; O element correlates with Na in the CZTS absorber)

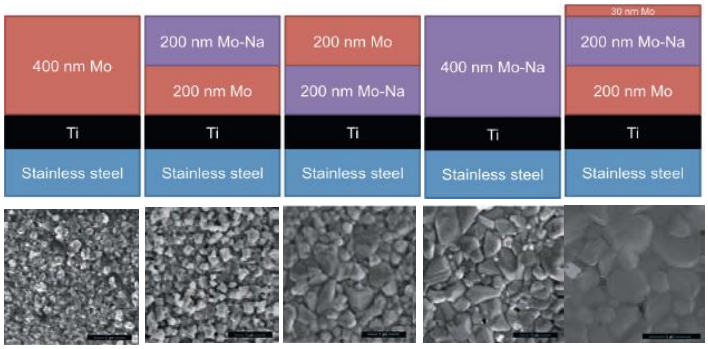

Figure PP2.2.17: J Schematics of different back contact configurations and SEM images of the CZTS absorber consequently.

Strategies for passivating the CdS/CZTS heterojunction interface are further explored. The ultrathin SnO_2 intermediate layer deposited by a successive ionic layer adsorption and reaction (SILAR) method was introduced into the hetero-interface of CZTS/CdS for interface defect passivation (see Figure PP2.2.10). CZTS solar cells with SnO_2 intermediate layers show higher open circuit voltage and fill factor compared to their counterpart cells without the SnO_2 intermediate layer, resulting in increased overall efficiency (see Figure PP2.2.11). The passivation effect is further affirmed by the improved carrier lifetime (see Figure PP2.2.12). ALD-Al_2O_3 is also studied as the interface passivation materials for CdS/CZTS heterojunction. The improved V_{OC} of CZTS solar cells agrees with previous reports (see Figure PP2.2.13). However, it is found that the effective role of ALD- Al_2O_3 in improving the V_{OC} of CZTS is not from Al_2O_3, which is different from previous reports. The revised paper resulting from this work is under review by Advanced Energy Materials. More detailed work is currently carried out to further optimise this process.

Zn/Cu disordering has been regarded as one of the major factors contributing to the V_{OC} loss of CZTS solar cells. Cd alloying, partially replacing Zn, is found capable of reducing the disordering. Photothermal deflection spectroscopy (PDS) measurement is used to reveal the correlation between disordering induced band tailing and Cd alloy amount. Urbach energy decreases and thus the band tailing problem is relieved with a certain amount of Cd alloying (see Figure PP2.2.14). The analysis of Z-contrast HADDF STEM images provides direct evidence of Cd participating in the CZTS lattice. With Cd-alloying, we report the beyond 11% efficient Cd-alloyed sulphide CCZTS ($Cu_2Zn_xCd_{1-x}SnS_4$) solar cell fabricated by combining sputtering and chemical bath deposition (CBD) method (see Figure PP2.2.15).

For CZTS solar cells grown on stainless steel, Na supply is realised by using Na-doped Mo (Mo-Na) back contact. While finding that direct contact of CZTS and Mo-Na layer leads to poor homogeneity and adhesion, a better back contact configuration with a Mo capping layer on Mo-Na layer is found helpful to maintain the advantages of Mo back contact while achieving well-controlled MoS_2 interface layer thickness. By integrating developed strategies for CZTS solar cells on stainless steel, such as stainless steel surface treatment, Ti barrier layer (see Figure PP2.2.16), Na-doped back contact (see Figure PP2.2.17), optimised sulfurisation process, ion soaking as well as buffer materials, we obtain around 8% efficiency flexible CZTS solar cells on 50 um thick stainless steel. However, this efficiency is still far lower than that on traditional soda line glass substrate with over 10% efficiency. Further investigation to optimise the Na profile, especially enhancing the Na incorporation at surface region and to reduce the interface recombination is needed for high energy conversion efficiency of flexible kesterite CZTS solar cells.

Highlights

- Following the two world record CZTS solar cells achieved in 2016, we established another two world record CZTS solar cells in 2017.
  - Established the confirmed world record 10% efficiency CZTS solar cell (total cell area 1.1 cm^2), which is certified by NREL and recorded in the Solar Cell Efficiency Tables (version 50 and version 51).
  - Established the confirmed world record 11% efficiency CZTS solar cell (total cell area 0.24 cm^2), which breaks our previous 9.5% record, certified by NREL and recorded in the Solar Cell Efficiency Tables (version 50 and version 51).

- Developed baseline of the Cd-free ALD-ZTO buffer and demonstrated 9.3% in-house measured Cd-Free CZTS solar cells, which is the highest reported so far for Cd-free CZTS solar cells.
- Developed several strategies of transferring CZTS solar cell technologies to stainless steel for BIPV application. Demonstrated around 8% efficiency CZTS solar cells on flexible stainless steel. The major performance loss from that on soda lime glass is analysed.

Future Work

Future work in 2018 will be focused on further improving the efficiency of CZTS solar cells to beyond 12%. Strategies will be developed to further reduce the V_{OC} deficit, such as integration of developed new buffer materials, band grading, surface passivation and further our understandings of the origin of short minority carrier lifetime and V_{OC} deficit.

References

Crovetto, A., Yan, C., Zhou, F., Stride, J., Schou, J., Hao, X.J. and Hansem, O., 2016, "Lattice-matched Cu2ZnSnS4/CeO2 solar cell with open circuit voltage boost", Applied Physics Letters, Vl.109, (23), DOI: 10.1063/1.4971779.

Gu, Y., Shen, H., Ye, C., Dai, X., Cui, Q., Li, J., Hao, F., Hao, X.J. and Lin H., 2018, "All solution-processed Cu2ZnSnS4 solar cell with self-depleted Na_2S back contact modification layer", Advanced Function Materials, DOI: 10.1002/adfm.201703369.

Huang, J., Yan, C., Sun, K., Liu, F., Sun, H., Pu, A., Green, M.A. and Hao X.J., 2018, "Boosting the kesterite Cu2ZnSnS4 solar cells performance by diode laser annealing", Solar Energy Materials and Solar Cells, 175, 71–76.

Liu, F., Huang, J., Sun, K., Yan, C., Shen, Y., Park, J., Pu, A., Zhou, F., Liu, X., Stride, J.A., Green, M.A. and Hao, X.J., 2017, "Beyond 8% ultrathin kesterite Cu2ZnSnS4 solar cells by interface reaction route controlling and self-organised nano-pattern at the back contact", NPG Asian Materials, 9, e401, doi:10.1038/am.2017.103

Liu, F., Yan, C., Sun, K., Zhou, F., Hao, X.J. and Green, M.A., 2017, "Light bias-dependent External Quantum Efficiency of Kesterite Cu2ZnSnS4 Solar Cells", ACS Photonics, DOI: 10.1021/acsphotonics.7b00151.

Liu, X., Cui, H., Hao, X.J., Huang, S. and Conibeer, G., "The effect of vacuum thermal annealing on the molybdenum bilayer back contact deposited by radio-frequency magnetron sputtering for chalcogenide and kesterite solar cells", Journal of the Korean Physical Society, 71(12), 968–973.

Park, J., Huang, J., Sun, K., Ouyang, Z., Liu, F., Yan, C., Sun, H., Pu, A., Green M.A. and Hao X.J., 2018, "The effect of thermal evaporated MoO3 intermediate layer as primary back contact for kesterite Cu2ZnSnS4 solar cells", Thin Solid Films, 648, 39–45.

Park, J., Kim, D., Chen, S., Huang, J., Liu, F., Zi, O., Sun, H., Yan, C., Kim, K., Yun, J., Seidel, J., Green, M.A. and Hao X.J., "The role of hydrogen from ALD-Al2O3 in kesterite Cu2ZnSnS4 solar cells: surface and grain boundary passivation", Advanced Energy Materials, (under review).

Pu, A., Ma, F., Yan, C., Huang, J., Sun, K., Green, M. and Hao X.J., 2017, "Sentaurus modelling of 6.9% Cu2ZnSnS4 device based on comprehensive electrical & optical characterisation", Solar Energy Materials and Solar Cells, 160, 372–381.

Sun, H., Sun, K., Huang, J., Yan, C., Liu, F., Park, J., Pu, A., Stride, J., Green, M.A. and Hao X.J., 2018, ""Efficiency enhancement of kesterite Cu2ZnSnS4 solar cells via solution-processed ultra-thin tin oxide intermediate layer at absorber/buffer interface", ACS Applied Energy Materials, 1(1), 154–160, DOI: 10.1021/acsaem.7b00044.

Sun, K., Huang, J., Yan, C., Pu, A., Liu, F., Sun, H., Liu, X., Stride, J.A., Green M.A. and Hao X.J., "Self-assembled nanometer-scale ZnS structure at the CZTS/ZnCdS hetero-interface for high efficiency wide bandgap Cu2ZnSnS4 solar cells", Chemistry of Materials (under review).

Sun, K., Liu, F., Huang, J., Yan, C., Song, N., Sun, H., Xue, C., Ou, A., Zhang, Y., Shen, Y., Stride, J.A., Green M.A. and Hao X.J., "Sodium-doped molybdenum back contacts for flexible kesterite Cu2ZnSnS4 solar cells on stainless steel substrates", Solar Energy Materials and Solar Cells (revised version under review).

Yan, C., Huang, J., Sun, K., Pu, A., Johnston, S., Zhang, Y., Liu, F., Eder, K., Yang, L., Cairney, J.M., Ekins-Daukes, N.J., Sun, H., Hameiri, Z., Stride, J.A., Chen, S., Green, M.A. and Hao X.J., "Heat treated heterojunction Cu2ZnSnS4 solar cell breaks 10% power conversion efficiency barrier", Nature Energy (under review).

Yan, C., Sun, K., Huang, J., Johnston, S., Liu, F., Veettil, B.P., Sun, K., Pu, A., Zhou, F., Stride, J.A., Green, M.A. and Hao X.J., 2017, "Beyond 11% efficient sulfide kesterite Cu2ZnxCd1-xSnS4 solar cell: effects of cadmium alloying", ACS Energy Letters, 2, (4), 930–936, DOI: 10.1021/acsenergylett.7b00129.

PP2.4a Hot Carrier Cells

Lead Partner
UNSW

UNSW Team
Prof Gavin Conibeer, A/Prof Santosh Shrestha, A/Prof Stephen Bremner, Dr Shujuan Huang, Dr Robert Patterson, Dr Yuanxun Liao

UNSW Students
Weijian Chen, Milos Dubajic, Hongze Xia, Jianfeng Yang, Bo Wang, Simon Chung, Zhilong Zhang, Wenkai Cao, Yi Zhang, Xi Dai

Funding Support
ARC Discovery, ACAP

Aim

Modeling and characterisation of both energy selective contacts and of the phonon properties of candidate hot carrier materials.

Progress

The hot carrier solar cell aims to tackle the carrier thermalisation loss after absorption of above bandgap photons. It has the potential to achieve very high efficiencies in a device that is essentially a single junction. Detailed balance calculations indicate limiting efficiencies as high as 65% under 1 sun and 85% under maximum concentration (Green, 2003). The key property for a hot carrier absorber is to slow the rate of carrier cooling from the picosecond timescale to at least 100s of ps, but preferably ns to be similar to the rate of radiative recombination. Hot carriers cool primarily by emission of LO phonons.

Low dimensional multiple quantum well (MQW) systems have been shown to have lower carrier cooling rates. Comparison of bulk and MQW materials has shown significantly slower carrier cooling in the latter. Bulk GaAs was compared to MQW GaAs/AlGaAs materials, using time resolved transient absorption, by Rosenwaks (Rosenwaks, 1993). This shows that the carriers stay hotter for significantly longer times in the MQW samples, particularly at the higher injection levels by one and a half orders of magnitude. This is due to an enhanced "phonon bottleneck" in the MQWs allowing the threshold intensity at which a certain ratio of LO phonon re-absorption to emission is reached which allows maintenance of a hot carrier population to be reached at a much lower illumination level. More recent work on strain balanced InGaAs/GaAsP MQWs by Hirst has also shown carrier temperatures significantly above ambient, as measured by PL (Hirst, 2012). Importantly increase in In content to make the wells deeper and to reduce the degree of confinement is seen to increase the effective carrier temperatures.

GaAs/AlAs MQW samples grown by MBE are used to comprehensively investigate these mechanisms behind the reduction of carrier cooling. A series of samples in which the well thickness is varied with constant barrier thickness is compared with a series in which the barrier thickness is varied at constant well thickness. Photoluminescence and XRD data are presented which indicate reasonably uniform material quality across the series. Time resolved photoluminescence, utilising time correlated single photon counting, is used to measure the carrier temperature with time after excitation and hence indicate carrier cooling rates. Comparison of the trends in the various series of samples is used to elucidate some insight into the nature of the reduced carrier cooling mechanisms.

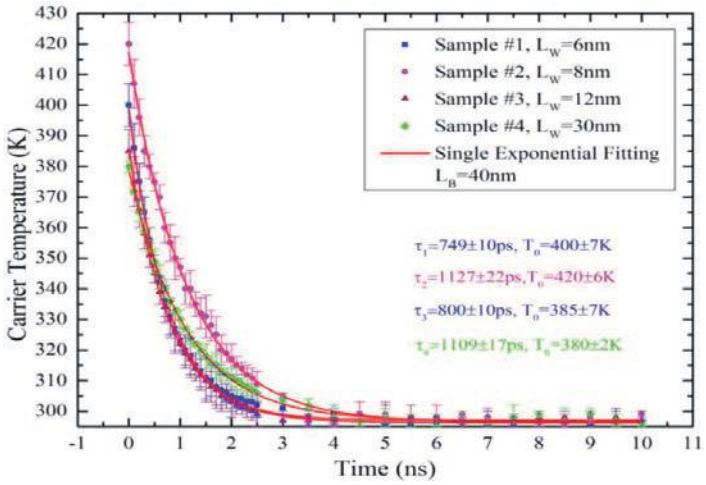

Figure PP2.4a.1: Carrier temperature evolution from "high energy tail fitting" for samples 1 to 4 with increasing QW LW, but fixed LB of 40 nm.

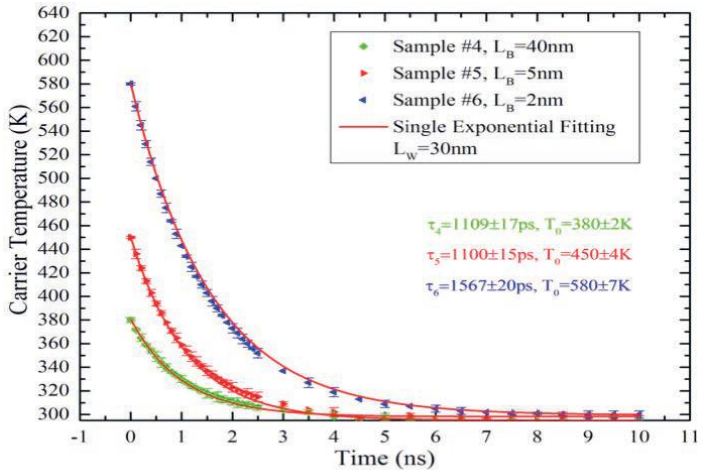

Figure PP2.4a.2: Carrier temperature evolution from "high energy tail fitting" for samples 4,5,6 with decreasing QW LB, but fixed LW of 30 nm.

The results in these two figures all show thermalisation times of over 700 ps, which is much longer than that of bulk materials. This is consistent with the long times seen in the other work on MQW carrier temperatures (Rosenwaks, 1993; Hirst, 2012). The carrier temperature and decay time constant data are plotted in Figure PP2.4a.3 as a function of the QW or barrier thickness.

With reference to Figure PP2.4a.3 primarily, these initial tr-PL measurements do indeed indicate long hot carrier lifetimes in these MQWs, consistent with significantly slower hot carrier cooling rates in MQWs.

Increasing well thickness, constant barrier thickness: In considering the samples with increasing QW width and fixed barrier width of 40 nm in the left half of Figure PP2.4a.3, there is a strong increase in both carrier temperature and hot carrier lifetime for QW widths from 6 nm to 8 nm. However, there is a decrease in carrier temperature for subsequent 12 nm and 30 nm QW samples, but a general increase in hot carrier lifetime for this same series. A potential explanation for this non-monotonic behaviour relies on the change of DOS as quantum confinement decreases for thin wells and on both a decrease in confined energy levels and an increase in effective material quality, as well thickness increases, for thicker wells.

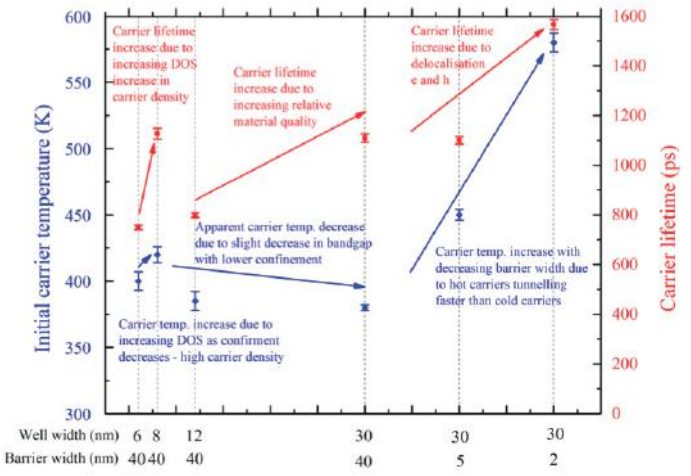

Figure PP2.4a.3: Comparison of initial carrier temperatures (blue diamonds) and hot carrier lifetimes (red squares) for varying well or barrier thicknesses.

For the increase in well thickness from 6 nm to 8 nm, there is a very strong decrease in quantum confinement, because this decreases exponentially with the thickness. This results in a strong increase in the DOS in the wells. As this is non-linear with well thickness it also leads to an increase in the carrier density for a given illumination intensity and consequent greater emission of optical phonons by hot carriers and hence earlier onset of a phonon bottleneck (in which optical phonons are restricted from decaying into acoustic phonons – the Klemens' mechanism – and are therefore re-absorbed by hot carriers) and hence the slowed carrier cooling rate leading to both higher carrier temperature and longer hot carrier lifetime. For thicker QWs of 12 nm and 30 nm there is a further reduction in quantum confinement, but again as this change is exponential, it is already quite small and so does not result in any appreciable increase in DOS in these thicker wells, although it does still have a small effect on reducing the ground state confined energy level. This results in very little change to the non-equilibrium hot carrier population but the slightly lower ground state means this population is shifted to slightly lower energies, thus giving an apparent decrease in carrier temperature.

However, the increase in QW width also increases the ratio of high quality bulk-like GaAs material to lower quality QW/barrier interface material. The radiative recombination efficiency will depend on the quality of the total GaAs thickness, so an increase in well width is likely to increase the radiative efficiency and give the increase in hot carrier radiative lifetime observed.

Decreasing barrier thickness, constant well thickness: Considering now the samples with fixed well width of 30 nm and decreasing barrier width in the right half of Figure PP2.4a.3, there is a very strong increase in carrier temperature as barrier width decreases. However, there is no change in the hot carrier lifetime going from 40 nm to 5 nm barriers, but then a strong increase in this lifetime for the sample with the thinnest 2 nm barriers. Because the barriers become thinner these effects are likely to be dominated by changes in the diffusion of hot carriers, differences in effective mass and hence mobility of holes and electrons and by the fact that initial excitation gives rise to the highest carrier population in the top few QWs.

More specifically, initial excitation of carriers in the QWs gives hot carrier populations isolated within each well, with the greatest excitation occurring in the top few wells dependent on the absorption coefficient of GaAs. As time progresses after the initial excitation, tunnelling diffusion of carriers occurs from the more highly populated upper wells into lower wells. This tunnelling effect will be exponentially dependent on the barrier thickness and much greater for the thinner barriers.

Because of their much smaller effective mass (0.03 cf. about 1 in GaAs), electrons will tunnel much faster than holes through a given barrier. At later measurement delay times this will tend to give a separation of charge carriers with electrons diffusing through to lower wells but holes remaining almost immobile in upper wells. This carrier separation (the Dember effect enhanced by tunnelling) delocalises electrons from holes in the depth direction and leads to a suppression of radiative recombination. For an assumed constant non-radiative recombination probability, this will lead to a longer observed hot carrier or thermalisation lifetime in the thinnest barrier sample.

However, hot electrons will tunnel significantly faster than cold electrons through a given barrier because they are closer to the top of the barrier and hence their tunnelling probability is exponentially enhanced. This difference in hot/cold electron diffusion will be strongest for thicker barriers, such that for the 40 nm barrier cold electrons will have negligible tunnelling probability but hot electrons will tunnel relatively fast into lower wells thus both cooling the population in the upper few wells and reducing the carrier density of these hot carriers as they diffuse to lower wells such that they no longer exhibit phonon bottleneck and cool relatively quickly. This therefore gives the observed relatively low carrier temperature with the thickest barriers, increasing to progressively higher temperatures as the barrier thickness decreases first to 5 nm and then to 2 nm.

This hot carrier diffusion effect to some extent counteracts the charge carrier separation effect on hot carrier lifetime such that there is almost no change in this lifetime in going from 40 nm to 5 nm barriers (even though there is the increase in carrier temperature because the reducing difference in hot/cold electron diffusion is little affected by the carrier delocalisation) but the large increase in both hot carrier lifetime and carrier temperature on going from 5 nm to 2 nm barriers (as the delocalisation becomes stronger but the indirectly connected differential hot/cold electron diffusion becomes weaker).

Overall effect of MQWs on hot carrier cooling: There is clearly further work that needs to be carried out to confirm (or deny) these rather qualitative explanations of MQW hot carrier behaviour, but what is certainly very clear is that thin barriers and thick wells in the MQWs give both high carrier temperatures, up to 300 K above ambient, and long hot carrier lifetimes, up to 1.5 ns. This bodes very well for the incorporation of such MQW structures as hot carrier cell absorbers. The necessary long-lived hot carrier properties appear to be approached in structures which will also facilitate good transport of hot carriers to the surfaces and hence to energy selective contacts for extraction of high energy and hence high voltage charge carriers. The role of the multiple interfaces in GaAs material that is close to being bulk-like would appear to be important. This would be very consistent with the very high figures of merit seen in thermoelectric MQW structures, in which electron transport is little impeded by thin low energy barriers, but phonon scattering is strongly enhanced by these same barriers which have a strong mismatch in acoustic impedance which strongly reflects and localises phonons. Work on comparing different numbers of QW interfaces in MQWs with thin widely spaced barriers will be carried out.

Highlights

- Multiple quantum well (MQW) samples in the GaAs/AlAs system either with varying QW thickness or with varying barrier thickness, have been used to investigate the mechanisms responsible for high carrier temperatures and long hot carrier lifetimes in MQWs.
- For variation in barrier thickness, thinner barriers are seen to give both higher carrier temperatures and longer hot carrier lifetimes with temperatures up to 300 degrees above ambient at lifetimes of approximately 1.5 ns, due to differential tunnelling through barriers for electrons and holes and for hot and cold carriers leading to carrier separation and suppression of recombination to give longer hot carrier lifetimes.

References

Conibeer, G., Zhang, Y., Shrestha, S. and Bremner, S., 2017, "Towards an understanding of hot carrier cooling mechanisms in multiple quantum wells", Japanese Journal of Applied Physics, 56(9) doi:10.7567/JJAP.56.091201.

Xia, H., Feng, Y., Chung, S., Zhang, Y., Shrestha, S., Huang, S., Uchiyama, H., Tsutsui, S., Sugiyama, M., Baron, A.Q.R. and Conibeer, G., 2017, "Inelastic X-ray scattering measurements of III-V multiple quantum wells", Applied Physics Letters, 110, 043102, doi: 10.1063/1.4974478.

Hirst, L.C., Fürher, M., Farrell, D.J., Le Bris, A., Guillemoles, J.F., Tayebjee, M.J.Y., Clady, R., Schmidt, T.W., Sugiyama, M., Wang, Y., Fujii, H. and Ekins-Daukes, N.J., 2012, "InGaAs/GaAsP quantum wells for hot carrier solar cells", Proc. of SPIE, v 8256, p 82560X, 2012.

Green, M.A., 2003, "Third Generation Photovoltaics", Springer-Verlag, 2003.

Rosenwaks, Y., M., Hanna, M., Levi, D., Szmyd, D., Ahrenkiel, R. and Nozik, A., 1993, " Hot-carrier cooling in GaAs: Quantum wells versus bulk", Phys Rev B, 48, 14675–14678.

Zhang, Y., Tayebjee, M., Smyth, S., Dvorak, M., Wen, X., Xia, H., Heilmann, M., Liao, Y., Zhang, Z., Williamson, T., Williams, J., Bremner, S., Shrestha, S., Huang, S., Schmidt, T.W. and Conibeer, G., 2016, "Extended Hot Carrier Lifetimes Observed in Bulk In0.265Ga0.735N Under High-Density Photoexcitation", Applied Physics Letters, 108(13), 131904, DOI: 10.1063/1.4945594

PP2.4b Silicon Nanostructure Tandem Cells

Lead Partners
UNSW, USyd

UNSW Team
Dr Ivan Perez-Wurfl, Prof Gavin Conibeer

UNSW Student
Keita Nomoto

Funding Support
UIPRS (UNSW)

Academic Partner
University of Sydney, Prof Simon Ringor

Aim

To characterise self-organised silicon quantum dot nanostructures in terms of composition and doping profiles.

Progress

Atom probe tomography has been used in conjunction with TEM to give very comprehensive 3D maps of the compositions of silicon quantum dots in SiO_2 matrix with the doping profiles of phosphorus and boron doping identified.

The project was completed very satisfactorily at the beginning of 2017.

Samples with varying silicon/oxygen composition have been annealed to produce silicon nanocrystals (Si NCs) embedded in an oxide matrix. These are prepared for analysis with Atom probe tomography (APT).

The results show that the microstructure of the Si NCs is different depending on the excess Si content, annealing conditions and presence of dopant atoms. Proximity histograms and cluster analyses reveal the distribution and incorporation of boron (B) and/or phosphorus (P) dopant atoms in the system of the Si NC/oxide matrix. The atomic scale analysis indicates that P atoms prefer to be located in the inside of the Si NCs, whereas B atoms are more likely to be positioned at the interface or in the oxide matrix. In addition, B and P are clustered together in Si NCs when they are co-doped.

Regardless of the sample fabrication methods, the size of the Si NC increases as the excess Si content and the annealing temperature increase. The presence of dopant atoms affects the microstructure of the Si NC due to the breaking of the Si dioxide barrier layers. Segregation- and bulk solubility–behaviour, kinetic and thermodynamic effects are used to explain the obtained B and P distribution. The measured optical and electrical properties can be explained by the microstructure of the Si NC and dopant distribution, which helps elucidate the relationship between the actual atomic structure and the measured macroscopic properties of Si NC films. Studying the detailed structure of the Si NCs paves the way towards improving the performance of devices that could be used for next generation optoelectronic devices.

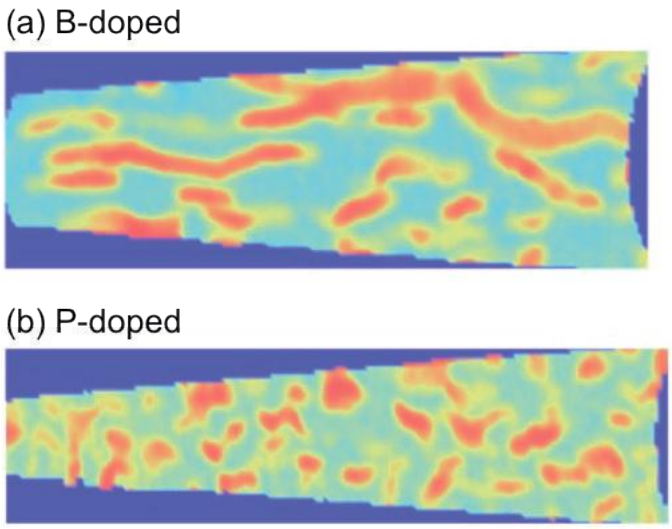

Figure PP4.2b.1: 2D silicon density map of (a) boron-doped sample annealed at 1100ºC; and (b) phosphorus-doped sample annealed at 1100ºC. The thickness of both slices is 100 nm and illustrates greater clustering of Si NCs in the B-doped material as compared to the P-doped material.

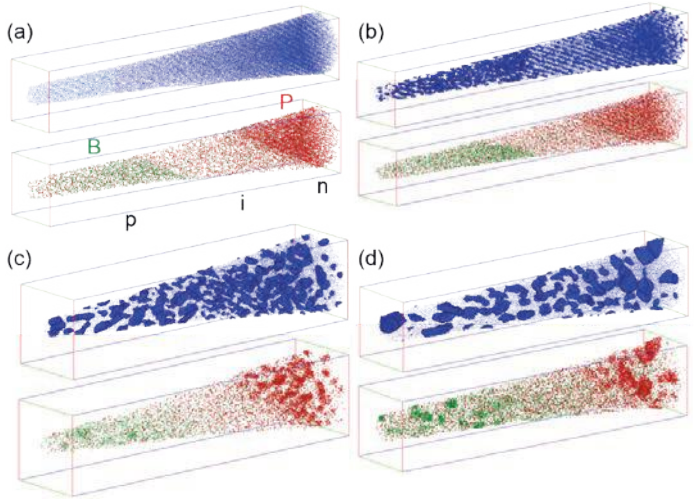

Figure PP4.2b.3: APT 3D reconstruction of p-i-n samples. (a) as-deposited (42 x 42 x 244 nm^3). Samples annealed at (b) 1000°C (45 × 45 × 305 nm^3); (c) 1100°C (46 × 46 × 202 nm^3); and (d) 1180°C (44 × 44 × 215 nm^3). These clearly indicate the B-doped regions on the left and P-doped on the right, with a co-doped region in the middle. This correlates very well with the electrical characterisation indicating a rectifying p-n junction between the B- and P-doped regions.

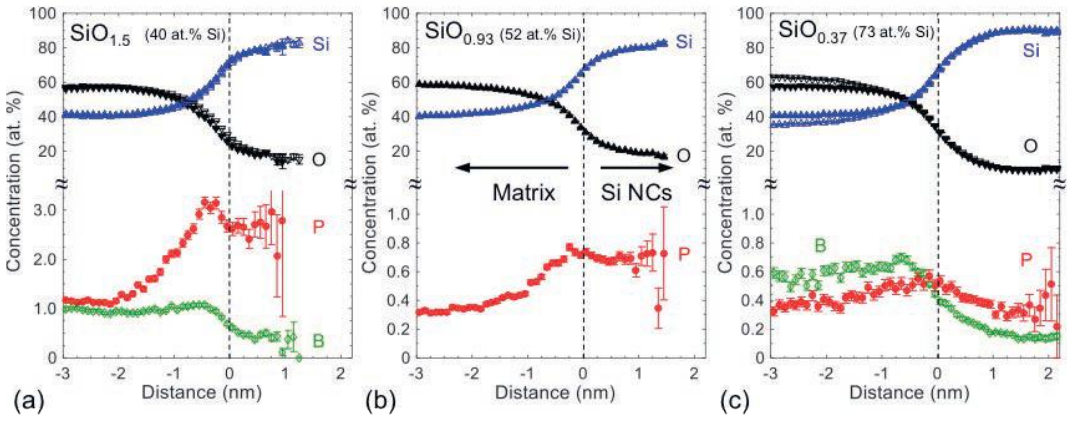

Figure PP4.2b.2: Proxigram analysis of P- and B-doped Si NCs in the oxide matrix. The composition of SRO is (a) $SiO_{1.5}$, (b) $SiO_{0.93}$ and (c) $SiO_{0.37}$. The surface of the NCs is determined to be when the Si and O atom concentrations are equal. The dopant incorporation is seen to be within the Si NCs for P atoms (+ve distance from NC surface) and to be more likely to be at the interface or in the SiO_2 matrix for B atoms (-ve distance from surface).

Highlights

- Detailed 3D atomic scale analysis of silicon NC nanostructures.
- Indications that Si clustering is affected by annealing conditions and P or B doping.
- Evidence that P atoms are located within Si NCs.
- Evidence that B atoms are located at the interface and in the SiO_2 matrix.
- The project has been completed very satisfactorily at the beginning of 2017.

References

Nomoto, K., Chien-Jen Yang, T., Ceguerra, A., Zhang, T., Lin, Z., Breen, A., Wu, L., Puthen-Veettil, B., Jia, X., Conibeer, G., Perez-Wurfl, I. and Ringer, S.P., 2017, "Microstructure analysis of silicon nanocrystals formed from silicon rich oxide with high excess silicon: Annealing and doping effects", Journal of Applied Physics, 122(2), DOI: 10.1063/1.4990983.

Nomoto, K., Hiller, D., Gutsch, S., Ceguerra, A., Breen, A., Zacharias, M., Conibeer, G., Perez-Wurfl, I. and Ringer, S., 2017, "Atom probe tomography of size controlled phosphorus doped silicon nanocrystals", Physica Status Solidi (RRL) – Rapid Research Letters, 11(1), 1600376, DOI: 10.1002/pssr.201600376.

Nomoto, K., Ceguerra, A., Breen, A., Zhang, T., Puthen-Veettil, B., Ringer, S., Conibeer, G., Perez-Wurfl, I., Wu, L., Jia, X. and Lin, Z., 2016, "Structural, optical, and electrical properties of silicon nanocrystals fabricated by high silicon content silicon-rich oxide and silicon dioxide bilayers", Applied Physics Express, 9(11), 115001, http://dx.doi.org/10.7567/APEX.9.115001.

Keita, N., Gutsch, S., Ceguerra, A., Breen, A., Sugimoto, H., Fujii, M., Perez-Würfl, I., Ringer, S. and Conibeer, G., "Atom probe tomography of phosphorus- and boron-doped silicon nanocrystals of various composition of silicon rich oxide", MRS Communications, 6(3), 283–288. DOI: 10.1557/mrc.2016.37.

Keita, N., Sugimoto, H., Breen, A., Ceguerra, A., Kanno, T., Ringer, S., Wurfl, I., Conibeer, G. and Fujii, M., "Atom Probe Tomography Analysis of Boron and/or Phosphorus Distribution in Doped Silicon Nanocrystals", Journal of Physical Chemistry – Part C, 120(31), 17845-17852. DOI: 10.1021/acs.jpcc.6b06197.

PP2.5 Perovskites

Lead Partners
UNSW, USyd

UNSW Team
Dr Ivan Perez-Wurfl, Prof Gavin Conibeer

UNSW Student
Keita Nomoto

Funding Support
UIPRS (UNSW)

Academic Partner
University of Sydney, Prof Simon Ringor

UNSW Team
Prof Martin Green, A/Prof Anita Ho-Baillie, Dr Shujuan Huang, Dr Trevor Young, Dr Jae Yun, Dr Meng Zhang, Dr Arman Mahboubi Soufiani

UoM Team
Prof Ken Ghiggino, Dr David Jones

Monash Team
Prof Udo Bach, Prof Yi-Bing Cheng, Prof Leone Spiccia, Dr Feng Li, Dr Alex Pascoe, Dr Steffen Meyer, Dr Jianfeng Lu

ANU Team
Prof Kylie Catchpole, Prof Klaus Weber, Dr Thomas White, Dr Daniel Walter, Dr Chog Barugkin, Dr Hemant Kumar Mulmudi, Dr Heping Shen

UQ Team
Prof Paul Burn, Prof Paul Meredith, Dr Hui Jin, Dr Aaron Raynor, Dr Ravi Chandra Raju Nagiri

CSIRO Team
Dr Gerry Wilson, Dr Fiona Scholes, Dr Mei Gao, Dr Doojin Vak, Dr Jyothi Ramamurthy, Dr Hasitha Weerasinghe, Dr Andrew Scully, Dr Anthony Chesman, Ms Regine Chantler, Mr Karl Weber, Mr Andrew Faulks, Dr Kallista Sears

Academic Partners

Prof Sang Il Seok, Korea Research Institute of Chemical Technology (KRICT), Ulsan National Institute of Science and Technology, Korea (UNIST)

Dr Samuel D. Stranks, University of Cambridge, and University of Oxford

Dr Xiaoming Wen, Centre for Micro-Photonics, Swinburne University of Technology

Prof Joanne Etheridge, Monash Centre for Electron Microscopy

Department of Chemistry, The University of Adelaide

Laboratoire National des Champs Magne´tiques Intenses, CNRS-UGA-UPS-INSA, France

Prof Nripan Mathews, Nanyang Technological University, Singapore (NTU)

P.C. Harikesh, NTU

Dr Ghanshyam Pilania, Los Alamos National Laboratory (LANL)

Prof Rohan Mishra, Washington University

Professor Dieter Neher, Potsdam University, Germany

The University of Toledo

Stanford University

Georgia Institute of Technology

Students
Qingshan Ma (UNSW), Sheng Chen (UNSW), Adrian Shi (UNSW), Jincheol Kim (UNSW), Xiaofan Deng (UNSW), Cho Fai Jonathan Lau (UNSW), Benjamin Wilkinson (UNSW), Jianghui Zheng (UNSW), Da Seul Lee (UNSW), Yongyoon Cho (UNSW), Jueming Bing (UNSW), Nathan Chang (UNSW), Yecheng Zhou (UoM), Liancong Jiang (Monash), Wuqiang Wu (Monash), Mathias Uller Rothmann (Monash), The Duong (ANU), Jun Peng (ANU), Yiliang Wu (ANU), Xiao Fu (ANU), Daniel Jacobs (ANU), Dale Grant (ANU), Qianqian Lin(UQ), Wei Jiang (UQ), Shanshan Zhang (UQ)

Aim

Since the establishment of AUSIAPV/ACAP SRI in 2012, mixed organic-inorganic halide perovskites have emerged as a new class of solar cell with potential as a material for the development of efficient, lower cost photovoltaic cells.

The potential of perovskites for PV cells as an absorber material lies in its ability to achieve good cell efficiencies, while being relatively cheap to produce and simple to manufacture (i.e. competitive cell efficiency at a lower cost).

A significant effort has been initiated internationally on this materials class, and ACAP has several unique advantages that place the proposed activities at the forefront of these international efforts. Foremost among these advantages are the different relevant perspectives that ACAP is able to offer given the expertise within the different groups constituting ACAP in the dye-sensitised, organic photovoltaics (OPV), inorganic thin-film and silicon cell and module areas, as well as the strong contacts to the commercial sector, and the coordination of this expertise and research effort made possible through the ACAP organisational structure.

To capture these research efforts within ACAP, a new program package for perovskite solar cells under PP2 Thin-Film, Third Generation and Hybrid Devices with additional funding has been established to carry out focused and highly collaborative Australian research and industry eengagement in perovskite photovoltaics. The aim is to establish an internationally leading activity in this exciting new materials group and, consistent with the original intent of ACAP, the team will undertake highly innovative and competitive research with a strategic focus on PV technologies that targets breakthroughs in the cost of solar energy. With a focus on issues that need to be resolved to enable low-cost, full-scale production, the work would enhance the commercial viability of perovskites.

The research is divided into the following main areas

1. Thorough understanding of basic material and device properties by taking full advantage of the expertise, facilities and experience within the partner organisations. The project will undertake research in a diverse range of applications of perovskite materials and devices to develop a path to cost-effective, stable perovskite solar cells.
2. Investigation of prospects for Pb-free perovskite materials.
3. Understanding the stability of these materials with respect to both material synthesis and on encapsulation approaches to address present stability and durability issues.
4. Development of tandem thin-film cells both within the perovskite material system and in combination with inorganic thin films (Si wafer tandems specifically excluded since they are covered by another ARENA project).
5. Scaling to commercially relevant devices including improving the performance of reasonably large devices

(>1 cm^2 in area) rather than on the tiny devices (<0.1 cm^2 in area) where a majority of international attention is focused. This task also includes the evaluation of manufacturing costs for the most promising of the fabrication approaches identified and scaling issues.

Progress

Materials and Device Properties

Hysteresis has been widely observed in perovskite solar cell current-voltage characteristics due to their complex dynamic behaviour. The process of measuring the efficiency of perovskite solar cells appears to be much more complicated than for other technologies. To investigate this, the first major inter-comparison of this PV technology was conducted. The participants included two labs accredited for PV performance measurement (CSIRO Energy and NREL) and eight PV research laboratories including the key nodes within ACAP (UNSW, UoM, Monash, UQ, ANU, CSIRO Manufacturing Flagship). It is found that the inter-laboratory measurement variability can be almost ten times larger for a slowly responding perovskite cell (see Figure PP2.5.1a) than for a control silicon cell. For such a cell, the choice of measurement method, far more so than measurement hardware, is the single-greatest cause for this undesirably large variability. Recommendations are provided for identifying the most appropriate method for a given cell, depending on its stabilisation and degradation behaviour see Figure PP2.5.1b). The results of this study suggest that identifying a consensus technique for accurate and meaningful efficiency measurements of perovskite solar cells will lead to an immediate improvement in reliability. This, in turn, should assist device researchers to correctly evaluate promising new materials and fabrication methods, and further boost the development of this technology (Dunbar et al., 2017).

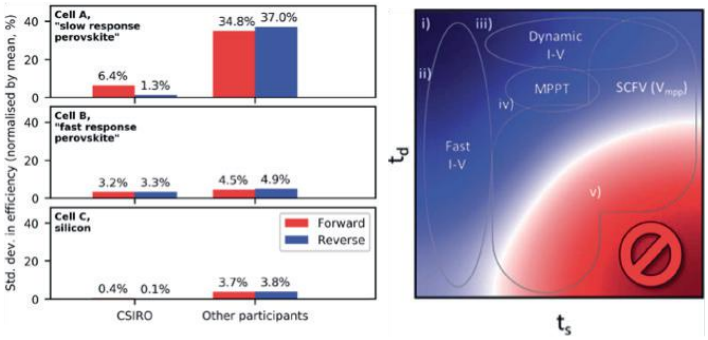

Figure PP2.5.1: (a) 1σ variability observed for the repeat host measurements (left) and non-accredited participants (right) for forward and reverse I–V measurements; and (b) schematic chart indicating recommended general measurement approaches for devices subject to degradation and extended stabilisation. The colour scale indicates the measurement error, E, associated with incomplete stabilisation and/or degradation for a device with a given combination of ts (indicative stabilisation time) and td (indicative degradation time). Red, white and blue indicate large, intermediate and small errors, respectively. The approaches are: fast I–V curves, maximum-power-point tracking (MPPT), stabilised current at fixed voltage (SCFV) and dynamic I–V.

Hot carrier properties of materials are important in photodetection, photocatalysis and light emission to improve the power efficiency and carrier dynamics, especially in high-power optoelectronic applications such as lasing. A hot carrier photovoltaic device is one of the means to achieve power conversion efficiency (PCE) beyond the Shockley–Queisser limit for single-junction solar cells. A strong phonon bottleneck effect is helpful to establish a long-lived hot carrier population for such a hot carrier photovoltaic device. The team at UNSW in collaboration with Swinburne University of Technology, the University of Adelaide and Monash have performed ultrafast optical characterisation and first-principle calculations on four kinds of lead halide perovskites (A=FA+/MA+/Cs+, X=I-/Br-) where FA=HC(NH$_2$)$_2$ and MA=CH$_3$NH$_3$ revealing different carrier-phonon dynamics (Yang et al., 2017). A stronger phonon bottleneck effect is observed in hybrid perovskites than in their inorganic counterparts (see Figure PP2.5.2a). Compared with the caesium-based system, a 10 times slower carrier-phonon relaxation rate is observed in FAPbI$_3$. The up-conversion of low energy phonons is proposed to be responsible for the bottleneck effect (see Figure PP2.5.2b). The presence of organic cations introduces overlapping phonon branches and facilitates the up-transition of low energy modes. The blocking of phonon propagation associated with an ultra-low thermal conductivity of the material also increases the overall up-conversion efficiency. This result also suggests a new and general method for achieving long-lived hot carriers in materials.

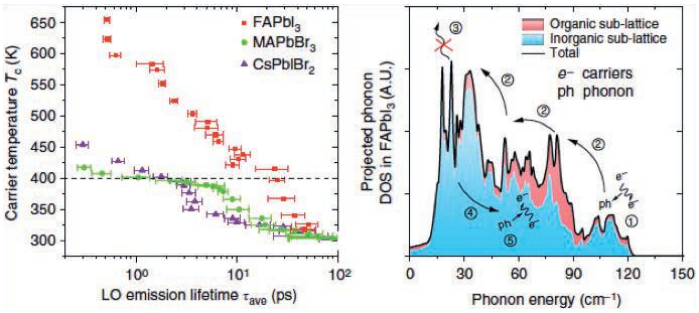

Figure PP2.5.2: Phonon dynamics and bottleneck effect in lead-halide perovskites. (a) Carrier temperature-dependent phonon emission lifetime in different lead halide perovskites with a similar initial carrier concentration of around 2 x 10^{18} cm^{-3}. The error bars shows the standard error of the average (s.e.m) emission lifetime. An emission lifetime that is about 10 times longer than the other materials is observed in FAPbI$_3$ with carrier temperature at and below 400 K; and (b) proposed phonon dynamics in the FAPbI$_3$. The solid black line shows the total phonon DOS, in which the contributions from the inorganic and organic sub-lattices are shown by the blue region on the bottom with the pink region stacked on top, respectively. The labelled phonon dynamic processes are: (1) Fröhlich interaction of carriers primarily on the lead halide framework; (2) relaxation of lead halide LO phonon, organic sub-lattice can be excited by phonon–phonon scattering; (3) propagation of acoustic phonon is blocked due to anharmonic phonon–phonon scatterings; (4) up-conversion of acoustic phonons; and (5) carrier reheating.

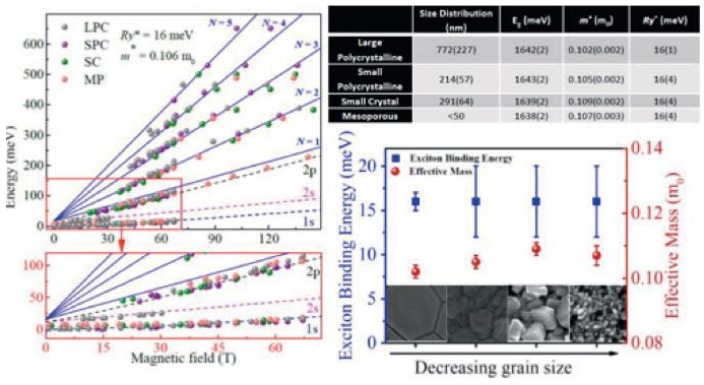

	Size Distribution (nm)	E_b (meV)	m^* (m_0)	Ry^* (meV)
Large Polycrystalline	772(227)	1642(2)	0.102(0.002)	16(1)
Small Polycrystalline	214(57)	1643(2)	0.105(0.002)	16(4)
Small Crystal	291(64)	1639(2)	0.109(0.002)	16(4)
Mesoporous	<50	1638(2)	0.107(0.003)	16(4)

Figure PP2.5.3: Comparison of the excitonic properties of the four different $MAPbI_3$ morphologies. (a) Overlaid fan chart of the LPC, SPC, SC and MP samples. The solid lines and the dashed lines are the fits to the set of Landau levels and the excitonic transitions, respectively; (b) the zoomed-in plot of the excitonic transitions region of the fan chart in panel (A); and (c) the bottom panel illustrates the change in Ry* and m for the various morphologies.

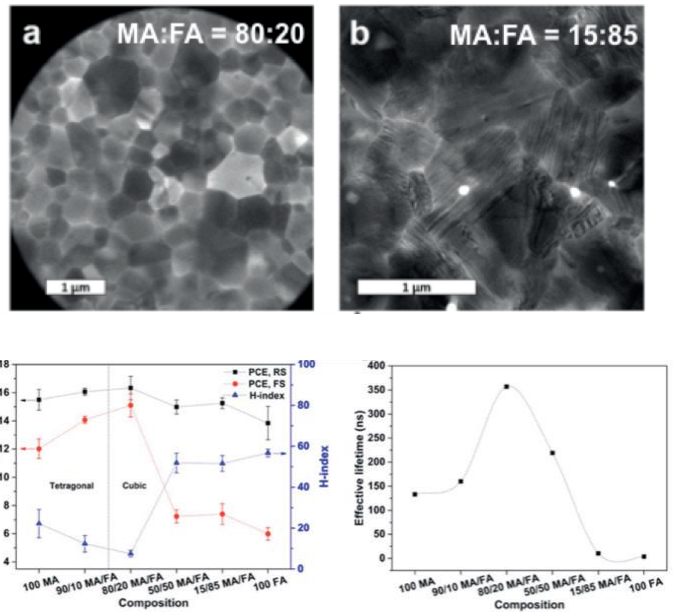

Figure PP2.5.4: (a) and (b) Bright field TEM image of mixed perovskite thin films with different MA:FA ratios; (c) power conversion efficiencies of mixed perovskite devices with different MA:FA ratios; and (d) effective lifetimes of mixed perovskite thin films with different MA:FA ratios.

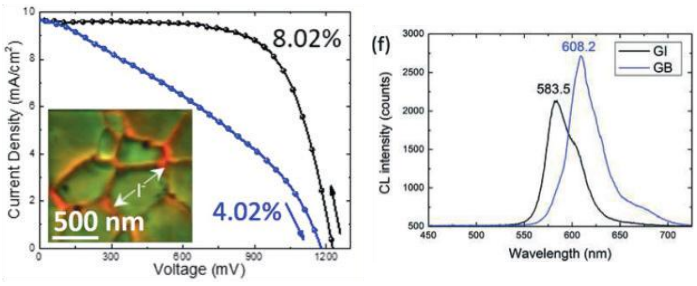

Figure PP2.5.5: (a) A superposition of two CL PMT mappings of the CsPbIBr2 film with different spectral windows. The orange regions indicate a longer emitted light wavelength (590–640 nm) than that of the green regions (530–590 nm). (b) CL spectra for the area inside a CsPbIBr2 grain (GI) and its grain boundary (GB).

An important parameter that dictates the design of a solar cell is the strength of the Coulomb interaction between the photo-generated electron in the conduction band and the hole in the valence band (i.e. the exciton binding energy). Recently, it has been suggested that the exciton binding energy of the perovskite material is influenced by the size of the grains of the perovskite film, and therefore a different device design will be required depending on the grain size. The team at UNSW in collaboration with researchers at Monash, Laboratoire National des Champs Magnétiques Intenses, CNRS-UGA-UPS-INSA, France, University of Cambridge and University of Oxford, performed magneto-optic measurements on films with different grain sizes (see Figures PP2.5.3a and PP2.5.3b). At low temperatures, in which thermal fluctuations of the interactions are frozen and the rotational disorder of the organic cation is negligible, the exciton binding energy and reduced effective mass of carriers remain effectively unchanged with grain size (see Figure PP2.5.3c). It is concluded that the microstructure plays a negligible role in the Coulomb interaction of the photocreated electron–hole pairs, in contrast to previous reports. In addition, excitons do not play a significant role in films with any of the polycrystalline morphologies studied. With the renewed understanding, it means that excitons should not be a factor for the design of optoelectronic devices based on polycrystalline $MAPbI_3$ and similar materials with different grain sizes, making future device architecture optimisation less constrained (Soufiani et al., 2017).

At Monash, advanced transmission electron microscopy (TEM) characterisation techniques developed over the last few years have proved to be very useful in showing the type and amount of crystallographic defects. The type of perovskite films studied has expanded from $CH_3NH_3PbI_3$ to mixed $MA_{1-X}FA_XPbI_3$ perovskites. It was found that the relative amount of the MA+ and FA+ cation in the material plays a critical role (see Figure PP2.5.4(a) and (b)). The optimum ratio of 80% MA+ and 20% FA+ ($MA_{0.8}FA_{0.2}PbI_3$) has no defects, the lowest solar cell hysteresis, the highest solar cell efficiency, and the longest charge carrier lifetime (see Figure PP2.5.4(c) and (d)). In another TEM study by Monash, photoluminescence and cathodo-luminescence are also used in conjunction to study charge carrier recombination and retrieve crystallographic and compositional information for all inorganic $CsPbIBr_2$ films on the nanoscale. It is found that under light and electron beam illumination, "iodide-rich" $CsPbI_{1+X}Br_{2-X}$ phases form at grain boundaries as well as segregate as clusters inside the film (see Figure PP2.5.5(a) and (b)). Phase segregation (which is irreversible caused by exposure to the electron beam or reversible caused by exposure to light) generates a high density of mobile ions moving along grain boundaries as ion migration "highways". These mobile ions can pile up at the perovskite/TiO_2 interface resulting in formation of larger injection barriers, hampering electron extraction and leading to current density–voltage hysteresis in the planar $CsPbIBr_2$ solar cells investigated (Li et al., 2017).

The team at ANU investigated light-induced phase segregation inside quadruple-cation perovskite material in a complete cell structure (see Figure PP2.5.6(a)) and found that the magnitude of this phenomenon is dependent on the operating condition of the solar cell. Under short-circuit and even under maximum power point conditions, phase segregation is found to be negligible compared to the magnitude of segregation under open-circuit conditions. In accordance with the finding, perovskite cells based on quadruple-cation perovskite with 1.73 eV bandgap retain 94% of the original efficiency after 12 h operation at the maximum power point, while the cell only retains 82% of the original efficiency after 12 h operation at the open-circuit condition (see Figure PP2.5.6(b)). This result

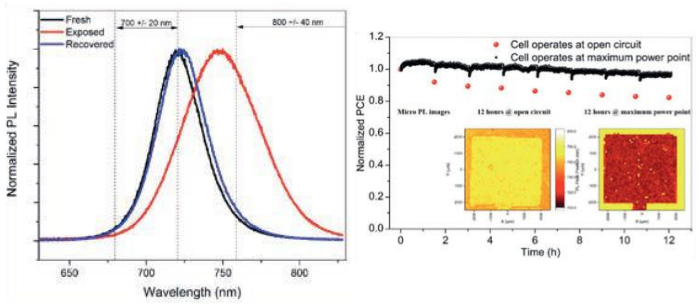

Figure PP2.5.6: (a) Change in PL spectrum of fresh, exposed, and recovered perovskite films indicating phase segregation that is reversible; and (b) evolution of power conversion efficiency of perovskite cells during 12 h operation at the maximum power point, and open-circuit condition.

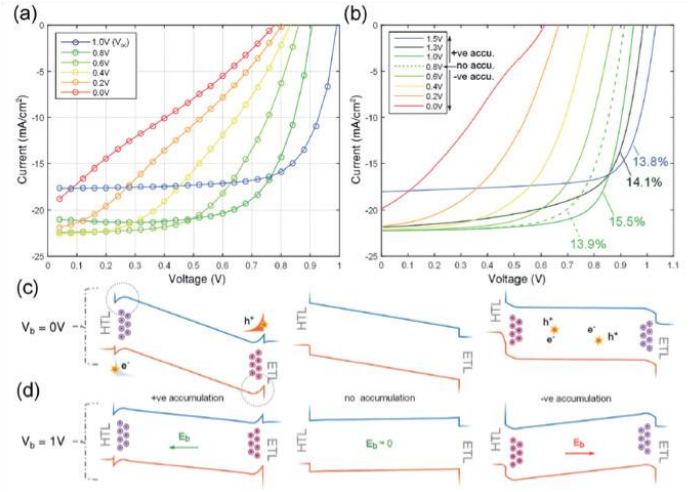

Figure PP2.5.7: (a) Rapid forward scan measurements (20 V s^{-1}) taken after equilibration at different bias voltages given in the legend. These results exhibit reduced J_{SC} after forward biasing, or "inverse hysteresis"; (b) simulated forward scans showing the joint effects of positive and negative ion accumulation: negative accumulation reduces V_{OC} and $J_{SC,}$ while positive accumulation enhances V_{OC}, but at the cost of J_{SC} under extreme positive accumulation (1.5 V pre-bias in our model). Power conversion efficiencies for some of the curves are shown in the labels; and (c and d) simulated band diagrams at 0 V (c) and 1 V (d) bias demonstrating the effects of positive (left) and negative (right) ionic accumulation, as compared with no accumulation (middle). Surface recombination caused by unfavourable band-bending (circled) reduces J_{SC} under severe positive accumulation, while the screened electric field under negative accumulation causes a similar reduction due to increased bulk recombination. At high forward bias the cell under positive accumulation enjoys the benefit of an enhanced bulk electric field (E_b) which enlarges the voltage as compared to cells under no or negative accumulation.

highlights the need to have standard methods including light/dark and bias condition for testing the stability of perovskite solar cells. Additionally, phase segregation is observed when the cell was forward biased at 1.2 V in the dark, which indicates that photo-excitation is not required to induce phase segregation (Duong et al., 2017).

In another study, the ANU team tested the limits of the ionic theory by attempting to account for a number of exotic characterisation results using a detailed numerical device model that incorporates ionic charge accumulation at the perovskite interfaces (see Figure PP2.5.7). The experimental observations include a temporary enhancement in open-circuit voltage following prolonged periods of negative bias, dramatically S-shaped current-voltage sweeps, decreased current extraction following positive biasing or "inverted hysteresis", and non-monotonic transient behaviours in the dark and the light. Each one of these phenomena can be reproduced and ultimately explained by the models, providing further evidence for the ionic theory of hysteresis as well as valuable physical insight into the factors that coincide to bring these phenomena about. In particular it was found that both interfacial recombination and carrier injection from the selective contacts are heavily affected by ionic accumulation, and are essential to explaining the non-monotonic voltage transients and S-shaped J-V curves. Inverted hysteresis is attributed to the occurrence of "positive" ionic accumulation, which may also be responsible for enhancing the stabilised open-circuit voltage in some perovskite cells (Jacobs et al., 2017). In another study, the role of stoichiometry and band alignment in inverted hysteresis observed in $CH_3NH_3PbI_3$ solar cells are further investigated (Shen et al., 2017).

In the third study at ANU (Walter, 2018), it was found that despite the hysteretic phenomena in perovskite solar cells, at steady-state, they are amenable to quantitative analysis of luminescence images. This is demonstrated by calculating the spatial distribution of series resistance from steady-state photoluminescence images. This study observes good consistency between the magnitude, voltage-dependence and spatial distribution of series resistance calculated from luminescence images and from cell-level current-voltage curves and uncalibrated luminescence images, respectively (see Figure PP2.5.8). This method has significant value for the development of PSC process control, design and material selection, and illustrates the possibilities for large-area, spatially resolved, quantitative luminescence imaging-based characterisation of PSCs.

At UQ, a simple modification of the anode with a triarylamine-based small molecule is reported (Lin et al., 2017), which avoids the need to use standard hole transport materials and delivers a relatively high open-circuit voltage of 1.08 V and a power conversion efficiency of 16.5% in a simple planar architecture (see Figure PP2.5.9). In addition, in collaboration with the University of Potsdam, an oxygen plasma treatment process for improving interlayer wetting and ionisation potential (which affects open circuit voltage of the completed device) has been demonstrated on ITO/interlayer/perovskite/C_{60}/BCP/Cu cell devices (see Figure PP2.5.10).

Another interlayer work by the team at UoM reported (Subbiah, 2017) the synthesis of fluorene-based conjugated polyelectrolytes (PFS-FTEG and PFS-FC) using an innovative aqueous Suzuki polycondensation approach with organic co-solvents in air (see Figure PP2.5.11(a)). The materials were then employed in perovskite solar cell devices as an interlayer in conjunction with ZnO (see Figure PP2.5.11(b)). The double interlayer led to enhanced power conversion efficiency of 15.1% (see Figure PP2.5.11(c) and (d)). Recently the team also achieved an efficiency of 17.4% using a low temperature processed TiO_x for a glass/ITO/TiO_x/$CH_3NH_3PbI_3$/Spiro-OMeTAD/Ag cell (see Figure PP2.5.12).

Interface engineering developed by various nodes have allowed the demonstrations of more than 20% efficiencies (measured in-house) on small-area (0.16 cm^2) devices such as 20.4% efficient quadruple cation cell with the perovskite/TiO_2 interface passivated by ultrathin polymer–fullerene film at ANU (see Figure PP2.5.13) (Peng et al., 2017); 20.2% efficient cell with the perovskite/hole conductor interface passivated by thiolbenzene derivatives such as MBN at Monash (see Figure PP2.5.14); and 21.7% efficient cell with the perovskite/hole transport material interface passivated by a layer mixed with 2-dimensional (2D) and 3D perovskite materials at UNSW (see Figure PP2.5.15).

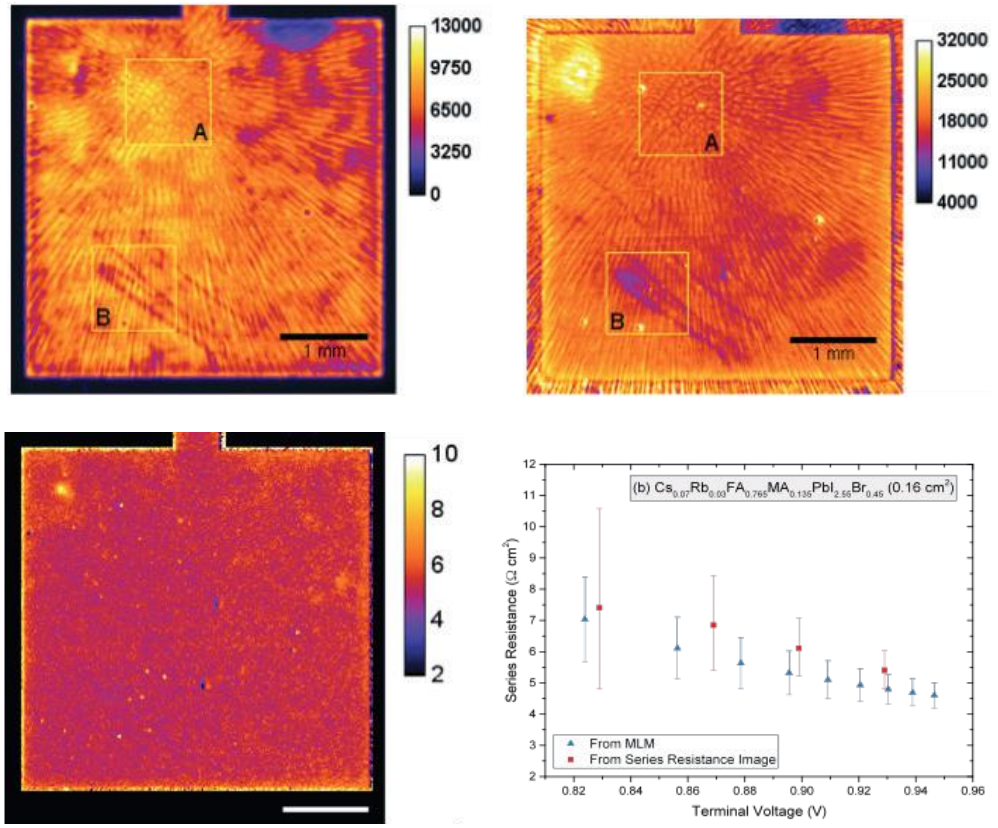

Figure PP2.5.8: (a) EL image; (b) biased-PL image; (c) map of series resistance at approximately the maximum power point terminal voltage (scale bar represents 1 mm, units are Ω cm2); and (d) comparison of aggregate local series resistance and global series resistance for multication PSC under investigation.

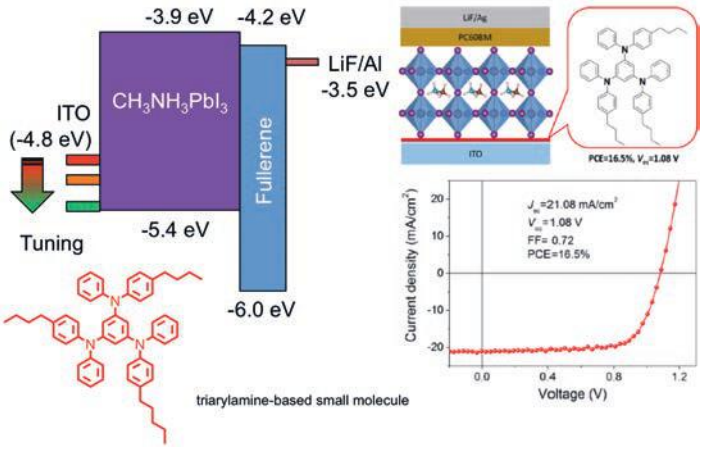

Figure PP2.5.9: (a) Proposed energy level diagram; (b) schematic illustration of the device architecture using the organohalide perovskite $CH_3NH_3PbI_3$ and modified ITO; and (c) current density-voltage (J-V) curve under 1 sun illumination of the champion device.

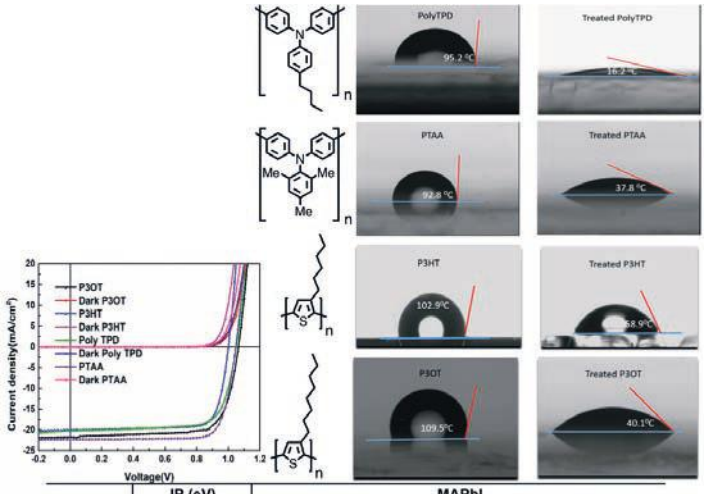

	IP (eV)		MAPbI$_3$			
	Neat	Treated	J_{sc} (mA/cm^2)	V_{oc} (V)	FF (%)	PCE (%) (Hero)
Poly TPD	5.2	5.4	20±0.5	1.05±0.01	0.75±0.02	16±0.2 (16.2)
PTAA	5.1	5.4	22±0.7	1.02±0.01	0.78±0.02	17.9±1.1 (19.0)
P3HT	4.7	5.2	20±0.4	0.97±0.01	0.77±0.02	16.0±0.1 (16.1)
P3OT	4.7	5.0	21±0.5	1.06±0.01	0.74±0.01	17.0±0.4 (17.4)

Figure PP2.5.10: (a) Current density-voltage (J-V) curves and electrical characteristics under 1 sun illumination for champion ITO/interlayer/perovskite/C_{60}/BCP/Cu cell devices using interlayers treated by oxygen plasma; (b) results of water contact angle measurements for neat and treated interlayers; and (c) ionization potentials (IP) of neat and treated interlayers.

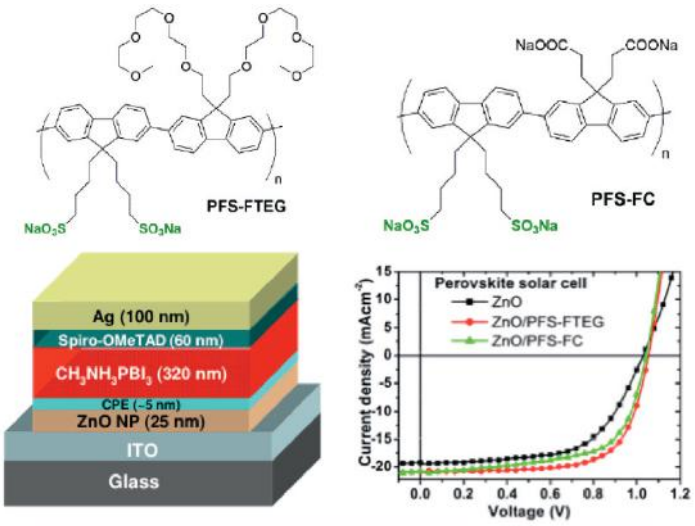

Interlayers	J_{sc} [mA cm^{-2}]	V_{oc} [V]	FF [%]	PCE [%]
ZnO	19.2 ± 0.20	1.02 ± 0.02	61 ± 3	11.75 ± 0.25 (12.0)
ZnO/PFS-FTEG	20.9 ± 0.25	1.04 ± 0.01	69 ± 2	14.90 ± 0.20 (15.1)
ZnO/PFS-FC	20.8 ± 0.35	1.04 ± 0.02	64 ± 3	13.60 ± 0.30 (13.9)

Figure PP2.5.11: (a) Conjugated polyelectrolyte (CPE) materials PFS-FTEG and PFS-FC; (b) schematic diagram of perovskite solar cell; (c) J-V curves of the perovskite devices with various electron transport layers (ETL) ZnO, ZnO/PFS-FTEG and ZnO/PFS-FC; and (d) statistics and best photovoltaic parameter for perovskite solar cells with various ETLs.

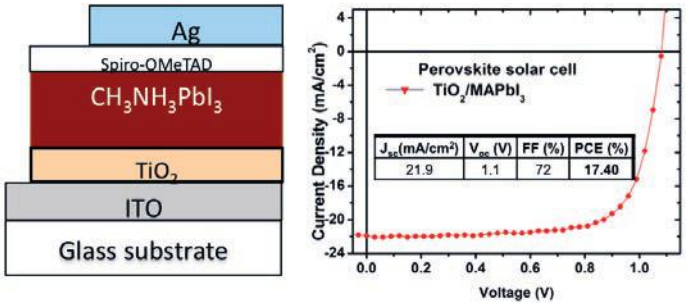

Figure PP2.5.12: (a) Schematic diagram; and (b) J-V curve of a perovskite device that uses low temperature processed TiO_x.

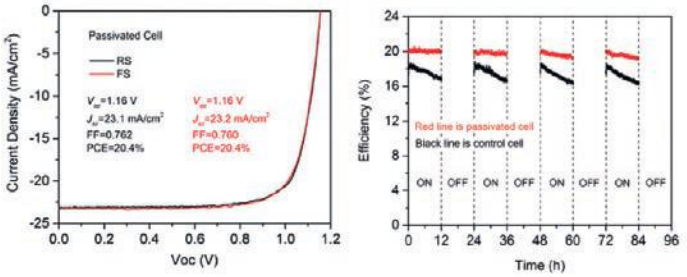

Figure PP2.5.13: (a) J-V curve; and (b) stability test result of quadruple cation cell with the perovskite/TiO_2 interface passivated by ultrathin polymer–fullerene film at ANU.

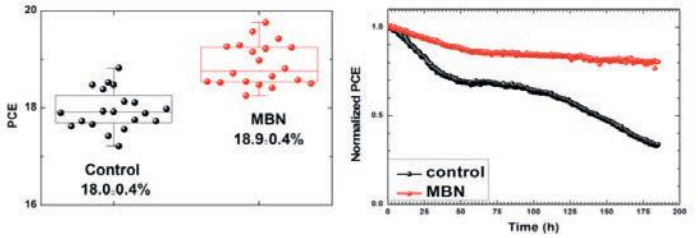

Figure PP2.5.14: (a) Power conversion efficiencies cells before (control) and after (MBN) perovskite/hole conductor interface passivation by thiolbenzene derivatives – MBN; and (b) stability test result of representative cell from each group at Monash.

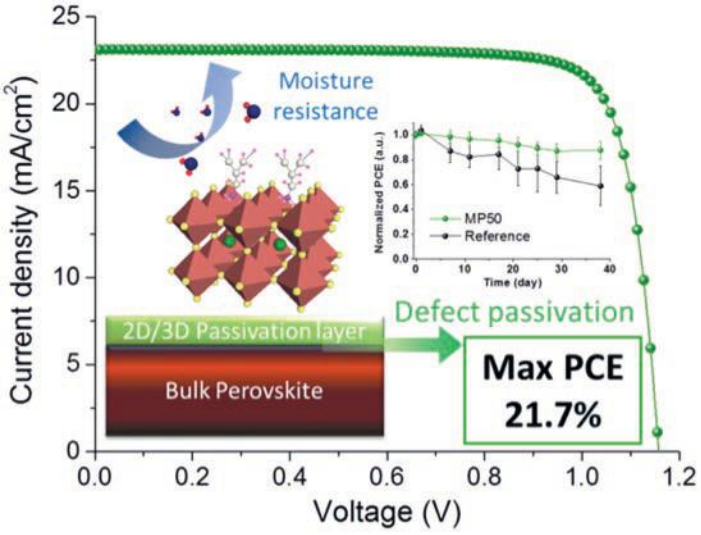

Figure PP2.5.15: J-V curve, schematic and stability test result of a cell with the perovskite/hole transport material interface passivated by a layer mixed with 2-dimensional (2D) and 3D perovskite materials at UNSW.

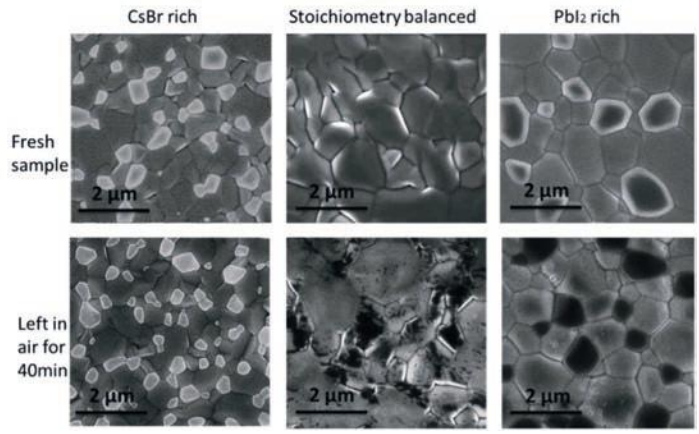

Figure PP2.5.16: Top view scanning electron microscope (SEM) images of fresh (top row) and air-exposed (bottom row) CsBr-rich, stoichiometrically balanced and PbI_2-rich $CsPbI_2Br$ films. The films are deposited on FTO glass substrates.

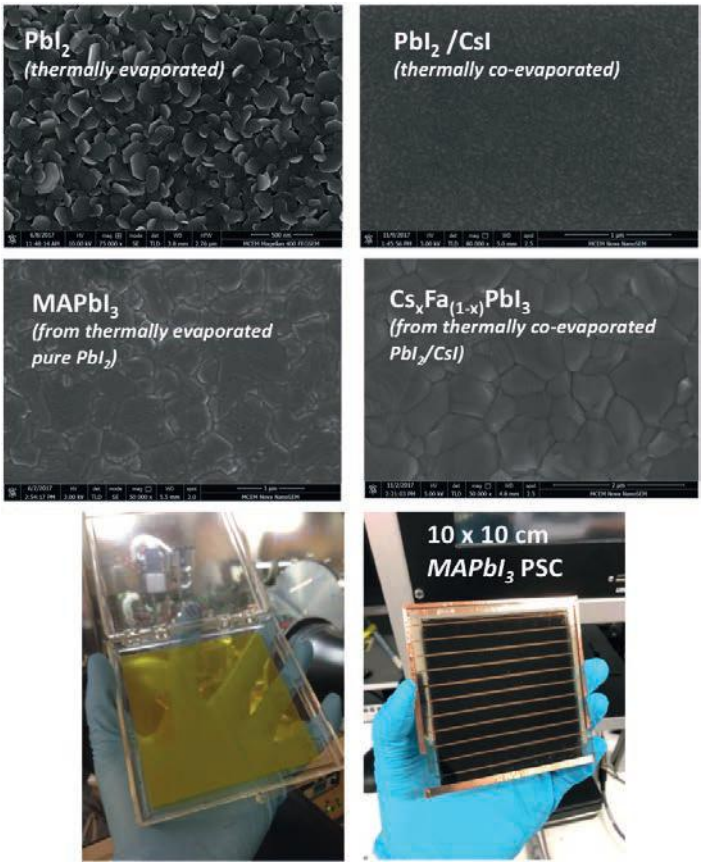

Figure PP2.5.17: Top view scanning electron microscope (SEM) images of thermally evaporated perovskite precursor and perovskite films. Photos showing thermally evaporated PbI_2 film and $MAPbI_3$ test device on 10 x 10 cm.

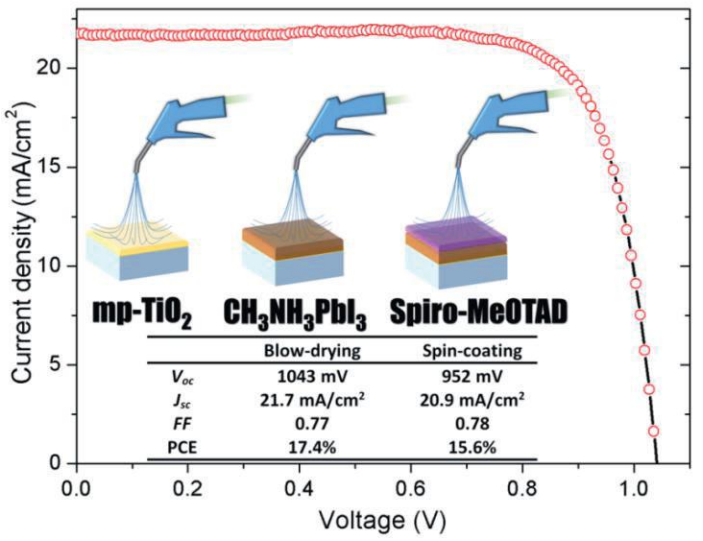

Figure PP2.5.18: J-V curve of champion cell that eliminates spin coating but uses blow-drying method for the depositions of mp-TiO_2; $CH_3NH_3PbI_3$ and Spiro-OMeTAD layers. Electrical characteristics of the spin coating free cell compared to the cell with layers deposited by spin coating.

Stabilities of these cells have also improved as a result of the interface engineering.

With regards to the development of scaleable deposition methods, various nodes have made progress. Thermal evaporation has been used at UNSW to deposit $CsPbIBr_2$ and $CsPbI_2Br$ cells (Ma et al. 2017). It has been found that by varying the stoichiometry of the precursor during the evaporation process, the stability of evaporated perovskite films varies significantly (see Figure PP2.5.16). In collaboration with ANU, the chemical analyses of these films have been performed.

Thermal evaporation for organic cation and mixed cation perovskite film is also developed at Monash. $MAPbI_3$ devices and $Cs_XFA_{1-X}PbI_3Br_{3-Y}$ devices on small areas (0.16 cm^2) by thermal evaporation have been successfully demonstrated achieving power conversion efficiencies at 17% and 12%, respectively. Scaling up to large areas is underway (see Figure PP2.5.17).

Apart from the spray process developed last year, UNSW has also developed a blow-drying method (Sheng et al., 2017) that eliminates spin coating for the deposition of all of the layers in the glass/FTO/c-TiO_2/mp-TiO_2/$CH_3NH_3PbI_3$/Spiro-OMeTAD/Au cell (see Figure PP2.5.18). It was found that blow-dried $MAPbI_3$ achieves better infiltration and more compact film with fewer pinholes. Spiro-MeOTAD deposited by blow-drying produces better perovskite/spiro- MeOTAD interface with fewer shunting paths and better hole extraction. This blow-drying method has several advantages. (1) The fabrication of perovskite layer does not require anti-solvent that is an additional component and a sacrificial component. (2) This method produces good quality and smooth layers. (3) The solution processing sequence is scaleable which combines one spraying process for c-TiO_2 with the other layers deposited by blow-drying. (4) The equipment specification for this method is simple. CSIRO has further improved the blow-drying method for the deposition perovskite film by adding NH_4Cl additive to the PbI_2 and CH_3NH_3I perovskite precursors during the "blowing-assisted drop-casting" (BADC) deposition in air. A PCE of 19.5% was achieved for a small-area device (0.1 cm^2) on glass. It was found that the advantage of NH_4Cl additive seen in the BADC fabricated perovskite film cannot be seen in the perovskite film fabricated by the conventional spin coating method (see Figure PP2.5.19). Scaling up to a large area using this method is underway.

Tandem

One advantage of perovskites is that their bandgap can be tuned by varying the composition. Higher bandgap perovskites can be used as a "top" sub-cell for multi-junction thin-film tandems. The team at UNSW in collaboration with University of Oxford, builds on previous work of a higher bandgap device and has successfully integrated an $MAPbBr_3$ cell with an $MAPbI_3$ cell demonstrating a monolithic perovskite/perovskite tandem solar cell (Sheng et al., 2017). The integration involves the use of a solution-processed PEDOT:PSS/C60 stack which serves as recombination layer and protective layer for the underlying sub-cell (see Figure PP2.5.20). A large open-circuit voltage of 1.96 V is achieved.

Other higher bandgap perovskite materials suitable for multi-junction tandems explored include $CsPbIBr_2$ (2.05eV); $CsPbI_2Br$ (1.90eV); and $CsPbI_3$ (1.72eV) as these inorganic materials can endure temperatures required by subsequent fabrication processes for integrating lower bandgap perovskite cells. The team at UNSW is the first to demonstrate a $CsPbIBr_2$ cell and has recently made great progress by partially replacing lead in $CsPbI_2Br$ with strontium (Sr) without reducing device stability or performance. The team has found an additional benefit of replacing Cs with strontium (Sr) in $CsPb_{1-x}Sr_xI_2Br$ resulting in an

Sr-rich surface passivating the perovskite (Lau et al., 2017). The best $CsPb_{0.98}Sr_{0.02}I_2Br$ cell which can also be processed at lower temperatures (100°C, lower than the commonly used 250°C) achieves a reverse scan efficiency at 11.3% and a stabilised efficiency at 10.8% which is the highest stabilised efficiency reported for a $CsPbI_2Br$ cell (see Figure PP2.5.21). The team has also successfully replaced Pb partially with an alkali earth metal in $CsPbI_3$ producing multiple benefits. Firstly, the reduction in the size of colloidal clusters in the $CsPbI_3$ precursor solution with alkali earth metal allows more uniform films with larger grains to be produced (see Figure PP2.5.22(a) to (c)). This morphology improvement provides a better contact at the interface between perovskite and the hole transport layer. Again, the surface of the perovskite film is passivated by an alkali earth metal rich oxide layer, improving cell performance. The champion cell achieves a reverse scan and stabilised efficiency at 13.3%, which is the highest for a $CsPbI_3$ cell (see Figure PP2.5.22(d)). As the partial replacement of Pb in these inorganic cells did not result in poorer stability, further understanding in the role of dopants may open pathways for developing lead-free inorganic perovskite solar cells.

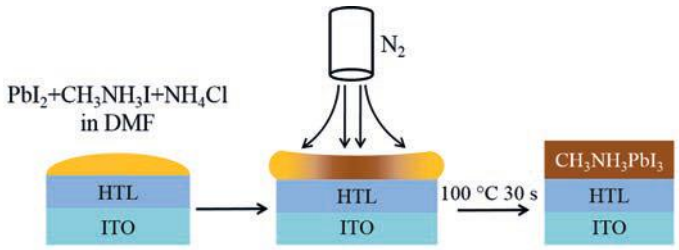

Figure PP2.5.19: Scheme of blowing-assisted drop-casting (BADC) method for the preparation of $CH_3NH_3PbI_3$ films.

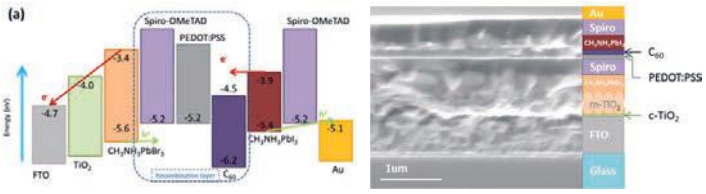

Figure PP2.5.20: (a) Schematic energy band diagram; and (b) cross-sectional SEM image of perovskite/perovskite tandem.

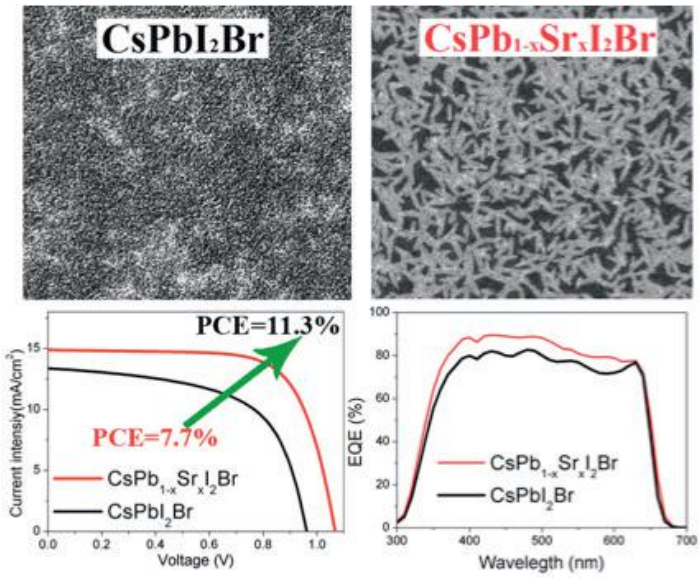

Figure PP2.5.21: Top view SEM images, J-V curves and EQE curves of $CsPbI_2Br$ perovskite film and device before and after Sr doping.

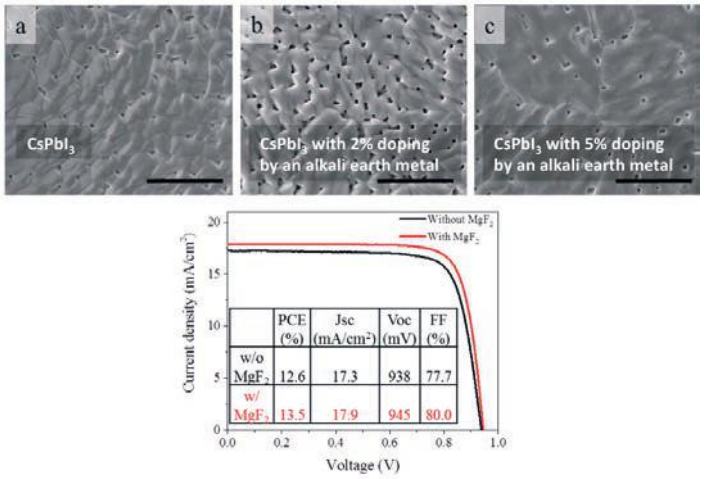

Figure PP2.5.22: (a) to (c) Top view SEM images of perovskite films produced using $CsPbI_3$ precursors with increasing amounts of alkali earth metal improving film morphology. Scale bar is 5 μm; and (d) J-V curves and electrical characteristics of champion $CsPbI_3$ cells with lead partially replaced by alkali earth metal before and after the application of MgF_2 anti-reflection coating.

Lead-free Perovskites

The team at ANU with collaborators at NTU, Singapore and Washington University has commenced the use of density functional theory (DFT) modelling to identify promising Bi-based perovskites and screening double perovskites and oxynitrides using advanced computing methods taking into consideration the thermodynamic stability of the compounds. Progress has been made in preparing $Cs_3Bi_2I_9$ single crystals and thin films for power resolved cathodo-luminescence (CL) measurements (see Figure PP2.5.23).

Device Durability

At UNSW, the team systematically investigated the degradation of $FAPbI_3$ perovskite at different levels of relative humidity (RH), which is shown to be critical for the onset of degradation processes (Yun et al., 2018). Below 30% RH, the black phase of the $FAPbI_3$ perovskite shows excellent phase stability over 90 days. Once the RH reaches 50%, degradation of the $FAPbI_3$ perovskite occurs rapidly (see Figure PP2.5.24(a)). Results from a Kelvin probe force microscopy study reveal that the formation of non-perovskite phases initiates at the grain boundaries and the phase transition proceeds towards the grain interiors. Also, ion migration along the grain boundaries is greatly enhanced upon degradation. A post-thermal treatment (PTT) is developed that removes chemical residues at the grain boundaries, which effectively slows the degradation process (see Figure PP2.5.24(b)). Finally, it is demonstrated that the PTT process improves the performance and stability of the $FAPbI_3$ device (see Figure PP2.5.24(c).

Building on last year's report by the Monash team on the "fatigue" behaviour of perovskite solar cells, cells of different structures were compared by exposure to multiple 12-h cycles of darkness and illumination. It is found that the cells using carbon electrodes are more stable than cells using NiO_x hole transport layers. These results are useful for future stable perovskite cell designs.

In the past year, the team at UNSW developed a low

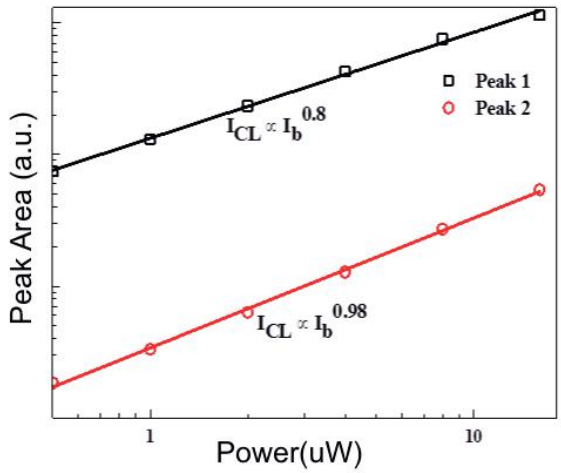

Figure PP2.5.23: Results of power-resolved cathodo-luminescence (CL) measurement of lead-free perovksites.

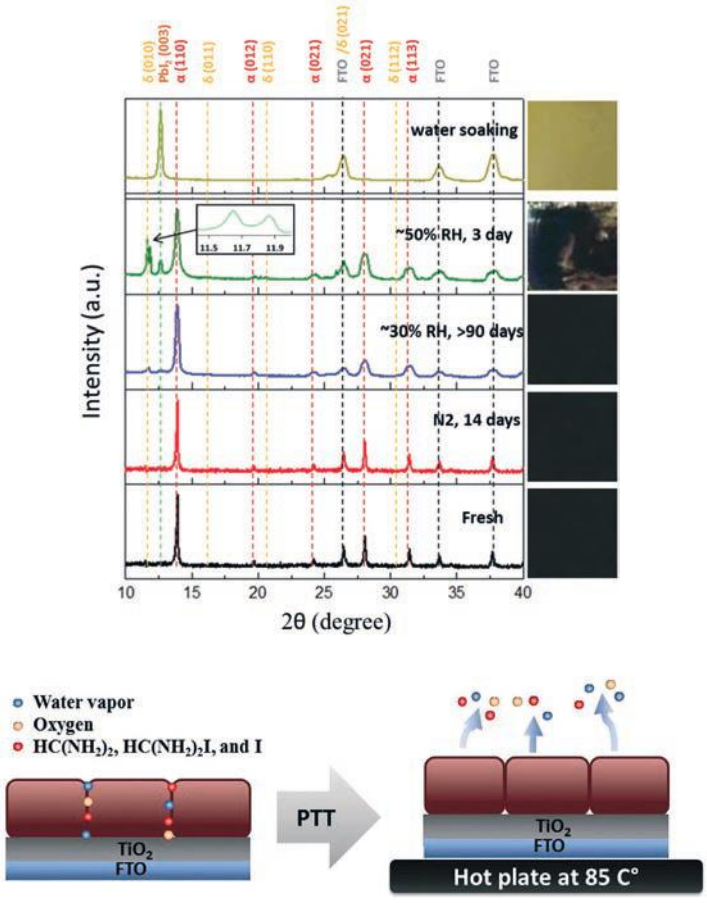

Figure PP2.5.24: (a) X-ray diffraction (XRD) patterns of $FAPbI_3$/c-TiO_2/FTO glass test structures when stored at different relative humidity levels at room temperature in the dark. The corresponding photos of the samples are also presented. Samples include the as-prepared film and those stored in N_2 for 14 days stored at ≈30% RH for over 90 days, stored at ≈50% RH for 3 days and those after soaking in water and drying; (b) illustration of possible chemical residues at the grain boundaries and the effect of a post-thermal treatment; and (c) distribution of device performances and the normalised power conversion efficiency as a function of time in ambient environment of reference and PTT (1 h at 85°C post-thermal treatment) treated $FAPbI_3$/c-TiO_2/FTO glass planar devices.

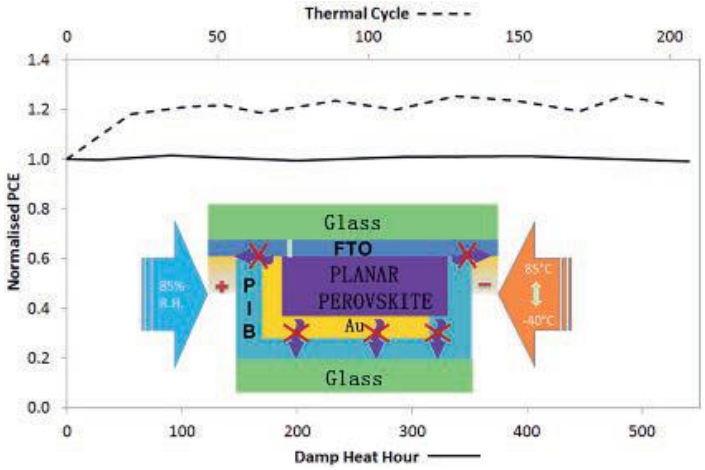

Figure PP2.5.25: Schematic showing an effective low temperature, glass–glass encapsulation technique using high performance polyisobutylene (PIB) for perovskite solar cells. Results of IEC61215:2016 damp heat and thermal cycling tests performed on planar glass/FTO/TiO_2/$FAPbI_3$/PTAA/gold perovskite solar cells encapsulated using this scheme.

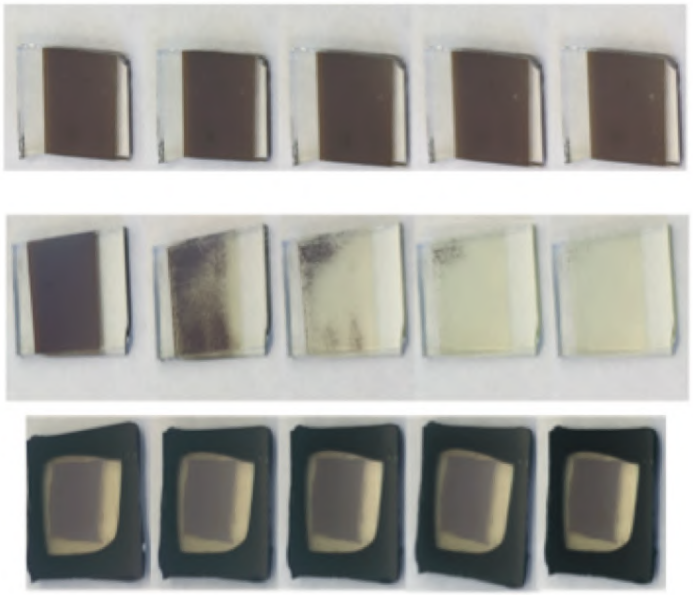

Figure PP2.5.26: Photos showing (a) un-encapsulated thermally evaporated CsBr-rich $CsPbI_2Br$ film; (b) un-encapsulated thermally evaporated stoichiometrically balanced $CsPbI_2Br$ film when the evaporating rate of CsBr is not sufficiently high; and (c) encapsulated stoichiometrically balanced $CsPbI_2Br$ film at different stages: freshly deposited, exposed to air for 5, 10, 20 and 40 minutes.

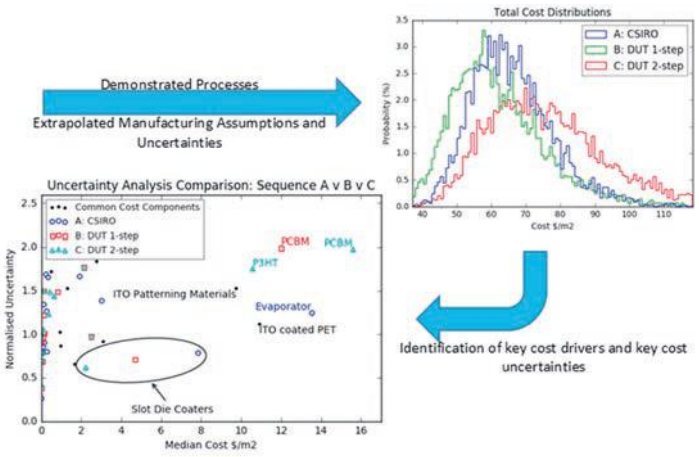

Figure PP2.5.27: Normalised uncertainty graphs comparing demonstrated processes identifying key cost drivers and distribution of total cost estimates allowing for uncertainties.

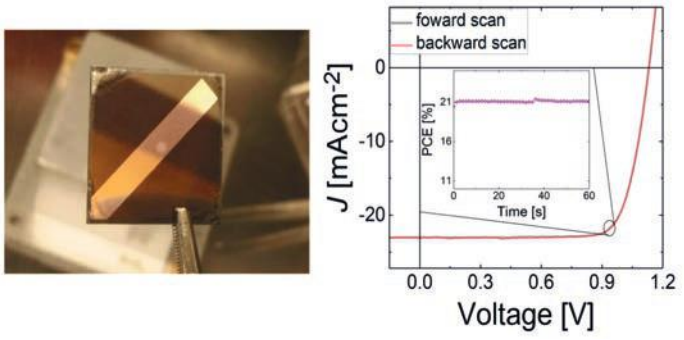

Figure PP2.5.28: Photo and J-V curve of "hero" 1 cm² solar cell with J_{SC} = 22.5 mA cm^{-2}, V_{OC} = 1.15 V, FF = 80% and PCE = 20.5% measured in-house.

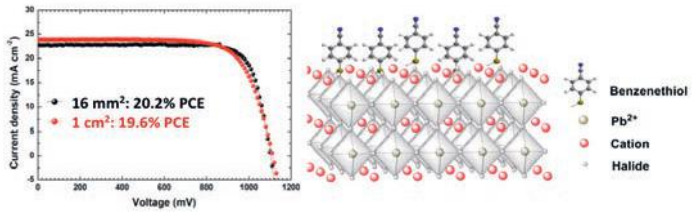

Figure PP2.5.29: (a) J-V curve of perovskite cell with hole-conductor passivated by thiolbenzene derivative (MBN); and (b) schematic for the passivation scheme.

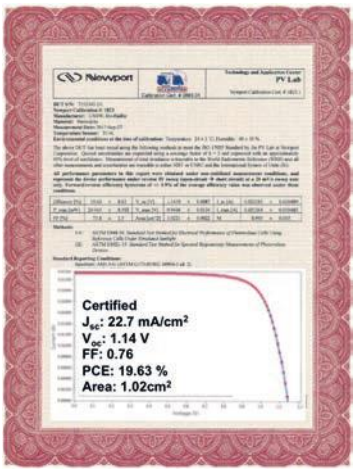

Figure PP2.5.30: Certification from Newport confirming power conversion efficiencies for a 1.02 cm² cell at 19.63%.

temperature, glass–glass encapsulation technique using high performance polyisobutylene (PIB) for perovskite solar cells, which could be applied as either an edge seal or blanket layer (Shi et al., 2017). Electrical connections to the encapsulated PSCs were provided by either the Au or FTO layer with the latter being most effective. A blanket encapsulation method is also most effective as it prevents the heat-induced escape of volatile decomposition products from the perovskite solar cell materials. Its effectiveness is demonstrated in the result of IEC61215:2016 damp heat (85°C and 85% relative humidity) and thermal cycling (-40°C to 85°C) tests performed on PIB encapsulated planar glass/FTO/TiO_2/$FAPbI_3$/PTAA/gold perovskite solar cells. These cells maintained the initial efficiency after 540 h of damp heat testing and 200 thermal cycles. These are among the best damp heat and thermal cycle test results for perovskite solar cells at the time of reporting (see Figure PP2.5.25). The same encapsulation technique has also been used to stabilise thermally evaporated $CsPbI_2Br$, which is unstable if the rate of CsBr evaporation is not sufficiently high and is not encapsulated (see Figure PP2.5.26(a) to (c)) (Ma et al., 2017). Planar $CsPbI_2Br$ solar cell encapsulated using the technique was able to withstand 240 hours damp heat testing. Given the modest performance of the cells (8% averaged from forward and reverse scans for $FAPbI_3$ planar cells and 5% to 7% for planar $CsPbI_2Br$ cells) and the challenges associated with these perovskite materials (e.g. yellow phase for $FAPbI_3$) tested in this work, it is envisaged that better stability results can be further achieved when higher performance perovskite solar cells are encapsulated using the PIB packaging techniques developed in this work.

Commercial prospects, upscaling and manufacturing costs

Building on the previous year's work that developed a method effective in evaluating the manufacturing cost for early-stage technology, which was applied to evaluate the costs of flat-plate perovskite photovoltaic modules, UNSW in collaboration with CSIRO analysed three demonstrated roll-to-roll (R2R) compatible manufacturing sequences and two potential optimised sequences (Chang et al., 2018). The cost analysis method provides for uncertainty in the input assumptions allowing quick identification and quantification of key cost barriers, which are: high cost materials P3HT and PCBM, the use of evaporation for the rear metal deposition, and the transparent ITO coating (see Figure PP2.5.27). It was projected that technology developments in these key areas would halve the expected manufacturing cost to US$37/m² ± 30%. With 68% geometric fill factor (GFF, which is a figure of merit for area usage), 10% PCE and a three-year lifetime, such R2R perovskite modules would be competitive with existing flexible PV products in the market on a $/W and power to weight basis. To compete with Si and CdTe in the flat plate PV market, PCE and lifetimes in excess of 15% and 15 years respectively would be required.

Excellent progress has been made in demonstrating 1 cm² devices. UQ in collaboration with Potsdam University has achieved a PCE of 20.5% (measured in-house) for a 1 cm² ITO/PTAA/$CsI_{0.05}[(FAPbI_3)_{0.83}(MAPbBr_3)_{0.17}]_{0.95}$/C60/BCP/Cu perovskite device (see Figure PP2.5.28). At Monash, a PCE of 19.6% was measured in-house for a 1 cm² perovskite cell that uses thiolbenzene derivatives (MBN) interface passivation (see Figure PP2.5.29). Most recently, UNSW's 1.02 cm² perovskite cell was independently certified by Newport, with an efficiency of 19.63% (see Figure PP2.5.30). This is encouraging for a certified perovskite cell larger than 1 cm² (which is larger than the certified 0.99 cm² 20.87% efficient cell by KRICT and more efficient than the certified 1 cm² 19.56% efficient cell by EPFL).

Many of the activities at CSIRO have a "lab-to-fab" focus aimed

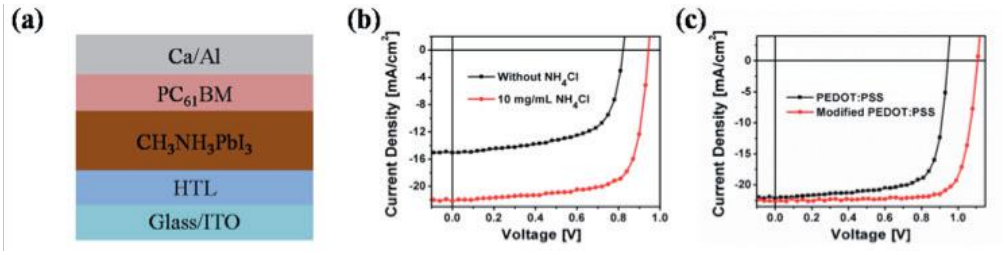

Figure PP2.5.31: (a) Device structure of perovskite solar cells; (b) J-V curves for perovskite solar cells fabricated without an NH_4Cl additive and with 10 mg/mL NH_4Cl additive; and (c) J-V curves for perovskite solar cells incorporating PEDOT:PSS and modified PEDOT:PSS as the HTL. Device area: 0.1 cm^2.

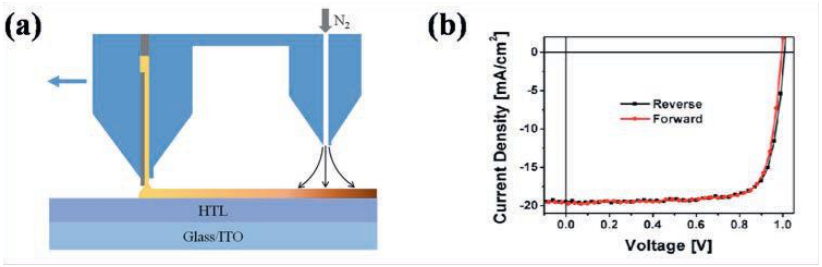

Figure PP2.5.32: (a) The slot-die coating process for preparing $CH_3NH_3PbI_3$ films; and (b) J-V curves for a perovskite solar cell incorporating a slot-die coated $CH_3NH_3PbI_3$ film under reverse and forward scan. Device area: 0.1 cm^2.

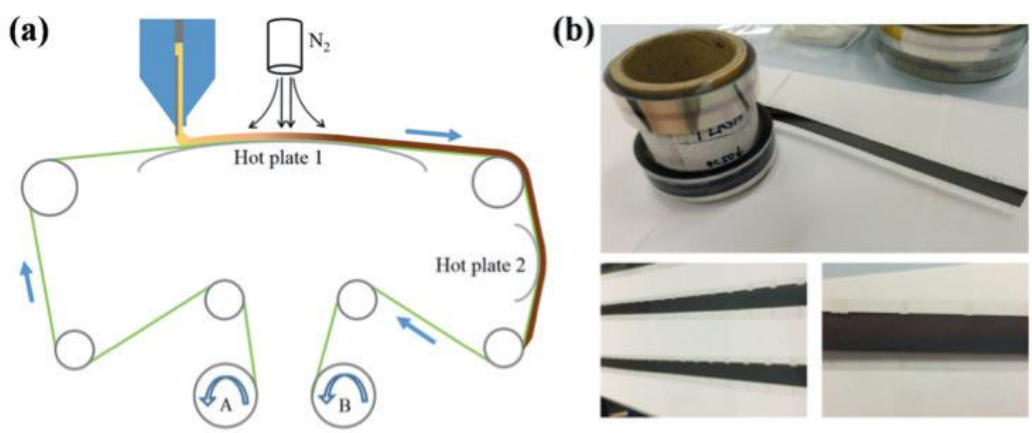

Figure PP2.5.33: (a) Roll-to-roll processing set-up for continuous preparation of $CH_3NH_3PbI_3$ film; and (b) photos of roll-to-roll prepared $CH_3NH_3PbI_3$ films. Device area: 0.1 cm^2.

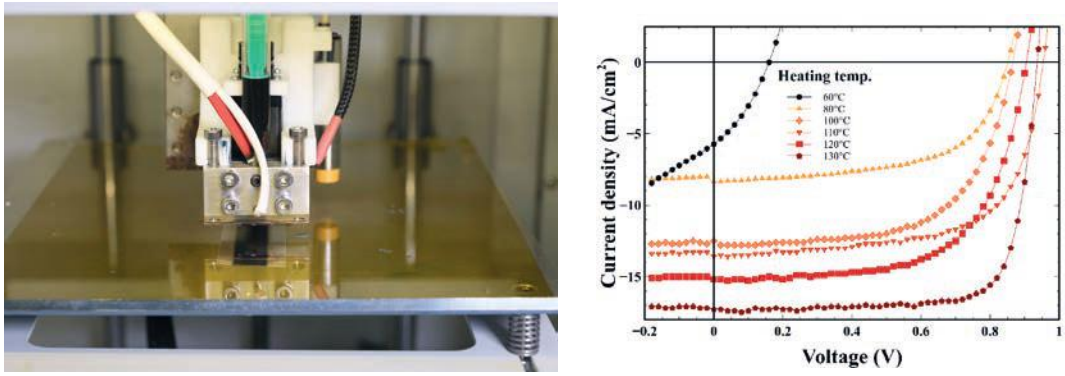

Figure PP2.5.34: (a) Upgraded 3D printer–based slot die coater featured with heating unit to 135°C for both substrate and coating head temperature; and (b) J-V curves for perovskite solar cells fabricated at different heating temperatures without blow-drying. Device area: 0.1 cm^2.

at accelerating the translation of laboratory-based small-scale results to large-scale devices using industry-relevant manufacturing methods. There is also a strong focus that all processes are to be done in air. In the last year, an improved blowing-assisted drop-casting (BADC) method was developed that involves the use of additives such as NH_4Cl producing perovskite $CH_3NH_3PbI_3$ films with excellent optical absorption, photoluminescence, crystallinity and morphology. Using these improved processes along with modified PEDOT:PSS (higher work function) as hole transport layer, $CH_3NH_3PbI_3$ device with high V_{OC} and a PCE of 19.5% on 0.1 cm^2 is demonstrated (see Figure PP2.5.31). The same approach was successfully translated to batch-to-batch slot-die coating (see Figure PP2.5.32(a)) and R2R coating (see Figure PP2.5.33(a)), enabling the continuous production of $CH_3NH_3PbI_3$ films. Cells with PCEs of 15.6% (see Figure PP2.5.32(b)) and 11.2% (see Figure PP2.5.33(b)) are the best reported so far for slot-die coating of perovskites on glass and R2R coating on PET in a one-step process, respectively. The developed BADC method facilitates practical application for further large-scale fabrication of perovskite cells.

Apart from targeting high device performance, reproducibility is also a key factor to be considered for scale-up. It has been found that it is challenging to reproduce blowing conditions in the roll-to-roll process in the current setup. A low-cost alternative to BADC, which allows devices to still be fabricated in air, is the heating of the precursor solution and heating of the substrate requiring an upgrade of the in-house slot-die coater (see Figure PP2.5.34(a)). Up to 14% PCE (device size of 0.1 cm^2) was achieved using this method on glass substrate (see Figure PP2.5.34b). Further optimisation will be explored.

The cohesion energy of perovskites containing various cations is also investigated. Perovskite shows lower cohesion energy than other types of thin-film solar cells. High efficiency devices with reduced grain sizes and with the inclusion of additional cations and PbI_2 additives exhibit a decreased cohesion (Rolston et al., 2017). This work is led by CSIRO and is also supported by ACAP international collaboration fund. More details can be found in PP6.12.

Highlights

- Appropriate methods for measuring perovskite solar cells taking into account their stabilisation and degradation behaviours are given which involves an inter-comparison among the accredited PV measurement laboratories (CSIRO Energy and NREL) and eight PV research laboratories including the key nodes within ACAP (UNSW, UoM, Monash, UQ, ANU, CSIRO Manufacturing Flagship).
- Hot carrier properties of materials are better understood. The up-conversion of low energy phonons is proposed to be responsible for the bottleneck effect, which can be capitalised on. A significantly slower carrier-phonon relaxation rate is observed in $FAPbI_3$ perovskites compared with caesium-based perovskites.
- A renewed understanding on the role of excitons is developed clarifying their independence from perovskite grain size and composition.
- Advanced transmission electron microscopy (TEM) has been further utilised to identify the type and amount of crystallographic defects depending on the composition of the perovskites. It was found that the relative amount of the MA^+ and FA^+ cation in the material plays a critical role with optimum ratio identified thus far to be 80% MA^+ and 20% FA^+.
- Phase segregation has been studied from various perspectives. TEM, photoluminescence and cathodo-luminescence measurements on $CsPbIBr_2$ films show light-induced and electron beam–induced segregation with "iodide-rich" $CsPbI_{1+X}Br_{2-X}$ phases formed predominantly at grain boundaries responsible for ion movement and therefore current density–voltage hysteresis. The extent of light-induced phase segregation is also dependent on the operating condition of the solar cell as observed in quadruple-cation perovskite solar cells. Under short-circuit and even maximum power point conditions, phase segregation is found to be negligible compared to the magnitude of segregation under open-circuit conditions, which results in more rapid degradation.
- The effect of ions is also modelled to explain experimental observations such as temporary enhancement in open-circuit voltage following prolonged periods of negative bias; dramatically S-shaped current-voltage sweeps; decreased current extraction following positive biasing or "inverted hysteresis", and non-monotonic transient behaviours in the dark and the light.
- Despite the hysteretic phenomena, a quantitative analysis of luminescence images can still be carried out such as the generation of spatial distribution of series resistance from steady-state photoluminescence images, which has significant value for PSC process control, design optimisation, material selection and development of large-area cells.
- Interface engineering has been the theme for many cell developments. More than 20% efficiencies have been achieved on small-area devices by various nodes.
- Great progress has been made in the demonstration of >1 cm^2 devices. In particular, certified efficiency at 19.63% has been achieved on a 1.02 cm^2 cell.
- Progress has been made in inorganic higher bandgap perovskite cells suitable for multi-junction tandems reporting some of the highest efficiencies for $CsPbI_2Br$ and $CsPbI_3$ cells.
- Identification of the critical relative humidity level for the onset of degradation in $FAPbI_3$ planar cells.
- Development of a post-thermal treatment (PTT) to remove chemical residues at the grain boundaries, slowing cell degradation process.
- Low-cost glass–glass encapsulation technique has been developed for perovskite solar cells. Encapsulated $FAPbI_3$ planar cells have been demonstrated to pass the IEC61215:2016 thermal cycling test.
- The translation of batch-printing-on-glass to roll-to-roll-printing-on-flexible-substrate has been successful achieving 11.6% PCE on small areas which is one of the best for R2R printed (in air) devices on flexible ITO/PET.
- Manufacturing cost analysis has been extended to three demonstrated roll-to-roll (R2R) compatible manufacturing sequences and two potential optimised sequences, which has identified key cost barriers. It was projected that technology developments in these key areas would halve the expected manufacturing cost. Key R2R perovskite module requirements such as geometric fill factor, PCE and lifetime have also been identified for the product to be competitive with existing flexible PV products in the market or existing flat plate PV products.

Future Work

- We will link theoretical models to the design of new perovskite materials, predicting the behaviours of material modification, then verification by synthesis of the new materials (including mixed cation, mixed halide and 2-dimensional/3-dimensional hybrid perovskites; new inter-layer materials) for better performance and stability.
- We will develop passivation and doping techniques to reduce or eliminate hysteresis, slow response, and instabilities in various types of perovskites.
- We will continue to develop advanced characterisation compatible with perovskite test structures and full device such as luminescence spectroscopy including photoluminescence and cathodoluminescence; EDX mapping under SEM; Kelvin probe force microscopy (KPFM); advanced TEM; and electron backscatter diffraction analysis (EBSD) to investigate micro-structure, device level properties and defects.
- We will develop further understanding of mechanisms behind light-induced degradation and fatigue behaviour of perovskite solar cells, thereby finding ways to reduce and eliminate such phenomena.
- We will continue to improve its lab-to-fab translation tools for optimising printing processes. We will continue to improve characterisation approaches as required for large-area and flexible devices.
- We will continue further scale up and continue studies on the electrical stability and mechanical integrity of printed devices collaborating broadly with ACAP and other academic and industry partners, where appropriate, to translate research outcomes to industry-relevant manufacturing methods and from rigid to flexible substrates.
- We will continue to explore other aspects relevant to manufacture, such as lifetime investigations on the R2R printed perovskite solar cells, and cost-reduction opportunities using alternative materials for module components.

References

Dunbar, R.B., Duck, B.C., Moriarty, T., Anderson, K.F., Duffy, N.W., Fell, C. J., Kim, J., Ho-Baillie, A., Vak, D., Duong, T., Wu, Y., Weber, K., Pascoe, A., Cheng, Y.-B., Lin, Q. Burn, P. L., Bhattacharjee, R., Wang H. and Wilson, G. J., (2017) "How reliable are efficiency measurements of perovskite solar cells? The first inter-comparison, between two accredited and eight non-accredited laboratories", J. Mater. Chem. A, 2017, 5, 22542–22558

Yang, J., Wen, X., Xia, H., Sheng, R., Ma, Q., Kim, J., Tapping, P., Harada, T., Kee, T.W., Huang, F. , Cheng, Y.-B., Green, M., Ho-Baillie, A., Huang, S., Shrestha, S., Patterson, R. and Conibeer, G., "Acoustic-optical phonon up-conversion and hot-phonon bottleneck in lead-halide perovskites", Nat. Commun. 8, 14120, doi: 10.1038/ncomms14120 (2017).

Mahboubi Soufiani, A., Yang, Z., Young, T., Miyata, A., Surrente, A., Pascoe, A., Galkowski, K., Abdi-Jalebi, M., Brenes, R., Urban, J. Zhang, N., Bulovic, V., Portugall, O., Cheng, Y.-B., Nicholas, R. J., Ho-Baillie, A., Green, M. A., Plochocka P. and Stranks, S. D., (2017), "Impact of microstructure on the electron–hole interaction in lead halide perovskites", Energy Environ. Sci., 10, 1358-1366

Li, W., Rothmann, M. U., Liu, A., Wang, Z., Zhang, Y., Pascoe, A. R., Lu, J., Jiang, L., Chen, Y., Huang, F., Peng, Y., Bao, Q., Etheridge, J., Bach and U., Cheng, Y.-B., (2019), "Phase Segregation Enhanced Ion Movement in Efficient Inorganic CsPbIBr2 Solar Cells", Adv. Energy Mater. 7, 1700946

Duong, T., Mulmudi, H.K., Wu, Y., Fu, X., Shen, H., Peng, J., Wu, N., Nguyen, H. T., Macdonald, D., Lockrey, M., White, T. P., Weber, K. and Catchpole, K., (2017), "Light and Electrically Induced Phase Segregation and Its Impact on the Stability of Quadruple Cation High Bandgap Perovskite Solar Cells", ACS Appl. Mater. Interfaces, 9(32), 26859–26866

Jacobs, D.A., Wu, Y., Shen, H., Barugkin, C., Beck, F.J., White, T.P., Weber, K. and Catchpole, K.R., (2017), "Hysteresis phenomena in perovskite solar cells: the many and varied effects of ionic Accumulation", Phys. Chem. Chem. Phys., 19, 3094-3103.

Shen, H., Jacobs, D.A., Wu, Y., Duong, T., Peng, J., Wen, X., Fu, X., Karuturi, S.K., White, T.P., Weber, K., and Catchpole, K.R., (2017), "Inverted Hysteresis in CH3NH3PbI3 Solar Cells: Role of Stoichiometry and Band Alignment", J. Phys. Chem. Lett., 8, 2672–2680.

Walter, D., Wu, Y., Duong, T., Peng, J., Jiang, L., Fong, K.C., and Weber, K., (2018), "On the Use of Luminescence Intensity Images for Quantified Characterization of Perovskite Solar Cells: Spatial Distribution of Series Resistance", Adv. Energy Mater., 8, 1701522

Lin, Q., Jiang, W., Zhang, S., Nagiri, R.C.R., Jin, H., Burn, P.L. and Meredith, P., (2017),"A Triarylamine-Based Anode Modifier for Efficient Organohalide Perovskite Solar Cells", ACS Appl. Mater. Interfaces, 9, 90969-9101

Subbiah, J., Mitchell, V.D., Hui, N.K.C., Jones, D.J., and Wong, W.W.H., (2017), "A Green Route to Conjugated Polyelectrolyte Interlayers for High-Performance Solar Cells", Angew. Chem., 129, 8551 –8554.

Peng, J., Wu, Y., Ye, W., Jacobs, D.A., Shen, H., Fu, X., Wan, Y., Duong, T., Wu, N., Barugkin, C., Nguyen, H.T., Zhong, D., Li, J., Lu, T., Liu, Y., Lockrey, M.N., Weber, K.J., Catchpole, K.R. and White, T.P., (2017), "Interface passivation using ultrathin polymer–fullerene films for high-efficiency perovskite solar cells with negligible hysteresis", Energy Environ. Sci., 10, 1792—1800.

Ma, Q., Huang, S., Chen, S., Zhang, M., Lau, C. F. J., Lockrey, M. N., Mulmudi, H. K., Shan, Y., Yao, J., Zheng, J., Deng, X., Catchpole, K., Green , M. A., and Ho-Baillie, A. W. Y., (2017), "The Effect of Stoichiometry on the Stability of Inorganic Cesium Lead Mixed-Halide Perovskites Solar Cells", J. Phys. Chem. C, 2017, 121 (36), pp 19642–19649.

Sheng, R., Hoerantner, M.T., Wang, Z., Jiang, Y., Zhang, W., Agosti, A., Huang, S., Hao, X., Ho-Baillie, A.W.Y., Green, M.A., Snaith, H.J., (2017), "Monolithic Wide Band Gap Perovskite/Perovskite Tandem Solar Cells with Organic Recombination Layers", J. Phys. Chem. C, DOI: 10.1021/acs.jpcc.7b05517

Lau, C.-F.J., Zhang, M., Deng, X., Zheng, J., Bing, J., Ma, Q., Kim, J., Hu, L., Green, M.A., Huang, S., and Ho-Baillie, A.W.Y., (2017), "Strontium-Doped Low-Temperature-Processed CsPbI2Br Perovskite Solar Cells", ACS Energy Lett., 2 (10), 2319–2325

Yun, J.S., Kim, J., Young, T., Patterson, R.J., Kim, D., Seidel, J., Lim, S., Green, M.A., Huang, S. and Ho-Baillie, A., (2017), "Humidity Induced Degradation via Grain Boundaries of HC(NH2)2PbI3 Planar Perovskite Solar Cells", Adv. Funct. Mater. 2018, 1705363

Shi, L., Young, T. L., Kim, J., Sheng, Y., Wang, L., Chen, Y., Feng, Z., Keevers, M.J., Hao, X., Verlinden, P.J., Green, M.A. and Ho-Baillie, A.W.Y., (2017), “Accelerated Lifetime Testing of Organic–Inorganic Perovskite Solar Cells Encapsulated by Polyisobutylene”, (2017) ACS Appl. Mater. Interfaces, 9 (30), pp 25073–25081

Chang, N.L., Ho-Baillie, A.W.Y., Vak, D., Gao, M., Green, M.A. and Egan, R.J., (2018), “Manufacturing cost and market potential analysis of demonstrated roll-to-roll perovskite photovoltaic cell processes”, Solar Energy Materials and Solar Cells, 174, 314-324.

Rolston, N., Printz, A.D., Tracy, J.M., Weerasinghe, H.C., Vak, D., Haur, L.J., Priyadarshi, A., Mathews, N., Slotcavage, D.J., McGehee, M.D., Kalan, R.E., Zielinski, K., Grimm, R.L., Tsai, H., Nie, W., Mohite, A.D., Gholipour, S., Saliba, M., Michael Grätzel, and Dauskardt, R.H., (2017), “Effect of Cation Composition on the Mechanical Stability of Perovskite Solar Cells”, Advanced Energy Materials, 10.1002/aenm.201702116

PP3 Optics and Characterisation

Overview

Program Package 3, "Optics and Characterisation", targets experimental demonstration that previously accepted theoretical conversion limits can be increased by use of structures that have a high local density of optical states, with particular emphasis on thin-film organic and inorganic solar cells. Of special interest are devices thinner than the wavelength of light where there are opportunities for much stronger absorption of light than would normally be expected from the device thickness involved.

Work at ANU takes a biomimicry approach, based on butterfly wings, to achieve and characterise wavelength selective light trapping to maximise and manage the absorption and consequent current generation.

Other work has developed and applied cutting-edge characterisation techniques for photovoltaics materials. Standard reflection-transmission (R/T) spectroscopy techniques are not sufficiently sensitive to measure the subtle effect of excitonic binding energy on absorption spectra. The system at UNSW is now operational for the detection band up to 1050 nm and has been used to measure a GaP sample and the results are currently being interpreted.

UNSW has also developed a new ultra-high-sensitivity tool, the Photothermal Deflection Spectrometer, which exceeded the performance of commercially available photo-absorption systems by three orders of magnitude and it is being improved, in partnership with Open Instruments, for commercialisation.

A partnership of UNSW, ANU and PV Lighthouse is developing and testing a light-trapping model to more accurately predict the behaviour of isotextured solar cells for various anti-reflection coatings, encapsulants and light sources. In parallel, UNSW has been checking the feasibility of using embedded dielectric structures for a practical and economical rear light-trapping layer for solar cells, through simulations and experiments. These methods are of particular interest for application in thin-film solar cells, where the films are too thin to allow the use of texturing for scattering the light, but might also be applied to wafer cells.

PP3.2 Plasmonic and Nanophotonic Light Trapping

Lead Partner
UNSW/ANU

ANU Team
Prof Kylie Catchpole, Assoc Prof Thomas White, Assoc Prof Klaus Weber, Dr Niraj Lal

ANU Students
Kevin Le, Thomas Allen, Simeon Baker-Finch

UNSW Team
Dr Supriya Pillai, Prof Martin A. Green, Dr Henner Kampwerth, Dr Michael Pollard, Dr Ivan Wurfl, Dr Malcolm Abbott, Dr Supriya Pillai, Prof Darren Bagnall

UNSW Students
Xiao Qi Xu, C. E Disney, Yuanchih Chang

Industry Partners
Open Instruments – Dr Henner Kampwerth
PV Lighthouse – Keith McIntosh, Malcolm Abbott

Funding Support
ARENA, ACAP, ANU, UNSW

Aims

Wavelength selective light trapping is being developed and characterised in several ways in order to maximise and manage the absorption and consequent current generation.

Develop an extremely sensitive reflection-transmission (R/T) spectroscopy tool to be able to experimentally determine the excitonic binding energy of photovoltaic materials.

Develop a photothermal deflection spectrometer tool to accurately explore the absorption spectrum.

Progress

The team at ANU combines the principles of moth-eye anti-reflection, Bragg scattering and thin-film interference to design and fabricate a short-wavelength scattering/long-pass filter with sharp cut-off, high transmission of infrared light, and strong reflection of visible light into high angles. Based on the lamellae-edge features on *Morpho didius* butterfly wings, nanostructures are self-assembled via sequential one-chamber chemical vapour deposition, metal nanoparticle formation and wet-chemical etching. Such structures have potential applications in light trapping for tandem solar cells.

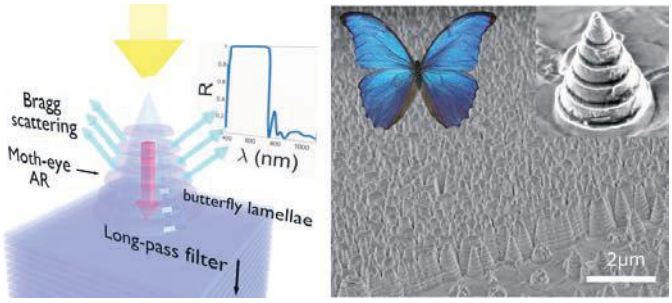

Figure PP3.2.1: (a) Schematic of a transparent long-pass scatterer with cut-off wavelength λ_c.; and (b) design of transparent long-pass scatterer incorporating moth-eye anti-reflection, long-pass Bragg filter, and short-wavelength scattering from butterfly wing lamellae (inset: *Morpho didius* butterfly (male)).

The effect of excitonic binding energy on absorption spectra is subtle, but important for material and cell optimisation. Theoretical values for silicon, CZTS and perovskites need to be experimentally verified. Standard reflection-transmission (R/T) spectroscopy techniques are not sufficiently sensitive to measure this. UNSW is building a customised system that is three orders of magnitude more sensitive to these spectral changes compared to standard systems. The technique measures differential changes of the R/T spectrum by forming a lock-in signal between two wavelengths instead of measuring absolute intensities.

The system is operational now for the detection band up to 1050 nm. The team has measured a GaP sample and is currently interpreting results.

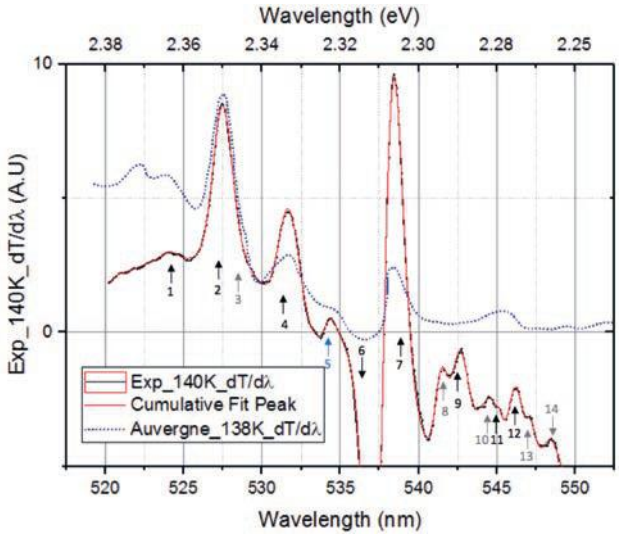

Figure PP3.2.2: The differential wavelength absorption spectrum of GaP at 140K. The blue dotted curve shows measurement data from Auvergne, et al. (1975), where the black and red solid lines are our measurement data, as well as its multi-Gaussian fits. The peaks and valleys of 1,2,4-7 are agreeing with the measurement from 1975, but smaller peaks and valleys disagree. Differences in sample purity are the likely cause.

Current research in photovoltaics seeks to employ increasingly thinner films of photoactive layers. Current examples are various CZTS and perovskite layers. As for all optimisation procedures, accurate measurement for process control is of central importance.

One of the most essential measurements, is the optical photo-absorption spectrum. Unfortunately, this is where most researchers face problems. Currently, available measurement instruments are not sufficiently sensitive to perform such measurement on thin films. This is especially the case for measurements in the so-called “sub-bandgap” region; a region that contains information on defects and Urbach tails. This situation of insufficient measurement capability remains true today.

In the years 2013–2015, ARENA funded the building of the first Photothermal Deflection Spectrometer (PDS) at UNSW. This instrument with ultra-high sensitivity fulfilled all expectations and exceeded the performance of commercially available photo-absorption systems by three orders of magnitude (x1,000). Since commissioning, it has become very popular among researchers in several research groups, having finally gained access to good measurement data.

This current project extends that work and has allowed a major step towards commercialisation. The most important hurdle that had to be overcome was the time-consuming opto-mechanical alignment phase, which could take up to an hour per sample. The ACAP funding allowed a collaboration between UNSW and Open Instruments Pty Ltd in which this alignment-hurdle was successfully overcome. The system will be, by a large margin, the world’s most sensitive photo-absorption spectrometer.

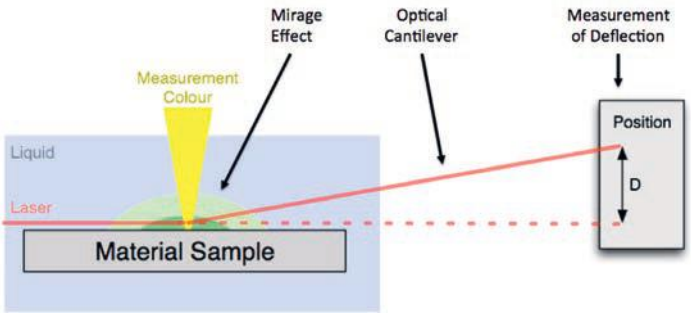

Figure PP3.2.3: The heart of the PDS system is the “mirage effect” that makes the very small amount of absorbed light measurable. It is doing so by suspending the material sample in a liquid (e.g. carbon tetrachloride, carbon disulphide) that changes its optical refractive index strongly with temperature. Light that is absorbed by the sample creates a tiny amount of heat, which then causes a refractive gradient (mirage) around that area in the liquid. This gradient is effectively forming a lens, that can deflect a probing laser beam. The deflection of a laser beam can then easily be measured by a position detector. The distance to that detector acts as an optical cantilever, making the entire system extremely sensitive.

Measurements of reflectance and transmittance are performed on isotextured Si wafers both before and after the deposition of thin films on their surfaces, to investigate light trapping in a partnership of UNSW, ANU and PV Lighthouse. The wafers have a variety of surface morphologies that were created by varying the isotexture etch duration. With an established light-trapping model, photovoltaic researchers can more accurately predict the behaviour of isotextured solar cells for various anti-reflection coatings, encapsulants and light sources.

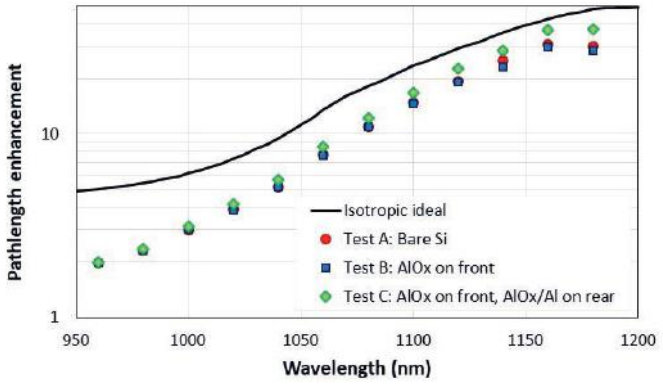

Figure PP3.2.4: Path length enhancement Z(λ) for a 3 μm isotextured experimental sample determined by ray tracing.

UNSW has been working to check the feasibility of using embedded dielectric structures, proposed earlier, to potentially act as a practical and economical rear light-trapping layer for solar cells. Simulations and experimental work were undertaken to ascertain the suitability of such structures.

Nanosphere (NS) lithography was used as part of the project where deposition was using spin-coating technique, which is a fast and cheap way of fabricating the structures. The spin-coating process was optimised and large area features were fabricated on whole wafers, the diffraction patterns clearly showing the uniformity of the layers. Quantitative analysis of such fabricated structures was performed using scanning electron microscope (SEM) images and Fourier transformation. The concentration of the different polystyrene nanospheres (PSNS) and the spin speeds were optimised.

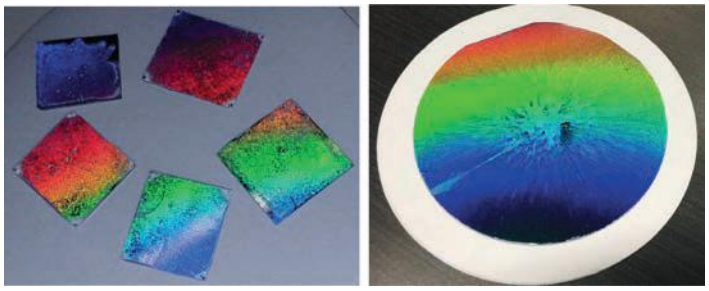

Figure PP3.2.5: Large area uniform deposition of the NS before metal overcoating clearly showing a strong diffraction pattern.

Figure PP3.2.5 is a representative image of the large area fabrication on full-size wafers accomplished showing clear diffraction patterns visually identified by the strong colours at different angles. In low magnification (large area) SEM images, we typically observe “grains” of closely packed NS with varying orientations as seen in Figure PP3.2.6 (a) and (b), even though the whole surface may be covered by a monolayer array. The accumulation of individual hexagonal patterns with different rotations results in the frequency profile showing ring patterns as shown in Figure PP3.2.6 (c) and sharp peaks in the line profile (Figure PP3.2.6 (d)). By integrating the line profiles taken from the centre to the edge over all in-plane angles, the quality (overall uniformity) of the NS films can be found. The appearance of a clear and sharp ring, with a spatial frequency matching the expected periodicity, indicates that the surface is covered by a uniform NS monolayer. Hence, the more intense and narrower the peak, the better the quality factor, signifying large area uniform arrays.

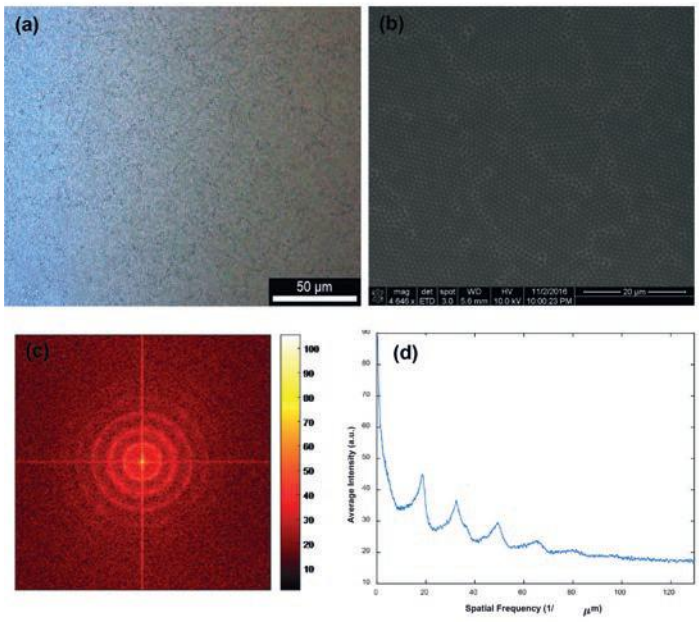

Figure PP3.2.6: Large area uniform 0.99 **µm** monolayers deposited by NS suspensions with optimal concentrations. Figure shows (a) 100x magnification optical microscope; (b) SEM image; (c) frequency domain profile of the SEM image in (b); and (d) intensity line profile of (c).

NS of different sizes and pitch were deposited onto thinned wafers and overcoated with silver (embedded NS). The schematic of the structure along with an SEM image is shown in Figure PP3.2.7. One of the challenges of the project was the thinning of the wafers to provide proof of concept as it is expected that the enhancement would be greater for the thinner samples. Wafers of 200 µm thickness were thinned using wet etching and thinned down to ~50 µm. The thinned samples were then bonded to fused silica.

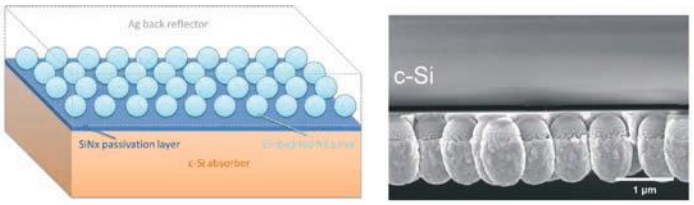

Figure PP3.2.7: (a) Designed (inverted view); and (b) SEM cross-section images of experimental-structure nanospheres overcoated with silver.

Spectral PL and PL imaging was used to measure the performance of the samples fabricated. A clear enhancement in the spectral PL was observed for the embedded NSs compared to planar reflectors for the same sample configuration as shown in Figure PP3.2.8(a). The results from the samples were further verified using PL imaging to account for variation in the large area samples as shown in Figure PP3.2.8(b). The PL counts from the PL images from different areas were averaged to arrive at the total PL count for the sample. Unlike spectral PL, PL imaging provides response form a larger area. Both results are compared to a planar silver reflector.

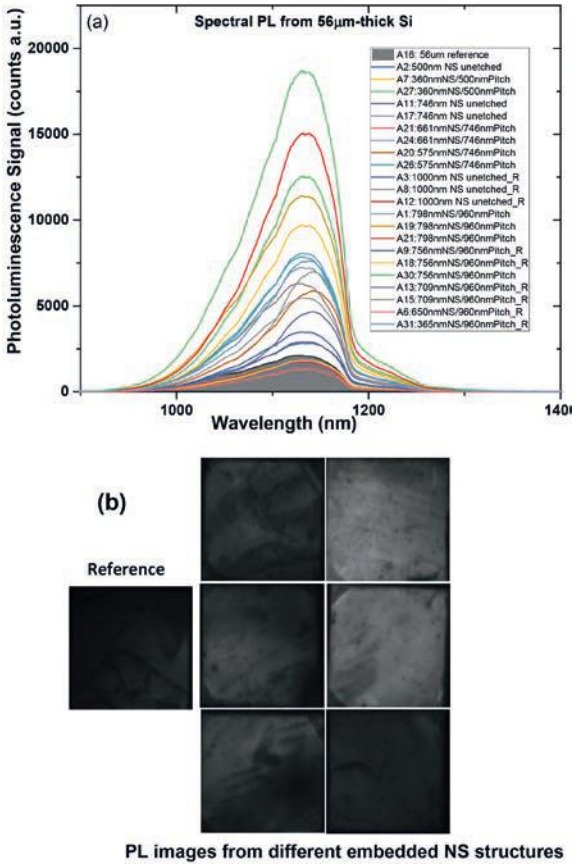

Figure PP3.2.8: (a) Spectral PL measurements of samples with different size and pitch of NSs overcoated with silver. The shaded region in grey represents the reference plots (planar metal reflector); and (b) PL images of some of the samples. Also shown is a reference sample for comparison.

Following concerns about parasitic absorption in the metal of such rear reflectors impeding useful absorption in Si, a detailed study was performed using simulations on different types of plasmonic rear reflectors to understand absorption in the metal vs. absorption in the semiconductor. It was found that for these types of structures, large angle scattering dominates in most cases, leaving a net positive impact relative to a rear mirror. However, this balance between parasitic absorption and large angle scattering should be factored in to selecting the correct geometries for nanotextured rear reflectors. Some of the results were presented in the previous annual report. Overall, it can be concluded that higher absorption in the metal need not always be problematic for plasmonic light-trapping structures and may not need to be avoided. Rather, it can potentially be associated with strong enhancements to absorption in the active layer of the cell (Disney, et al., 2017).

Highlights

- Finite-element modelling demonstrates strong (>45%) reflection into the first diffracted order for short wavelengths, while retaining >80% transmission for longer wavelengths.
- Fabricated nanostructures couple more than 50% of reflected light into angles of >10° while enabling broadband long-pass transmission.
- The world's first alignment free sample stage for an ultra-sensitive PDS system was successfully built and tested. A significant hurdle for commercialisation has been overcome and we press ahead for the first commercialisation phase at the end of 2018. This system is available for use at UNSW from now on.
- Path length enhancement of up to 42 times demonstrated on isotextured Si wafers and established that, unlike external reflectance, light trapping in isotextured wafers depends only weakly on the isotexture etch time (for practical etch durations).
    - The spherical-cap model, which is extended to account for internal rays within the isotexture, can be applied to predict the transmittance and escape reflectance and, hence, the light trapping in isotextured wafers.
    - The model predicts the AM1.5G generation current to within ± 1% and the reflectance and transmittance to within ± 2% absolute for $\lambda < 1100$ nm (and to within ± 4% for $\lambda < 1200$ nm for most samples).
- Large area fabrication of plasmonic rear reflectors using dielectric nanospheres and proof of concept to check the feasibility of these embedded dielectric structures to potentially act as a rear light-trapping layer for solar cells.

Future Work

It is planned that a commercialisation phase for the PDS system will be initiated by Q1 of 2018. It is intended that first versions of the tool will be made commercially available for selected research partners in the second half of 2018. In addition, theoretical work was initiated to solidify the underlying mathematical algorithms to interpret the measurement data. This will further enhance the general usability and usefulness of the system.

References

Lal, N.N., Le, K.N., Thomson, A.F., Brauers, M., White, T.P. and Catchpole, K.R., 2017, "Transparent Long-Pass Filter with Short-Wavelength Scattering Based on Morpho Butterfly Nanostructures", ACS Photonics, 4(4), 741–745.

Xu, X., Kampwerth, H., Puthen-Veettil, B. and Green, M.A., 2015, "A double beam wavelength modulation spectroscopy using two lock-in amplifiers", 25th International Photovoltaic Science Engineering Conference, Busan, Korea, 15–20 November 2015.

Auvergne, D., Merle, P. and Mathieu, H., 1975, Phys. Rev. B 12, 1371.

McIntosh, K.R., Allen, T.G., Baker-Finch, S.C. and Abbott, M.D., 2017, "Light Trapping in Isotextured Silicon Wafers", IEEE Journal of Photovoltaics, 7(1), 110–117.

Disney, C., Pillai, S. and Green, M.A., 2017, "The Impact of parasitic loss on solar cells with plasmonic nano-textured rear reflectors", Scientific Reports, 7(1) 12826.

PP4 Manufacturing Issues

PP4.1 Cost Evaluations

Lead Partner
UNSW

UNSW Team
Dr Anita Ho-Baillie, Dr Richard Corkish, Assoc Prof Renate Egan, Dr Xiaojing Hao, Prof Martin Green

UNSW Students
Nathan Chang, Marina Monteiro Lunardi, Chang Yan

ACAP Partners
CSIRO, ANU, Monash, UoM, UQ

Academic Partners
NREL
Dr Juan Pablo Alvarez Gaitan, Prof Stephen Moore (UNSW School of Civil and Environmental Engineering)

Overview

Solar power presents the lowest cost form of new electricity generation in an increasing fraction of the world's developed and developing economies. Solar power purchase agreements on large plant auctions is routinely coming in at less than 3c/kWhr (USD) – lower than the cost of coal, gas or wind in the same bid.

In sunbelt countries, such as most of Australia, residential solar delivers electricity at less than 7c/kWhr (USD).

Despite large-scale deployment of existing technology being super competitive, there remains opportunity for further price reductions and for development of solar materials, cells and modules for different markets, including in replacing fuels for transport, generating fuels for storage and lightweight solar for non-conventional roofs. The technologies being developed within ACAP aim to contribute to the ongoing improvements in cost and/or efficiency.

The Manufacturing Issues program seeks to deliver methods for assessing module manufacturing costs for emerging technologies. The objective is (i) to quantify the potential of new technologies; (ii) to inform decision making around research priorities; and (iii) to guide resources to cost ($) and performance (W) opportunities.

Targets for these manufacturing costs are set to a level such that the PV technology developed is internationally competitive, taking into consideration all aspects of the costs for PV manufacturing and will be competitive with other electricity generation options.

Aim

Driven by a need to provide a framework for costing of new technologies, the aim of the PP4 program is to deliver a methodology for assessing manufacturing costs for the different technologies under investigation under the ACAP program. Modelling of the cost and competitiveness will quantify the potential of new technologies and inform decision making around priority areas for research, giving consideration to potential benefit, risk, scale and capital cost.

The SunShot targets are used as benchmarks for comparison of the outcomes of the cost calculations. The aims for ACAP are to develop technologies with costs lower than the SunShot targets and ultimately to provide the stimulus needed to encourage serious investment in the new technology developments.

Targets

Consistent with the alignment of ACAP with US Sunshot Initiative, the ACAP manufacturing costings are compared to the US Department of Energy targets for photovoltaics. The relevance of these cost reduction targets is that their achievement would be recognised as a very major technological advance internationally and would provide the stimulus needed to encourage serious investment in the new technology.

The SunShot targets are thoroughly documented and regularly reviewed. The 2020 SunShot targets for the unsubsidised, levelised cost of electricity (LCOE) are shown in Table 4.1.1, along with module targets for lifetime, cost and efficiency to reach these LCOE costs.

Sunshot Targets	Residential	Commercial	Utility
LCOE ($/kWh)	0.09	0.07	0.06
System Cost ($/Wp)	1.50	1.25	1.00
Degradation rate			0.2%/yr
System lifetime			30 years
Module cost			40c/Wp
Module efficiency			20%

Table 4.1.1: US SunShot targets for residential, commercial and utility-scale solar in 2020. The breakdown for utility scale solar into module lifetime, cost and efficiency is shown.

The utility-scale PV system cost target for 2020 is $1/W and an LCOE of $0.06/kWh. To achieve this LCOE, the SunShot PV program has the following input targets:

- module cost to the end customer of $0.40/W
- module efficiency of 20%
- degradation rate of 0.2%/annum.

In late 2016, the SunShot Initiative proposed new 2030 targets for residential, commercial and utility scale. These longer term values recognising the "transformative solar progress to date and the potential for further innovation" and reduce the average unsubsidised LCOE of utility-scale PV to 3¢/kWh, commercial-scale to 4¢/kWh and residential rooftop PV costs to 5¢/kWh by 2030 [SunShot, 2016].

The ACAP research program aims to contribute to meeting these cost targets through new materials and device developments, described in PP1, 2 and 3. The Manufacturing Issues program (PP4) provides the framework for comparing the manufacturability and competitiveness of the innovative technologies under investigation within the ACAP group.

Progress

A key outcome of the efforts under PP4 is to provide a resource for assessing the cost of different processes with a view to informing research efforts on the key cost drivers and opportunities, and to understand how the technology fits on the costs and marketing roadmaps for photovoltaics.

Over 2017, the cost methodology has been expanded in its scope and analytical methods to take new aspects of uncertainty into consideration, and has been applied to further variations of standard c-Si manufacturing alternatives at varying levels of commercialisation including PERC, plating, hydrogenation and silicon heterojunction technologies.

4.1.1 Costing Methodology

Manufacturing cost estimation methods are commonly used in industry to optimise and incrementally improve performance and the cost of production. In ACAP, we are working on next-generation technologies, where the processes are less refined and the costs less well understood. With solar becoming increasingly competitive, researchers are motivated to conduct an early assessment of the cost impact of new technologies to better direct research effort, but these assessments need to take into account the relative maturity of the emerging technology.

Normal practice in manufacturing costing is to apply a bottom-up analysis using commercial software packages. These calculators have limited application for new technology developments in that they do not take into account uncertainties in the expected processes and costs. At an early stage of development, it can be difficult to define final processes and challenging to obtain precise cost information from equipment and material suppliers.

Within ACAP, we have developed novel methods for use during the early stages of process development to identify areas where cost reductions are necessary to bring an emerging PV technology to commercialisation and reduce the total time to commercialise a technology.

The ACAP cost analysis methodology has continued to be improved over 2017 to extend the model to include the impact and uncertainty associated with improved performance, the market premium paid for high power modules and early work on balance of system costs to deliver an LCOE value. The program has been extended to consider life cycle analysis and new work is proposed in module recycling and market assessments for emerging thin-film technologies (see Section PP4.2).

These enhancements to the model has enabled greater insights into the key benefits of different technologies, as well as bringing focus onto the key factors that must be addressed in order for a technology to be competitive in the market.

To begin a cost analysis, a manufacturing process sequence is derived from consultations with the researchers developing the processes. Process sequences are documented that reflect the demonstrated research processes, but are scaled to industrial throughput. The cost to manufacture is then calculated using a bottom-up 'Cost of Ownership' approach, considering costs such as materials, equipment, utilities, labour, building, maintenance and overheads. The main materials and suitable manufacturing tools are identified for each step, and the best available manufacturing cost data are obtained from various sources, such as publications, cost reports and price lists.

To account for uncertainties, for every cost parameter, a 'Nominal', 'High' and 'Low' value is determined. These data, together with other assumptions (such as factory yield, labour costs and depreciation schedules), are used to calculate the module manufacturing cost. Monte Carlo analysis is used to assess the impact of the uncertainty in each parameter. Typically 5000 scenarios are generated. For each scenario, the value of each cost parameter is generated randomly according to its two half-normal distribution, and then the cost calculations are completed using these generated values. The distribution of the cost outputs from the 5000 scenarios can then be analysed to understand the uncertainty of these cost estimates. Alternative process sequences can then be analysed and compared on both a median cost and cost uncertainty basis.

This costing methodology can be used iteratively as processes and knowledge develop.

With each iteration, the key cost drivers and the impact of the uncertainty from each parameter can be seen and can be used to inform research, resourcing and refinement of cost parameters to reduce uncertainty.

The methodology was developed under ACAP in 2016 and applied to a range of technologies.

1. Perovskite on Glass. [Chang, et al., 2017]
2. Roll-to-Roll Perovskite Printing. [Chang, et al., 2018a]
3. III-Vs on Silicon using Mechanical Bonding.
4. Silicon Cell Technology using laser doped selective emitter (LDSE) technologies.

In line with ACAP milestones, the methodology continues to be developed and new technologies costed each year.

4.1.2 Variations of Standard c-Si Sequences

Building on the work of previous years, where aluminium back surface field (Al-BSF) and LDSE technologies have been assessed, in 2017 further variations of c-Si processing have been analysed reflecting process variations at different stages of research, development and commercialisation: Passivated Emitter and Rear Cell (PERC), Advanced Hydrogenation, Inkjet Patterning and Silicon Heterojunctions (SHJ).

4.1.2.1 Passivated Emitter and Rear Cell (PERC) (Wenham, UNSW).

PERC processing, developed at UNSW, currently holds approximately 20% of the market share of total PV module production and is expected to increase to over 40% by 2021. The 2017 analysis confirms the benefit of PERC compared to the current industry standard Al-BSF technology.

4.1.2.2. Advanced Hydrogenation of Mono c-Si Cells (Wenham, UNSW).

Advanced Hydrogenation technologies, developed at UNSW are currently being tested in manufacturing, primarily to address carrier-induced degradation, known to impact performance and thus yield for modules in the field.

Cost modelling of these sequences compared to standard Al-BSF can be seen in Figures 4.1.1 to 4.1.3, showing, in Figure 4.1.1a, the additional cost per module of the two advanced sequences (PERC and PERC + Advanced Hydrogenation). The incorporation of uncertainty results in a probability distribution of cost, rather than a single number.

The new process sequences are more expensive on a $ per module basis, but manufacturing considerations go beyond the cost per module. The next step is to consider the power benefit from the new process.

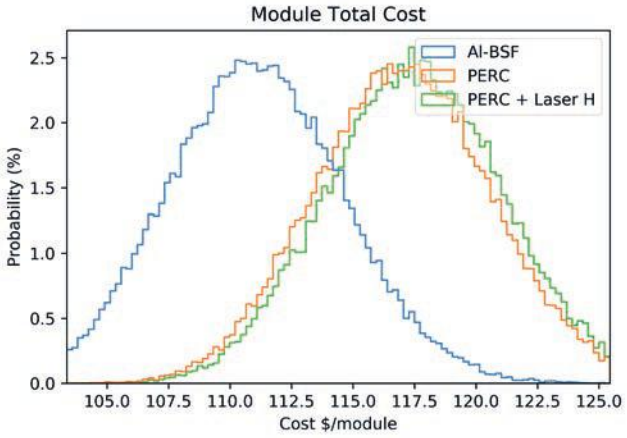

Figure PP4.1.1a: Total module cost ($ per module) for the two advanced sequences (PERC and PERC + Advanced Hydrogenation) compared with the Al-BSF process (Chang, et al., 2018b).

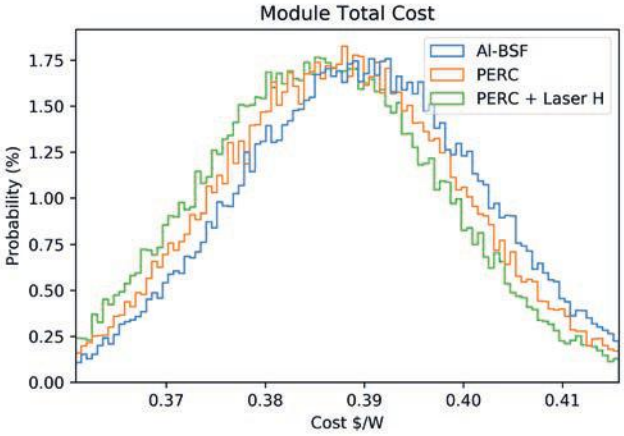

Figure PP4.1.1b: Total module cost in $/W for the two advanced sequences (PERC and PERC + Advanced Hydrogenation) compared with the Al-BSF process (Chang, et al., 2018b).

In Figure PP4.1.1b, the impact of improved efficiency is included, to give a module cost in $/W. Taking efficiency into consideration, the PERC and PERC + Advanced Hydrogenation processes are competitive with the Al-BSF process.

The manufacturing cost analysis then considers the additional benefits assigned to higher efficiency and the PERC and Advanced Hydrogenation technologies.

In Figure PP4.1.1c various market price factors such as increased selling prices (in $/W) for higher power modules and degradation free modules are included to show the expected margin per module. This last figure shows the clear commercial incentive to manufacturers of the advanced sequences compared to the baseline that is not evident when considering only the $/W cost results.

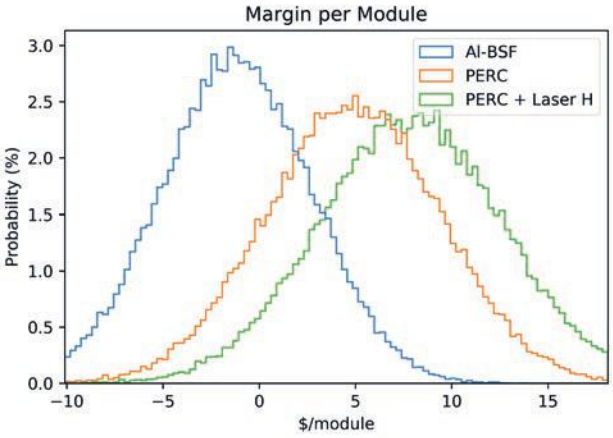

Figure PP4.1.1c: Margin per module in $/module for the two advanced sequences (PERC and PERC + Advanced Hydrogenation) compared with the Al-BSF process (Chang, et al., 2018b).

4.1.2.3 Inkjet Patterning (with Zhongtian Li, UNSW).

ACAP is supporting the early-stage development of an inkjet dielectric patterning method that can improve the efficiency of LDSE cells. The 2017 cost analysis found that the expected efficiency improvement is not yet sufficient to counteract the increased processing costs. The normalised uncertainty analysis identified the most important cost to be the use of novel chemicals. The chemical is used to strip off the epoxy layer used as a mask in inkjet printing. Research will focus on reducing this cost by replacing or improving utilisation of this chemical.

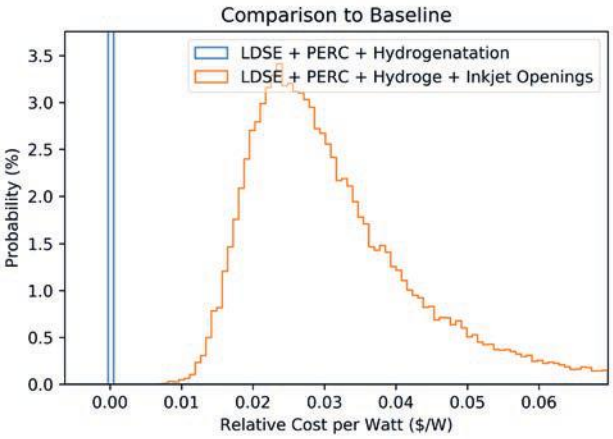

Figure PP4.1.2a: Relative cost in $/Watt when adding a novel Inkjet Process to the LDSE+PERC+Advanced Hydrogenation process.

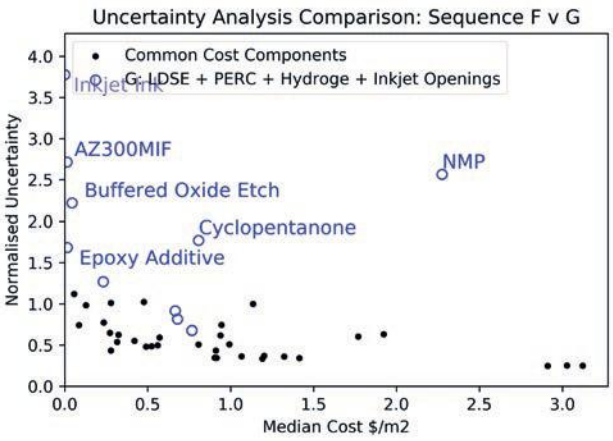

Figure PP4.1.2b: Normalised uncertainty analysis identifies the key cost drivers and uncertainties for new processes under development. In this case, identifying the cost and risk associated with novel process chemicals.

4.1.2.4 Silicon Heterojunction Solar Cells and Variations (with Hallam, UNSW).

Silicon heterojunction (SHJ) solar cells are attractive to the photovoltaics industry because of their higher efficiencies compared to standard Al-BSF and PERC cells. However, one of their disadvantages is that, to reach these efficiencies, they require n-type wafers with lower impurity levels compared to p-type wafers. In the photovoltaics industry, n-type wafers have a much lower market share compared to p-type wafers and are therefore more expensive.

Recent progress in Advanced Hydrogenation processes has opened the possibility of high performance SHJ cells using p-type wafers.

We have built an SHJ cost model based on a baseline process sequence, and then analysed a variation developed at UNSW that uses lower cost p-type wafers. This new sequence is not expected to match the efficiency of a standard SHJ cell, however it can potentially be much cheaper.

Over 2017, we assessed the potential costs and benefits of SHJ cells using p-type wafers, compared with n-type wafers, as well as a comparison to standard p-type mono PERC cells.

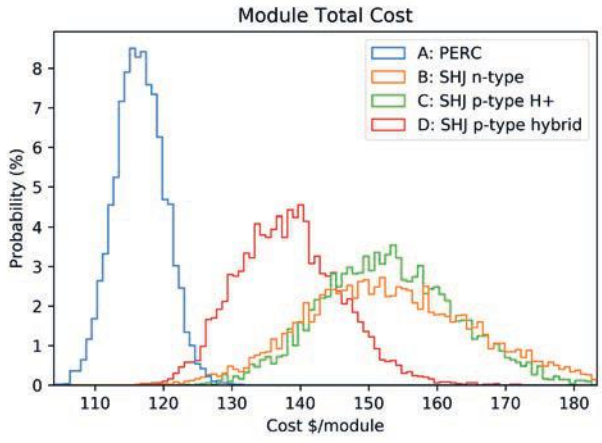

Figure PP4.1.3a: Cost per module in $/module for n-type and p-type SHJ technologies, including with advanced hydrogenation.

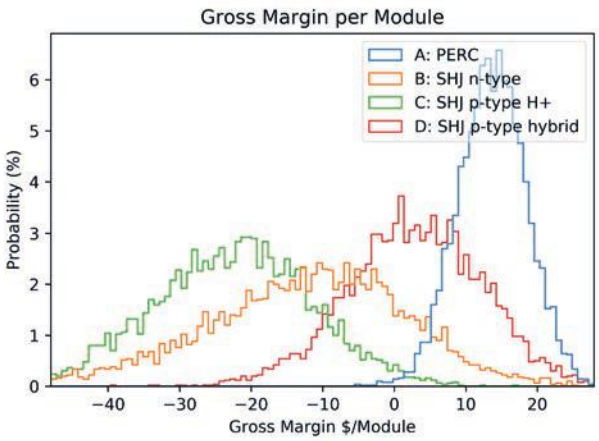

Figure PP4.1.3b: Margin per module in $/module for n-type and p-type SHJ technologies, including with advanced hydrogenation.

We found the key cost and performance parameters for these technology comparisons to be the usage/cost of the low temperature silver paste used in SHJ cells, the price premium of n-type wafers compared to p-type wafers, and the cell efficiencies that can be obtained with each sequence.

For the p-type vs. n-type SHJ comparison, the key uncertainties impacting the analysis are the expected cell efficiency difference and the n-type wafer cost premium.

For the p-type hybrid SHJ vs. p-type PERC comparison, the key uncertainties are the expected efficiency gain and the cost of the low temperature silver paste.

For both of these comparisons, guidance is provided on the research targets (efficiency and key cost drivers) necessary for each to be competitive compared to the baseline.

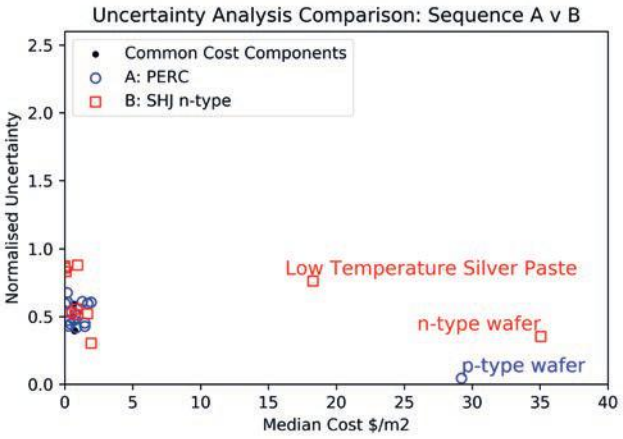

Figure PP4.1.3c: Normalised uncertainty analysis for n-type SHJ identifies the key cost drivers and uncertainties for new processes under development. In this case, identifying the cost and risk associated with n-type wafers and low temperature silver paste.

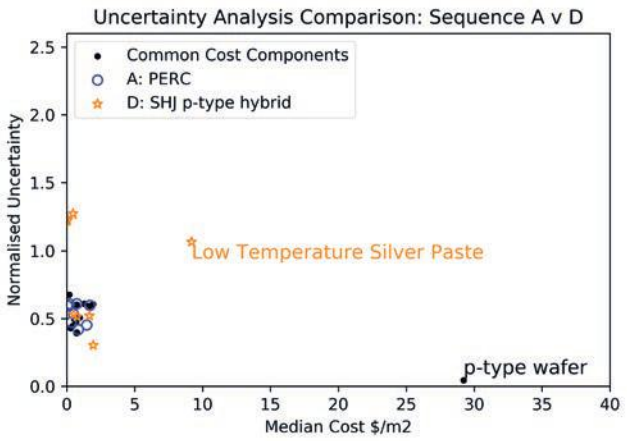

Figure PP4.1.3d: Normalised uncertainty analysis for p-type SHJ identifies the key cost drivers and uncertainties for new processes under development. In this case, identifying the cost and risk associated with the low temperature silver paste.

PP4.2 Life Cycle Assessments

Overview

Photovoltaic (PV) researchers and industry are continuously looking for technologies that can reduce costs and produce better efficiencies for solar cells and modules (Green, 2016). There are continuous developments being reported for several alternative PV materials but silicon (Si) remains the dominant commercial PV technology in the industry (Fraunhofer Institute for Solar Energy Systems, 2017). It continues to dominate the market (Frankl, et al., 2010) because Si is abundant, non-toxic, stable and has benefited from developments for the semiconductor industry. The technology is proven, modules are robust, and the manufacturing costs are low and falling. However, the search for new PV materials and device design is necessary as Si solar cells are approaching maturity when cost and performance improvements are becoming marginal in the absence of major breakthroughs.

The idea of a tandem solar cell (see Section 1.3) has been proposed and demonstrated (Green, et al., 2016; Almansouri, et al., 2015; Green, 2014; Wanlass, et al., 1989). Thin-film materials have been developed, providing potentially low-cost, flexible geometries and using relatively small material quantities. These technologies have led to several options for PV modules such as amorphous and microcrystalline Si films ("micromorph cells"), chalcogenide compounds such as cadmium telluride (CdTe), copper indium diselenide or disulphide (CIS), copper indium gallium diselenide (CIGS) and copper zinc tin sulfide (CZTS) and the recently emerged perovskite solar cells (see Section 2.5) (Green, 2007; Green, et al., 2017).

Along with these developments, there is also a concern with the environmental impacts that the production process, use phase and end of life may cause. Life Cycle Assessment (LCA) is a methodology used to analyse any product or process from an environmental perspective (Owens, 1997). The initial step of an LCA is defining the goal and scope of the study. The next phase is to produce an inventory, followed by the impact assessment, where the inventory data is translated into environmental impacts. Finally and based on the results, recommendations are made in order to have lower environmental impacts (Duda and Shaw, 1997).

Aim

At UNSW, a comprehensive LCA was conducted on chalcogenide/Si tandem solar modules (Monteiro Lunardi et al., 2018b) and advanced technologies on Si solar modules. The chalcogenide technologies chosen were CIGS, CZTS and AZTS (Ag_2ZnSnS_4) and the advanced techniques include two different processes of hydrogenation. The studies compare these solar modules, with the aid of GaBi LCA software (GaBiSoftware, 2016) to assess different environmental impacts of these technologies.

These LCAs are carried out with the aim of guiding research efforts towards cell designs with minimum environmental impact according to these criteria: global warming potential (GWP), human toxicity (cancer and non-cancer effects), freshwater eutrophication, freshwater ecotoxicity and abiotic depletion potential (ADP) impacts as well as energy payback time.

Progress

In 2016 we performed an LCA for perovskite/Si tandem solar modules (Monteiro Lunardi, et al., 2017). The current poor stability of perovskite material leads to poor environmental outcomes for perovskite/Si tandem modules. It was found that the replacement of the metal electrode with indium tin oxide or a metal grid reduces the environmental impacts significantly. Aluminium, compared to silver and gold, gives better environmental outcomes, including for energy payback time. The avoidance of using 2,2',7,7'-tetrakis(N,N-di-p-methoxyphenylamine)9,9'-spirobifluorene (Spiro-OMeTAD) and the reduction of solvent usage are also environmentally beneficial. Better environmental impacts are possible if perovskite materials become transparent and electrically conductive when they fail (Monteiro Lunardi, et al., 2017).

For chalcogenide/Si tandem solar modules it was found that, for global warming potential, the CZTS/Si and AZTS/Si tandem structures studied have better outcomes than Si modules (p/n and heterojunction with intrinsic thin-layer HIT structures). However the CIGS/Si tandem structure has worse impacts compared with silicon (p/n). Better results could be achieved if the energy used during the production process can be reduced. Also, if the efficiency can be increased the GWP impacts could be better for the tandem structures when compared with both types of silicon. For human toxicity (cancer and non-cancer), freshwater eutrophication and freshwater ecotoxicity the main impacts come from the CdS layer. Because of the presence of Cd in its composition, this layer is very toxic, not just for humans but also for fauna and flora. We suggested that researchers should focus on alternative layers to CdS with the same efficiency. Much work has already been done for this with CIS and CIGS (Bhattacharya and Ramanathan, 2004; Chelvanathan et al., 2010; Kushiya, et al., 1996; Asaduzzaman, et al., 2017) but there is still a lot to be done to find a strong replacement for this layer. The ADP shows that the use of metals and other materials is also a problem. The recycling of toxic elements as well as scarce metals is also very important to reduce the environmental impacts in all categories evaluated, but mostly ADP. Specifically for CIGS, indium is a key element and its scarcity is a concern for scaling up CIGS module production to the Terawatt level (Polman, et al., 2016). The results are shown in Figure PP4.2.1.

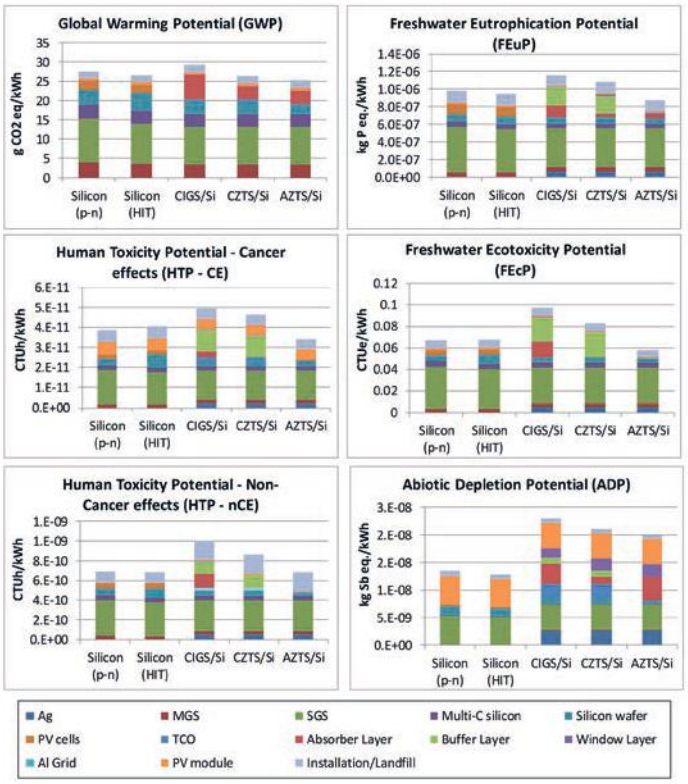

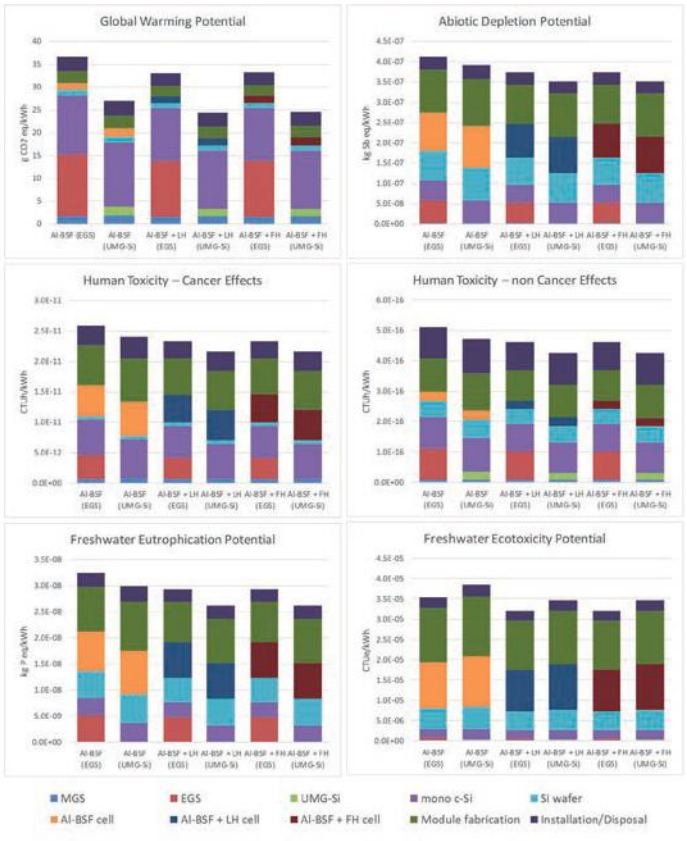

We conducted an LCA comparing Al-BSF and PERC (Monteiro Lunardi, et al., 2018a). The results demonstrate that the increase in the performance of the cells and modules using the PERC technology can produce better environmental impacts. Also, the energy payback time (EPBT) analysis demonstrates the importance of higher efficiency modules, not only for the best environmental results but also for the effective use of energy input. It is important to emphasise that the most significant contribution to low environmental impacts is from the use of UMG-Si (see Section PP1.1), and a smaller portion from the PERC improvements.

For advanced silicon solar modules (considering electronic grade silicon (EGS) and UMG-Si feedstocks with hydrogenation processes; see Section PP1.1) we find out that the silicon purification and treatment processes have the most significant impacts. Alternative technologies for the Cz process (mono c-Si) should be implemented to reduce this impact. Comparing the EGS and the UMG-Si processes we can observe that there is a decrease on the GWP results, due to the lower use of electricity in the UMG-Si process. The hydrogenation processes improves the cell's efficiency and reduces its light-induced degradation effects, which influences positively in the environmental outputs, due to the lower energy usage to produce the same amount of energy during the module's lifetime. The key finding of this LCA, related to the GWP impacts, is that the UMG-Si combined with the hydrogenation methods result in better environmental outcomes for this category. In other words, the processes with higher efficiency have the lower impacts, which means that the hydrogenation helps to produce better environmental outcomes for the technologies studied in this LCA. The advanced technologies studied in this LCA show better EPBT, which demonstrates the importance of the hydrogenation processes not only for the best environmental results but also for the effective use of energy input. However, these results could be different since we are not considering losses due to distribution and/or poor weather conditions. The results are shown in Figure PP4.2.2.

Summary

The manufacturing costing program continues to develop methods for assessing the manufacturing costing of new technologies. The cost and uncertainty methods developed allow uncertainties in individual process costs, performance and market value to be assessed. These uncertainties are combined using a Monte Carlo simulation.

The methods used do not require precise information on every data parameter and so allow for rapid analysis of emerging technologies, and in doing so, the analysis reveals the key drivers, technology risks and critical uncertainties to guide research directions.

The 2017 costing analyses included an assessment of variations of c-Si processing, reflecting process variations at different stages of research, development and commercialisation: Passivated Emitter and Rear Cell (PERC), Advanced Hydrogenation, Inkjet Patterning and Silicon Heterojunctions (SHJ).

LCA was used to compare the environmental impacts of different approaches to making silicon-based tandem cells.

Highlights

- Costing methodology expanded to include the impact and uncertainty of module performance and market factors, increasing the sensitivity of the analysis for more mature technologies.
- Identification of the key factors impacting commercialisation to allow focus by researchers and manufacturers on the factors with the most leverage.
- 2017 costing analyses included an assessment of variations of c-Si processing, reflecting process variations at different stages of research, development and commercialisation.

- LCA of chalcogenide/Si tandem solar modules:
  - Replacing the CdS buffer layer with a non-toxic and more transparent material is a key finding of this work.
  - The recycling of toxic elements as well as scarce metals is also very important to reduce the environmental impacts in all categories evaluated, but mostly abiotic depletion potential.
  - The use of energy during the processes is alarming. Alternative processes should be studied to find new routes that can produce good quality materials using lower quantities of energy.
- LCA of advanced silicon solar modules:
  - Comparing the EGS and the UMG-Si, the UMG-Si has lower environmental outcomes, due to the lower use of electricity during its production process.
  - The hydrogenation processes improve the cells which influences positively in the environmental outputs.
  - The key finding of this LCA, related to the GWP impacts, is that the UMG-Si combined with the hydrogenation methods result in better environmental outcomes for this category.

Future Work

In future years, we will continue to develop the cost analysis techniques, and apply them to additional technologies within ACAP. Potential areas for 2018 include silicon/perovskite tandems, advanced hydrogenation with multi wafers and CZTS.

Not many LCAs include the end of life of solar modules, mainly because of the lack of data for this process. However, it is important to consider this step of the process, since the European Waste Electrical and Electronic Equipment Directive confirms the potential environmental risks associated with the management and treatment of this waste. For future work we will consider different methods of recycling for all processes studied.

References

Almansouri, I., Ho-Baillie, A. & Green, M.A., 2015, "Ultimate efficiency limit of single-junction perovskite and dual-junction perovskite/silicon two-terminal devices", Japanese Journal of Applied Physics, 54(8S1).

Asaduzzaman, M., Hosen, M.B., Ali, M.K. and Bahar, A.N., 2017, "Non-Toxic Buffer Layers in Flexible Cu(In,Ga)Se2 Photovoltaic Cell Applications with Optimized Absorber Thickness", International Journal of Photoenergy, 8.

Bhattacharya, R. and Ramanathan, K., 2004, "Cu(In,Ga)Se2 thin film solar cells with buffer layer alternative to CdS", Solar Energy, 77(6), 679–683.

Chang, N.L., Ho-Baillie, A.W.Y., Basore, P.A., Young, T.L., Evans, R. and Egan, R.J., 2017, " A manufacturing cost estimation method with uncertainty analysis and its application to perovskite on glass photovoltaic modules", Progress in Photovoltaics, 25(5), 390–405, DOI: 10.1002/pip.2871

Chang, N.L., Ho-Baillie, A.W.Y., Vak, D., Gao, M., Green, M.A. and Egan, R.J., 2018a, "Manufacturing cost and market potential analysis of demonstrated roll-to-roll perovskite photovoltaic cell processes", Solar Energy Materials and Solar Cells, 174, 314–324, DOI: 10.1016/j.solmat.2017.08.038N.

Chang, N.L, Ho-Baillie, A., Wenham, S.,Woodhouse, M., Evans, R., Tjahjono, B., Qi, F., Chong, C.M. and Egan, R.J., 2018, "Guiding Research Directions for c-Si Photovoltaics –Manufacturing Cost Analysis for Standard and New Silicon Solar Cell Technologies", Under Review (Energy and Environmental Science).

Chelvanathan, P., Hossain, M. I. and Amin, N., 2010, "Performance analysis of copper–indium–gallium–diselenide (CIGS) solar cells with various buffer layers by SCAPS", Current Applied Physics, 10(3), S387–S391.

Duda, M. and Shaw, J.S., 1997, "Life cycle assessment", Society, 35(1), 38–43.

Frankl, P., Nowak, S., Gutschner, M., Gnos, S. and Rinke, T., 2010, "International energy agency technology roadmap: solar photovoltaic energy".

Fraunhofer Institute for Solar Energy Systems, 2017 "Photovoltaics Report" [Online]. www.ise.fraunhofer.de. [Accessed 20/01/2016].

GaBiSoftware. 2016. GaBi LCA Software [Online]. thinkstep Global Headquarters. Available: http://www.gabi-software.com/australia/index/ [Accessed 20/01/2016].

Green, M.A., 2007, "Thin-film solar cells: review of materials, technologies and commercial status", Journal of Materials Science: Materials in Electronics, 18(S1), 15–19.

Green, M.A., 2016, "Commercial progress and challenges for photovoltaics", Nature Energy, 1(15015).

Green, M.A., "Silicon wafer-based tandem cells: The ultimate photovoltaic solution?" SPIE OPTO, 2014. International Society for Optics and Photonics, 89810L-89810L-6.

Green, M.A., Emery, K., Hishikawa, Y., Warta, W. and Dunlop, E.D., 2016, "Solar cell efficiency tables (version 47)", Progress in Photovoltaics, 24(1), 3–11.

Green, M.A., Hishikawa, Y., Warta, W., Dunlop, E.D., Levi, D.H., Hohl-Ebinger, J. and Ho-Baillie, A.W., 2017, "Solar cell efficiency tables (version 50)", Progress in Photovoltaics: Research and Applications, 25(7), 668–676.

Kushiya, K., Nii, T., Sugiyama, I., Sato, Y., Inamori, Y. and Takeshita, H., 1996, "Application of Zn-compound buffer layer for polycrystalline CuInSe2-based thin-film solar cells", Japanese Journal of Applied Physics, 35(8R), 4383.

Monteiro Lunardi, M., Alvarez-Gaitan, J.P., Chang, N.L. and Corkish, R., 2018a, "Life Cycle Assessment on PERC Solar Modules", Under review for publication in Solar Energy Materials and Solar Cells.

Monteiro Lunardi, M., Alvarez-Gaitan, J.P., Moore, S., Yan, C., Hao, X. and Corkish, R., 2018b, "A Comparative Life Cycle Assessment of CIGS/Si, CZTS/Si and AZTS/Si Tandem Solar Cells". Energy (accepted, EGY-D-17-05734R1).

Monteiro Lunardi, M., Ho-Baillie, A.W.Y., Alvarez-Gaitan, J.P., Moore, S. and Corkish, R., 2017, "A life cycle assessment of perovskite/silicon tandem solar cells", Progress in Photovoltaics: Research and Applications.

Chang, N.L., Hallam, B., Chen, D. and Egan, R.J., 2018c, "Techno-economic analysis of silicon heterojunction cell production sequences using hydrogenated p-type wafers", Submitted to World Conference on Photovoltaic Energy Conversion, Hawaii.

Owens, J., 1997, "Life cycle assessment", Journal of Industrial Ecology, 1(1), 37–49.

Polman, A., Knight, M., Garnett, E.C., Ehrler, B. and Sinke, W.C., 2016, "Photovoltaic materials: Present efficiencies and future challenges", Science, 352(6283), aad4424.

Wanlass, M.W., Emery, K.A., Gessert, T.A., Horner, G.S., Osterwald, C.R. and Coutts, T.J., 1989, "Practical Considerations in Tandem Cell Modeling", Solar Cells, 27(1-4), 191–204.

PP5 Education, Training and Outreach

Nodes Involved
All nodes involved

Academic Partners
Swinburne University of Technology

Industry Partners
Australian Photovoltaics Association (APVI)

Funding Support
All nodes, ACAP, Melbourne Lord Mayor's Charitable Foundation

Overview

Within the PP5 Education, Training and Outreach package, ACAP has specific targets for high quality publications and for the number of researchers in different categories who benefit from the infrastructural support it provides, as well as for the number and length of researcher exchanges. A significant number of outreach events are also targeted for each year. As well as major events such as those reported in the PP5 section of this annual report, other outreach activities in 2017 included public lectures on material relevant to ACAP's activities, newspaper and magazine articles, and visits, information papers and presentations for policy developers and their advisors.

Again in 2017, there was very strong international interest in the articles by ACAP researchers in leading journals. A remarkably high number of these were "Hot Papers" and "Highly Cited Papers", as identified by the Clarivate Analytics' Web of Science. See Chapter 2 of this report for further information. In general, interest in and citations of AUSIAPV/ACAP's work have grown considerably over the year.

The ACAP nodes continue to educate the future practitioners, researchers and educators to support the necessary rapid expansion of the national and global photovoltaics (PV) industry and to develop more effective educational tools.

Aim

The work described here is about, promoting knowledge of the success of Australian photovoltaics leadership, adding to the global body of knowledge, engaging the next generation of researchers and sharing knowledge.

Progress

ACAP holds an annual research conference near the end of each year in order to keep ARENA and its National Steering Committee informed, and to exchange research results, enhance collaboration and reinforce one-on-one contacts between students and staff from the different nodes. The program includes an oral summary of progress and plans for each Program Package as well as oral and poster presentations of technical progress from staff and student researchers and a situation summary presentation by ARENA.

The 2017 conference, the fifth, ran as a session on the final day of the Fourth Asia-Pacific Solar Research Conference (APSRC), followed by a workshop for ACAP participants on Day Two (APVI, 2018). Day One was held at the Bayview Eden Melbourne and Day Two was hosted by the Melbourne University node.

The ACAP proceedings began with inspiring plenary presentations from invited guest speakers, Dr Gregory Wilson, Director of the Materials Applications and Performance Center and the Co-Director of the National Center for Photovoltaics (NCPV) at the National Renewable Energy Laboratory (NREL), USA, entitled "Photovoltaics – Low Cost Electricity Leading to a Multi-TW Future"; Dr Pierre Verlinden, Vice-President and Chief Scientist, Trina Solar on "The Future of p-type Multi- and Mono-crystalline Si PERC Cells"; and Jenny Riesz, Principal – Market Policy Development with the Australian Energy Market Operator on "Solar Deployment and Integration".

The plenary session was followed by two invited technical presentations from each of the six nodes, describing detailed progress in selected tasks from within the ACAP program. Later, attendees at both conferences read and discussed the showcase posters invited from each node.

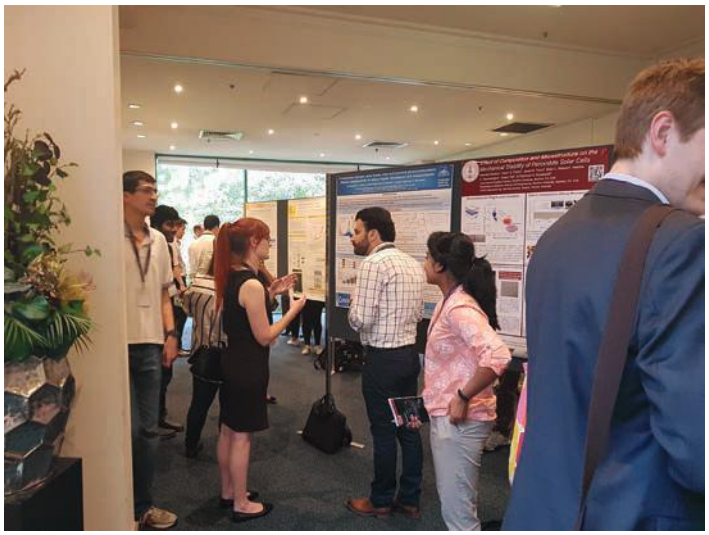

Figure PP5.1: The ACAP poster session generated considerable interest and interaction.

Day Two followed with an ARENA presentation and summary presentations of progress in each of the Program Packages. The ninth ACAP National Steering Committee meeting and the eighteenth Management Committee meeting were held on the afternoon of the second day of the conference.

The Australian PV Institute's APSRC, mentioned above, aims to provide a forum for development and discussion of content specific to Australia and its region, and an opportunity to foster collaboration between institutes, and to promote engagement between industry and academics. ACAP partners with the APVI to support the development of the conference program through participation in its organisation and through scheduling ACAP presentations as a session of the conference.

Figure PP5.2: Figure 5.1 Day three of the Fourth APVI Asia-Pacific Solar Research Conference, Melbourne, December 2017.

The Fourth APSRC was held on 5–7 December 2017 at Melbourne. The host ACAP node was Monash University and the Chair was Assoc Prof Jacek Jasieniak. Representatives of ACAP and of the UNSW ACAP node were involved in the organising committee. Staff and students from the nodes participated in academic review committees and contributed papers and posters to the conference. The conference drew nearly 300 participants from academia, government and industry, and ran parallel streams covering such areas as organic PV, PV devices, solar heating and cooling, policy and field experience. The list of invited plenary speakers included ACAP Director, Prof Martin Green and the principal investigators of two collaborating international research institutions: Dr Gregory Wilson (NREL) and Dr Pierre Verlinden (Trina Solar), whose presentations are described above.

In addition to involvement in the APSRC, ACAP has continuing strong engagement with the Australian Photovoltaics Institute (APVI), one of the more effective vehicles for Australian policy development through its focus on data, analysis and collaborative research. ACAP became a founding "Large Organisation" member of the Australian Photovoltaics Institute (APVI) and ACAP partners were active members of APVI throughout 2017. ACAP collaborators contributed to and participated in Australian representation on the Executive Committee for the International Energy Agency, Photovoltaic Power Systems.

All the nodes are involved in undergraduate and postgraduate education as capacity building for the next generations of photovoltaics researchers. Of particular note for 2017:

- approximately 40 students participated in the undergraduate course, "Nanoscience: Synthesis", run by the School of Chemistry and Molecular Bioscience at the University of Queensland
- the University of Melbourne node continued to deliver a Masters course in "Organic Electronics" with content that covers topics ranging from materials synthesis and characterisation to device applications, including organic photovoltaics
- UNSW is moving to a new academic calendar model from 2019, "UNSW 3+", consisting of three normal terms and an optional summer term. The normal terms will be 10 weeks each and the summer term will be five weeks. In order to fit the UNSW 3+ calendar, revised study plans for SPREE undergraduate and postgraduate coursework programs have been developed. In addition, teaching strategies of all SPREE courses have been reviewed and teaching plans were revised to suit the 10-week terms.

Figure PP5.3: UNSW Students Meet Industry night.

During 2017, UNSW's Women in Renewable Energy (WIRE) hosted, with the UNSW node's support, a broad range of events, providing its members with opportunities to socialise with other students, network with industry contacts, and expand their understanding of the renewables sector. WIRE hosted fortnightly picnics, attracting a great mix of regular attendees and new faces. A movie night was co-hosted with UNSW Women In Engineering Society, a great event for engineering students from different backgrounds to meet. An end-of-semester cocktail night, and a board games afternoon at the Whitehouse bar, were other casual events which allowed WIRE members to relax and socialise.

WIRE organised with Lendlease for members to attend a building tour of Barangaroo Tower Three, providing insight into application of sustainable design practices. An Industry Networking Night with the theme of "Diversity within Renewable Energy" gave WIRE members the chance to hear from two fantastic speakers about their careers, and the future of the renewables sector. WIRE also hosted its first ever Careers Night, inviting SPREE alumni to give presentations about their career progression, advice on gaining graduate positions, and tips on a smooth progression from study to working life. This event was a huge success, with many students commenting on how it removed much of the uncertainty surrounding starting a career. The strength of all these events was the space for open discussion, between industry contacts, SPREE staff and WIRE members, encouraging students to seek out information and providing a network for advice and support.

Figure PP5.4: UNSW's Women in Renewable Energy (WIRE) at (a) a fortnightly picnic; and (b) the 2017 Industry night.

Following on from the success of the CSIRO–Monash collaboration, industrial design and MBA students in previous years, in 2017 the CSIRO team engaged with Swinburne University postgraduate students as part of an industry-engaged innovation project for their Masters of Design program. A cross-disciplinary team of students from technical, business and design backgrounds worked with CSIRO researchers to develop a portable aquaculture (aesthetic) prototype incorporating printed solar films (see Figure PP5.5). This may later be developed into a functional prototype to further explore potential paths to market for printed PV.

Towards the end of the year, a detailed selection for ARENA-funded ACAP Fellowships was completed and offers were made to 20 outstanding young researchers to take up postdoctoral positions in cutting-edge projects across the nodes during the next three years.

The recipients and their projects, are:

Nathan Chang
"Techno-economic analysis of PV cell and module fabrication technologies"

The Duong
"Development of practical high-efficiency perovksite-silicon tandem modules"

Kean Chern Fong
"Transparent doped LPCVD polysilicon"

Phillip George Hamer
"Hydrogen drift and diffusion in solar cell architectures at intermediate temperatures"

Figure PP5.5: CSIRO working with Swinburne University Masters of Design students to develop a prototype portable aquaculture unit incorporating printed solar films.

Wenchao Huang
"Characterisation of microstructure formation in solution-processed photovoltaic perovskite thin films with synchrotron-based X-ray scattering techniques"

Wei Jiang
"Synthesis and characterisation of high dielectric constant semiconductors for homojunction organic photovoltaics"

Yajie Jiang
"Practical 50% efficient spectrum splitting CPV receivers using intermediate Bragg reflectors"

Mattias Klaus Juhl
"Determination of defect energy levels from injection dependent trapping"

Jincheol Kim
"High performance large area perovskite-silicon tandem solar cells"

Dongchen Lan
"Towards a 50% efficient multijunction photovoltaic system"

An Yao Liu
"New impurity removal technologies for low-cost, high-efficiency silicon solar cells"

Valerie Mitchell
"Block coplymers for high performance, thermally robust organic photovoltaic devices via an industrially relevant printing process"

Hieu Nguyen
"Multiscale and depth-resolved spectral photoluminescence for characterising solar cells"

Hang Cheong Sio
"Overcoming the material limitations of multicrystalline silicon for high efficiency solar cells"

Kaiwen Sun
" Device architecture design for commercial kesterite single-junction and multi-junction solar cells"

Daniel Walter
"Comprehending charge transport in perovskite-silicon tandem solar cells"

Yimao Wan
"Dopant-free silicon solar cells: rational design of transition metal oxide heterocontacts"

Chang Yan
"Towards 20% efficiency Cu_2ZnSnS_4 thin film solar cell by defect engineering and band grading engineering"

Jae Sung Yun
"Advanced nanoscale characterisation of local structures and defects for large bandgap materials for tandem solar cells"

Chuantian Zuo
"Semitransparent flexible perovskite solar cells for laminated tandem cell".

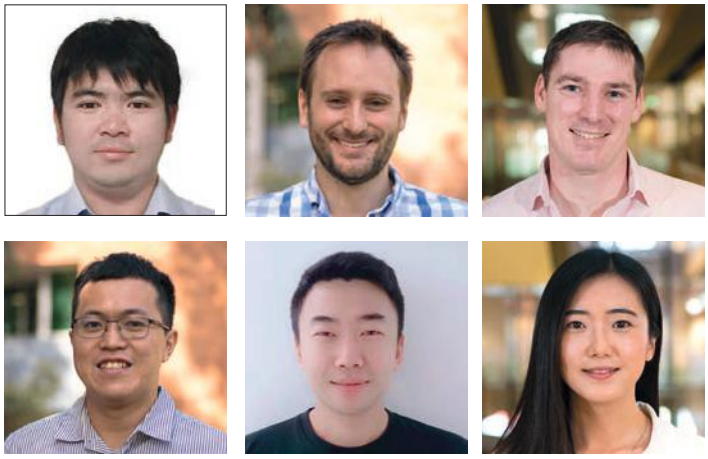

Figure PP5.6: Some of the twenty inaugural ACAP Fellows.

The impetus for release of additional funds from ARENA was the 2016 mid-term review report, in which the Review Panel (2016) noted that ACAP had requested "additional funding for postdoctoral fellowships to aid capacity building" and recommended that "ACAP substantiate this request to highlight likely benefits arising beyond those generated through ACAP's existing capacity building activities". ACAP subsequently made a formal request,with justifications, and ACAP and ARENA went on to negotiate an effective capacity building program. The positions are being offered by the institutions and taken up in late 2017 and early 2018.

An additional educational and training aspect, supported by ACAP, is researcher exchange. The frequency and depth of exchange activity has ramped up, strongly supported by the collaboration grants, reported in Chapter 6.

ACAP was very active on outreach and engagement in 2017. ACAP Director, Prof Martin Green, spoke on behalf of ACAP (Green 2017) at the ARENA Innovating Energy Summit in the Great Hall, Parliament House, Canberra on 14 August 2017. This talk was entitled, "Solar PV boosts Australian resources demand while reducing CO2!". ANU node leader, Prof Andrew Blakers, spoke on " Why our future is in pumped hydro" (Blakers 2017).

Next door to the auditorium, also In the Great Hall, ACAP and the UNSW and ANU nodes were represented at stands, engaging with politicians, public officials and other visitors through the day at the ARENA Innovating Energy Showcase.

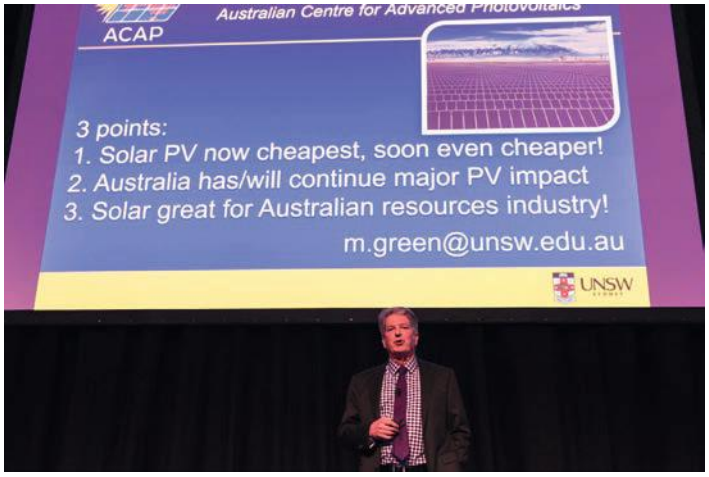

Figure PP5.7: ACAP director, Prof Martin Green, delivers his message of sustainable production In the Great Hall of Parliament House (Image: ARENA).

Figure PP5.8: Minister Josh Frydenberg visited the ACAP stand and showed great interest in the prototype Power Cube high efficiency spectrum splitting mini-module (see Section 6.1 of this report) (Image: ARENA, enhanced by UNSW).

Figure PP5.9: Chief Operating Officer, Richard Corkish, was kept busy all day explaining ACAP activities and achievements (Image: ARENA).

Tanya Plibersek MP, Deputy Leader of the Opposition and Shadow Minister for Education, in an address to the Universities Australia Conference in Canberra on 2 March 2017, used UNSW and ACAP as her example of Australian research tackling climate change.

> "Research at UNSW is just one example. The University's Centre for Advanced Photovoltaics recently set a new world-record in solar energy efficiency. Breakthroughs like this can underpin our future prosperity – if we work out how to harness them."
>
> **Tanya Plibersek MP, Deputy Leader of the Opposition and Shadow Minister for Education Canberra, 2 March 2017.**

The CSIRO node was active for National Science Week (12–20 August 2017), with a stand at "Living Science at the Market" at Melbourne's Queen Victoria Market.

Figure PP5.10: CSIRO researcher Dr Mei Gao sharing her knowledge on printed solar films with visitors to the Queen Victoria Market for the "Living Science at the Market" event as part of National Science Week.

The UNSW Sunswift "Violet" was, unfortunately, a non-starter in the 2017 World Solar Challenge. The car experienced a suspension failure while undergoing race testing at the Sydney Motorsport Park in Eastern Creek on 14 September. No-one was hurt, but the car was damaged too badly for it to be fixed in time for the race, from 8 to 13 October 2017. Sunswift Violet, a sleek four-seat sedan designed and built by engineering students at UNSW, was going through intense speed braking tests when a bolt on the left-hand front suspension fractured, causing the car to drop onto the roadway and skid for some 30 metres. Nevertheless, the car and the Sunswift team had already been very active in engaging the next generation of solar energy researchers, engineers, technicians and promoters.

UNSW's record-breaking Power Cube (see Section 6.1 of this report) features in the Sydney Powerhouse Museum as an outstanding example of Australian researchers pushing the boundaries of technology to beat the climate change problem.

ACAP researchers were involved in a huge range of technical presentations to the community and a few examples are mentioned here. ACAP sponsored the inaugural Research Symposium of the Australasian Community for Advanced Organic Semiconductors, 4–6 December 2017 (AUCAOS, 2017), including participation from the UQ and Melbourne nodes.

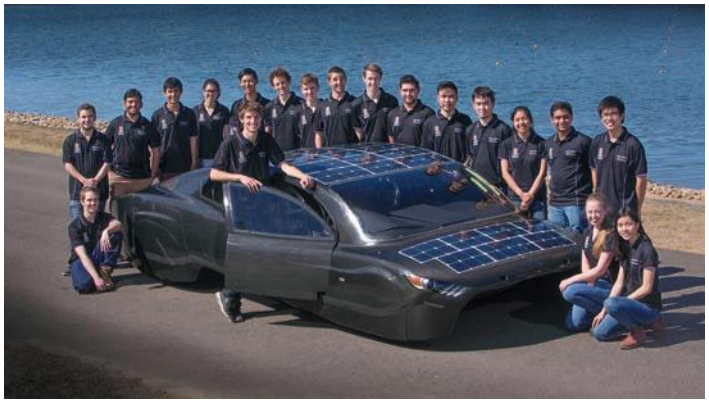

Figure PP5.11: The Sunswift student team with Violet.

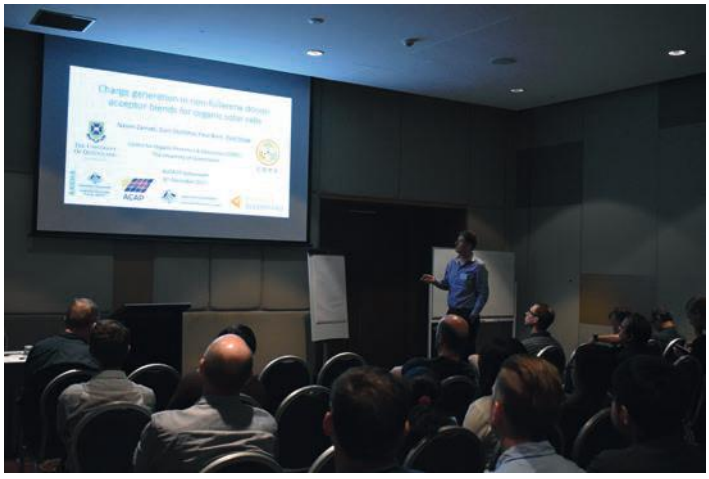

Figure PP5.12: Nasim Zarrabi presents to the AUCAOS in December 2017.

Jacek Jasieniak (Monash) and Fiona Scholes (CSIRO) were prominent thought leaders and participants in the 2017 CRC for Polymers seminar, engaging with industry, investors and other researchers.

Figure PP5.13: CRC for Polymers seminar.

The 2017 ANU Energy Update and Solar Oration featured Ms Audrey Zibelman, CEO of the Australian Energy Market Operator (AEMO), who discussed the intersection of the rise of renewables, grid stability and emission reductions and ANU's annual Energy Update included a keynote address by the Chief Scientist, Dr Alan Finkel, on "Implementing the National Electricity Market Review".

UNSW hosted 36 public lunchtime research seminars in 2017, with a large number of them having direct relevance to ACAP research and with many having a video recording made publicly available (UNSW, 2018). A couple of high points were the presentations of Prof Henry Snaith, University of Oxford, on "Metal halide perovskites: A new family of semiconductors for photovoltaics and optoelectronics" and Prof Albert Polman, of the FOM Institute for Atomic and Molecular Physics (AMOLF) in the Netherlands, on "Light management in photovoltaic materials".

ACAP researchers were again prominent in news reports. Sadly, one of the more prominent matters was the premature death of UNSW's Prof Stuart Wenham on 23 December 2017 (see Obituary in this report). On a brighter note, the PERC and hydrogenation technologies, for which he was a technology leader, were the talk of the industry, with a feature article in the SNEC Daily newspaper of 19 April 2017 at the influential International Photovoltaic Power Generation and Smart Energy Conference & Exhibition (SNEC Daily, 2017) and in PV Magazine on 26 January 2017. The updated Melbourne website, "Making any surface solar", excited a great deal of interest (University of Melbourne, 2017). ACAP COO, Richard Corkish, made a splash in the very "hot" Indian market with a well-received article, "Solar cells can be made cheaper", in The Hindu on 6 August 2017.

CSIRO's Flexible Electronics Laboratory showroom continues to function as an exciting destination for CSIRO visitors. In 2017, over 45 tours of the laboratory were conducted (see FigurePP5.14) including visitors from various high profile research institutions (e.g. Gwangju Institute of Science and Technology, Georgia Institute of Technology, University of Oxford), Australian SMEs and larger businesses (e.g. Fuji-Xerox, Toyota, GE) as well as both local and international government representatives (e.g. Saudi Arabian Prince, Nepal Consul General, Singapore High Commissioner).

Throughout 2017, the CSIRO team also worked on various design-related outreach activities with an industrial design intern (Mr Rowan Muller, recent RMIT graduate). These included the development of high quality concept images featuring printed solar films, which will be used for future outreach activities (see Figure PP5.15). The design of a large-scale printed solar film demonstrator was also finalised (see Figure PP5.15), the construction of which received additional support from the Lord Mayor's Charitable Foundation with installation at Melbourne Zoo scheduled for completion in early 2018.

The CSIRO team also continued its engagement with local public events, participating in "Living Science at the Market" as part of National Science Week at the Queen Victoria Market (see Figure PP5.10) and the Scientists and Mathematicians in Schools (SMiS) program. One work experience secondary school student was hosted at Monash and three were hosted at CSIRO to provide assistance with fabrication and characterisation of OPVs and perovskites.

Figure PP5.14: CSIRO's Flexible Electronics Laboratory showroom and some of the visitors from over 45 tours in 2017.

Figure PP5.15: Industrial design concept images developed for future outreach activities (top, bottom right) and design concept for printed solar film demonstrator at Melbourne Zoo (bottom left) (images by Mr Rowan Muller, CSIRO industrial design intern, RMIT graduate).

Highlights

- Selection of 20 new ACAP Fellows.
- The fourth Asia-Pacific Solar Research Conference was held, in conjunction with the ACAP, ASTRI and CSIRO annual meetings. With the theme of information, collaboration and integration, the event was chaired by Jacek Jasieniak from ACAP node and Monash University, and brought close to 300 participants to Melbourne.
- Interest in the ARENA Innovating Energy Summit and Showcase was unprecedented.
- The CSIRO Flexible Electronics Laboratory hosted more than 45 tours for visitors from high profile research institutions, industry and government.
- Development of high quality printed solar film concept images and a large-scale demonstrator design for Melbourne Zoo through collaboration with an industrial design intern.

Future Work

The next ACAP Conference will be held in coordination with the Fifth Asia-Pacific Solar Research Conference, at UNSW in December 2018. The first day will again overlap with the final day of the Asia-Pacific Solar Research Conference and the ACAP presentations on that day will form a special session of the broader conference.

Ongoing representation on the Executive Committee for the International Energy Agency, Photovoltaic Power Systems, including hosting of the Executive Committee meeting in Melbourne in late 2017.

References

ANU, 2017, ANU Solar Oration 2017, The Australian Energy Transition, http://energy.anu.edu.au/news-events/anu-solar-oration-2017-australian-energy-transition [accessed 20 February 2018].

APVI, 2018, Solar Research Conference, http://apvi.org.au/solar-research-conference/ [accessed 19 February 2018].

AUCAOS, 2017, Research Symposium 2017, http://aucaos.org.au/2017/01/10/research-symposium/ [accessed 20 February 2018].

Blakers, A., 2017, “Why our future is in pumped hydro”, presentation at ARENA Innovating Energy Summit: Powering Australia’s Future, Great Hall, Parliament House, Canberra, https://www.youtube.com/watch?v=HrCL1m6BO0s [accessed 20 February 2018].

Green, M.A., 2017, “Solar PV boosts Australian resources demand while reducing CO2!”, presentation at ARENA Innovating Energy Summit: Powering Australia’s Future, Great Hall, Parliament House, Canberra, https://www.youtube.com/watch?v=csqMkjudLNM&feature=youtu.be [accessed 20 February 2018].

Review Panel, 2016, “Mid-term Review Panel Report”, Australian Centre for Advanced Photovoltaics (ACAP), August.

SNEC Daily, 19 April 2017, www.pv-magazine.com/2017/04/19/issue-one-of-the-snec-daily-newspaper-published-on-first-day-of-snec-exhibition/ [accessed 20 February 2018].

University of Melbourne, 2017, “Making Any Surface Solar”, https://pursuit.unimelb.edu.au/features/making-any-surface-solar/ [accessed 20 February 2018].

AUSIAPV International Activities

Overview

The Australia–US Institute for Advanced Photovoltaics (AUSIAPV) encompasses the local activities of the Australian Centre for Advanced Photovoltaics (ACAP) as well as international collaborations with US-based partner organisations. The AUSIAPV program is directed at the highest level through an International Advisory Committee, with representatives from the key partners in Australia and the US, with engagement fostered through the development of collaborative research programs and the annual AUSIAPV/ACAP conference.

Section 6.1 describes the simplification of the overall design for the one-sun high-efficiency spectrum splitting modules by inclusion of the bandpass filter into the cell fabrication sequence.

Specific project activities that leverage the benefits of the AUSIAPV relationship also include key projects in Section 6.2 regarding the development of dye-sensitised solar cells in partnership with the University of California, Los Angeles and Section 6.3 as part of the Foundation Program to Advanced Cell Efficiency II (FPACE II) as well as a collaboration under the US Department of Energy SunShot Inititiave, where UNSW is involved in a program led by Arizona State University.

The AUSIAPV collaboration described in Section 6.4 is a long-standing one that records the .status of a whole range of photovoltaic technologies in the maintenance and publication of Solar Cell Efficiency Tables and that reported in Section 6.5, a project with collaborating organisation, PV Lighthouse, has grown into a leading tool for teaching photovoltaics manufacturing globally.

Since late 2015 and through 2016 the organisation has had three rounds of small grants to researchers based at ACAP nodes and another round was opened in Q4 of 2017. Many of the hot topics of the advancing silicon cell technology are being addressed by the collaboration grants. Their progress reports are presented online at www.acap.net.au/annual-reports.

In addition to the specific activities captured in this chapter, many of the reports already presented as detailed research reports also involve collaborations with US partners. These include the silicon tandem cell reported in PP1.3a and section 6.16, where well-established collaborations with institutes such as NREL, Arizona State University, Ohio State University, Colorado School of Mines, Yale University and University of Delaware are complemented by industry partner contributions from key players in the semiconductor foundry industries including Epistar Corp., Veeco and Amberwave, plus other partners from around the world.

Finally, the education, training and outreach activities reported in PP5 include a wide range of international interactions, the ACAP Conference, regular and special public lectures, and partnership arrangements in teaching and on-line learning, such as the development and delivery of courses between institutes in the US and Australia.

6.1 Improved Sunlight to Electricity Conversion Efficiency: Above 40% for Direct Sunlight and Above 30% for Global

Lead Partner
UNSW

UNSW Team
Dr Mark Keevers, Prof Martin Green, Dr Jessica Yajie Jiang

UNSW Student
Bruno Concha Ramon

NREL Team
Dr Keith Emery, Larry Ottoson, Tom Moriarty

Industry Partners
RayGen: Ian Thomas, John Lasich
Spectrolab: Dr Richard King (now ASU)
Trina Solar: Dr Pierre Verlinden, Yang Yang, Xueling Zhang
AZUR SPACE: Werner Bensch

Funding Support
ASI/ARENA, AUSIAPV, NREL, Spectrolab, RayGen, Trina Solar, AZUR SPACE, UNSW

Aim

The original aim of the project was to design, fabricate and test a proof-of-concept, prototype spectrum splitting concentrating photovoltaic (CPV) module demonstrating an independently confirmed efficiency above 40%. The combination of such a spectrum splitting or "Power Cube" receiver and a CPV power tower system (see Figure 6.1.1) has the potential to reduce the cost of utility-scale photovoltaics. With the targeted record performance level achieved in 2014, the project was extended in 2015 to target 42% CPV module efficiency and over 30% efficiency for a non-concentrating, flat-plate implementation of the approach.

As a contribution to the AUSIAPV program, NREL has provided extensive independent testing of module performance and advice on module design.

Progress

Prototype design

The original CPV prototype design was based on reflective concentration optics, a custom bandpass (spectrum splitting) filter, and two 1 cm› high efficiency commercial CPV cells, one Si and the other a triple-junction III-V cell, each mounted on a concentrator cell assembly (CCA) and a water-cooled heatsink, with an optional reflective secondary optical element (SOE) to improve flux uniformity. The mechanical design – based on optomechanical components – was iterated to achieve a lightweight, robust and fully adjustable structure, enabling optimisation about all critical linear and rotation axes.

More design details are given in the 2013, 2014, 2015 and 2016 ACAP Annual Reports. A photograph of the actual system under testing at UNSW in 2014 is shown in Figure 6.1.2. The triple-junction cell used in the prototype was a commercial Spectrolab concentrator cell (C3MJ+ cell, nominally 39.2% efficient at 500 suns–concentration, mounted on a ceramic substrate), while the Si cell was a SunPower back-contact cell of circa 1998 vintage (nominally 26% efficient at 200 suns), mounted on a ceramic substrate and encapsulated under glass by ENEA, Italy, followed by MgF_2 anti-reflection coating (ARC) at UNSW. This combination gave a record 40.4% efficiency in testing at NREL at the end of 2014, the first demonstrated conversion of sunlight to electricity with efficiency over 40%.

In 2015, an improved mirror was custom-designed and fabricated by Omega Optical Inc., likely setting a record for high reflectance over solar wavelengths. Independent measurements by NIST (US National Institute of Standards and Technology) confirming R = 99.7% Å ± 0.2% over the 400–1800 nm range. An improved version of the 287 cm^2 aperture area prototype using this improved parabolic mirror was independently tested at NREL's outdoor test facility in Colorado in 2016, again in a four-terminal configuration with efficiency of 40.6% ± 2% at air mass 1.5 certified, a new world record for a system of this size.

One-sun module

The project was extended in 2015 to investigate how the spectrum splitting approach could be applied to standard non-concentrating solar modules that have to respond to sunlight from a wide range of incident angles.

The approach adopted was based on an earlier UNSW discovery (Mills and Guitronich, 1978) of the near-ideal angular response properties of glass prisms. The module concept is shown in Figure 6.1.3. Light reflected from the first cell along the prism hypotenuse is channelled to the second cell.

Our present design uses prisms with a 30-degree apex angle. In this design, this approximately halves the area of III-V cells required while maintaining an acceptance angle of 118-degrees for on-axis light to hit both cells, with better performance for skew rays (Mills and Guitronich, 1978).

For our initial module, given the cells available, it was decided to implement the same design as in Figure 6.1.3 but with the III-V and silicon cell positions reversed with the final minimodule shown in Figure 6.1.4, being held by Dr Keevers. The 4 x 8 cm III-V cells were GaInP/GaInAs/Ge triple-junction cells designed for one-sun application (Bett et al., 2009), acquired from Azur Space while the 4 x 4 cm Si cells were high performance interdigitated back-contact (IBC) cells specially fabricated by Trina Solar for the project with anti-reflection (AR) coating optimised for the narrow band illumination involved.

An efficiency of 34.5% in a four-terminal configuration was independently confirmed in April 2016 by NREL for the 28 cm^2 minimodule, the highest ever one-sun measurement for a solar module of this size, far above the previous record of 24.1% (albeit for an appreciably larger area module). Presently, the approach is being used to fabricate a much larger 800 cm^2 device with similarly high efficiency targeted.

During this work, it was realised that there was an interest from space cell manufacturers in including a Bragg reflector between the III-V cells and the Ge cell in the three-cell stack to improve the cell radiation resistance. Modifying the design of this reflector for the present purposes would remove the need for external bandpass filters, as well as improving the angular response and reducing costs. This approach is the subject of a more detailed study.

Highlight

Simplification of overall design by inclusion of the bandpass filter into the cell fabrication sequence.

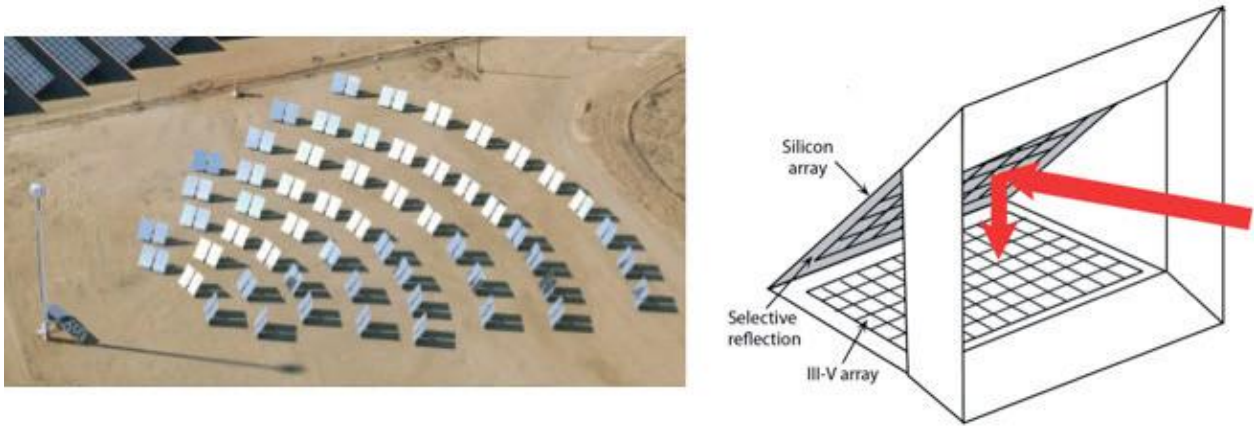

Figure 6.1.1: Photovoltaic power tower: (a) a heliostat field directs sunlight to a central tower housing a dense photovoltaic array receiver in the CPV system being developed by RayGen (artist's impression; image courtesy of RayGen); and (b) possible design of an advanced receiver implementing the demonstrated improvements at scale.

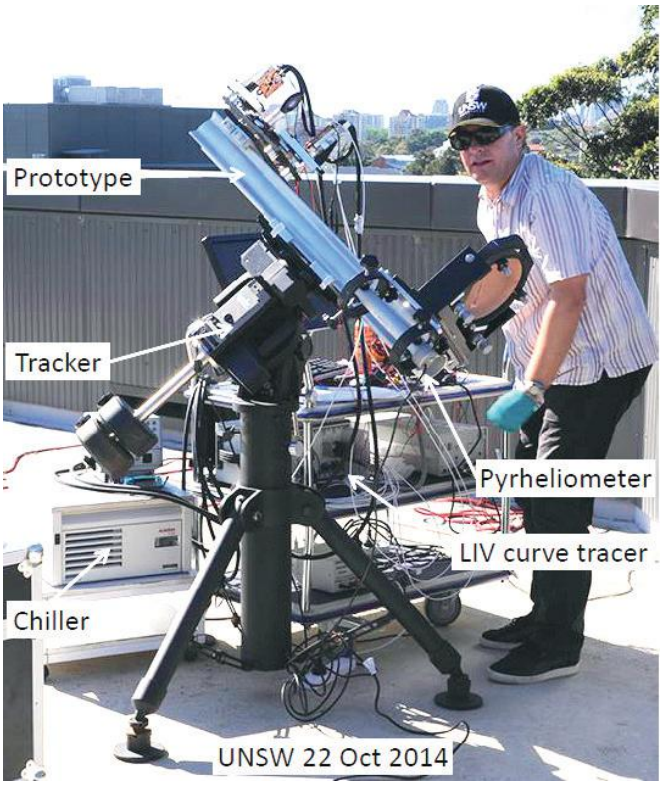

Figure 6.1.2: The prototype under testing at UNSW on 22 October 2014 with an efficiency of over 40% measured on that day.

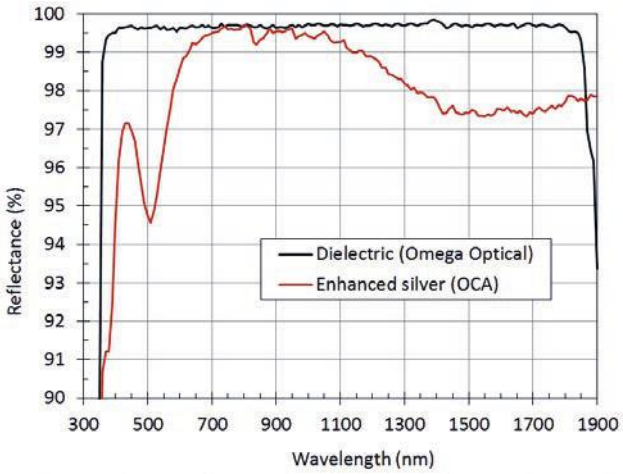

Figure 6.1.3: Initial one-sun module design concept where prisms are used to steer light reflected from one cell to the second for a wide range of incidence angles.

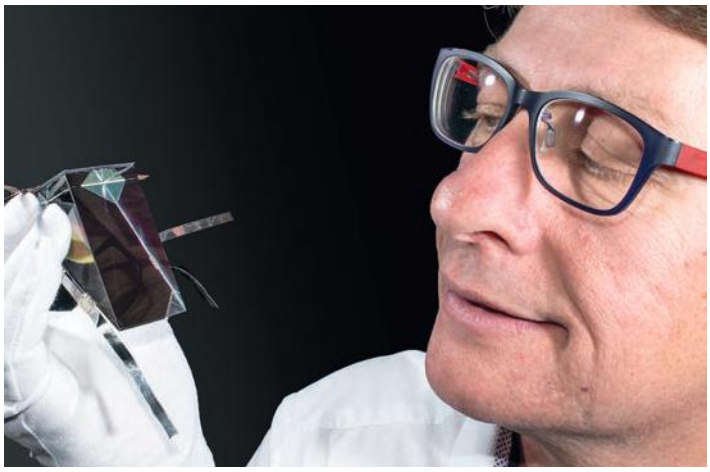

Figure 6.1.4: Dr Mark Keevers holding the record one-sun minimodule, with a III-V cell supplied by Azur Space along the prism hypotenuse combined with an Si cell supplied by Trina Solar. An efficiency of 34.5% was certified at NREL.

Future Work

Further refinement of the concentrator prototype design is expected to allow an efficiency of 42% to be demonstrated, increasing the margin over the alternative CPV and solar thermal approaches. Applying a similar approach to a standard non-concentrating, flat-plate module is expected to result in confirmation of record efficiency well over 30% for an 800 cm^2 module in 2018.

Reference

Mills, D. and Giutronich, J., 1978, "Ideal Prism Solar Concentrators", Solar Energy, 21, 423.

6.2 Dye-Sensitised Solar Cells

Lead Partner
Monash

Monash Team
Prof Yi-Bing Cheng

Monash Student
Wenchao Huang

Academic Partner
University of California, Los Angeles, Prof Yang Yang

Funding Support
ACAP, ARENA, ARC, Monash

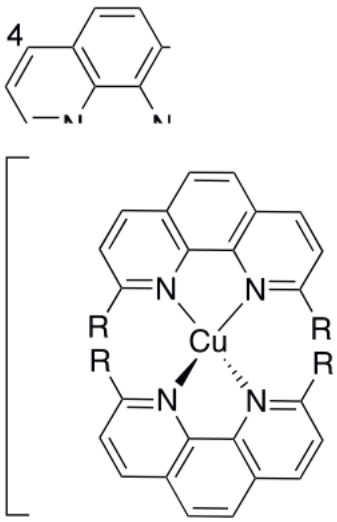

Figure 6.2.1: Molecular structure of the copper complex redox mediators, Cu(dmp) and Cu(dpp), studied in this work.

Aim

Due to the thinness of the active layer, light absorption is a critical issue limiting further improvements in organic photovoltaic (OPV) device performance. In order to use solar radiation more efficiently, a promising approach is to use tandem solar cells combining two photoactive layers to improve light absorption. The aim of this project is to collaborate with UCLA to develop highly efficient tandem organic, dye-sensitised-based solar cells.

Progress

The team at Monash have reported that, for copper-based redox mediators for DSCs, the structural reorganisation between Cu(I) and Cu(II) phenanthroline complexes can be minimised through modification of substituents at the phenanthroline ligand. Using DFT calculations we could show that the reorganisation is mainly dominated by the bulkiness of substituents on the 2,9-position of phenanthroline while substituents at the 4,7-positions have a minor influence. Cu(I/II) complexes of methyl (dmp) and phenyl (dpp) substituted phenanthroline have been synthesised, characterised and tested in solar cell devices. We have found that both substituents show similar charge transport properties in symmetrical and standard solar cells. However, if 4-*tert*-butylpyridine (TBP), a common additive to improve the solar cell performance, is added to the electrolyte solution, the charge transporting property of the phenyl substituted phenanthroline is significantly reduced. We attribute this behaviour to the more flattened structure of $[Cu(dpp)_2]^+$ which allows for stronger coordination of TBP to the copper centre.

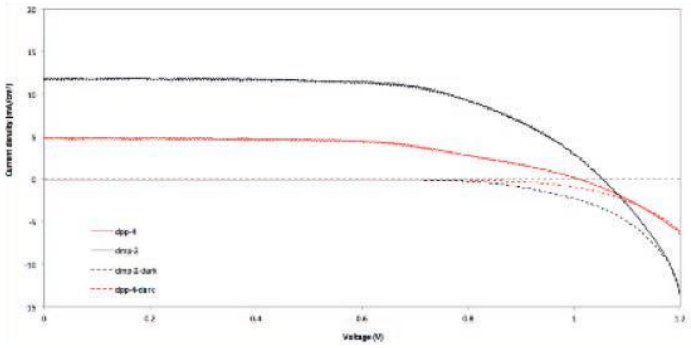

Figure 6.2.2: J-V curves of DSCs with Cu(dpp) and Cu(dmp) redox mediator electrolytes under AM1.5G (solid) and dark (dashed) conditions. All devices are composed of Y123-sensitised TiO_2 film (5 µm + 3 µm), a ITO-Pedot counter electrode and an acetonitrile-based electrolyte.

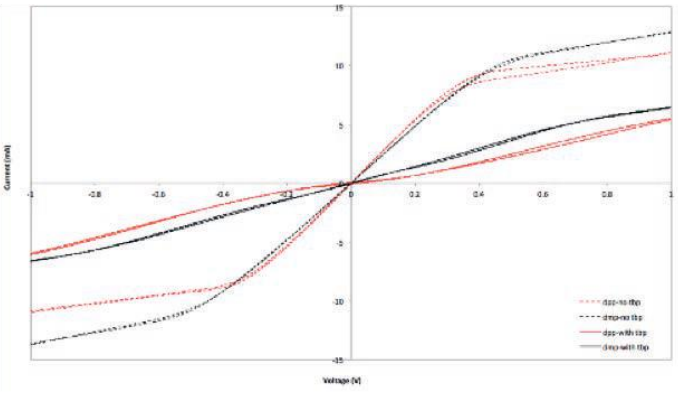

Figure 6.2.3: Cyclic voltammograms of symmetrical PEDOT sandwich cells with Cu(dpp) and Cu(dmp) redox mediators, with tBP (solid) and without tBP (dashed) under dark conditions.

6.3 Carrier Selective Contacts for Boosting Silicon Solar Cell Efficiency

Lead Partner
UNSW

UNSW Team
A/Prof S. Bremner, Dr A. Ho-Baillie, Dr F. Ma

UNSW Student
Jing Zhao

Academic Partner
Arizona State University

Arizona State University Team
A/Prof Stuart Bowden, Prof Christiana Honsberg

Funding Support
None

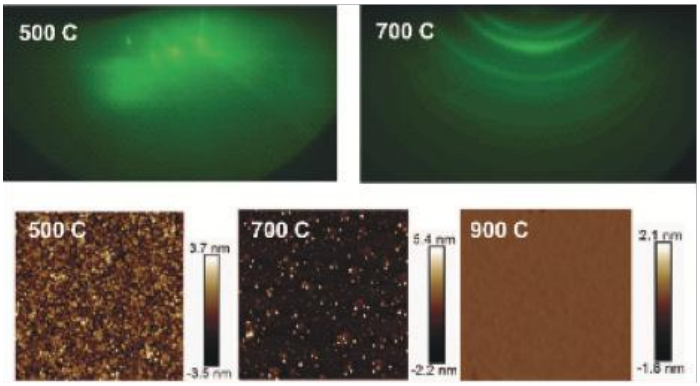

Figure 6.3.1: Top: Reflective High Energy Electron Diffraction (RHEED) patterns for NiO_x deposition at temperatures of 500˚C (left), showing bright streaks indicating high crystallinity, and 700˚C (right), showing a hazy ring pattern indicative of amorphous material. Bottom: Atomic Force Microscopy images of the corresponding surfaces (500˚C left, 700˚C middle, 900°C right) ex situ, showing improved surface smoothness with increased deposition temperature.

Aim

The aim is to develop novel device structures for ultrathin crystalline silicon (c-Si) solar cells based on "carrier selective contacts". UNSW contributes device modelling (e.g. using Sentaurus TCAD), materials deposition (e.g. spin coating), characterisation and integration of selected wide bandgap materials including transition metal oxides (e.g. NiO_x, VO_x) as carrier selective contacts (CSC) for the novel silicon cell structure as part of a collaborative effort. Refer also to the completed project undertaken by ANU with University of California, Berkeley and Lawrence Berkeley National Laboratories, including the Molecular Foundry, reported in Section 6.7 of the 2016 Annual Report.

Progress

Previously we have studied the use of transition metal oxides on silicon via sol-gel deposition, focusing on nickel oxide (NiO_x) and vanadium oxide (VO_x) (Zhao et al., 2017). In order to investigate in more detail the impact of different interface quality on carrier selective contact performance NiO_x layers were deposited by pulsed laser deposition on float zone n-type silicon wafers at temperatures of 300˚C, 500˚C, 700˚C, and 900˚C. This approach allowed for in situ monitoring of the deposition via Reflective High Energy Electron Diffraction (RHEED), which gives a pattern of the electron scattering from the top few atomic layers of a crystal. A selection of the resulting patterns is shown in Figure 6.3.1, with the RHEED patterns in the top line showing that a bright streaky pattern is seen for 500˚C (this indicates good crystallinity and layer-by-layer deposition), but when the temperature is 700 ˚C and above a hazy ring-like pattern (suggesting an amorphous layer deposition) is seen. After depositing approximately 10 nm NiO for each temperature, samples were removed and the surface probed by atomic force microscopy (AFM). The results on the bottom line of Figure 6.3.1 corresponding to 500˚C and 700˚C deposition show an increasingly smooth surface with deposition temperature, a trend confirmed by the 300˚C and 900˚C results (not shown).

In general, contact selectivity towards a particular carrier type can be evaluated via its specific contact resistivity ρ_c. The specific contact resistance ρ_c for our samples were measured using the transfer length method (TLM) for contacts fabricated with Al metal pads on the NiO_x layers. The thin NiO_x (~10 nm) being deposited at 700˚C and 900˚C improved dramatically the contact behaviour relative to lower deposition temperatures, giving ohmic contact with much lower specific contact resistance between the Al electrode and the p-Si substrate compared to the sample without NiO_x. The low resistance for hole transport provided by the NiO_x/Al contact structure is likely attributed to (a) a reduction in the work function, compared to that of Al, and/or (b) electron tunnelling through a reduced barrier width, similar to the mechanism of the ohmic contact between heavily phosphorus-doped p+ c-Si and the direct Al contact. The samples with NiO_x grown under 300˚C and 500˚C exhibit rectifying behaviour, i.e. they are not ohmic, likely caused by a large surface potential barrier at the interface or Fermi-level pinning due to a large defect density. Moreover, when a ~2 nm SrO interlayer between Al and NiO_x was included the ρ_c of the sample (the SrO enhances the passivation of the c-Si surface, as presented later), showed a higher ρ_c than the sample without SrO under the same growth temperature. This phenomenon can be related to the bulk resistivity of the SrO interlayer, introducing an additional hindrance to current transport. Nevertheless, it is notable that the insertion of a thin SrO layer increases the contact resistivity only moderately.

In order to study the passivation quality of the pulse laser deposition (PLD) NiO_x, the effective minority carrier lifetime was assessed by PL imaging, as the small size of PLD samples didn't allow standard photoconductance-based measurements. PL images of the NiO_x samples deposited under 300˚C, 500˚C, 700˚C and 900˚C with an SrO interlayer are shown in Figure 6.3.2. The relative minority carrier lifetime is quantified by PL intensity as the steady-state PL intensity scales linearly with the lifetime. These results show the average PL intensity over the whole area increases with the growth temperature. This is most likely due to less defect states within the NiO_x and less interface defect states at the NiO_x/Si interface (a reduction of interface recombination velocity) under high growth temperature. Furthermore, after the insertion of a thin interlayer film of SrO, the PL intensity significantly increased by around 20%, indicating an equivalent increase in effective lifetime. This can be attributed to the native-oxide-free surface for the NiO growth by including the 2 nm SrO layer, which reduces the interface defect density and thus improves the passivation.

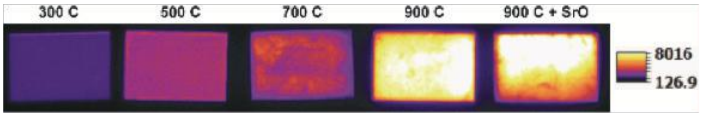

Figure 6.3.2: Photoluminescence imaging results showing counts (higher counts indicates higher minority carrier lifetime) for different deposition temperatures, showing improved passivation with increased deposition temperature. A sample with an SrO layer between the Si and NiO is also included, with good passivation also seen.

Highlights

- Investigation of the effect of crystallinity on carrier selective contact performance of nickel oxide deposited using pulsed laser deposition.
- Amorphous material at higher deposition temperature shows best results in terms of surface morphology, surface passivation and contact resistivity.
- Inclusion of an interlayer of strontium oxide saw promising initial results with improved passivation seen. Higher contact resistivity needs to be addressed, though the increase was moderate.

Future Work

Incorporation of alternate passivation layers such as aluminium oxide by various methods will be undertaken in the near future. As part of this work the use of the in situ strontium oxide–based de-oxidation process will be included. These results will be used in conjunction with simulation results to determine the best method for forming CSC using nickel oxide. The use of PLD for depositing VO_x layers will also be attempted this year. Further adaptation of the simulation tools will continue with expansion into simulating 2-dimensional dichalcogenides as the front CSC already being performed using a model previously developed for graphene (Zhao et al., 2018).

References

Zhao, J., et al., 2017, “Transition Metal Oxide-Silicon Carrier Selective Contact Solar Cell”, Presented at 44th IEEE PVSC, Washington DC.

Zhao, J., et al., 2018, “Advanced interface modelling of n-Si/HNO_3 doped graphene solar cells to identify pathways to high efficiency,” Applied Surface Science, 434, 102–111.

6.4 Solar Cell Performance Documentation

Lead Partner
UNSW

UNSW Team
Prof Martin Green, Dr Anita Ho-Baillie

NREL Team
Keith Emery, Dr Dean Levi

Academic Partners
Fraunhofer Institute, JRC Ispra, AIST Japan

Funding Support
ACAP

Aim

To improve accuracy and quality of photovoltaic device measurement and reporting.

Progress

A long-standing research collaboration between UNSW and NREL, now being conducted as an AUSIAPV collaborative project, involves the reliable documentation of the status of the whole range of photovoltaic

technologies worldwide. This is by the biannual publication of the “Solar Cell Efficiency Tables” in the Wiley journal, *Progress in Photovoltaics*.

By enforcing guidelines for the inclusion of solar cell efficiency results into these Tables, this not only provides an authoritative summary of the current state of the art but also ensures measurements are reported on a consistent basis. One criterion that has been important to enforce has been that results be independently certified at one of a limited but increasing number of “designated test centres”, generally of a national facility status, with a certified measurement capability and additionally involving international “round robin” testing. Two more test centres were added to the list in 2017, after careful review.

This rigour has been important particularly as new device technologies come to the fore and groups relatively inexperienced with cell testing suddenly are thrust into the limelight. The other important role has been in developing measurement standards when international standards are not available. Figure 6.4.1 shows standards in this category developed for defining the area used for efficiency determination for experimental laboratory cells.

Several results from the AUSIAPV/ACAP program have set new world standards and are featured in these Tables. In 2017, this included two new record efficiencies for CZTS cell performance, with 10.0% confirmed for a 1 cm^2 device and 11.0% for a smaller device.

ACAP partner, Trina Solar, also featured prominently, setting a new world record for commercially dominant multicrystalline cells, with 19.9% reported for a large-area commercially sized module based on the UNSW-developed PERC (Passivated Emitter and Rear Cell) approach.

The Tables are widely used and referenced by the photovoltaic research community. According to the ISI Web of Knowledge, the ten versions prepared since 2013 under the banner of AUSIAPV have all been among the most cited papers published since then in the engineering discipline worldwide.

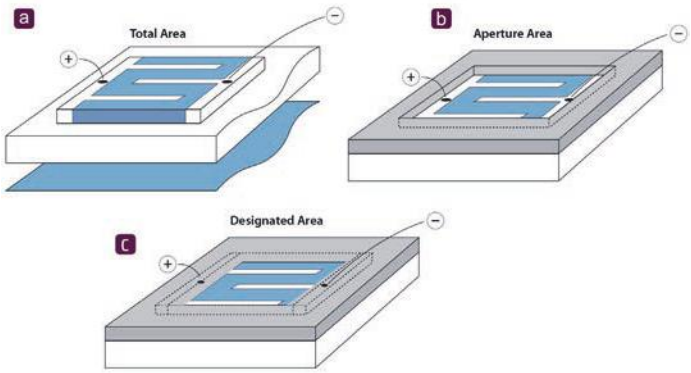

Figure 6.4.1: Cell area definitions: (a) total area; (b) aperture area; and (c) designated illumination area.

Highlight

- Value of Tables validated by exceptionally high citation rates.

Future Work

- Publish two updated versions of the Tables during 2018.

6.5 PV Manufacturing Education

Lead Partner
UNSW

UNSW Team
A/Prof Bram Hoex

QESST Team
Prof Stuart Bowden, Dr Andre Augusto

Industry Partner
PV Lighthouse

Funding Support
ACAP, UNSW

Aims

Many students come to UNSW wanting to learn how solar cells are manufactured. However, silicon solar cell manufacturing involves a diverse range of processing, ranging from chemical etching, plasma physics and metal alloying to screen printing. Understanding all of these processes, and how they interact in a production line, is challenging, to say the least, especially when it is not possible to take students to see a cell production line. Combined with the need for students to learn how to optimise a process with so many interrelated steps, a major educational challenge arises. To address this challenge, in 2001–2002 Professor Stuart Wenham and Dr Anna Bruce from the School of Photovoltaic and Renewable Energy Engineering at UNSW developed a simulation of the production of screen-printed silicon solar cells, called the Virtual Production Line (VPL).

In 2014, PV Factory (a cloud-based simulation platform) was developed through an ACAP-supported collaboration involving PV Lighthouse, UNSW and Arizona State University as a teaching application that could engage PV and Solar Energy Engineering students as they learned about how solar cells are made. This platform utilised revised versions of many of the earlier algorithms developed for VPL. Hosting of the simulation in the cloud has made it simpler for students to use the simulation – with the software hosted in the cloud there is no limitation regarding downloads nor version control. Cloud-based delivery has also enabled the implementation of leaderboards where students can compete with their classmates and users across the world to achieve the highest cell efficiency. PV Factory was released to the public in January 2015 and can be accessed at: https://factory.pvlighthouse.com.au.

PV Factory has attracted more than 2,000 unique users since its inception and is currently used in at least five universities in their teaching programs (including UNSW and ASU). PV Factory has processed close to 300,000 solar cell batches and has produced close to 3 million solar cells. Hence, it is clear that PV Factory has been found to be extremely useful in international PV manufacturing education.

Progress

In 2017, the main focus was on the development of the online textbook about PV manufacturing (accessible via PV-Manufacturing.org). This online resource contains a wide collection of written content, complemented with videos and animations about the solar cell manufacturing process. This is described in more detail in Section 6.29 “Development of online educational resources for PV manufacturing education”, available online at www.acap.net.au/annual-reports.

Highlights

- The PV Factory platform has been running consistently for over three years now and is formally used by five universities worldwide to run classes in their PV education programs.
- It Is now complemented by an online textbook on PV-manufacturing.org.

Future Work

- The focus will be on improving the first iteration of the online textbook based on user feedback.

References

Abbott, M.D., McIntosh, K.R., Lennon, A.J., Cotter, J.E., Li, Y., Lu, Z. and Li, A., 2015, “Online education with PV Factory”, 2015 IEEE 42nd Photovoltaic Specialist Conference, New Orleans, 14–19 June 2015.

Lennon, A., Abbott, M. and McIntosh, K., 2015, “Chasing Higher Solar Cell Efficiencies Engaging Students in Learning how Solar Cells are Manufactured”, IEEE International Conference on Teaching, Assessment, and Learning for Engineering (TALE), Zhuhai, China, 267.

Whipp, C., 2016, “Upgrading PV Factory as an Educational Tool”, BSc Thesis, UNSW.

Collaboration Grants

ACAP's competitively selected Collaboration Grants, whose titles are shown below, are reported online at http://www.acap.net.au/annual-reports.

6.6 Metal Plating for Next Generation Silicon Solar Cells

Lead Partner
UNSW

UNSW Team
A/Prof Alison Lennon, Dr Udo Römer, Dr Pei-Chieh Hsiao

Academic Partner
National Renewable Laboratories (NREL), Dr Paul Stradins, Dr Mathew Page, Dr Manuel Schnabel

Funding Support
ACAP

6.8 GaAs/Si Elongate Tandem Cells for Moderate Concentration

Lead Partner
ANU

ANU Team
Dr Matthew Stocks, Prof Andrew Blakers

Academic Partner
NREL

Funding Support
ARENA, ANU, NREL

6.9 Advanced Hole-Selective Contacts to Replace Boron Diffusion

Lead Partner
ANU

ANU Team
Dr Yimao Wan, Prof Andres Cuevas, Mr Chris Samundsett, Dr Jie Cui, Ms Josephine McKeon

ANU Students
Thomas Allen, Peiting Zheng, Di Yan, Xinyu Zhang

ACAP Team
Dr James Bullock, Dr Mark Hettick, Professor Ali Javey (UCB, LBNL)

Academic Partners
University of California, Berkeley (UCB), Lawrence Berkeley National Laboratory (LBNL, including the Molecular Foundry)

Funding Support
ARENA, ACAP

6.10 Advanced Light-Trapping for High Efficiency Si Cells

Lead Partner
ANU

ANU Team
Prof Andrew Blakers, Dr Ngwe Zin

AUSIAPV Partner
Georgia Institute of Technology (GIT), USA
University Center of Excellence for Photovoltaics (UCEP) – Ajay D Upadhyaya, Prof Ajeet Rohatgi

Academic Partners
University of Central Florida (UCF) (added following Dr Zin's move to UCF)
Florida Solar Energy Center (FSEC)

Funding Support
ARENA, ANU, GIT

6.11 Advanced Luminescence Studies of Si Wafers and Cells

Lead Partner
ANU

ANU Team
Prof Daniel MacDonald, Dr Hieu Nguyen

Academic Partner
Dr Mowafak Al-Jassim, Dr Steve Johnston, National Renewable Energy Laboratory (NREL), USA

Funding Support
ARENA, ANU, NREL

6.12 De-cohesion Analysis of Printed Solar Modules

Lead Partner
CSIRO

CSIRO Team
Dr Fiona Scholes, Dr Hasitha C Weerasinghe, Dr Doojin Vak

CSIRO Student
Xiaojin Peng (PhD Student)

Academic Partners
Stanford University (USA), Prof Reinhold H. Dauskardt / Nick Rolston (PhD Student)
Georgia Institute of Technology (USA), Prof Samuel Graham

Funding Support
ACAP / AUSIAPV

6.13 Determining Charge Lifetime and Mobility Dynamics in Organic Semiconductors for Photovoltaic Applications

UoM Team
A/Prof Trevor Smith, Dr Wallace Wong, Dr David Jones

UoM Students
Ms Kyra Schwarz, Mr Ahmed Alqatari

NREL / University of Colorado Boulder, USA Team
Prof Garry Rumbles, Dr Obadiah Reid

Funding Support
AUSIAPV, ARC, UoM, NREL

6.14 Screening Singlet Fission in Organic Semiconductors for Photovoltaic Applications

UoM Team
Dr David Jones, Prof Ken Ghiggino, A/Prof Trevor Smith, Dr Lars Goerigk

UoM Students
Ms Kyra Schwarz, Ms Saghar Masoomigadarzi

Princeton University (USA)
Prof Gregory Scholes

Georgia Tech, USA
Prof Seth Marder

RMIT University
A/Prof Yasuhiro Tachibana

Funding Support
AUSIAPV, ARC, UoM, Princeton University, Georgia Tech.

6.16 Design Optimisation of Silicon Sub-Cells in GaAsP/Si Tandem Cells

Lead Partner
UNSW

UNSW Team
A/Prof S. Bremner, A/Prof A. Ho-Baillie, Dr H. Mehrvarz, Prof M. Green

UNSW Student
Chuqi Yi

Academic Partner
Ohio State University: Dr T. Grassman, Prof S. Ringel

Funding Support
ARENA, ACAP

6.17 PP4 Cost Evaluation of Emerging PV Technologies

Lead Partner
UNSW

UNSW Team
Dr Anita Ho-Baillie, A/Prof Renate Egan, Prof Martin Green

UNSW Student
Nathan Chang

ACAP Team
CSIRO, Monash

Academic Partners
NREL

6.18 Studying Thermal Effects of Boron-Oxygen (B-O)–Related Light-Induced-Degradation (LID)

Lead Partner
UNSW

UNSW Team
Dr Brett Hallam

UNSW Student
Moonyong Kim

Academic Partner
University of North Carolina, Charlotte (UNCC)

Ohio State University Team
Prof. Abasifreke Ebong

Funding Support
ARENA

6.19 PP1 Origin of Interface Defect Levels for High Efficiency Silicon Solar Cells

Lead Partner
UNSW

UNSW Team
Dr Ziv Hameiri

UNSW Students
Yan Zhu, Shuai Nie

Academic Partner
Arizona State University, Dr Mariana Bertoni

Funding Support
ACAP Collaboration Grant, UNSW MREII, ARC DECRA

6.20 Developing Laser Processed Large-Area Front Deep Junctions and Heterojunction Passivated Back Contacts

Lead Partner
UNSW

UNSW Team
Dr Ivan Perez-Wurfl

UNSW Students
Tian Zhang, Zibo Zhou

Academic Partner
NIST (USA), Dr Brian Simonds

Funding Support
ACAP, NIST (in-kind)

6.21 Novel Light-Trapping Technique in Solar Cells

Lead Partner
UNSW

UNSW Team
Dr Supriya Pillai, Dr Michael E. Pollard, Prof Darren Bagnall

UNSW Students
Claire E.R. Disney, Atom Chang

Academic Partner
Arizona State University, Prof Christiana Honsberg, Prof Stuart Bowden, Dr. Som Dahal, Mr Sangpyeong Kim

Funding Support
ACAP, ARENA, UNSW

6.22 Interfacial Engineering for High Performance Organic Tandem Solar Cells and Perovskite Solar Cells

Lead Partner
Monash University

Monash Team
Dr Wenchao Huang, Prof Yi-Bing Cheng

International Partner
Professor Yang Yang, University of California, Berkeley and Lawrence Berkeley Laboratories

6.23 Rear Contact Solar Cells with Nanophotonic Light Trapping

Lead Partner
UNSW

UNSW Team
Dr Michael Pollard, A/Prof Bram Hoex, Dr David Payne, Prof Darren Bagnall

UNSW Students
Alexander To, Yuan-Chih Chang

USA Partner
Prof Harry Atwater (California Institute of Technology)

European Partners
Professor Albert Polman, Andrea Cordaro, Verena Neder, Dimitry Lamers (AMOLF, the Netherlands)
Dr Alexander Sprafke (MLU Halle-Wittenburg, Germany)
Dr Tasmiat Rahman, Dr Stuart Boden (University of Southampton, UK)

6.24 Alignment-free Photothermal Deflection Spectrometer: From University to Industry

Lead Partner
UNSW

UNSW Team
Dr Michael Pollard, Dr Ivan Perez-Wurfl, Dr Binesh Puthen-Veettil

Industry Partner
Open Instruments Pty Ltd: Dr Henner Kampwerth

Funding Support
ARENA, ACAP

6.25 Development of GaAsBi-Bbased 1.0-1.2 eV Sub-Cells for Multi-Junction Solar Cells on Silicon Substrates

Lead Partner
UNSW

UNSW Team
A/Prof S. Bremner, Dr Anita Ho-Baillie

UNSW Students
Hongfeng Wang, Hayden Lobry

Academic Partner
Arizona State University

Arizona State University Team
Prof Christiana Honsberg, Prof Richard King

Funding Support
ARENA, ACAP

6.26 Advanced Hydrogenation and Mitigation of LeTID on PERCs Made From 1366 Technologies Direct Wafer® Multi-Crystalline Silicon Material

Lead Partner
UNSW

UNSW Team
Dr Catherine Chan, Dr Alison Ciesla, Scientia Prof Stuart Wenham

USA Partner
1366 Technologies

Team
Dr Adam Lorenz, Dr Rob Steeman

6.27 Silicon Nanocrystal Carrier Selective Contacts for Silicon Solar Cells

Lead Partner
UNSW

UNSW Team
Prof Gavin Conibeer, Dr Ivan Perez-Wurfl, Dr Robert Patterson

USA Partners
Natcore Technology Inc, Rochester NY

Team
Dr Dennis Flood, Dr David Levy

6.28 P-type Hybrid Heterojunction Solar Cells

Lead Partner
UNSW

UNSW Team
Dr Brett Hallam

UNSW Student
Daniel Chen, Moonyong Kim

Academic Partner
Arizona State University

Team
Prof Zachary Holman

Funding Support
ARENA

6.29 Development of Online Educational Resources for PV Manufacturing Education

Lead Partner
UNSW

UNSW Team
A/Prof Bram Hoex

UNSW Students
Jing Zhao, Daniel Chen, Moonyong Kim, Alex To, Jack Colwell, Utkarshaa Varshney

QESST Team
Prof Stuart Bowden, Dr Andre Augusto

Funding Support
ACAP, UNSW

6.30 Rapid Optical Modelling of Black Silicon

Lead Partner
UNSW

UNSW Team
Dr David Payne, Dr Malcolm Abbott, Tsun Fung

Australian Partner
PV Lighthouse Pty Ltd, Dr Keith McIntosh

Academic Partner
Technical University of Denmark, Dr Rasmus Davidson, Dr Maksym Plakhotnyuk

Funding Support
ACAP

6.31 Optical Characterisation of Passivated Contacts for Silicon Solar Cells

Lead Partner
ANU

ANU Team
Prof Andrew Blakers, Dr Kean Fong

Academic Partner
University of Central Florida, Dr. Soe Zin Ngwe

Industry Partner
PV Lighthouse, Dr Keith McIntosh,

Funding Support
ARENA, AUSIAPV, ANU

6.32 High Efficiency Heterojunction Solar Cells Based on Low-Cost Solar-Grade Silicon Wafers

Lead Partner
ANU

ANU Team
Prof Daniel Macdonald, Dr Chang Sun, Mr Rabin Basnet

Academic Partner
A/Prof Zachary Holman, Arizona State University (ASU)

Funding Support
ARENA, ANU, ASU

6.33 Discovering and Developing Lead-Free Perovskites for Photovoltaic Application

Lead Partner
ANU

ANU Team
Dr Hemant Kumar Mulmudi, A/Prof Klaus Weber

ANU Students
Nandi Wu

USA Partners
Dr Ghanshyam Pilania, Los Alamos National Laboratory (New Mexico)
A/Prof Rohan Mishra, Washington University in St Louis

6.34 In-Situ X-ray Characterisation of Printed Organic Solar Cell Films

UoM Team
Dr David Jones, Dr Jegadesan Subbiah

CSIRO
Dr Gerry Wilson, Dr Doojin Vak, Dr Mei Gao

NIST (USA)
Dr Lee Richter, Dr Sebastian Engmann

University of Bayreuth (Germany)
Prof Anna Köhler, Mr Daniel Kroh (student)

Funding Support
AUSIAPV, UoM, CSIRO, NIST, University of Bayreuth (UoM-Bayreuth Polymer/Colloid Network).

Financial Summary

In December 2012, a grant of $33.1 million from the Australian Government through ARENA was announced to support the 8-year program of the Australia-US Institute for Advanced Photovoltaics (AUSIAPV). This support leveraged an additional $55.4 million cash and in-kind commitment from AUSIAPV participants taking the total value of the project to $88.5 million.

AUSIAPV commenced on 1 February 2013 after the signing of the Head Agreement between ARENA and UNSW, and with the receipt of letters of confirmation of participation under the terms of the Head Agreement by the other project participants. Collaboration Agreements with the Australian participants in the Australian Centre for Advanced Photovoltaics (ACAP) were completed on 1 July 2013.

An extension to the program, to undertake an Australian Solar PV Cell and Module Research Infrastructure Plan and Feasibility Study was signed in October 2014, generating an additional milestone, 4A. This project was completed and Milestone 4A was paid in October 2015. A further extension was formalised through Variation #4, executed in February 2016. It extended perovskites research in ACAP and generated two new Milestones (4B and 5B) for 2016 and others in subsequent years. Both the new 2016 Milestones were met and paid. The Milestone 5 and 6 payments from ARENA to UNSW were also paid, in 2016 and 2017, respectively. Disbursements were made to each node following confirmation of institutional cash contributions.

Variation #5 in June 2016 added a new partner, Dyesol Pty Ltd (now known as Greatcell Pty Ltd) and pooled the cash and in-kind contributions of most of the collaborating international research institutions and of the collaborating industry participants.

Good progress was made in 2014 - 2016 towards regaining the original budgetary expenditure timelines. Variation #6 in October 2017 and #6A in December 2017 implemented many of the changes proposed by the Mid-Term Review Panel in 2016, including the provision of additional funding for Capacity Building (Fellowships) and Small Grants, and made several minor updates and corrections. These variations brought the total funds granted to $46.0 million. A robust and transparent process to distribute Small Grants was developed in 2015 and also implemented in a small first funding round in that year. Two larger, rounds were undertaken during 2016 and a fourth round was offered in Q1 of 2018. In addition, twenty Fellowships were offered in Q4 of 2017.

All technical milestones for 2017 were achieved, apart from one that was delayed, with ARENA approval, by a damaging fire in one of the ACAP laboratories.

The breakdown by institution of the $11.3 million total cash and in-kind budget for 2017 is shown in Figure 7.1(a). The actual total 2017 cash and in-kind expenditure was $14.0 million and its breakdown is shown in Figure 7.1(b), with additional irrevocable cash commitments carried into 2018.

A new collaborating industry participant, Raygen Resources Pty. Ltd., joined during 2017 and an Agreement Letter was signed with the Georgia Institute of Technology.

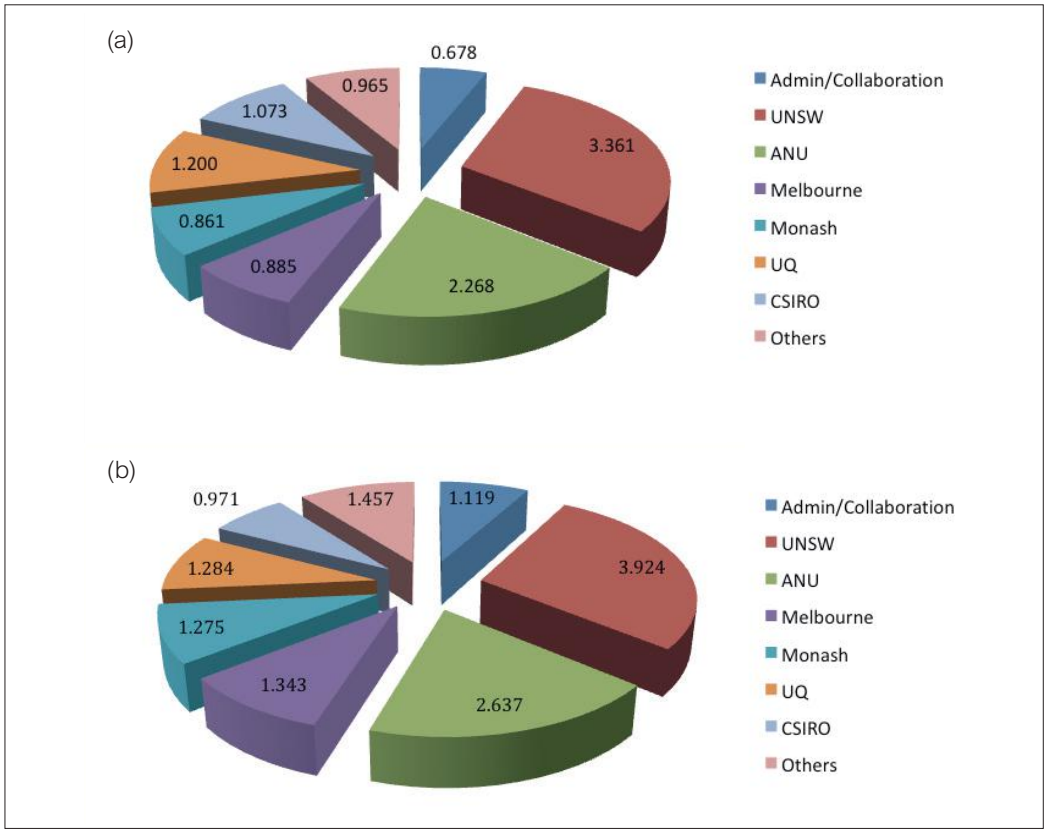

Figure 7.1: (a) Total AUSIAPV/ACAP cash and in-kind expenditure budget ($m) for 2017 broken down by institution; (b) Actual cash and in-kind expenditure ($m) breakdown by institution for 2017.

Publications

8.2 Book Chapters

Angmo, D., Gao, M. and Vak, D. (2017). "Organic-Inorganic Hybrid Perovskite Solar Cells with Scalable and Roll-to-Roll Compatible Printing/Coating Processes", in "Printable Solar Cells", Ch. 10, pp. 313-362, Wiley, DOI: 10.1002/9781119283720.ch10.

Corkish, R. (2017). "Undergraduate and Postgraduate Education in Renewable Energy", in "Renewable and Alternative Energy: Concepts, Methodologies, Tools, and Applications", Mehdi Khosrow-Pour (Ed. In Chief), IGI Global, DOI: 10.4018/978-1-5225-1671-2.ch003.

Green, M. (2017). "Advanced Concepts" in "Photovoltaic Solar Energy: From Fundamentals to Applications", A. Reinders, P. Verlinden, W. van Sark, A. Freundlich (editors), Wiley, Chichester, pp.160-166.

Hoex, B. (2017). "Surface Passivation and Emitter Recombination Parameters", in "Photovoltaic Solar Energy From Fundamentals to Applications". John Wiley & Sons, pp. 114-124.

Liu, Z., Hao, X., Ho-Baillie, A. and Green, M. (2017). "Epitaxial Growth of Ge on Si by Magnetron Sputtering" Chapter in "Epitaxy", Open Access Book, M. Zhong (ed.), InTechOpen, September.

Lunardi, M.M., Alvarez-Gaitan, J.P., Bilbao J.I. and Corkish, R. (2017), "A Review of Recycling Processes for Photovoltaic Modules", in Solar Panels and Photovoltaic Materials, Intech 2018, ISBN: 978-953-51-6173-8 (in proof)

8.3. Patent Applications

Abbott, M., Wenham, S., Hamer, P., Hallam, B., "A method for processing silicon material", National Phase, Australia, 2016232981, 2017; China, 201680015469.X, 2017; Europe, 16764058, 2017; South Korea, 10-2017-7026864, 2017; Singapore, 11201706676S, 2017; USA, 15/557215, 2017.

Ciesla, A., Hallam, B., Chan, C., Chong, C. M., Chen, D., Bagnall, D., Payne, D., Mai, L., Abbott, M., Kim, M., Chen, R., Wenham, S., Fung, T. H., Shi, Z., "Advanced hydrogen passivation that mitigates hydrogen-induced recombination (HIR) and surface passivation deterioration in PV devices", PCT, PCT/AU2017/051290, 2017; National Phase, Taiwan, 106140628, 2017

Ciesla, A., Hallam, B., Chan, C., Chong, C. M., Chen, D., Bagnall, D., Payne, D., Mai, L., Abbott, M., Kim, M., Chen, R., Wenham, S., Fung, T. H., Shi, Z., "A method for improving wafer performance for photovoltaic devices", PCT, PCT/AU2017/051289, 2017; National Phase, Taiwan, 106140627, 2017.

Hao, X., Li, W. Green, M., Ho-Baillie, A., Liu, Z., "A method for forming a virtual germanium substrate using a laser", National Phase, USA, 15/508975, 2017

Hao, X., Liu, F., Huang, J., Yan, C., Sun, K., Green, M., "A copper-based chalcogenide photovoltaic device and a method of forming the same", PCT, PCT/AU2017/050630, 2017

Lennon, A., Allen, V., "A method and an apparatus for treating a surface of a TCO material in a semiconductor device", PCT, PCT/AU2017/050164, 2017; National Phase, Taiwan, 106106496, 2017.

Lennon, A., Ouyang, Z., Hall, C., Song, N., Wang, X., Hsiao, P., "A method for fabricating a photovoltaic module", Provisional, Australia, 2017902821, 2017

Lennon, A., Ouyang, Z., Lou, S. N., Jiang, Y., "An electrochemical capacitor and an integrated energy-generation and energy-storage device", PCT, PCT/AU2017/050369, 2017

Li, Z., Lennon, A., "A method of patterning a layer", National Phase, USA, 15/517156, 2017; National Phase, China, 201710223617.3, 2017

Shi, L., Young, T., "A thin film photovoltaic device and a method for encapsulating the same", Provisional, Australia, 2017902609, 2017

Shi, Z., Wenham, S., Chen, R., Chan, C., Ciesla, A., "Improving wafer performance for photovoltaic devices through the use of crystallographic imperfections", Provisional, Australia, 2017902441, 2017

Uddin, A. Elumalai, N., "A photovoltaic cell and a method of forming a photovoltaic cell", PCT, PCT/AU2017/051115, 2017

Uddin, A., "A photovoltaic cell and a method of forming a photovoltaic cell", National Phase, USA, 15/503075, 2017

Uddin, A., Elumalai, N., "A method of forming a light absorbing layer for a photovoltaic cell and a photovoltaic cell comprising the light-absorbing layer", PCT, PCT/AU2017/051114, 2017

Wenham, S., Ciesla, A., Hallam, N., Chan, C., Chong, C. M., Chen, R., Abbott, M., Payne, D., "A method for processing silicon material", PCT, PCT/AU2017/050560, 2017; National Phase, Taiwan, 106118747, 2017.

Wenham, S., Hallam, B., Einhaus, R., "A method for manufacturing a photovoltaic device", PCT, PCT/AU2017/050719, 2017; National Phase, Taiwan, 106123382, 2017

Western, N., Bremner, S., "A method of forming a contact for a photovoltaic cell", Divisional, Singapore, 10201701426T, 2017

8.4 Papers in Refereed Scientific and Technical Journals

Allen, T. G, Bullock, J., Jeangros, Q., Samundsett, C. , Wan, Y., Cui, J., Hessler-Wyser, A., De Wolf, S., Javey, A., and Cuevas, A., (2017). "A Low Resistance Calcium/Reduced Titania Passivated Contact for High Efficiency Crystalline Silicon Solar Cells," Advanced Energy Materials, 1602606.

Armin, A., Shoaee, S., Lin, Q., Burn, P. L., and Meredith, P., (2017). "On the unipolarity of charge transport in methanofullerene diodes", NPJ Flexible Electronics, 1(13).

Armin, A., Stoltzfus, D. M., Donaghey, J. E., Clulow, A. J., Nagiri, R. C. R., Burn, P. L., Gentle, I. R., and Meredith, P., (2017). "Engineering dielectric constants in organic semiconductors", Journal of Materials Chemistry C, 5, 3736–3747.

Banal, J. L.; Zhang, B.; Jones, D. J.; Ghiggino, K. P.; Wong, W. W. H., (2017). "Emissive Molecular Aggregates and Energy Migration in Luminescent Solar Concentrators" Acc. Chem. Res., 50(1), 49-57. DOI: 10.1021/acs.accounts.6b00432

Bazaka, K., Ahmad, J., Oelgemöller, M., Uddin, A., and Jacob, M. V. (2017). "Photostability of plasma polymerized γ-terpinene thin films for encapsulation of OPV." Scientific Reports, 7, 45599 doi:10.1038/srep45599

Bonilla, R. S., Hoex, B., Hamer, P., and Wilshaw, P. R. (2017). "Dielectric surface passivation for silicon solar cells: A review", Physica Status Solidi (A) Applications and Materials Science, 214(7).

Bourret-Sicotte, G., Hamer, P., Bonilla, R. S., Collett, K., Ciesla, A., Colwell, J., and Wilshaw, P. R. (2017). "Shielded hydrogen passivation – A potential in-line passivation process", Physica Status Solidi (A) Applications and Materials Science, 214(7).

Bremner, S. P., Yi, C., Almansouri, I., Ho-Baillie, A., and Green, M. A. (2017). "Corrigendum to "Optimum band gap combinations to make best use of new photovoltaic materials" [Solar Energy 135 (2016) 750–757] (S0038092X16302237) (10.1016/j.solener.2016.06.042)", Solar Energy, 150, 621.

Cazzaniga, A., Crovetto, A., Yan, C., Sun, K., Hao, X., Ramis Estelrich, J., Canulescu, S., Stamate, E., Pryds, N., Hansen, O., and Schou, J. (2017). "Ultra-thin Cu2ZnSnS4 solar cell by pulsed laser deposition", Solar Energy Materials and Solar Cells, 166, 91-99.

Chan, C., Fung, T. H., Abbott, M., Payne, D., Wenham, A., Hallam, B., Chen, R., and Wenham, S. (2017). "Modulation of Carrier-Induced Defect Kinetics in Multi-Crystalline Silicon PERC Cells Through Dark Annealing", SOLAR RRL, 1(2).

Chan, C., Hamer, P., Bourret-Sicotte, G., Chen, R., Ciesla, A., Hallam, B., Payne, D., Bonilla, R. S., and Wenham, S. (2017). "Instability of Increased Contact Resistance in Silicon Solar Cells Following Post-Firing Thermal Processes", SOLAR RRL, 1(11).

Chan, K. H., Elumalai, N. K., Tayebjee, M. J. Y., Uddin, A., and Pillai, S. (2017). "Dark carrier dynamics and electrical characteristics of organic solar cells integrated with Ag-SiO2 core-shell nanoparticles", Synthetic Metals, 223, 34-42.

Chandrasekharan, A., Hambsch, M., Jin, H., Maasoumi, F., Shaw, P. E., Raynor, A., Burn, P. L., Lo, S.-C., Meredith, P., and Namdas, E. B., (2017). "Effect of capping group on the properties of non-polymeric diketopyrrolopyrroles for solution-processed bulk heterojunction solar cells", Organic Electronics, 50, 339–346.

Chang, N. L., Yi Ho-Baillie, A. W., Basore, P. A., Young, T. L., Evans, R., and Egan, R. J. (2017). "A manufacturing cost estimation method with uncertainty analysis and its application to perovskite on glass photovoltaic modules." Progress in Photovoltaics: Research and Applications, 25(5), 390-405.

Chang, N.L., Ho-Baillie, A.W., Vak, D., Gao, M., Green, M.A., and Egan, R.J., (2018). "Manufacturing cost and market potential analysis of demonstrated roll-to roll perovskite photovoltaic cell processes", Solar Energy Materials and Solar Cells, 174, 314–324

Chen, D., Edwards, M., Wenham, S., Abbott, M., and Hallam, B. (2017). "Laser enhanced gettering of silicon substrates." Frontiers in Energy, 11(1), 23-31.

Chen, D., Kim, M., Stefani, B. V., Hallam, B. J., Abbott, M. D., Chan, C. E., Chen, R., Payne, D. N. R., Nampalli, N., Ciesla, A., Fung, T. H., Kim, K., and Wenham, S. R. (2017). "Evidence of an identical firing-activated carrier-induced defect in monocrystalline and multicrystalline silicon." Solar Energy Materials and Solar Cells, 172, 293-300.

Chen, G., Zheng, J., Zheng, L., Yan, X., Lin, H., and Zhang, F. (2017). "Crack-free CH3NH3PbI3 layer via continuous dripping method for high-performance mesoporous perovskite solar cells." Applied Surface Science, 392(C), 960-965.

Chen, S., Wen, X., Huang, S., Huang, F., Cheng, Y. B., Green, M., and Ho-Baillie, A. (2017). "Light Illumination Induced Photoluminescence Enhancement and Quenching in Lead Halide Perovskite." SOLAR RRL, 1(1).

Chen, S., Wen, X., Yun, J. S., Huang, S., Green, M., Jeon, N. J., Yang, W. S., Noh, J. H., Seo, J., Seok, S. I., and Ho-Baillie, A. (2017). "Spatial Distribution of Lead Iodide and Local Passivation on Organo-Lead Halide Perovskite." ACS Applied Materials and Interfaces, 9(7), 6072-6078.

Chen, W., Wen, X., Latzel, M., Yang, J., Huang, S., Shrestha, S., Patterson, R., Christiansen, S., and Conibeer, G. "Nanoscale characterization of GaN/InGaN multiple quantum wells on GaN nanorods by photoluminescence spectroscopy."

Chung, D., Mitchell, B., Goodarzi, M., Sinton, R. A., Macdonald, D., and Trupke, T. (2017). "Uncertainty in Photoluminescence Metrology on Multicrystalline Silicon Bricks and Cross Validation with Wafers." IEEE Journal of Photovoltaics, 7(6), 1701-1709.

Chung, D., Mitchell, B., Goodarzi, M., Sun, C., Macdonald, D., and Trupke, T. (2017). "Bulk Lifetimes up to 20 ms Measured on Unpassivated Silicon Discs Using Photoluminescence Imaging." IEEE Journal of Photovoltaics, 7(2), 444-449.

Chung, S., Wen, X., Huang, S., Gupta, N., Conibeer, G., Shrestha, S., Harada, T., and Kee, T. W. (2017). "Nanosecond long excited state lifetimes observed in hafnium nitride." Solar Energy Materials and Solar Cells, 169, 13-18.

Chung, S., Wen, X., Huang, S., Gupta, N., Harada, T., Kee, T. W., Conibeer, G., and Shrestha, S. (2017). "Corrigendum to "Nanosecond long excited state lifetimes observed in hafnium nitride" [Sol. Energy Mater. Sol. Cells 169 (2017) 13–18] (S0927024817302064) (10.1016/j.solmat.2017.04.037))." Solar Energy Materials and Solar Cells, 171, 302.

Conibeer, G., Zhang, Y., Bremner, S. P., and Shrestha, S. (2017). "Towards an understanding of hot carrier cooling mechanisms in multiple quantum wells." Japanese Journal of Applied Physics, 56(9).

Conrad, B., Lochtefeld, A., Gerger, A., Barnett, A., and Perez-Wurfl, I. (2017). "Optical characterisation of III-V alloys grown on Si by spectroscopic ellipsometry." Solar Energy Materials and Solar Cells, 162, 7-12.

Cui, J, Phang, S , Sio, H , Wan, Y, Cuevas, A, (2017). "Passivation of phosphorus diffused black multi-crystalline silicon by hafnium oxide", PSS Rapid Research Letters.

Cui, H., Liu, X., Sun, L., Liu, F., Yan, C., and Hao, X. (2017). "Fabrication of Efficient Cu2ZnSnS4 Solar Cells by Sputtering Single Stoichiometric Target." Coatings, 7(2).

Cui, J., Wan, Y., Cui, Y., Chen, Y., Verlinden, P., and Cuevas, A., "Highly effective electronic passivation of silicon surfaces by atomic layer deposited hafnium oxide," Applied Physics Letters, 110, 021602, 2017.

Disney, C. E. R., Pillai, S., and Green, M. A. (2017). "The Impact of parasitic loss on solar cells with plasmonic nano-textured rear reflectors." Scientific Reports, 7(1).

Dumbrell, R., Juhl, M. K., Trupke, T., and Hameiri, Z. (2017). "Comparison of terminal and implied open-circuit voltage measurements." IEEE Journal of Photovoltaics, 7(5), 1376-1383.

Dunbar, R. B., Duck, B. C., Moriarty, T., Anderson, K. F., Duffy, N. W., Fell, C. J., Kim, J., Ho-Baillie, A., Vak, D., Duong, T., Wu,

Y., Weber, K., Pascoe, A., Cheng, Y. B., Lin, Q., Burn, P. L., Bhattacharjee, R., Wang, H., and Wilson, G. J. (2017). "How reliable are efficiency measurements of perovskite solar cells? the first inter-comparison, between two accredited and eight non-accredited laboratories." Journal of Materials Chemistry A, 5(43), 22542-22558.

Dunbar, R. B., Duck, B. C., Moriarty, T., Anderson, K. F., Duffy, N. W., Fell, C. J., Kim, J., Ho-Baillie, A., Vak, D., Duong, T., Wu, Y., Weber, K., Pascoe, A., Cheng, Y. B., Lin, Q., Burn, P. L., Bhattacharjee, R., Wang, H. & Wilson, G. J., (2017). "How reliable are efficiency measurements of perovskite solar cells? The first inter-comparison, between two accredited and eight non-accredited laboratories", Journal of Materials Chemistry A, 5, 22542–22558.

Dunbar, RB., Moustafa, W., Pascoe, AR., Jones, TW., Anderson, KF., Cheng, YB., Fell, CJ., Wilson, GJ., "Device Pre-Conditioning And Steady-State Temperature Dependence Of CH3NH3PbI3 Perovskite Solar Cells", Progress In Photovoltaics: Research And Applications, 25 (7), 533-544, 2017

Duong, T., Wu, Y., Shen, H., Peng, J., Fu, X., Jacobs, D., Wang, E., Kho, TC., Fong, KC., Stocks, M., Franklin, E., Blakers, A., Zin, N., Mcintosh, K., Li, W., Cheng, YB., White, TP., Weber, K., Catchpole, K., "Rubidium Multication Perovskite With Optimized Bandgap For Perovskite-Silicon Tandem With Over 26% Efficiency", Advanced Energy Materials, 7 (14), 2017

Evans, R., and Boreland, M. (2017). "Multivariate Data Analytics in PV Manufacturing: Four Case Studies Using Manufacturing Datasets." IEEE Journal of Photovoltaics, 8(1).

Fan, Y., Yang, J., Jiang, L., Wang, Y., Ng, B. K., Sun, H., Lai, Y., Li, J., and Liu, F. (2017). "Effects of illumination on the electrochemical behavior of selenium electrodeposition on ITO substrates." Journal of the Electrochemical Society, 164(4), H225-H231.

Gao, C., Xu, M., Ng, B. K., Kang, L., Jiang, L., Lai, Y., and Liu, F. (2017). "In situ growth of Sb2S3 thin films by reactive sputtering on n-Si(100) substrates for top sub-cell of silicon based tandem solar cells." Materials Letters, 195, 186-189.

Gendron, D., Maasoumi, F., Armin, A., Pattison, K., Burn, P. L., Meredith, P., Namdas, E. B., and Powell, B. J., (2017). "A thiocarbonyl-containing small molecule for optoelectronics", RSC Advances, 7, 10316–10322.

Gong, L., Liu, Y. Z., Liu, F. Y., and Jiang, L. X. (2017). "Room-temperature deposition of flexible transparent conductive Ga-doped ZnO thin films by magnetron sputtering on polymer substrates." Journal of Materials Science: Materials in Electronics, 28(8), 6093-6098.

Gong, L., Liu, Y., Jiang, L., and Liu, F. (2017). "Study on the adhesive mechanism between the Ga doped ZnO thin film and the polycarbonate substrate." Materials Science in Semiconductor Processing, 66, 105-108.

Green, M. A. (2017). "Corrigendum to: Solar cell efficiency tables (version 49) (Prog. Photovolt: Res. Appl, (2017), 25, (3–13), 10.1002/pip.2855)." Progress in Photovoltaics: Research and Applications, 25(4), 333-334.

Green, M. A., and Ho-Baillie, A. (2017). "Perovskite Solar Cells: The Birth of a New Era in Photovoltaics." ACS Energy Letters, 2(4), 822-830.

Green, M. A., Emery, K., Hishikawa, Y., Warta, W., Dunlop, E. D., Levi, D. H., and Ho-Baillie, A. W. Y. (2017). "Solar cell efficiency tables (version 49)." Progress in Photovoltaics: Research and Applications, 25(1), 3-13.

Green, M. A., Hishikawa, Y., Warta, W., Dunlop, E. D., Levi, D. H., Hohl-Ebinger, J., and Ho-Baillie, A. W. H. (2017). "Solar cell efficiency tables (version 50)." Progress in Photovoltaics: Research and Applications, 25(7), 668-676.

Guo, J., Lin, S., Bilbao, J. I., White, S. D., and Sproul, A. B. (2017). "A review of photovoltaic thermal (PV/T) heat utilisation with low temperature desiccant cooling and dehumidification." Renewable and Sustainable Energy Reviews, 67, 1-14.

Hallam, B. J., Chan, C. E., Chen, R., Wang, S., Ji, J., Mai, L., Abbott, M. D., Payne, D. N. R., Kim, M., Chen, D., Chong, C., and Wenham, S. R. (2017). "Rapid mitigation of carrier-induced degradation in commercial silicon solar cells." Japanese Journal of Applied Physics, 56(8).

Hallam, B. J., Hamer, P. G., Bonilla, R. S., Wenham, S. R., and Wilshaw, P. R. (2017). "Method of Extracting Solar Cell Parameters from Derivatives of Dark I-V Curves." IEEE Journal of Photovoltaics, 7(5), 1304-1312.

Hallam, B., Chen, D., Kim, M., Stefani, B., Hoex, B., Abbott, M., and Wenham, S. (2017). "The role of hydrogenation and gettering in enhancing the efficiency of next-generation Si solar cells: An industrial perspective." Physica Status Solidi (A) Applications and Materials Science, 214(7).

Hallam, B., Herguth, A., Hamer, P., Nampalli, N., Wilking, S., Abbott, M., Wenham, S., and Hahn, G. (2017). "Eliminating light-induced degradation in commercial p-Type Czochralski silicon solar cells." Applied Sciences (Switzerland), 8(1).

Hallam, B., Kim, M., Abbott, M., Nampalli, N., Nærland, T., Stefani, B., and Wenham, S. (2017). "Recent insights into boron-oxygen related degradation: Evidence of a single defect." Solar Energy Materials and Solar Cells, 173, 25-32.

Hameiri, Z. (2017). "Photovoltaics literature survey (No. 131)." Progress in Photovoltaics: Research and Applications, 25(1), 132-136.

Hameiri, Z. (2017). "Photovoltaics literature survey (no. 132)." Progress in Photovoltaics: Research and Applications, 25(2), 201-205.

Hameiri, Z. (2017). "Photovoltaics literature survey (no. 133)." Progress in Photovoltaics: Research and Applications, 25(3), 264-267.

Hameiri, Z. (2017). "Photovoltaics literature survey (no. 134)." Progress in Photovoltaics: Research and Applications, 25(4), 335-337.

Hameiri, Z. (2017). "Photovoltaics literature survey (No. 135)." Progress in Photovoltaics: Research and Applications, 25(6), 470-474.

Hameiri, Z. (2017). "Photovoltaics literature survey (no. 136)." Progress in Photovoltaics: Research and Applications, 25(8), 746-752.

Hameiri, Z. (2017). "Photovoltaics literature survey (No. 137)." Progress in Photovoltaics: Research and Applications, 25(10), 878-884.

Hameiri, Z. (2017). "Photovoltaics literature survey (no. 138)." Progress in Photovoltaics: Research and Applications, 25, 1077-1083.

Hameiri, Z., Borojevic, N., Mai, L., Nandakumar, N., Kim, K., and Winderbaum, S. (2017). "Low-absorbing and thermally stable industrial silicon nitride films with very low surface recombination." IEEE Journal of Photovoltaics, 7(4), 996-1003.

Hamer, P., Bourret-Sicotte, G., Martins, G., Wenham, A., Bonilla, R. S., and Wilshaw, P. (2017). "A novel source of atomic hydrogen

for passivation of defects in silicon." Physica Status Solidi - Rapid Research Letters, 11(5).

Heo, Y.-J.; Kim, J.-E.; Weerasinghe, H.; Angmo, D.; Qin, T.; Sears, K.; Hwang, K.; Jung, Y.-S.; Subbiah, J.; Jones, D. J.; Gao, M.; Kim, D.-Y.; Vak, D., (2017). "Printing-friendly sequential deposition via intra-additive approach for roll-to-roll process of perovskite solar cells" Nano Energy, 41, 443-451, 2017. DOI: 10.1016/j.nanoen.2017.09.051

Heo, Y-J., Kim, J-E., Weerasinghe, H.C., Angmo, D., Qin, T., Sears, K., Hwang, K., Jung, Y-S., Subbiah, J., Jones, D.J., Gao, M., Kim, D-Y., and Vak, V., (2017). "Printing-friendly sequential deposition via intra-additive approach for roll-to-roll process of perovskite solar cells", Nano Energy, 41, 443-451.

Hu, L., Patterson, R. J., Hu, Y., Chen, W., Zhang, Z., Yuan, L., Chen, Z., Conibeer, G. J., Wang, G., and Huang, S. (2017). "High Performance PbS Colloidal Quantum Dot Solar Cells by Employing Solution-Processed CdS Thin Films from a Single-Source Precursor as the Electron Transport Layer." Advanced Functional Materials, 27(46).

Huang, F., Pascoe, AR., Wu, W., Ku, Z., Peng, Y., Zhong, J., Caruso, RA., Cheng, YB., "Effect Of The Microstructure Of The Functional Layers On The Efficiency Of Perovskite Solar Cells", Advanced Materials, 29 (20), 2017

Huang, S., Cao, W., Yuan, L., Patterson, R., Wen, X., Tapping, P., Kee, T., Puthen-Veettil, B., Zhang, P., Zhang, Z., Oiuyang, Z., Reece, P., Bremner, S., Shrestha, S., and Conibeer, G. (2017). "Difference in hot carrier cooling rate between Langmuir-Blodgett and drop cast PbS QDs films due to strong electron-phonon coupling." Nanoscale 9, 17133-17142.

Huang, W., Gann, E., Chandrasekaran, N., Prasad, SKK., Chang, S., Thomsen, L., Kabra, D., Hodgkiss, JM., Cheng, YB., Yang, Y., McNeill, CR., "Influence Of Fullerene Acceptor On The Performance, Microstructure And Photophysics Of Low Bandgap Polymer Solar Cells", Advanced Energy Materials, 7 (11), 2017

Iskra, A., Juhl, M. K., Weber, J. W., Wong, J., and Trupke, T. (2017). "Detection of Finger Interruptions in Silicon Solar Cells Using Line Scan Photoluminescence Imaging." IEEE Journal of Photovoltaics, 7(6), 1496-1502.

J. Xu, B. Zhang, M. Jansen, L. Goerigk, W. W. H. Wong, C. Ritchie, (2017). 'Highly Fluorescent Pyridinium Betaines for Light Harvesting' Angew. Chem. Int. Ed., 56, 13882–13886. DOI: 10.1002/anie.201704832.

Jia, X., Lin, Z., Zhang, T., Puthen-Veettil, B., Yang, T., Nomoto, K., Ding, J., Conibeer, G., and Perez-Wurfl, I. (2017). "Accurate analysis of the size distribution and crystallinity of boron doped Si nanocrystals: Via Raman and PL spectra." RSC Advances, 7(54), 34244-34250.

Jin, X., Bai, J., Gu, X., Chang, C., Shen, H., Zhang, Q., Li, F., Chen, Z., and Li, Q. (2017). "Efficient light-emitting diodes based on reverse type-I quantum dots." Optical Materials Express, 7(12), 4395-4407.

Jin, X., You, L., Chen, Z., and Li, Q. (2018). "High-efficiency platinum-free quasi-solid-state dye-sensitized solar cells from polyaniline (polypyrrole)-carbon nanotube complex tailored conducting gel electrolytes and counter electrodes." Electrochimica Acta, 260, 905-911.

Juhl, M. K., Abbott, M. D., and Trupke, T. (2017). "Relative External Quantum Efficiency of Crystalline Silicon Wafers from Photoluminescence." IEEE Journal of Photovoltaics, 7(4), 1074-1080.

Karimkashi Arani, S., Hawkes, E. V. A. T. T., Bolla, M. I. C. H. E. L. E., Wang, H., Im, H., and Arias, P.

Kashif, MK, Benesperi, I., Milhuisen, RA., Meyer, S., Hellerstedt, J., Zee, D., Duffy, NW., Halstead, B., Fuhrer, MS., Cashion, J., Cheng, YB., Spiccia, L., Simonov, AN., Bach, U., "Polypyridyl Iron Complex As A Hole-Transporting Material For Formamidinium Lead Bromide Perovskite Solar Cells", ACS Energy Letters, 2 (8), 1855-1859, 2017

Kim, J., Park, N., Yun, J. S., Huang, S., Green, M. A., and Ho-Baillie, A. W. Y. (2017). "An effective method of predicting perovskite solar cell lifetime–Case study on planar CH3NH3PbI3 and HC(NH2) 2PbI3 perovskite solar cells and hole transfer materials of spiro-OMeTAD and PTAA." Solar Energy Materials and Solar Cells, 162, 41-46.

Kim, J., Yun, J. S., Cho, Y., Lee, D. S., Wilkinson, B., Soufiani, A. M., Deng, X., Zheng, J., Shi, A., Lim, S., Chen, S., Hameiri, Z., Zhang, M., Lau, C. F. J., Huang, S., Green, M. A., and Ho-Baillie, A. W. Y. (2017). "Overcoming the challenges of large-area high-efficiency perovskite solar cells." ACS Energy Letters, 2, 1978-1984.

Kim, K. H., Winderbaum, S., and Hameiri, Z. (2017). "In-situ diagnostics of PECVD AlOx deposition by optical emission spectroscopy." Surface and Coatings Technology, 328, 204-210.

Kim, M., Abbott, M., Nampalli, N., Wenham, S., Stefani, B., and Hallam, B. (2017). "Modulating the extent of fast and slow boron-oxygen related degradation in Czochralski silicon by thermal annealing: Evidence of a single defect." Journal of Applied Physics, 121(5).

Kim, Y., Cho, I. W., Ryu, M. Y., Kim, J. O., Lee, S. J., Ban, K. Y., and Honsberg, C. B. (2017). "Stranski-Krastanov InAs/GaAsSb quantum dots coupled with sub-monolayer quantum dot stacks as a promising absorber for intermediate band solar cells." Applied Physics Letters, 111(7).

Kivisaari, P., Berg, A., Karimi, M., Storm, K., Limpert, S., Oksanen, J., Samuelson, L., Pettersson, H., and Borgström, M. T. (2017). "Optimization of Current Injection in AlGaInP Core'Shell Nanowire Light-Emitting Diodes." Nano Letters, 17(6), 3599-3606.

Lal, NN., Dkhissi,Y., Li, W., Hou, Q., Cheng, YB., Bach, U., "Perovskite Tandem Solar Cells", Advanced Energy Materials, 7 (18), 2017

Lambert, D. S., Murphy, S. T., Lennon, A., and Burr, P. A. (2017). "Formation of intrinsic and silicon defects in MoO3 under varied oxygen partial pressure and temperature conditions: An ab initio DFT investigation." RSC Advances, 7(85), 53810-53821.

Lan, D., and Green, M. A. "Up-conversion of sunlight by GaInP/GaAs/Ge cell stacks: Limiting efficiency, practical limitation and comparison with tandem cells."

Latzel, M., Büttner, P., Sarau, G., Höflich, K., Heilmann, M., Chen, W., Wen, X., Conibeer, G., and Christiansen, S. H. (2017). "Significant performance enhancement of InGaN/GaN nanorod LEDs with multi-layer graphene transparent electrodes by alumina surface passivation." Nanotechnology, 28(5).

Lau, C. F. J., Zhang, M., Deng, X., Zheng, J., Bing, J., Ma, Q., Kim, J., Hu, L., Green, M. A., Huang, S., and Ho-Baillie, A. (2017). "Strontium-Doped Low-Temperature-Processed CsPbI2Br Perovskite Solar Cells." ACS Energy Letters, 2(10), 2319-2325.

Lee, C. Y., Aziz, M. I. A., Wenham, S., and Hoex, B. (2017). "Characterisation of thermal annealed WOx on p-type silicon for hole-selective contacts." Japanese Journal of Applied Physics, 56(8).

Li, F., You, L., Li, H., Gu, X., Wei, J., Jin, X., Nie, C., Zhang, Q., and Li, Q. (2017). "Emission tunable CdZnS/ZnSe core/shell quantum dots for white light emitting diodes." Journal of Luminescence, 192, 867-874.

Li, F., You, L., Nie, C., Zhang, Q., Jin, X., Li, H., Gu, X., Huang, Y., and Li, Q. (2017). “Quantum dot white light emitting diodes with high scotopic/photopic ratios.” Optics Express, 25(18), 21901-21913.

Li, H., Hallam, B., Wenham, S., and Abbott, M. (2017). “Oxidation Drive-In to Improve Industrial Emitter Performance by POCl3 Diffusion.” IEEE Journal of Photovoltaics, 7(1), 144-152.

Li, H., Ma, F. J., Hameiri, Z., Wenham, S., and Abbott, M. (2017). “An advanced qualitative model regarding the role of oxygen during POCl3 diffusion in silicon.” Physica Status Solidi - Rapid Research Letters, 11, 1700046.

Li, H., Ma, F. J., Hameiri, Z., Wenham, S., and Abbott, M. (2017). “On elimination of inactive phosphorus in industrial POCl3 diffused emitters for high efficiency silicon solar cells.” Solar Energy Materials and Solar Cells, 171, 213-221.

Li, M., Ma, F. J., Peters, I. M., Shetty, K. D., Aberle, A. G., Hoex, B., and Samudra, G. S. (2017). “Numerical Simulation of Doping Process by BBr3 Tube Diffusion for Industrial n -Type Silicon Wafer Solar Cells.” IEEE Journal of Photovoltaics, 7(3), 755-762.

Li, Q., Li, H., Shen, H., Wang, F., Zhao, F., Li, F., Zhang, X., Li, D., Jin, X., and Sun, W. (2017). “Solid Ligand-Assisted Storage of Air-Stable Formamidinium Lead Halide Quantum Dots via Restraining the Highly Dynamic Surface toward Brightly Luminescent Light-Emitting Diodes.” ACS Photonics, 4(10), 2504-2512.

Li, W., Zhao, L., Zhang, K., Sun, H., Lai, Y., Jiang, Y., Jiang, L., Liu, F., and Jia, M. (2017). “Fabrication of Cu2ZnSnS4 thin film solar cells by annealing of reactively sputtered precursors.” Journal of Alloys and Compounds, 701, 55-62.

Li, Y., Liu, X., Chen, X., Wang, D., and He, Y. (2017). “Photoelectric properties of graphene oxide–ZnO composite nanosheets vertically grown on substrate.” Journal of Alloys and Compounds, 699, 468-478.

Liang, R.-Z.; Babics, M.; Seitkhan, A.; Wang, K.; Geraghty, P. B.; Lopatin, S.; Cruciani, F.; Firdaus, Y.; Caporuscio, M.; Jones, D. J.; Beaujuge, P. M., (2017). “Additive-Morphology Interplay and Loss Channels in “All-Small-Molecule” Bulk-heterojunction (BHJ) Solar Cells with the Nonfullerene Acceptor IDTTBM” Adv. Funct. Mater., pp.28(7), 1705464. DOI: 10.1002/adfm.201705464

Liao, Y., Zhang, P., Bremner, S., Shrestha, S., Huang, S., and Conibeer, G. (2017). “Resonant Tunneling through Monolayer Si Colloidal Quantum Dots and Ge Nanocrystals.” Advanced Functional Materials, 27(21).

Liao, Y., Zhou, D., Shrestha, S., Huang, S., Bremner, S., and Conibeer, G. (2017). “Interfacial Area between Hetero-Epitaxial γ-Al2O3 and Silicon.” Advanced Materials Interfaces, 4(17).

Limpert, S., Burke, A., Chen, I. J., Anttu, N., Lehmann, S., Fahlvik, S., Bremner, S., Conibeer, G., Thelander, C., Pistol, M. E., and Linke, H. (2017). “Bipolar Photothermoelectric Effect Across Energy Filters in Single Nanowires.” Nano Letters, 17(7), 4055-4060.

Limpert, S., Burke, A., Chen, I. J., Anttu, N., Lehmann, S., Fahlvik, S., Bremner, S., Conibeer, G., Thelander, C., Pistol, M. E., and Linke, H. (2017). “Single-nanowire, low-bandgap hot carrier solar cells with tunable open-circuit voltage.” Nanotechnology, 28(43).

Lin, Q., Jiang, W., Zhang, S., Nagiri, R. C. R., Jin, H., Burn, P. L., and Meredith, P., (2017). “A Triarylamine-Based Anode Modifier for Efficient Organohalide Perovskite Solar Cells”, ACS Applied Materials & Interfaces, 9, 9096–9101.

Liu, F., Huang, J., Sun, K., Yan, C., Shen, Y., Park, J., Pu, A., Zhou, F., Liu, X., Stride, J. A., Green, M. A., and Hao, X. (2017). “Beyond 8% ultrathin kesterite Cu2ZnSnS4 solar cells by interface reaction route controlling and self-organized nanopattern at the back contact.” NPG Asia Mater, 9, e401.

Liu, F., Yan, C., Sun, K., Zhou, F., Hao, X., and Green, M. A. (2017). “Light-Bias-Dependent External Quantum Efficiency of Kesterite Cu2ZnSnS4 Solar Cells.” ACS Photonics, 4(7), 1684-1690.

Liu, X., Cui, H., Hao, X., Huang, S., and Conibeer, G. J. (2017). “The effect of vacuum thermal annealing on the molybdenum bilayer back contact deposited by radio-frequency magnetron sputtering for chalcogenide and kesterite based solar cells.” Journal of the Korean Physical Society, 71(12), 968–973 .

Liu, X., Huang, J., Zhou, F., Liu, F., Stride, J. A., and Hao, X. (2017). “Spatial Grain Growth and Composition Evolution during Sulfurizing Metastable Wurtzite Cu2ZnSnS4 Nanocrystal-Based Coatings.” Chemistry of Materials, 29(5), 2110-2121.

Liu, Y., Tang, Y., Zeng, Y., Luo, X., Ran, J., Luo, Y., Su, X., Ng, B. K., Liu, F., and Jiang, L. (2017). “Colloidal synthesis and characterization of single-crystalline Sb2 Se3 nanowires.” RSC Advances, 7(40), 24589-24593.

Liu, Z., Hao, X., Ho-Baillie, A., and Green, M. A. (2017). “Effects of Al thickness on one-step aluminium-assisted crystallization of Ge epitaxy on Si by magnetron sputtering.” Materials Letters, 209, 32-35.

Liu, Z., Hao, X., Ho-Baillie, A., and Green, M. A. (2017). “In situ X-ray diffraction study on epitaxial growth of SixGe1−x on Si by aluminium-assisted crystallization.” Journal of Alloys and Compounds, 695, 1672-1676.

Liu, Z., Hao, X., Huang, J., Ho-Baillie, A., Varlamov, S., and Green, M. A. (2017). “Diode laser annealing of epitaxy Ge on sapphire (0 0 0 1) grown by magnetron sputtering.” Materials Letters, 208, 35-38.

Lu, J., Jiang L., Li W., Li F., Pai N.K., Scully, A.D., Tsai C.M., Simonov A.N., Bach U., Cheng Y.B., and Spiccia, L., “Diammonium and monoammonium mixed-organic-cation perovskites for high performance solar cells with improved stability”, (2017). Advanced Energy Materials, 7, 17000444.

Lu, J., Jiang, L., Li, W., Li, F., Pai, NK., Scully, AD., Tsai, C., U. Bach, A.N. Simonov, Y.B. Cheng, L. Spiccia, “Diammonium And Monoammonium Mixed-Organic-Cation Perovskites For High Performance Solar Cells With Improved Stability”, Advanced Energy Materials, 7 (18), 2017

Lund, C., Pryor, T., Jennings, P., Blackmore, K., Corkish, R., Saman, W., Miller, W., and Woods-McConney, A. (2017). “Sustainable Energy Education: Addressing the Needs of Students and Industry.” Renewable Energy and Environmental Sustainability, 2.

Ma, Q., Huang, S., Chen, S., Zhang, M., Lau, C. F. J., Lockrey, M. N., Mulmudi, H. K., Shan, Y., Yao, J., Zheng, J., Deng, X., Catchpole, K., Green, M. A., and Ho-Baillie, A. W. Y. (2017). “The Effect of Stoichiometry on the Stability of Inorganic Cesium Lead Mixed-Halide Perovskites Solar Cells.” Journal of Physical Chemistry C, 121(36), 19642-19649.

Ma, Q., Huang, S., Chen, S., Zhang, M., Lau, C. F. J., Lockrey, M. N., Mulmudi, H. K., Shan, Y., Yao, J., Zheng, J., Deng, X., Catchpole, K., Green, M. A., and Ho-Baillie, A. W. Y. (2017). “The Effect of Stoichiometry on the Stability of Inorganic Cesium Lead Mixed-Halide Perovskites Solar Cells.” Journal of Physical Chemistry C, 121(36), 19642-19649.

Mahboubi Soufiani, A., Yang, Z., Young, T., Miyata, A., Surrente, A., Pascoe, A., Galkowski, K., Abdi-Jalebi, M., Brenes, R., Urban, J., Zhang, N., Bulovic, V., Portugall, O., Cheng, YB., Nicholas, RJ., Ho-Baillie, A., Green, MA., Plochocka, P., Stranks, SD., “Impact Of Microstructure On The Electron-Hole Interaction In Lead Halide

Perovskites", Energy And Environmental Science, 10 (6), 1358-1366, 2017

Mahboubi Soufiani, A., Yang, Z., Young, T., Miyata, A., Surrente, A., Pascoe, A., Galkowski, K., Abdi-Jalebi, M., Brenes, R., Urban, J., Zhang, N., Bulovi‍ɣ, V., Portugall, O., Cheng, Y. B., Nicholas, R. J., Ho-Baillie, A., Green, M. A., Plochocka, P., and Stranks, S. D. (2017). "Impact of microstructure on the electron-hole interaction in lead halide perovskites." Energy and Environmental Science, 10(6), 1358-1366.

Mahmud, M. A., Elumalai, N. K., Upama, M. B., Wang, D., Chan, K. H., Wright, M., Xu, C., Haque, F., and Uddin, A. (2017). "Low temperature processed ZnO thin film as electron transport layer for efficient perovskite solar cells." Solar Energy Materials and Solar Cells, 159, 251-264.

Mahmud, M. A., Elumalai, N. K., Upama, M. B., Wang, D., Gonçales, V. R., Wright, M., Xu, C., Haque, F., and Uddin, A. (2017). "A high performance and low-cost hole transporting layer for efficient and stable perovskite solar cells." Physical Chemistry Chemical Physics, 19(31), 21033-21045.

Mahmud, M. A., Elumalai, N. K., Upama, M. B., Wang, D., Haque, F., Wright, M., Xu, C., and Uddin, A. (2017). "Controlled nucleation assisted restricted volume solvent annealing for stable perovskite solar cells." Solar Energy Materials and Solar Cells, 167, 70-86.

Mahmud, M. A., Elumalai, N. K., Upama, M. B., Wang, D., Puthen-Veettil, B., Haque, F., Wright, M., Xu, C., Pivrikas, A., and Uddin, A. (2017). "Controlled Ostwald ripening mediated grain growth for smooth perovskite morphology and enhanced device performance." Solar Energy Materials and Solar Cells, 167, 87-101.

Mahmud, M. A., Elumalai, N. K., Upama, M. B., Wang, D., Soufiani, A. M., Wright, M., Xu, C., Haque, F., and Uddin, A. (2017). "Solution-processed lithium-doped ZnO electron transport layer for efficient triple cation (Rb, Ma, Fa) perovskite solar cells." ACS Applied Materials and Interfaces, 9(39), 33840-33854.

Mahmud, M. A., Elumalai, N. K., Upama, M. B., Wang, D., Zarei, L., Gonçales, V. R., Wright, M., Xu, C., Haque, F., and Uddin, A. (2018). "Adsorbed carbon nanomaterials for surface and interface-engineered stable rubidium multi-cation perovskite solar cells." Nanoscale, 10(2), 773-790.

Mao, W., Zheng, J., Zhang, Y., Chesman, ASR., Ou, Q., Hicks, J., Li, F., Wang, Z., Graystone, B., Bell, TDM., Rothmann, MU., Duffy, NW., Spiccia, L., Cheng, YB., Bao, Q., Bach, U., "Controlled growth of monocrystalline organo-lead halide perovskite and its application in photonic devices", Angewandte Chemie - International Edition, 56 (41), 12486-12491, 2017

McIntosh, K. R., Allen, T. G., Baker-Finch, S. C., and Abbott, M. D. (2017). "Light trapping in isotextured silicon wafers." IEEE Journal of Photovoltaics, 7(1), 110-117.

Mitchell, B., Chung, D., He, Q., Zhang, H., Xiong, Z., Altermatt, P. P., Geelan-Small, P., and Trupke, T. (2017). "PERC Solar Cell Performance Predictions from Multicrystalline Silicon Ingot Metrology Data." IEEE Journal of Photovoltaics, 7(6), 1619-1626.

Mitchell, V. D.; Gann, E.; Huettner, S.; Singh, C. R.; Subbiah, J.; Thomsen, L.; McNeill, C. R.; Thelakkat, M.; Jones, D. J., (2017). "Morphological and Device Evaluation of an Amphiphilic Block Copolymer for Organic Photovoltaic Applications" Macromolecules, 50 (13), 4942-4951. DOI: 10.1021/acs.macromol.7b00377

Mitchell, V. D.; Wong, W. W. H.; Thelakkat, M.; Jones, D. J., (2017). "The synthesis and purification of amphiphilic conjugated donor-acceptor block copolymers" Polym. J., 49 (1), 155-161. DOI: 10.1038/pj.2016.97

Monteiro Lunardi, M., Richard Corkish, R. C., Stephen Moore, S. M., J.P. Alvarez-Gaitan, J. P. A. G., and Anita Ho-Baillie, A. H. B. (2017). "A Life Cycle Assessment of Perovskite/Silicon Tandem Solar Cells." Progress in Photovoltaics: Research and Applications, 25(8) 679–695

Nampalli, N., Fung, T. H., Wenham, S., Hallam, B., and Abbott, M. (2017). "Statistical analysis of recombination properties of the boron-oxygen defect in p-type Czochralski silicon." Frontiers in Energy, 11(1), 4-22.

Nampalli, N., Li, H., Kim, M., Stefani, B., Wenham, S., Hallam, B., and Abbott, M. (2017). "Multiple pathways for permanent deactivation of boron-oxygen defects in p-type silicon." Solar Energy Materials and Solar Cells, 173, 12-17.

Nguyen H. T., and Macdonald, D., (2017). "On the composition of luminescence spectra from heavily doped p-type silicon under low and high excitation", Journal of Luminescence, 181 223-229.

Nguyen, H. T., Jensen, M. A., Li, L., Samundsett, C., Sio, H. C., Lai, B. , Buonassisi, T., Macdonald, D., (2017). "Microscopic distributions of defect luminescence from subgrain boundaries in multicrystalline silicon wafers", IEEE Journal of Photovoltaics, 7 772-780.

Nguyen, H. T., Johnston, S., Basnet, R., Guthrey, H., Dippo, P., Zhang, H., Al-Jassim, M. M., and Macdonald, D., (2017). "Imaging the thickness of passivation layers for crystalline silicon with micron‍ɣscale spatial resolution using spectral photoluminescence", Solar RRL, vol. 1.

Nguyen, H. T., Johnston, S., Paduthol, A., Harvey, S. P., Phang, S. P., Samundsett, C., Sun, C., Yan, D., Trupke, T., Al-Jassim, M. M., and Macdonald, D. (2017). "Quantification of Sheet Resistance in Boron-Diffused Silicon Using Micro-Photoluminescence Spectroscopy at Room Temperature." Solar RRL, 1(10), DOI: 10.1002/solr.201700088.

Nguyen, H. T., Mokkapati, S., Macdonald, D., (2017). "Detecting dopant diffusion enhancement at grain boundaries in multicrystalline silicon wafers with micro-photoluminescence spectroscopy", IEEE Journal of Photovoltaics, 7, 598-603.

Nomoto, K., Yang, T. C. J., Ceguerra, A. V., Zhang, T., Lin, Z., Breen, A., Wu, L., Puthen-Veettil, B., Jia, X., Conibeer, G., Perez-Wurfl, I., and Ringer, S. P. (2017). "Microstructure analysis of silicon nanocrystals formed from silicon rich oxide with high excess silicon: Annealing and doping effects." Journal of Applied Physics, 122(2).

Pakhuruddin, M. Z., Huang, J., Dore, J., and Varlamov, S. (2017). "Enhanced light-trapping in laser-crystallised silicon thin-film solar cells on glass by optimised back surface reflectors." Solar Energy, 150, 477-484.

Pakhuruddin, M. Z., Huang, J., Kühnapfel, S., Dore, J., Gall, S., and Varlamov, S. (2017). "Properties of laser-crystallised silicon thin-film solar cells on textured glass." Journal of Materials Science: Materials in Electronics, 28(14), 10391-10399.

Pandey, R., Vats, G., Yun, J., Bowen, C. R., Ho-Baillie, A. W. Y., and Seidel, J. "Perovskites for Solar and Thermal Energy Harvesting: State of the Art Technologies, Current Scenario and Future Directions." https://arxiv.org/abs/1705.05529

Park, J., Ouyang, Z., Yan, C., Sun, K., Sun, H., Liu, F., Green, M., and Hao, X. (2017). "Hybrid Ag nanowire-ITO as transparent conductive electrode for pure Sulfide Kesterite Cu2ZnSnS4 Solar Cells." Journal of Physical Chemistry C, 121(38), 20597-20604.

Pascoe, A., Gu, Q., Rothmann, M., Li, W., Zhang, Y., Scully, A.D., Lin, X., Spiccia, L., Bach, U., and Cheng, Y.B., (2017). "Directing nucleation and growth kinetics in solution-processed perovskite thin-films", China Science Materials, 60, 612-628.

Pascoe, AR., Gu, Q., Rothmann, M.U., Li, W., Zhang, Y., Scully, AD., Lin, X., Spiccia, L., Bach, U., Cheng, YB., "Directing Nucleation And Growth Kinetics In Solution-Processed Hybrid Perovskite Thin-Films", Science China Materials, 60 (7), 617-628, 2017

Payne, D. N. R., Vargas, C., Hameiri, Z., Wenham, S. R., and Bagnall, D. M. (2017). "An advanced software suite for the processing and analysis of silicon luminescence images." Computer Physics Communications, 215, 223-234.

Peng, J, Wu, Y , Wang, Y, Jacobs, D, Shen, H , Fu, X, Wan, Y., Doung, T, Wu, N, Barugkin, C , Nguyen, H, Zhong, D, Li, J , Lu, T, Liu, Y , Lockrey, M, Weber, K , Catchpole, K, White, T , (2017)."Interface passivation using ultrathin polymer-fullerene films for high-efficiency perovskite solar cells with negligible hysteresis," Energy & Environmental Science.

Peng, X. Yuan, J., Shen, S., Gao, M., Yin, H., Cheng, J., Zhang, Q., and Angmo, D., (2017). "Progress on inkjet printing of organic and perovskite solar cells", Advanced Functional Material, 27, 1703704.

Pu, A., Ma, F., Yan, C., Huang, J., Sun, K., Green, M., and Hao, X. (2017). "Sentaurus modelling of 6.9% Cu2ZnSnS4 device based on comprehensive electrical & optical characterization." Solar Energy Materials and Solar Cells, 160, 372-381.

Puthen Veettil, B., König, D., Huang, S., Patterson, R., and Conibeer, G. (2017). "Morphology effects on the bandgap of silicon nanocrystals - Numerically modelled by a full multi-grid method." Journal of Applied Physics, 121(5).

Qin, T, Huang, W., Kim, J., Vak, D., Forsyth, C., McNeill, CR., Cheng, YB., "Amorphous Hole-Transporting Layer In Slot-Die Coated Perovskite Solar Cells", Nano Energy, 31, 210-217, 2017

Qin, T., Huang, W., Kim, J-E., Vak, D., Forsyth, C., McNeill, C. R., Cheng, Y., (2017). "Amorphous hole-transporting layer in slot-die coated perovskite solar cells", Nano Energy, 31, 210-27.

Quiroz, C. O. R., Shen, Y., Salvador, M., Forberich, K., Schrenker, N., Spyropoulos, G. D., Heumüller, T., Wilkinson, B., Kirchartz, T., Spiecker, E., Verlinden, P. J., Zhang, X., Green, M. A., Ho-Baillie, A., and Brabec, C. J. (2018). "Balancing electrical and optical losses for efficient Si-perovskite 4-terminal solar cells with solution processed percolation electrodes." Journal of Materials Chemistry A(8), DOI: 10.1039/C7TA10945H.

Rautela, R.; Joshi, N.; Novakovic, Wong, W. W. H.; White, J.M.; Ghiggino, K. P.; Paige, M. F.; Steer, R. P., (2017). "Determinants of the efficiency of photon upconversion by triplet-triplet annihilation in the solid state: zinc porphyrin derivatives in PVA", Phys. Chem. Chem. Phys., 19, 23471-23482. DOI: 10.1039/c7cp04746k

Rodriguez, J., Zhang, W., Lim, S., and Lennon, A. (2017). "Improved metal adhesion with galvanic nickel plating to silicon solar cells." Solar Energy Materials and Solar Cells, 165, 17-26.

Rolston, N., Printz, A.D., Tracy, J.M., Weerasinghe, H.C., Vak, V., Priyadarshi, A., Mathews, N., Slotcavage, D.J., McGehee, M.D., Kalan, R.E., Grimm, R.L., Nie, W., Mohite, A.D., Tsai, H., Saliba, M., Grätzel, M., and Dauskardt, R.H., (2017). "Effect of Cation Composition on the Mechanical Stability of Perovskite Solar Cells", Advanced Energy Materials, 10.1002/aenm.201702116

Rothmann, MU., Li, W., Etheridge, J., Cheng, YB., "Microstructural Characterisations Of Perovskite Solar Cells - From Grains To Interfaces: Techniques, Features, And Challenges", Advanced Energy Materials, 2017

Rothmann, MU., Li, W., Zhu, Y., Bach, U., Spiccia, L., Etheridge, J., Cheng, YB., "Direct Observation Of Intrinsic Twin Domains In Tetragonal CH3NH3PbI3", Nature Communications, 8, 2017

Rougieux, F. E., Nguyen, H. T., Macdonald, D. H., Mitchell, B., and Falster, R. (2017). "Growth of Oxygen Precipitates and Dislocations in Czochralski Silicon." IEEE Journal of Photovoltaics, 7(3), 735-740.

Sears, K.K., Fievez, M., Gao, M., Weerasinghe, H.C., Easton, C.D., and Vak, D., (2017). "ITO-Free Flexible Perovskite Solar Cells Based on Roll-to-Roll, Slot-Die Coated Silver Nanowire Electrodes", Solar RRL, DOI: 10.1002/solr.201700059

Sepalage G.A., Meyer S., Pascoe A.R., Scully A.D., Bach U., Cheng Y.B., and Spiccia L., (2017). "A facile deposition method for CuSCN: Exploring the influence of CuSCN on J-V hysteresis in planar perovskite solar cells", Nano Energy, 32, 310–319.

Sepalage, GA., Meyer, S., Pascoe, AR., Scully, AD., Bach, U., Cheng, YB., Spiccia, L., "A Facile Deposition Method For CuSCN: Exploring The Influence Of CuSCN On J-V Hysteresis In Planar Perovskite Solar Cells", Nano Energy, 32, 310-319, 2017

Shen, D., Sun, C., Zheng, P., Macdonald, D., and Rougieux, F., (2017). "Carrier induced degradation in compensated n-type silicon solar cells: Impact of light-intensity, forward bias voltage, and temperature on the reaction kinetics", Japanese Journal of Applied Physics, 56, 08MB23

Shen, H., Jacobs, D. A., Wu, Y., Duong, T., Peng, J., Wen, X., Fu, X., Karuturi, S. K., White, T. P., Weber, K., and Catchpole, K. R. (2017). "Inverted Hysteresis in CH3NH3PbI3 Solar Cells: Role of Stoichiometry and Band Alignment." Journal of Physical Chemistry Letters, 8(12), 2672-2680.

Sheng, R., Hörantner, M. T., Wang, Z., Jiang, Y., Zhang, W., Agosti, A., Huang, S., Hao, X., Ho-Baillie, A., Green, M., and Snaith, H. J. (2017). "Monolithic Wide Band Gap Perovskite/Perovskite Tandem Solar Cells with Organic Recombination Layers." Journal of Physical Chemistry C, 121(49), 27256-27262.

Shi, J., Pollard, M. E., Angeles, C. A., Chen, R., Gates, J. C., and Charlton, M. D. B. (2017). "Photonic crystal and quasi-crystals providing simultaneous light coupling and beam splitting within a low refractive-index slab waveguide." Scientific Reports, 7(1).

Shi, L., Young, T. L., Kim, J., Sheng, Y., Wang, L., Chen, Y., Feng, Z., Keevers, M. J., Hao, X., Verlinden, P. J., Green, M. A., and Ho-Baillie, A. W. Y. (2017). "Accelerated Lifetime Testing of Organic-Inorganic Perovskite Solar Cells Encapsulated by Polyisobutylene." ACS Applied Materials and Interfaces, 9(30), 25073-25081.

Shrestha, S., Chung, S., Liao, Y., Wang, P., Cao, W., Wen, X., Gupta, N., and Conibeer, G. (2017). "Potential of HfN, ZrN, and TiH as hot carrier absorber and Al2O3/Ge quantum well/Al2O3 and Al2O3/PbS quantum dots/Al2O3 as energy selective contacts." Japanese Journal of Applied Physics, 56(8).

Soeriyadi, A. H., Wang, L., Conrad, B., Li, D., Lochtefeld, A., Gerger, A., Barnett, A., and Perez-Wurfl, I. (2017). "Extraction of Essential Solar Cell Parameters of Subcells in a Tandem Structure With a Novel Three-Terminal Measurement Technique." IEEE Journal of Photovoltaics, . 8(1), 327-332.

Song, N., Huang, J., Green, M. A., and Hao, X. (2017). "Diode laser annealing on sputtered epitaxial Cu2ZnSnS4 thin films." Physica Status Solidi - Rapid Research Letters, 11(5).

Soufiani, A. M., Hameiri, Z., Meyer, S., Lim, S., Tayebjee, M. J. Y., Yun, J. S., Ho-Baillie, A., Conibeer, G. J., Spiccia, L., and Green, M. A. (2017). "Lessons learnt from spatially resolved electro- and photoluminescence imaging: Interfacial delamination in CH3NH3PbI3 planar perovskite solar cells upon illumination." Advanced Energy Materials, 7(9), 1602111-1602111.

Sprafke, A., Behrendt, A., Liu, J., Spencer, L., and Tang, J. (2017). "Feature issue introduction: Light, Energy and the Environment, 2016." Optics Express, 25(8), A444-A446.

Subbiah, J.; Mitchell, V. D.; Hui, N. K. C.; Jones, D. J.; Wong, W. W. H., (2017). "A Green Route to Conjugated Polyelectrolyte Interlayers for High-Performance Solar Cells" Angewandte Chemie (International ed. in English) 56 (29), 8431-8434. DOI: 10.1002/anie.201612021

Sun, C., Nguyen, H. T., Rougieux, F. E., and Macdonald, D., (2017). "Precipitation of Cu and Ni in n-and p-type Czochralski-grown silicon characterized by photoluminescence imaging", Journal of Crystal Growth, 460, 98-104

Sun, C., Nguyen, H. T., Sio, H. C., Rougieux, F. E., and Macdonald, D., (2017). "Activation kinetics of the boron-oxygen defect in compensated n- and p-type silicon studied by high-injection micro-photoluminescence", IEEE Journal of Photovoltaics, 7, 988-995

Telford, A. M., Thickett, S. C., and Neto, C. (2017). "Functional patterned coatings by thin polymer film dewetting." Journal of Colloid and Interface Science, 507, 453-469.

Teymouri, A., Pillai, S., Ouyang, Z., Hao, X., Liu, F., Yan, C., and Green, M. A. (2017). "Low-temperature solution processed random silver nanowire as a promising replacement for indium tin oxide." ACS Applied Materials and Interfaces, 9(39), 34093-34100.

To, A., and Hoex, B. (2017). "Extracting dielectric fixed charge density on highly doped crystalline-silicon surfaces using photoconductance measurements." Journal of Applied Physics, 122(19).

To, A., Tahir, S., Garavaglia, A., Li, W. M., Li, X., and Hoex, B. (2017). "The Effect of Bifacial AlOx Deposition on PERC Solar Cell Performance." IEEE Journal of Photovoltaics, 7(6), 1528-1538.

Tong, J., To, A., Lennon, A., and Hoex, B. (2017). "Unintentional consequences of dual mode plasma reactors: Implications for upscaling lab-record silicon surface passivation by silicon nitride." Japanese Journal of Applied Physics, 56(8).

Tong, J., Wan, Y., Cui, J., Lim, S., Song, N., and Lennon, A. (2017). "Solution-processed molybdenum oxide for hole-selective contacts on crystalline silicon solar cells." Applied Surface Science, 423, 139-146.

Upama, M. B., Elumalai, N. K., Mahmud, M. A., Sun, H., Wang, D., Chan, K. H., Wright, M., Xu, C., and Uddin, A. (2017). "Organic solar cells with near 100% efficiency retention after initial burn-in loss and photo-degradation." Thin Solid Films, 636, 127-136.

Upama, M. B., Elumalai, N. K., Mahmud, M. A., Wang, D., Haque, F., Gonçales, V. R., Gooding, J. J., Wright, M., Xu, C., and Uddin, A. (2017). "Role of fullerene electron transport layer on the morphology and optoelectronic properties of perovskite solar cells." Organic Electronics: Physics, Materials, Applications, 50, 279-289.

Upama, M. B., Elumalai, N. K., Mahmud, M. A., Wright, M., Wang, D., Xu, C., Haque, F., Chan, K. H., and Uddin, A. (2017). "Interfacial engineering of electron transport layer using Caesium Iodide for efficient and stable organic solar cells." Applied Surface Science, 416, 834-844.

Upama, M. B., Wright, M., Elumalai, N. K., Mahmud, M. A., Wang, D., Chan, K. H., Xu, C., Haque, F., and Uddin, A. (2017). "High performance semitransparent organic solar cells with 5% PCE using non-patterned MoO3/Ag/MoO3 anode." Current Applied Physics, 17(2), 298-305.

Upama, M. B., Wright, M., Elumalai, N. K., Mahmud, M. A., Wang, D., Chan, K. H., Xu, C., Haque, F., and Uddin, A. (2017). "Optical modelling of P3HT:PC71BM semi-transparent organic solar cell." Optical and Quantum Electronics, 49(1).

Upama, M. B., Wright, M., Elumalai, N. K., Mahmud, M. A., Wang, D., Xu, C., and Uddin, A. (2017). "High-Efficiency Semitransparent Organic Solar Cells with Non-Fullerene Acceptor for Window Application." ACS Photonics, 4(9), 2327-2334.

Upama, M. B., Wright, M., Mahmud, M. A., Elumalai, N. K., Mahboubi Soufiani, A., Wang, D., Xu, C., and Uddin, A. (2017). "Photo-degradation of high efficiency fullerene-free polymer solar cells." Nanoscale, 9(47), 18788-18797.

Vargas, C., Zhu, Y., Coletti, G., Chan, C., Payne, D., Jensen, M., and Hameiri, Z. (2017). "Recombination parameters of lifetime-limiting carrier-induced defects in multicrystalline silicon for solar cells." Applied Physics Letters, 110(9).

Walter, D., Wu, Y., Duong, T., Jiang, L., Fong, K.C., and Weber, K.J., (2017). "On the Use of Luminescence Intensity Images for Quantified Characterization of Perovskite Solar Cells: Spatial Distribution of Series Resistance," Adv. Energy Mater. Published online 10.1002/aenm.201701522.

Wan,Y., Samundsett, C., Bullock, J., Hettick, M., Allen, T., Yan, D., et al., (2017). "Conductive and Stable Magnesium Oxide Electron-Selective Contacts for Efficient Silicon Solar Cells," Advanced Energy Materials, pp. 1601863-n/a.

Wang, D., Chan, K. H., Elumalai, N. K., Mahmud, M. A., Upama, M. B., Uddin, A., and Pillai, S. (2017). "Interfacial engineering of hole transport layers with metal and dielectric nanoparticles for efficient perovskite solar cells." Physical Chemistry Chemical Physics, 19(36), 25016-25024.

Wang, D., Su, B., Jiang, Y., Li, L., Ng, B. K., Wu, Z., and Liu, F. (2017). "Polytype 1T/2H MoS_2 heterostructures for efficient photoelectrocatalytic hydrogen evolution." Chemical Engineering Journal, 330, 102-108.

Wang, H., He, B., Liu, F., Stevens, C., Brady, M. A., Cai, S., Wang, C., Russell, T. P., Tan, T. W., and Liu, Y. (2017). "Orientation transitions during the growth of imine covalent organic framework thin films." Journal of Materials Chemistry C, 5(21), 5090-5095.

Wang, L., Pollard, M. E., Klaus Juhl, M., Conrad, B., Soeriyadi, A., Li, D., Lochtefeld, A., Gerger, A., Bagnall, D. M., Barnett, A., and Perez-Wurfl, I. (2017). "Spectral response of steady-state photoluminescence from GaAs1-xPx layers grown on a SiGe/Si system." Applied Physics Letters, 111(12).

Wang, P., Iles, G. N., Mole, R. A., Yu, D., Wen, X., Aguey-Zinsou, K. F., Shrestha, S., and Conibeer, G. (2017). "Hot carrier transfer processes in nonstoichiometric titanium hydride." Japanese Journal of Applied Physics, 56(8).

Wang, Q., Lyu, M., Zhang, M., Yun, J. H., and Wang, L. (2017). "Configuration-centered photovoltaic applications of metal halide perovskites." Journal of Materials Chemistry A, 5(3), 902-909.

Wang, S., Mai, L., Wenham, A., Hameiri, Z., Payne, D., Chan, C., Hallam, B., Sugianto, A., Chong, C. M., Ji, J., Shi, Z., and Wenham, S. (2017). "Selective emitter solar cell through simultaneous laser doping and grooving of silicon followed by self-aligned metal plating." Solar Energy Materials and Solar Cells, 169, 151-158.

Wang, Y., Chen, J., Jiang, L., Liu, F., Lai, Y., and Li, J. (2017). "Characterization of Bi2S3 thin films synthesized by an improved successive ionic layer adsorption and reaction (SILAR) method." Materials Letters, 209, 479-482.

Wang, Y., Jiang, L., Chen, J., Liu, F., and Lai, Y. (2017). "Realization of nanostructured N-doped p-type Bi2S3 thin films." Materials Letters, 193, 228-231.

Wang, Y., Jiang, L., Liu, Y., Tang, D., Liu, F., and Lai, Y. (2017). "Facile synthesis and photoelectrochemical characterization of

Sb2O3 nanoprism arrays." Journal of Alloys and Compounds, 727, 469-474.

Wright, M., Lin, R., Tayebjee, M. J. Y., and Conibeer, G. (2017). "Effect of Blend Composition on Bulk Heterojunction Organic Solar Cells: A Review." SOLAR RRL, 1(3-4).

Wu, N., Wu, Y., Walter, D., Shen, H., Duong, T., Grant, D., Barugkin, C., Fu, X., Peng, J., White, T.P., Catchpole, K.R., and Weber, K.J., (2017). "Identifying the cause of voltage and fill factor losses in perovskite solar cells using luminescence measurements", Energy Technology Vol. 5, pp. 1827 – 1835.

Wu, W., Chen, D., Li, F., Pascoe, AR., Cheng, YB., Caruso, RA., "Integrated Planar And Bulk Dual Heterojunctions Capable Of Efficient Electron And Hole Extraction For Perovskite Solar Cells With >17% Efficiency", Nano Energy, 32, 187-194, 2017

Wu, W., Chen, D., McMaster, WA., Cheng, YB., Caruso, RA., "Solvent-Mediated Intragranular-Coarsening Of Ch3NH3PbI3 Thin Films Toward High-Performance Perovskite Photovoltaics", ACS Applied Materials And Interfaces, 9 (37), 31959-31967, 2017

Wu, Y., Yan, D., Peng, J., Duong, T., Wan, Y., Pheng Phang, S., Shen, H., Wu, N., Barugkin, C., Fu, F., Surve, S., Grant, D., Walter, D., White, T.P., Catchpole, K.R., and Weber, K.J, "Monolithic perovskite/silicon-homojunction tandem solar cell with over 22% efficiency," Energy and Environ. Sci. 10, 2472 – 2479,.

Xia, H., Patterson, R., Smyth, S., Feng, Y., Chung, S., Zhang, Y., Shrestha, S., Huang, S., Uchiyama, H., Tsutsui, S., Sugiyama, M., Baron, A. Q. R., and Conibeer, G. (2017). "Inelastic X-ray scattering measurements of III-V multiple quantum wells." Applied Physics Letters, 110(4).

Yan, C., Sun, K., Huang, J., Johnston, S., Liu, F., Veettil, B. P., Sun, K., Pu, A., Zhou, F., Stride, J. A., Green, M. A., and Hao, X. (2017). "Beyond 11% Efficient Sulfide Kesterite Cu2ZnxCd1–xSnS4 Solar Cell: Effects of Cadmium Alloying." ACS Energy Letters, 2(4), 930-936.

Yan, C., Sun, K., Liu, F., Huang, J., Zhou, F., and Hao, X. (2017). "Boost Voc of pure sulfide kesterite solar cell via a double CZTS layer stacks." Solar Energy Materials and Solar Cells, 160, 7-11.

Yang, J., Chen, W., Wang, B., Zhang, Z., Huang, S., Shrestha, S., Wen, X., Patterson, R., and Conibeer, G. "Selective optical contacting for solar spectrum management.", Proc. SPIE 10099, Physics, Simulation, and Photonic Engineering of Photovoltaic Devices VI, 1009917 (23 February 2017); doi: 10.1117/12.2251197

Yang, J., Li, Y., Zhang, K., Yuan, T., Jiang, L., Liu, F., Lai, Y., and Li, J. (2017). "Preparation and photovoltaic characterization of Cu2ZnSnS4 thin films fabricated by electrodeposition of alloy precursor followed by annealling." Zhongnan Daxue Xuebao (Ziran Kexue Ban)/Journal of Central South University (Science and Technology), 48(4), 917-924.

Yang, J., Wen, X., Xia, H., Sheng, R., Ma, Q., Kim, J., Tapping, P., Harada, T., Kee, T. W., Huang, F., Cheng, Y. B., Green, M., Ho-Baillie, A., Huang, S., Shrestha, S., Patterson, R., and Conibeer, G. (2017). "Acoustic-optical phonon up-conversion and hot-phonon bottleneck in lead-halide perovskites." Nature Communications, 8.

Yang, T. C. J., Nomoto, K., Puthen-Veettil, B., Lin, Z., Wu, L., Zhang, T., Jia, X., Conibeer, G., and Perez-Wurfl, I. (2017). "Properties of silicon nanocrystals with boron and phosphorus doping fabricated via silicon rich oxide and silicon dioxide bilayers." Materials Research Express, 4(7).

Yang, X., Weber, K., Hameiri, Z., and De Wolf, S. (2017). "Industrially feasible, dopant-free, carrier-selective contacts for high-efficiency silicon solar cells." Progress in Photovoltaics: Research and Applications, 11, 896-904.

Yang, Y., Wen, X., Xia, H., Sheng, R., Ma, Q., Kim, J., Tapping, P., Harada, T., Kee, TW., Huang, F., Cheng, YB., Green, M., Ho-Baillie, A., Huang, S., Shrestha, S., Patterson, R., Conibeer, G., "Acoustic-Optical Phonon Up-Conversion And Hot-Phonon Bottleneck In Lead-Halide Perovskites", Nature Communications, 8, 2017

Yuan, L., Patterson, R., Wen, X., Zhang, Z., Conibeer, G., and Huang, S. (2017). "Investigation of anti-solvent induced optical properties change of cesium lead bromide iodide mixed perovskite ($CsPbBr_{3-x}I_x$) quantum dots." Journal of Colloid and Interface Science, 504, 586-592.

Zarrabi, N., Stoltzfus, D. M., Burn, P. L., and Shaw, P. E., (2017). "Charge Generation in Non-Fullerene Donor–Acceptor Blends for Organic Solar Cells", The Journal of Physical Chemistry C, 121, 18412–18422.

Zhang, B., Soleimaninejad, H., Jones, D. J., White, J. M., Ghiggino, K. P., Smith, T. A., Wong, W. W. H., (2017). "Highly fluorescent molecularly insulated perylene diimides: effect of concentration on photophysical properties" Chem. Mater., 29 (19), 8395-8403. DOI: 10.1021/acs.chemmater.7b02968

Zhang, C., Kim, Y., Faleev, N. N., and Honsberg, C. B. (2017). "Improvement of GaP crystal quality and silicon bulk lifetime in GaP/Si heteroepitaxy." Journal of Crystal Growth, 475, 83-87.

Zhang, M., Yun, J. S., Ma, Q., Zheng, J., Lau, C. F. J., Deng, X., Kim, J., Kim, D., Seidel, J., Green, M. A., Huang, S., and Ho-Baillie, A. W. Y. (2017). "High-Efficiency Rubidium-Incorporated Perovskite Solar Cells by Gas Quenching." ACS Energy Letters, 2(2), 438-444.

Zhang, Q., Gu, X., Chen, Z., Jiang, J., Zhang, Z., Wei, J., Li, F., Jin, X., Song, Y., and Li, Q. (2017). "Enhancing extraction efficiency of quantum dot light-emitting diodes by surface engineering." Optics Express, 25(15), 17683-17694.

Zhang, Q., Nie, C., Chang, C., Guo, C., Jin, X., Qin, Y., Li, F., and Li, Q. (2017). "Highly luminescent red emitting CdZnSe/ZnSe quantum dots synthesis and application for quantum dot light emitting diodes." Optical Materials Express, 7(11).

Zhang, Z., Chen, Z., Yuan, L., Chen, W., Yang, J., Wang, B., Wen, X., Zhang, J., Hu, L., Stride, J. A., Conibeer, G. J., Patterson, R. J., and Huang, S. (2017). "A New Passivation Route Leading to Over 8% Efficient PbSe Quantum-Dot Solar Cells via Direct Ion Exchange with Perovskite Nanocrystals." Advanced Materials, 29(41).

Zhang, Z., Huang, Y., Reece, P. J., and Bremner, S. P. (2017). "Influence of GaAsSb structural properties on the optical properties of InAs/GaAsSb quantum dots." Physica E: Low-Dimensional Systems and Nanostructures, 94, 7-14.

Zhang, Z., Tan, S., Kim, Y., Liu, Z., Reece, P. J., and Bremner, S. P. (2017). "Effect of Sb and As spray on emission characteristics of InAs quantum dots with AlAs capping layer." Journal of Physics D: Applied Physics, 50(40).

Zhao, X., Li, D., Zhang, T., Conrad, B., Wang, L., Soeriyadi, A. H., Han, J., Diaz, M., Lochtefeld, A., Gerger, A., Perez-Wurfl, I., and Barnett, A. (2017). "Short circuit current and efficiency improvement of SiGe solar cell in a GaAsP-SiGe dual junction solar cell on a Si substrate." Solar Energy Materials and Solar Cells, 159, 86-93.

Zheng, J., Zhang, M., Lau, C. F. J., Deng, X., Kim, J., Ma, Q., Chen, C., Green, M. A., Huang, S., and Ho-Baillie, A. W. Y. (2017). "Spin-coating free fabrication for highly efficient perovskite solar cells." Solar Energy Materials and Solar Cells, 168, 165-171.

Zheng, P., Rougieux, F. E., Zhang, X., Degoulange, J., Einhaus, R., Rivat, P., and Macdonald, D. H., (2017). "21.1% UMG silicon solar cells", IEEE Journal of Photovoltaics, 7, 58-61.

Zhu, B. L., Liu, F., Li, K., Lv, K., Wu, J., Gan, Z. H., Liu, J., Zeng, D. W., and Xie, C. S. (2017). "Sputtering deposition of transparent conductive F-doped SnO2 (FTO) thin films in hydrogen-containing atmosphere." Ceramics International, 43(13), 10288-10298.

Zhu, Y., Juhl, M. K., Trupke, T., and Hameiri, Z. (2017). "Photoluminescence imaging of silicon wafers and solar cells with spatially inhomogeneous illumination." IEEE Journal of Photovoltaics.

Zhu, Y., Le Gia, Q. T., Juhl, M. K., Coletti, G., and Hameiri, Z. (2017). "Application of the Newton–Raphson method to lifetime spectroscopy for extraction of defect parameters." IEEE Journal of Photovoltaics, 7, 4, 1092-1097.

8.5 Conference Papers and Presentations

Angmo, D., "Organic-based Non-fullerene Charge-transport Layer towards Upscaling of Perovskite Solar Cells", 5th ACAP Conference and 4th Asia Pacific Solar Research Conference, Melbourne, Dec 5-7, 2017.

Bach, U., "Back-Contact Dye-Sensitized and Perovskite Solar Cells", HOPV17, Japan, February 2017

Bach, U., "Back-Contact Perovskite Solar Cells", ANFF Showcase, Sydney, November 2017

Bach, U., "Back-Contact Perovskite Solar Cells", CCCF 2017 Conference, Gold Coast, July 2017

Bach, U., "Back-Contact Perovskite Solar Cells", EMRS Conference, Poland, September 2017

Bach, U., "Back-Contact Perovskite Solar Cells", UQ Conference, Brisbane, August 2017

Bach, U., "Characterisation of CH3NH3PbI3 Perovskite Solar Cells by TEM", Helmholtz Berlin, Germany, May 2017

Bach, U., "Dipole-Field-Assisted Charge Extraction in Schottky Junction Perovskite Solar Cells", HOPV Lausanne, Switzerland, May 2017

Bach,U., "Novel Redox Mediators for Dye-Sensitized Solar Cells", ACCC6 Conference, Melbourne, July 2017

Basnet, R., Rougieux .F.E. and Macdonald, D., "Impact of firing temperatures on hydrogen passivation of ring defects in Czochralski silicon", 27th International Photovoltaic Science and Engineering Conference, Shiga, Japan, 2017.

Basnet, R., Rougieux, F.E., Nguyen, H.T., and Macdonald, D., "Investigating relationship between local oxygen precipitates and their recombination activities in n-type Cz silicon", 27th International Photovoltaic Science and Engineering Conference, Shiga, Japan, November 12-17, 2017

Basnet, R., Rougieux, F.E., Nguyen, H.T., and Macdonald, D., "Investigating relationship between local oxygen precipitates and their recombination activities in n-type Cz silicon", 4th Asia Pacific Solar Research Conference, Melbourne, December 5-7, 2017

Bhoopathy, R., Kunz, Juhl, trupke, and Hameiri, Z., "Outdoor photoluminescence measurements of photovoltaic modules under full sunlight illumination", 27th International Photovoltaic Science and Engineering Conference, Shiga, Japan, 2017.

Burn, P.L., "A computational approach to elucidating the film structure in organic semiconducting films", Mainz, Germany, 8 September 2017.

Burn, P.L., "Interlayer engineering for high Voc perovskite solar cells", International Conference on Solution Processed Innovative Solar Cells (SPINS17), Barcelona, Spain, September 4-8 2017.

Burn, P.L., "Interlayer engineering for high Voc perovskite solar cells", SPIE, San Diego, USA, 6 – 10 August 2017.

Chen, Z., Zhang, Z., Patterson, R., Conibeer, G. and Huang, S., "Optimizing the Front Contacts of PbSe Quantum Dot Solar Cell with Additional Au Grids", 27th International Photovoltaic Science and Engineering Conference, Shiga, Japan, 2017.

Cheng, YB., "High efficiency perovskite solar cells – processing, microstructures and properties", 11th Aseanian Conf on Nano-Hybrid Solar cells, Himeiji, Japan, October 2017

Cheng, YB., "Microstructure studies of hybrid perovskite solar cells", HOPV 17, Japan, February 2017

Cheng, YB., "Perovskite Solar Cells", Australia-China Forum on Advanced Materials and Manufacturing, Sydney, October 2017

Cheng, YB., "Perovskite Solar Cells", Kyoto University, Japan, October 2017

Cheng, YB., "Printing of Solar Cells", National Institute of Clean Energy, China, August 2017

Chin, R.L., Pollard, M., Trupke, T., Hameiri, Z., "Selectively probing surface and bulk carrier dynamics in semiconductors via two-photon photoluminsescence", 27th International Photovoltaic Science and Engineering Conference, Shiga, Japan, 2017.

Chong, C.M. and Wenham, S.R., " Eliminating B-O CID in Commercial Solar Cells with Industrial Hydrogenation Tools", 33rd European Photovoltaic Solar Energy Conference, Amsterdam, The Netherlands, 2017.

Ciesla, A., Chen, D., Chan, C., Payne, D., Zafirovska, I., Sen, C., Colwell, J., Hallam, B., Chen, R., Abbott ,M., Wenham, S.R., Chong, C.M.and Bourret-Sicotte, G., "New Insight into LID in Multi-PERC Solar Cells and Modules", 33rd European Photovoltaic Solar Energy Conference, Amsterdam, The Netherlands, 2017.

Concha-Ramon, B., Keevers, M.J., Jiang, Y. and Green, M.A., "A One-Sun Spectrum-Splitting Minimodule Using Prismatic Encapsulation: Simulation and Outdoor Testing", 33rd European Photovoltaic Solar Energy Conference, Amsterdam, The Netherlands, 2017.

Conibeer, G., Zhang, Y., Bremner, S., and Shrestha, S., "Hot carrier cooling mechanisms in multiple quantum wells." SPIE Proceedings 10099, Physics, Simulation, and Photonic Engineering of Photovoltaic Devices VI, 2017, 100990K, doi: 10.1117/12.2251927.

Conibeer, G.J., Perez-Wurfl, I. and Puthen-Veetil, B., "Silicon Quantum Dot Nanostructures as Passivating Contacts for Carrier Selective Contact Cells", 33rd European Photovoltaic Solar Energy Conference, Amsterdam, The Netherlands, 2017.

Corkish, R., "Australia-US Institute for Advanced Photovoltaics & Australian Centre for Advanced Photovoltaics", University of Delaware, 20 June 2017.

Dumbrell, R. W., Juhl, M. K., Li, M., Trupke, T., and Hameiri, Z., "Metal induced contact recombination measured by quasi-steady-state photoluminescence." 44th IEEE Photovoltaic Specialists Conference, Washington, DC., 2017.

Dumbrell, R. W., Juhl, M. K., Trupke, T., and Hameiri, Z., "On the use of voltage measurements for determining carrier lifetime at high illumination intensity." 44th IEEE Photovoltaic Specialists Conference, Washington, DC., 2017.

Ekins-Daukes, N., Phillips, C., Pusch, A., Vaquero, A., Yoshida, M. and Schmidt, T., "THE Role of ratchets in photovoltaics ", 27th International Photovoltaic Science and Engineering Conference, Shiga, Japan, 2017.

Ernst, M., Franklin, E., Chong, T.K., Wang, E.C., Fong, K.C., Kho, T. and Blakers, A., "High Efficiency Locally Laser Doped IBC Solar Cells", 33rd European Photovoltaic Solar Energy Conference, Amsterdam, The Netherlands, 2017.

Fell, A., Glunz, S.W., and Walter, D., "A Fast and Easy Perovskite Solar Cell Simulation Tool Featuring Ion Migration", 33rd European Photovoltaic Solar Energy Conference, Amsterdam, The Netherlands, 2017.

Fu, X., and White, T. P., "Investigating transient recombination in perovskite film and extracting material properties by fitting steady-state PL and transient PL," 3rd International Conference on Perovskite Solar Cells and Optoelectronics (PSCO2017), Oxford, UK, Sept 2017.

Fung, T. H., Chan, C. E., Hallam, B. J., Payne, D. N. R., Abbott, M. D., and Wenham, S. R.,. "Impact of annealing on the formation and mitigation of carrier-induced defects in multi-crystalline silicon." Energy Procedia, 124, September 2017, Pages 726-733

Fung, T.H., "Impact of Annealing on the Formation and Mitigation of Carrier-induced Defects in Multi-crystalline Silicon", 7th International Conference on Silicon Photovoltaics, SiliconPV 2017, 3-5 April 2017, Freiburg, Germany

Gao, M., "Highly Efficient Perovskite Solar Cells via Roll-to-Roll Process", 5th ACAP Conference and 4th Asia Pacific Solar Research Conference, Melbourne, Dec 5-7, 2017 .

Geraghty, P., Wang, H., Lee, C., Jegadesan Subbiah, J. and Jones, D. "High performance molecular donors for organic solar cells, materials design and device optimization" 2017, IEEE PVSC-44, Washington DC., 2017 .

Ghiggino, K., "Light harvesting and energy conversion in organic photovoltaic materials", RACI South Australia Physical Chemistry Symposium, Adelaide, November 24, 2017.

Ghiggino, K., "Photon harvesting and concentration for solar energy conversion", Thin Films and Photonics and Organic Electronics Interdisciplinary Workshop, Shandong University, Jinan, China, September 26-27, 2017.

Ghiggino, K., Banal, J., Zhang,B. and W. Wong, W., "Concentration quenching resistant fluorophores for light concentration", 15th Conference on Methods and Applications of Fluorescence (MAF2017), Bruges, Belgium, September 10-13, 2017.

Ghiggino, K., K. Schwarz, K. and Smith, T., "Ultrafast spectroscopy of charge generation in organic photovoltaic materials", RACI Centenary Congress, Melbourne, July 23-28, 2017.

Green, M.A. and Ho-Baillie, A.W.Y., "Progress with Perovskite/Silicon and All-Perovskite Tandem Solar Cells", 33rd European Photovoltaic Solar Energy Conference, Amsterdam, The Netherlands, 2017.

Green, M.A., 2017, "Current Status and Future Prospects of Photovoltaic Research and Technology", invited keynote talk, GADEST 2017, Lopota Resort, Georgia, 1-6 October 2017.

Green, M.A., 2017, "How did silicon solar cells get so cheap", Commonwealth Science Conference, Singapore, 13-16 June 2017.

Green, M.A., 2017, "Overview of Photovoltaics: Where Might Perovskites Make Impact?", Tutorial, 3rd International Conference on Perovskite Solar Cells & Optoelectronics (PSCO-2017), Oxford, UK, 18-20 September 2017.

Green, M.A., 2017, "Photovoltaics: Global Green Energy Applications and Future Perspectives", Invited keynote talk, International Green Energy Development Conference, Yangzhong City, China, 16 September 2017.

Green, M.A., 2017, "Photovoltaics: Recent Progress and Future Prospects", Plenary talk, 2017 Asia-Pacific Solar Research Conference, Melbourne, 5-7 December 2017.

Green, M.A., 2017, "Silicon Solar Cells: What Comes After PERC?", Invited Keynote talk, World Solar Congress, Shanghai, 5-6 September 2017.

Green, M.A., 2017, "Tandem Perovskite Solar Cells: Challenges and Progress", invited keynote talk, AP-HOPV Conference, Yokohama, Japan, 2-4 February 2017.

Green, M.A., 2017, "UNSW PV Impact", Solar Asia Summit, Sydney, 27 April 2017.

Green, M.A., 2017, "UNSW PV Research and Collaboration Opportunities", Seminar, China Electronics Technology Group Corporation (CETC), Tianjin, 11 September, 2017.

Green, M.A., and Ho-Baillie, A.W.Y., 2017, "Progress with Perovskite/Silicon and All-Perovskite Tandem Solar Cells", 3CP.1.4, 33rd European Photovoltaic Solar Energy Conference, Amsterdam, 25-29 September 2017.

Haedrich, I., Thomson, A., Ernst, M., Macdonald, D., Zheng, P., Zhang, X. and Jin, H., "How Cell Texturing Impacts Annual Yield of Solar Modules and the Role of Module Embedding", 33rd European Photovoltaic Solar Energy Conference, Amsterdam, The Netherlands, 2017.

Hallam, B., "New Insights into Boron-oxygen Related Degradation", 7th International Conference on Silicon Photovoltaics, SiliconPV 2017, 3-5 April 2017, Freiburg, Germany

Hallam, B., Chan, C., Chen, R., Wang, S., Ji, J., Mai, L., Abbott, M., Kim, M., Chen, D.,

Jacobs, D., Pfeffer, F., Shen, H., Peng, J., Beck, F., White, T., and Catchpole, K., "Impedance Spectroscopy for Perovskite Cells: Utility and Interpretation,", 3rd International Conference on Perovskite Solar Cells and Optoelectronics (PSCO2017), Oxford, UK, Sept 2017.

Jensen, M., Zhu, Y., Looney, E., Morishige, A., Castrillon, C., Hameiri, Z., and Buonassisi, T. (2017). "Assessing the defect responsible for LeTID: Temperature- and injection-dependent lifetime spectroscopy." 44th IEEE Photovoltaic Specialists Conference, Washington, DC.

Jensen, M., Zhu, Y., Nakajima, K., Juhl, M. K., Youssef, E., Looney, E. E., Hameiri, Z., Sander, R., and Buonassisi, T. (2017). "Defect engineering for material-quality improvements in low-capex crystalline silicon—an application of temperature- and injection-dependent lifetime spectroscopy." MRS Fall Meeting, Boston.

Jiang, Y., Keevers, M.J., Green, M.A., (2017). "Design of Bragg Reflectors in III-V Solar Cells for Spectrum Splitting to Si", Proceedings of the Asia Pacific Solar Research Conference 2017, Australian PV Institute, Dec 2017, ISBN: 978-0-6480414-1-2.

Jin, H., "Efficient Small Molecule Organic Photovoltaic Cells on Single Layer Graphene Transparent Conductive Electrodes", 2017 ANFF & AMMRF Research Showcase - Make & Measure, Camperdown, Sydney, NSW, Australia, November 2017.

Jin, H., "Graphene anodes for thin film organic solar cells", 5th ACAP Conference, Melbourne, Victoria, Australia, December 2017.

Jin, H., "Graphene anodes for thin film organic solar cells", Inaugural Australasian Community for Advanced Organic Semiconductors (AUCAOS) Symposium, Kingscliff, New South Wales, Australia, December 2017

Jones, D. "High Performance Molecular Donors for Printed OPV-Synthesis and Scale-up", Materials Research Society (MRS) Meeting, Phoenix, Az. 17-21 April 2017.

Jones, D. “Molecular donors for high performance organic solar cells“, Georgia Institute of Technology, Feb 2017.

Jones, D. “Molecular donors for high performance organic solar cells”, 13th International Conference on Materials Chemistry (RCS MC13), Liverpool, UK. 12 July 2017.

Jones, D. “Side-Chain Engineering in High Performance p-Type Organic Semiconductors for Printed OPV”, University of St Andrews, 14th July 2017.

Juhl, M.K., Pollard, M.E., Paduthol, A.R., Trupke, T. and Hameiri, Z., “Contactless Determination of Dielectric Absorption from the Spectral Response of Photoluminescence”, 33rd European Photovoltaic Solar Energy Conference, Amsterdam, The Netherlands, 2017.

Kho, T., “ONO for Silicon Solar Cell”, 7th International Conference on Silicon Photovoltaics, SiliconPV 2017, 3-5 April 2017, Freiburg, Germany

Kim, J., “Effect of substrate and solution temperatures on morphology and performance of slot die coated perovskite solar cells”, 5th ACAP Conference and 4th Asia Pacific Solar Research Conference, Melbourne, Dec 5-7, 2017.

Kim, M., Chen, D., Abbott, M., Wenham, S. and Hallam, B., “Investigating the Influence of Interstitial Iron on the Study of Boron-Oxygen Defects”, 33rd European Photovoltaic Solar Energy Conference, Amsterdam, The Netherlands, 2017.

Lan, D. and Green, M.A., “Detailed Investigation of a GaInP/GaAs/Ge Up-Conversion System: Efficiency Loss Analysis and Possible Route to Improvement”, 33rd European Photovoltaic Solar Energy Conference, Amsterdam, The Netherlands, 2017.

Lee Chin, R. A., Pollard, M., Trupke, T., and Hameiri, Z., “Numerical Modeling of Two-photon Photoluminescence in Semiconductors for Probing Bulk and Surface Kinetics.” 27th International Photovoltaic Science and Engineering Conference, Japan, 2017.

Lee, C.-Y., Zhang, T., Khoo K., Hoex, B., Abdallah, A.A., Rashkeev, S. and Tabet, N., “Thermal Stability of Novel Hole-Selective Contacts for Silicon Wafer Solar Cells”, 33rd European Photovoltaic Solar Energy Conference, Amsterdam, The Netherlands, 2017.

Li, H., Ma, F. J., Hameiri, Z., Wenham, S., and Abbott, M., “Towards “defect-free” n-type emitters using oxygen during POCl3 diffusion.” 33rd European Photovoltaic Solar Energy Conference and Exhibition, Amsterdam, 2017.

Li, H., Ma, F.-J., Hameiri, Z., Wenham, S.R. and Abbott, M., “Towards “Defect-Free” n-Type Emitters Using Oxygen during POCl3 Diffusion”, 33rd European Photovoltaic Solar Energy Conference, Amsterdam, The Netherlands, 2017.

Li, M., Stangl, R, Aberle, A.G., Ma, F.-J., Hoex, B. and Samudra, G.S., “Investigation on the Ag-Al Metal Spiking into Boron-Diffused p+ Layer of Industrial Bifacial n-Type Silicon Wafer Solar Cells by Numerical Simulation”, 33rd European Photovoltaic Solar Energy Conference, Amsterdam, The Netherlands, 2017.

Liao, A., Western, N.J. and Bremner, S.P., “Full Area Emitter IBC Cells Fabricated with Point-Contacting by Localized Dielectric Breakdown”, 33rd European Photovoltaic Solar Energy Conference, Amsterdam, The Netherlands, 2017.

Lunardi, M.M., Alvarez-Gaitan, J.P., Chang, N.L. and Corkish, R., “Life Cycle Assessment of Hydrogenation Processes on Silicon Solar Modules”, 7th World Conference on Photovoltaic Energy Conversion, 10 -15 June 2018, Waikoloa, Hawaii (manuscript submitted)

Lunardi, M.M., Alvarez-Gaitan, J.P., Chang, N.L., Moore, S., Corkish, R., “Life Cycle Assessment on of Advanced Silicon Solar Cells”, Proceedings of the Asia Pacific Solar Research Conference 2017, Australian PV Institute, Dec 2017, ISBN: 978-0-6480414-1-2.

Lunardi, M.M., Moore, S., Alvarez-Gaitan, J.P., Yan, C., Hao, X., Corkish, R., “A Comparative Life Cycle Assessment of CIGS/Si, CZTS/Si and AZTS/Si Tandem Solar Cells”, 33rd European Photovoltaic Solar Energy Conference (EU PVSEC 2017) , Amsterdam, 25 - 29 September 2017., Amsterdam

McGregor, S.K.M., “Investigating the Relationship between Phase Behaviour and Photovoltaic Performance”, 2nd Queensland Annual Chemistry Symposium, Organic and Medicinal Chemistry, Queensland University of Technology, Brisbane, Australia, December 2017.

McGregor, S.K.M., “Investigating the Relationship between Phase Behaviour and Photovoltaic Performance”, Inaugural Australian Community for Advanced Organic Semiconductors Symposium, Kingscliff, Australia, December 2017.

McGregor, S.K.M., “Organic semiconductors for thin film photovoltaic devices”, Asia Pacific Solar Research Conference, Australian Centre for Advanced Photovoltaics (ACAP), Monash University, Melbourne, December 2017.

Nampalli, N., “ Multiple Pathways for Permanent Deactivation of Boron-oxygen Defects in p-Type Silicon”, 7th International Conference on Silicon Photovoltaics, SiliconPV 2017, 3-5 April 2017, Freiburg, Germany

Nguyen, H. T., and Macdonald, D., “Detection of diffused dopants in silicon wafers using micro photoluminescence spectroscopy,” 26th Workshop on Crystalline Silicon Solar Cells and Modules: Materials and Processes, Vail, USA, July 30 – August 2, 2017

Nguyen, H. T., Jensen, M. A., Li, L., Samundsett, C., Sio, H. C., Lai, B., Buonassisi, T., and Macdonald, D., “Microscopic distribution of luminescence from dislocation clusters in multicrystalline silicon wafers,” 44th IEEE Photovoltaic Specialists Conference, Washington, USA, June 25-30, 2017

Nie, S., Zhu, Y., Bernardini, S., Bertoni, M., Hameiri, Z., “Advanced temperature-dependent characterization of silicon nitride surface passivation layer”, 27th International Photovoltaic Science and Engineering Conference, Shiga, Japan, 2017.

Paduthol, A.R., Juhl, M.K., Hameiri, Z., Trupke, T., Nogay, G. and Löper, P., “Efficient carrier injection from amorphous silicon into crystalline silicon determined from photoluminescence”, 33rd European Photovoltaic Solar Energy Conference, Amsterdam, The Netherlands, 2017. (EU PVSEC Student Award Winner)

Payne, D., Claville Lopez, A., Zeng, Y., Bagnall, D.M., Abbott, M.D., McIntosh. K.R., Cruz-Campa, J., Schmidt, R.D. and Plakhotnyuk, M., “Rapid Optical Modelling of Plasma Textured Silicon”, 33rd European Photovoltaic Solar Energy Conference, Amsterdam, The Netherlands, 2017.

Peng, X., “Fully Printed/Coated, ITO-free Perovskite Solar Cells under Ambient Conditions”, 5th ACAP Conference and 4th Asia Pacific Solar Research Conference, Melbourne, Dec 5-7, 2017.

Raynor, A., “NDI and its uses within all polymer solar cells”, Australasian Community for Advanced Organic Semiconductors Symposium, Kingscliff, Australia, December 2017.

Römer, U Nie, S., Zhu, Y., Bernardini, S., Bertoni, M., and Hameiri, Z., “Advanced temperature charctrisation of silicon nitride surface passivation layer.” Presented at 27th International Photovoltaic Science and Engineering Conference, Japan 2017.

Römer, U., “Decoupling the Metal Layer of Back Contact Solar Cells – Optical and Electrical Benefits”, 7th International Conference on Silicon Photovoltaics, SiliconPV 2017, 3-5 April 2017, Freiburg, Germany

Rougieux, F., Nguyen, H.T., Macdonald, D., Mitchell, B., and Falster R., “Oxygen Precipitates in Czochralski Silicon: Influence of Growth Conditions on the Minority Carrier Lifetime”, 33rd European Photovoltaic Solar Energy Conference, Amsterdam, The Netherlands, 2017.

Saker Neto, N., Wong, W.W.H., Jones, D.J., “Monodisperse Conjugated Polymer Synthesis using Exponential Iterative Coupling”, AUCAOS Symposium, December 4-6, 2017.

Shen, H., Duong, T., Karuturi, S., Wu, N., Peng, J., Fu, X., Wu, Y., Weber, K., White, T. P., and Catchpole, K. R., “Compositional Engineering of Multi-cation - High Bandgap Perovskite Enables Perovskite-CIGS Tandem with Efficiency Approaching 24%,” 3rd International Conference on Perovskite Solar Cells and Optoelectronics (PSCO2017), Oxford, UK, Sept 2017.

Shi, J., Pollard, M. E., Gates, J., and Charlton, M.D.B. (2017) “Design and fabrication quasiperiodic photonic crystals for simultaneous slab waveguide coupling and splitting.” Conference on Lasers and Electro-Optics OSA Technical Digest (Optical Society of America, 2017), paper JW2A.130, https://doi.org/10.1364/CLEO_AT.2017.JW2A.130.

Shi, J., Pollard, M. E., Wang, Z. L., Wilkinson, J., and Charlton, M.D.B. (2017). “Photonic crystal slab sensor for monolayer detection.” Conference on Lasers and Electro-Optics OSA Technical Digest (Optical Society of America, 2017), paper JTu5A.8 https://doi.org/10.1364/CLEO_AT.2017.JTu5A.8.

Shi, L., Keevers, M., Hao, X., Ho-Baillie, A., Young, T., Green, M., “Accelerated lifetime testing of organic-inorganic perovskite solar cells encapsulated by low cost Polyisobutylene based polymer”, 27th International Photovoltaic Science and Engineering Conference, Shiga, Japan, 2017.

Song, N., Li, Z., Li, Y., Zhang, X., Shengzhao, Y., Verlinden, P. J., and Lennon, A. (2017) “Decoupling the metal layer of back contact solar cells - Optical and electrical benefits.” Energy Procedia 124, 907-913.

Subbiah,J., Mitchell, V. D., Wong, W.W.H. and Jones, D. “Organic Nanostructured metal oxide interlayer for efficient organic and perovskite solar cells”, 9th International conference on Materials for Advanced Technologies (ICMAT-2017), 18-23, June 2017, Singapore, 2017.

Subbiah,J., Geraghty, P., Mitchell, V.D., Wong, W.W.H. and Jones, D.J., “High performance ternary blend organic solar cells using conjugated polymer and molecular materials”, 254th ACS National Meeting, August 20-24, 2017, Washington, DC, USA.

Sun, K., Huang, J., Yan, C., Liu, F., Hao X. and Green, M.A., 2017 “New Strategy to Deal with the Interface Problem - Improving Pure Sulfide Cu2ZnSnS4 Solar Cell towards 10% Efficiency”, 3BO.11.2, 33rd European Photovoltaic Solar Energy Conference, Amsterdam, 25-29 September 2017.

Sun, K., Huang, J., Yan, C., Liu, F., Hao, X., Green, M.A. and Johnson, S.W., “New Strategy to Deal with the Interface Problem - Improving Pure Sulfide Cu2ZnSnS4 Solar Cell towards 10% Efficiency”, 33rd European Photovoltaic Solar Energy Conference, Amsterdam, The Netherlands, 2017.

To, A., “Exploiting Bifacial Deposition of ALD AlOx for p-Type PERC Solar Cells”, 7th International Conference on Silicon Photovoltaics, SiliconPV 2017, 3-5 April 2017, Freiburg, Germany

To, A., Min Li, W., Li, X., and Hoex, B. (2017). “The effects of bifacial deposition of ALD AlOx on the contact properties of screen-printed contacts for p-type PERC solar cells.” Energy Procedia 124, 914-921 DOI: 10.1016/j.egypro.2017.09.291.

Vak, D. “Hot slot die coating for high performance roll-to-roll produced organic photovoltaic devices”, Australasian Community for Advanced Organic Semiconductors (AUCAOS) symposium, Kingscliff, Dec 4-6, 2017.

Vak, D. “Organic-Inorganic Hybrid Perovskites: Drop-In Replacement of Organic Based Photoactive Materials in Printed Solar Films?”, 4th International Conference on Perovskite Solar Cells and Optoelectronics (PSCO), Oxford, 18-20, Sep 2017.

Vak, D., “Hot Slot Die Coating for Organic and Perovskite Solar Cells”, 5th ACAP Conference and 4th Asia Pacific Solar Research Conference, Melbourne, Dec 5-7, 2017.

Vargas Castrillon, C. A., Kim, K., Coletti, G., Payne, D. N. R., Chan, C., Wenham, S., and Hameiri, Z., (2017). “Influence of silicon nitride and its hydrogen content on carrier-induced degradation in multicrystalline silicon wafer.” 33rd European Photovoltaic Solar Energy Conference and Exhibition, Amsterdam, the Netherlands, 2017.

Vargas Castrillon, C., Kim, K., Payne, D., Chan, C., Wenham, S.R. and Hameiri Z. and Coletti, G., “Influence of Silicon Nitride and Its Hydrogen Content on Carrier-Induced Degradation in Multicrystalline Silicon”, 33rd European Photovoltaic Solar Energy Conference, Amsterdam, The Netherlands, 2017.

Wan, Y., “‘Mg’nificent Electron Contacts for n-Type Silicon Solar Cells: Metal, Oxide, and Fluoride”, 7th International Conference on Silicon Photovoltaics, SiliconPV 2017, 3-5 April 2017, Freiburg, Germany

Wang X., “ITO-free thin film solar cells”, 5th ACAP Conference, Melbourne, Victoria, Australia, December 2017.

Wang X., “ITO-free thin film solar cells”, Inaugural Australasian Community for Advanced Organic Semiconductors (AUCAOS) Symposium, Kingscliff, New South Wales, Australia, December 2017.

Wang, B., Patterson, R., Huang, S., Shrestha, S. and Conibeer, G., “Ab inition calculation of transport properties between PbSe quantum dots facets with halide ligands (CL, BR, I)”, 27th International Photovoltaic Science and Engineering Conference, Shiga, Japan, 2017.

Weerasinghe H., “Long-term Stable Roll-to-Roll Processed Organic Photovoltaic Modules”, 5th ACAP Conference and 4th Asia Pacific Solar Research Conference, Melbourne, Dec 5-7, 2017.

Weerasinghe H.,Dkhissi Y., Cheng Y., Youn-Jung, Vak D. “Organic and Perovskite-based Photovoltaics on Flexible substrates: Fabrication and Encapsulation”, EMN Americas Meetings (Energy Materials Nanotechnology), Florida, USA, Dec 4-8, 2017.

Western, N. and Bremner, S.P., “Preclusion of Light Induced Degradation in Multi-Crystalline by Low Temperature Metallization”, 33rd European Photovoltaic Solar Energy Conference, Amsterdam, The Netherlands, 2017.

Wilkinson, B.M.W. Green, M.A. and Ho-Baillie, A.W.Y. , “Scaling Limits to Large Area Perovskite Solar Cell Efficiency”, 3CO.4.1, 33rd European Photovoltaic Solar Energy Conference, Amsterdam, 25-29 September 2017.

Wilkinson, B.M.W., Green, M.A. and Ho-Baillie, A.W.Y., “Designing Highly Efficient Perovskite Solar Cells”, 33rd European Photovoltaic Solar Energy Conference, Amsterdam, The Netherlands, 2017.

Wilkinson, B.M.W., Green, M.A. and Ho-Baillie, A.W.Y., “Scaling Limits to Large Area Perovskite Solar Cell Efficiency”, 33rd

European Photovoltaic Solar Energy Conference, Amsterdam, The Netherlands, 2017.

Wilson, G., "Renewable Energy in CSIRO" 3rd Australia-Korea Joint Committee on Science and Technology (JCST), Seoul, South Korea, Apr 19, 2017.

Wilson, G., "Roll-to-roll printing of OPV and perovskites on flexible and rigid substrates" (Plenary talk), International Workshop for Piezoelectric Materials and Applications, 12th Annual Energy Harvesting Workshop, 1st Annual Energy Harvesting Society Meeting, Falls Church, Virginia, US, Sep 11-14, 2017.

Wong, W.W.H., "A Green Route to Conjugated Polyelectrolyte Interlayers for High Performance Solar Cells", 13th International Symposium on Functional Pi-Electron Systems, Hong Kong, June 4-9, 2017.

Wong, W.W.H., "Controlled Synthesis of Conjugated Polymers", PolymerVic, Melbourne, September 27-28, 2017.

Wong, W.W.H., "Light Harvesting using Emissive Aggregates", 9th International Conference on Materials for Advanced Technologies (ICMAT-2017), Singapore, June 18-23, 2017.

Wu, H., Nguyen, H.T. and Macdonald, D., "Reconstructing photoluminescence spectra from heavily doped regions of silicon solar cells",

Yang, X., Weber, K. and De Wolf, S., "Industrially feasible, dopant-free, carrier-selective contacts for high-efficiency crystalline silicon solar cells", 27th International Photovoltaic Science and Engineering Conference, Shiga, Japan, 2017.

Yang, X., Weber, K., Hameiri, Z., and De Wolf, S., "Industrially feasible dopant-free, carrier-selective passivating contacts for high-efficiency crystalline silicon solar cells." 27th International Photovoltaic Science and Engineering Conference, Japan, 2017.

Yang, Y., Liua, R., McIntosh, K.R., Abbott, M., Sudbury, B., Holovsky, J., Yea, F., Deng, W., Feng, Z., Verlinden, P.J. and Altermatt, P.P., "Combining ray tracing with device modeling to evaluate experiments for an optical analysis of crystalline Si solar cells and modules", 7th International Conference on Silicon Photovoltaics, SiliconPV 2017, 3-5 April 2017, Freiburg, Germany; Energy Procedia, 124, 240-249.

Zafirovska, I., Juhl, M. K., and Trupke, T., "Efficient Detection of Finger Interruptions from Photoluminescence Images." 33rd European Photovoltaic Solar Energy Conference, Amsterdam, The Netherlands, 2017.

Zhang, Z., Chen, Z., Yuan, L., Conibeer, G., Patterson, R. and Huang, S., "Passivatin lead selenide quantum dot thin film solar cells with inorganic perovskite nanoparticles", 27th International Photovoltaic Science and Engineering Conference, Shiga, Japan, 2017.

Zhu, Y., Juhl, M. K., Trupke, T., and Hameiri, Z. "Applications of DMD-based inhomogeneous illumination photoluminescence imaging for silicon wafers and solar cells." 44th IEEE Photovoltaic Specialists Conference, Washington D.C., 2017.

Zhu, Y., Juhl, M., Coletti, G., and Hameiri, Z. "Impact of transient trapping on steady state photoconductance lifetime measurements." 27th International Photovoltaic Science and Engineering Conference, Shiga, Japan, 2017.

Zhu, Y., Juhl, M., Heinz, F., Schubert, M., Trupke, T., and Hameiri, Z. "Photoluminescence imaging at uniform excess carrier density using non uniform illumination." 27th International Photovoltaic Science and Engineering Conference, Shiga, Japan, 2017.

Zhu, Y., Juhl, M.K., Coletti, G., Hameiri, Z., "Impact of transient trapping on steady state photoconductance lifetime measurements", 27th International Photovoltaic Science and Engineering Conference, Shiga, Japan, 2017.

Zuo C., "Efficient Planar Perovskite Solar Cells Prepared By Using A Nitrogen Blowing Method In Air", 5th ACAP Conference and 4th Asia Pacific Solar Research Conference, Melbourne, Dec 5-7, 2017.

8.6 Theses

Allen, Thomas, "Addressing optical, recombination and resistive losses in crystalline silicon solar cells", PhD, ANU, 2017

Banal, James, "Spectral downshifting by molecular aggregates in planar concentrators for solar energy conversion", PhD, University of Melbourne, 2016

Benesperi, I., Novel hole transporting materials for perovskite solar cells, PhD, Monash,Nov 2017

Bullock, James, "Advanced Contacts For Crystalline Silicon Solar Cells", PhD, ANU, 2016

Cao, Wenkai, "Investigation and fabrication of nanostructured thin films for hot carrier solar cells using colloidal Lead Sulfide QDs", PhD, UNSW, 2017

Chan, Kah Howe, "Integration of Multi-functional Plasmonic Materials in Organic and Perovskite Solar Cell", PhD, UNSW, 2017

Chen, Jian, "Kesterite Thin Film Solar Cell Fabricated By Sulphurising Sputtered Metallic/Metal-Sulphide Precursor", PhD, UNSW, 2016

Chung, Simon, "Hot carrier solar cells: hafnium nitride as an absorber material", PhD, UNSW, 2017

Ciesla, Alison, "Advanced laser processing for next-generation silicon wafer solar cells", PhD, UNSW, 2017

Conrad, Brianna, "Improvement of GaAsP/SiGe tandem solar cell on silicon by optical characterisation, modelling, analysis, and design", PhD, UNSW, 2017

Diaz, Martin, "Improvement of GaAsP/SiGe tandem solar cell on silicon by optical characterisation, modelling, analysis, and design", PhD, UNSW, 2017

Disney, Claire, "Rear Located plasmonic Structures for Light Trapping in Solar Cells", PhD, UNSW, 2017

Dkhissi, Yasmina Delphine, "Solid-state thin films solar cells on polymer substrates", PhD, Melbourne, 2015

Duan, Ruoyu, "Design and Synthesis of Non-fullerene Acceptors", MSc, University of Melbourne, 2017

Fabig, Thomas, "Physical and Photophysical Characterisation of Organic Photovoltaic Nanoparticles", MSc, University of Melbourne, 2017

Gaveshana Anuradha Sepalage, "Application of Inorganic Hole Transporting Materials in Perovskite Solar Cells", PhD, Monash, 2017

Geraghty, Paul, "Materials Development to Achieve Thermally Robust High Performance Organic Photovoltaic Devices", PhD, University of Melbourne, 2017

Hetti Arachchige, Ishanie Rangeeka Perera, "Novel redox mediators for dye sensitized solar cells", PhD, Monash, 2015

Juhl, Mattias, "Application of the spectral response of photoluminescence in photovoltaics", PhD, UNSW, 2016

Kobomoto, Naoya, "Research on Colloidal Quantum Dot Solar Cell using Selective Ligand Exchange Process", Masters, UNSW, 2017

Li, Dun, "Material characterization and device optimization of silicon germanium solar cells grown on silicon substrates", PhD, UNSW, 2016

Li, Hongzhao, “Mitigation of Emitter and Bulk Defects for Industrial p-type Si Solar Cells by Thermal Processes”, PhD, UNSW, 2017

Limpert, Steven, “Heterostructure semiconductor nanowires for hot carrier photovoltaics and photothermoelectric detectors: theory and experiment”, PhD, UNSW, 2017

Lin, Ziyun, “Vertically structured Silicon quantum dot solar cell based on Molybdenum conductive contact substrate”, PhD, UNSW, 2017

Ma, Qingshan, “Perovskite solar cells via vapour deposition processes”, PhD, UNSW, 2017

Mahboubi Soufiani, Arman, “Opto-electronic Characterization of Perovskite Solar Cells”, PhD, UNSW, 2017

McKinley, Arnold, “The physics and mathematical theory of nano-scaled ring resonators and loop antennas”, PhD, ANU, 2014

Mitchell, Valerie, “The design and evaluation of amphiphilic block copolymers for organic photovoltaic active layers with enhanced self-assembly and solubility in green solvents”, PhD, University of Melbourne, 2017

Nampalli, Nitin, “Characterisation and passivation of boron-oxygen defects in p-type Czochralski silicon”, PhD, UNSW 2017

Nguyen, Hieu Trong, “Applications of Spectrally-Resolved Photoluminescence in Silicon Photovoltaics”, PhD, ANU, 2016

Nomoto, Keita, “Material Characteristics of Silicon Nanocrystals for Optical and Electrical Applications”, PhD, UNSW, 2017

Osorio Mayon, Yahuitl, “Engineering Nanoscale Materials for Solar Cells”, PhD, ANU, 2016

Park, Jongsung, “Advanced laser processing for next-generation silicon wafer solar cells”, PhD, UNSW, 2017

Schwarz, Kyra, “Charge Generation in Morphology-Controlled Organic Photovoltaic Materials”, PhD, University of Melbourne, 2017

Seow, Jiayi, “New Molecular Geometries for Solid-State Photon Upconversion”, MSc, University of Melbourne, 2017

Sepalage, Gaveshana Anuradha “Application of Inorganic Hole Transporting Materials in Perovskite Solar Cells”, PhD, Monash, 2017

Sheng, Rui, “CH3NH3PbBr3 Perovskite Solar Cells for Tandem Application – Demonstrations and Characterizations”, PhD, UNSW, 2017

Song, Aaron, “Functional conjugated polymers - from design to devices”, PhD, University of Melbourne, 2015

Sun, Chang, “Recombination activity of metal-related and boron-oxygen defects in crystalline silicon”, PhD, ANU, 2017

Teng, Peinan, “Study of limited junction area approach on silicon solar cells”, PhD, UNSW, 2017

To, Alexander, “Improved carrier selectivity of diffused silicon wafer solar cells”, PhD, UNSW, 2017

Wang, Li, “High efficiency three terminal GaAsP/SiGe dual junction solar Cell on silicon substrate”, PhD, UNSW, 2017

Wang, Xi, “Cost-effective and Reliable Copperplated Metallisation for Silicon Solar Cells: A Development Path”, PhD, UNSW, 2017

Woo, Sanghun, “Broad-Band Sensitised Upconverters for a Crystalline Silicon Solar Cell”, PhD, UNSW, 2016

Wu, Lingfeng, “Silicon nanocrystal solar cells on dielectric substrates”, PhD, UNSW, 2016

Xiao, Manda, “High performance hybrid thin film solar cells”, PhD, Monash, 2016

Yan, Chang, “Developing high efficiency Cu2ZnSnS4 (CZTS) thin film solar cells by sputtering”, PhD, UNSW, 2016

Zhang, Qiuyang, “Energy Selective Contacts Based on Quantum Well Structures of Al2O3 and Group IV Materials for Hot Carrier Solar Cells”, PhD, UNSW, 2014

Zhang, Tian, “PECVD Fabrication, Electrical Characterization and Laser Dopant Activation of Silicon Nanocrystals”, PhD, UNSW, 2016

Zhang, Yi, “Study on III-V materials for hot carrier solar cell absorbers”, PhD, UNSW, 2017

Zheng, Peiting, “Material properties of n-type silicon and n-type UMG solar cells”, PhD, ANU, 2016

Professor Stuart Ross Wenham

FTSE FIEEE FIEAust

15 July 1957 – 23 December 2017

Obituary

written by Professor Martin Green, AM FRS FAA FTSE

It is with great sense of loss that we report the sudden passing of Professor Stuart Wenham, Director of the Australian Research Council (ARC) Photovoltaics Centre of Excellence at UNSW Sydney (The University of New South Wales) and leader of the Advanced Hydrogenation Group.

Stuart was one of the world's foremost photovoltaic device researchers, inventing or co-inventing several solar cell structures brought into manufacturing. These include the buried contact solar cell, marketed under licence by BP Solar from 1992 to 2006 as the company's "Saturn" product and the self-aligned, selective emitter cell marketed by Suntech as the company's "Pluto" product from 2009 to 2013, both with over AU$1 billion in sales. He was also co-inventor of the advanced hydrogenation processes crucial to the recent uptake of the PERC (Passivated Emitter Solar Cell) technology, accounting for over AU$10 billion in sales in 2017.

Stuart also contributed to the recent cost reductions apparent for photovoltaics through assisting former UNSW colleague, Dr Zhengrong Shi, establish and scale up manufacturing in China. This was initially via process refinement and staff training, beginning in 2002. In 2005, Stuart was appointed Chief Technology Officer (part-time) prior to Suntech's listing on the New York Stock Exchange. Stuart was very effective in the preceding "roadshows" intended to encourage strong investor support, undoubtedly contributing to this becoming the largest technology float of 2005.

Stuart was born in Sydney, completing the BSc/BEng double degree at UNSW in 1980, topping the year and receiving the University Medal. In his final year, he took Professor Martin Green's postgraduate solar cell course, stimulating his interest in photovoltaics as well as beginning a lifelong friendship and collaboration with Green. On graduating, Stuart worked with Green's former PhD student, Dr Bruce Godfrey, establishing Australia's first solar cell production line. One customer was BP Solar who bought the line in 1985 when BP decided to manufacture its own cells, since it was producing the best cells then available.

Stuart returned to UNSW in 1983, employed on the team developing the world's first 20% efficient silicon cell, achieved in 1985, also playing a key role in increasing this efficiency to 25% in 1999. In parallel to the earlier work, he continued his part-time PhD under Green's supervision, working on the laser processing of cells. In 1984, patent applications were filed on the buried contact cell, mentioned above, later assessed by the Australian Academy of Technology and Engineering as one of the "Top 100 Australian inventions of the 20th century". Stuart was awarded his PhD in 1986 and was appointed as Lecturer at UNSW in 1988, Professor in 1998 and Scientia Professor in 2003.

Stuart was a superb teacher, winning the 1995 Vice-Chancellor's Award for "Teaching Excellence". In 1999, he was awarded an ARC Key Centre in Photovoltaic Engineering, initiating the launch of the world's first undergraduate degree program in photovoltaics in 2000 and the formation of a separate School of Photovoltaic and Renewable Energy Engineering in 2006. Approximately 500 undergraduate students are presently enrolled, together with 100 PhD students. In 2003, the Key Centre was merged with an ARC Special Research Centre awarded to Green, to form the ARC Photovoltaics Centre of Excellence, with Stuart as Director until the present.

Stuart was awarded several local and international prizes during his career. These include the 1992 CSIRO External Medal and the 1999 Australia Prize, both jointly with Green, plus the 2009 IEEE William R. Cherry Award and the 2011 IEEE J.J. Ebers Award, the Electron Devices Society's most prestigious award, and the 2013 IET A.F. Harvey Engineering Research Prize, all as sole awardee. He was selected as 2010 Professional Engineer of the Year by the Institute of Engineers, Australia and as one of "Australia's Top 100 Most Influential Engineers" by the Institute for the following four years.

A memorial service was held on 8 January 2018, at the Sir John Clancy Auditorium on UNSW's Kensington campus. Over 800 people from around the world attended, including many former students.

Australian Centre for Advanced Photovoltaics
Australia-US Institute for Advanced Photovoltaics

UNSW Sydney NSW 2052 Australia

Tel +61 2 9385 4018
Fax +61 2 9662 4240
Email: acap@unsw.edu.au

www.ausiapv.net.au
www.acap.net.au

Director: Scientia Professor Martin Green

Acknowledgements

Written and compiled by

Australian Centre for Advanced Photovoltaics
Australia-US Institute for Advanced Photovoltaics

Photos, figures and graphs
Courtesy of Centre staff, students and others

CRICOS Provider Code: 00098G.